

Homogeneously catalyzed hydroformylation in supercritical carbon dioxide : kinetics, thermodynamics, and membrane reactor technology for continuous operation

Citation for published version (APA):

Koeken, A. C. J. (2008). *Homogeneously catalyzed hydroformylation in supercritical carbon dioxide : kinetics, thermodynamics, and membrane reactor technology for continuous operation*. [Phd Thesis 1 (Research TU/e / Graduation TU/e), Chemical Engineering and Chemistry]. Technische Universiteit Eindhoven. <https://doi.org/10.6100/IR631964>

DOI:

[10.6100/IR631964](https://doi.org/10.6100/IR631964)

Document status and date:

Published: 01/01/2008

Document Version:

Publisher's PDF, also known as Version of Record (includes final page, issue and volume numbers)

Please check the document version of this publication:

- A submitted manuscript is the version of the article upon submission and before peer-review. There can be important differences between the submitted version and the official published version of record. People interested in the research are advised to contact the author for the final version of the publication, or visit the DOI to the publisher's website.
- The final author version and the galley proof are versions of the publication after peer review.
- The final published version features the final layout of the paper including the volume, issue and page numbers.

[Link to publication](#)

General rights

Copyright and moral rights for the publications made accessible in the public portal are retained by the authors and/or other copyright owners and it is a condition of accessing publications that users recognise and abide by the legal requirements associated with these rights.

- Users may download and print one copy of any publication from the public portal for the purpose of private study or research.
- You may not further distribute the material or use it for any profit-making activity or commercial gain
- You may freely distribute the URL identifying the publication in the public portal.

If the publication is distributed under the terms of Article 25fa of the Dutch Copyright Act, indicated by the "Taverne" license above, please follow below link for the End User Agreement:

www.tue.nl/taverne

Take down policy

If you believe that this document breaches copyright please contact us at:

openaccess@tue.nl

providing details and we will investigate your claim.

**Homogeneously Catalyzed Hydroformylation in
Supercritical Carbon Dioxide:
Kinetics, Thermodynamics, and Membrane Reactor
Technology for Continuous Operation**

PROEFSCHRIFT

ter verkrijging van de graad van doctor aan de
Technische Universiteit Eindhoven, op gezag van de
Rector Magnificus, prof.dr.ir. C.J. van Duijn, voor een
commissie aangewezen door het College voor
Promoties in het openbaar te verdedigen
op donderdag 17 januari 2008 om 16.00 uur

door

Adrianus Cornelis Jacobus Koeken

geboren te Oosterhout

Dit proefschrift is goedgekeurd door de promotor:

prof.dr.ir. J.T.F. Keurentjes

Copromotor:

dr. L.J.P. van den Broeke

A catalogue record is available from the Eindhoven University of Technology Library

ISBN: 978-90-386-1189-1

© 2007 by Adrianus C. J. Koeken

This project is supported with a grant (EETK01115) of the Dutch Programme EET (Economy, Ecology, Technology) a joint initiative of the Ministries of Economic Affairs, Education, Culture and Sciences and of Housing, Spatial Planning and the Environment.

Cover design: Ard Koeken and Paul Verspaget

Printed at the Universiteitsdrukkerij, Eindhoven University of Technology

Contents

Chapter 1	Introduction: The use of alternative solvents and membrane technology for the immobilization of homogeneous catalysts	1
Chapter 2	Evaluation of pressure and correlation to reaction rates during homogeneously catalyzed hydroformylation in supercritical carbon dioxide	15
Chapter 3	Chemoselectivity and regioselectivity of 1-octene hydroformylation in supercritical carbon dioxide	39
Chapter 4	Modeling of the kinetics of 1-octene hydroformylation in supercritical carbon dioxide	59
Chapter 5	Hydroformylation of 1-octene in supercritical carbon dioxide and organic solvents using trifluoromethyl substituted triphenylphosphine ligands	83
Chapter 6	Selectivity of rhodium catalyzed hydroformylation of 1-octene during batch and semi-batch operation using trifluoromethyl substituted ligands	97
Chapter 7	Permeation of gases and supercritical fluids through a supported microporous titania membrane	115
Chapter 8	Integration of reaction and separation at supercritical conditions using a titania membrane	133
Summary		151
Samenvatting		155
Curriculum Vitae		159
Dankwoord		161

Chapter 1

Introduction: The use of alternative solvents and membrane technology for the immobilization of homogeneous catalysts

Abstract

The application of alternative solvents, membrane technology, and dedicated catalysts are important starting points for the design of environmentally benign processes. An overview is given of different techniques to recover and recycle homogeneous catalysts, with an emphasis on the role of supercritical fluids. The aim of this thesis is to evaluate the possible advantages of supercritical carbon dioxide over organic solvents and the potential of membrane technology for the recovery of homogeneous catalysts used for the hydroformylation of long-chain alkenes.

Green process development

Stricter environmental legislation and the strive for cleaner and more efficient processes has prompted the chemical process industry to develop “greener” production processes. It is likely that, in addition to the benefits to the environment, the application of “green” technology will also improve the image of the chemical process industry. Green chemistry encompasses a number of themes: efficient use of raw materials and energy, reduction of waste, and safer chemical syntheses or production methods.^[1] Solvent replacement in conjunction with the development of dedicated catalysts is often quoted as one of the most promising means to achieve “greener” production processes. Supercritical fluids have received considerable attention as an environmentally benign alternative to organic solvents.^[1-7] A considerable amount of research is devoted to the study of environmentally benign chemical synthesis methods, where the beneficial aspects of both catalysis and supercritical fluids are combined.

Supercritical fluids

Most organic solvents currently used in industry pose certain risks including toxicity and flammability. Also, most common organic solvents, for example ethanol, toluene, and dichloromethane, are volatile, thus emission to the environment is difficult to prevent. There are a number of candidates to replace organic solvents. Water is abundant and cheap. However, organic nonpolar substances only dissolve in water to a limited extent and this limits the application of water. On the other hand, this also can be used to carry out certain difficult separations. Ionic liquids have a very low vapor pressure, which makes the emission to the environment by evaporation unlikely. A large range of organic substances is soluble in ionic liquids. Although the availability of ionic liquids with suitable properties is increasing, exact knowledge on their physical properties and chemical stability is still limited.^[8] Additionally, the viscosity of ionic liquids is relatively high and this can cause mass transfer limitations.^[9] The low solubility of permanent gases in water, ionic liquids, and organic solvents requires attention when performing reactions with a combination of gaseous and liquid reactants, which is the case for hydrogenation, hydroformylation, and possibly oxidation reactions. For fast reactions the transport of the gaseous reactant to the catalyst, usually dissolved or suspended in the liquid phase, can be rate limiting.

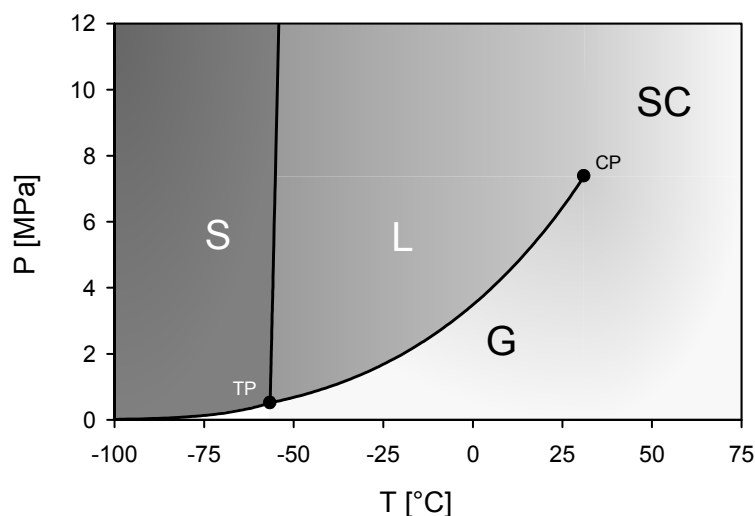


Figure 1. Part of the phase diagram of carbon dioxide.^[10]

In this respect, supercritical fluids (SCF), another class of alternative solvent media, have a clear advantage over liquid solvents; permanent gases have a high solubility in SCF. In particular CO₂ is of interest since CO₂ has a low toxicity and a moderate critical pressure and temperature. Furthermore, carbon dioxide is an abundant substance and it is nonflammable, which can retard the risk of fire or explosion in case of leakage. However, to apply CO₂ as a solvent, either as a liquid or in the supercritical phase, requires the use of pressure equipment.

In Figure 1 a part of the phase diagram of carbon dioxide is depicted. At 20 °C the vapor pressure of carbon dioxide is 5.7 MPa. When the temperature is increased the vapor pressure of carbon dioxide increases up to the critical point. At this point, 31 °C and 7.4 MPa, the liquid and vapor phase cease to exist and merge into the supercritical phase.

Table 1. Comparison of typical physical properties of gases, SCFs, and liquids.^[11-13]

Physical property	Gas (ambient T and P)	SCF (T _c , P _c)	Liquid (ambient T and P)
Density [kg m ⁻³]	0.6 – 2	100 – 800	600 – 1600
Dynamic viscosity [mPa s]	0.01 – 0.3	0.01 – 0.1	0.2 – 3
Diffusion coefficient [10 ⁻⁶ m ² s ⁻¹]	10 – 40	0.07 – 0.1	0.0002 – 0.002

The properties of a SCF are between those of a gas and a liquid, see Table 1. SCF densities approach liquid-like values and solubility generally increases with increasing solvent density. In the near critical region, just above the critical temperature and pressure, the density

of a SCF can change considerably with a relatively small change in pressure or temperature. From a process engineering point of view this can be an advantageous characteristic, because a small adjustment in pressure and/or temperature can separate products, including homogeneous catalysts, from a process stream. Properties like viscosity, diffusivity, and surface tension are also in between those of a gas and liquid^[12] and also show a pressure and temperature dependence.^[14]

It is possible to dissolve reactants and a homogeneous catalyst in one single supercritical phase. Optimal use can then be made of the higher diffusion rates, higher concentrations of gaseous reactants, and the lower viscosity. Consequently, conversion rates and selectivity can possibly be enhanced. A high degree of process intensification can be established making use of a supercritical reaction system. The one-phase reaction system in combination with a continuous flow process allows for high throughput experimentation using relatively small-scale reactors.^[5,11]

Catalysis in supercritical fluids

Catalysis is an important tool to achieve a chemical conversion with a maximum selectivity for the desired product combined with a minimum amount of waste produced. In Table 2 a comparison is made between the characteristics of heterogeneous and homogeneous catalysis.^[15]

Table 2. Comparison between aspects of heterogeneous and homogeneous catalysis, adapted from [6].

	Homogeneous	Heterogeneous
1. Activity	High	Variable
2. Selectivity	High	Variable
3. Reaction conditions	Mild	Harsh
4. Service life of catalysts	Variable	Extended
5. Sensitivity for catalyst poisons	Variable	High
6. Diffusion/mass transfer problems	Low	Important
7. Catalyst recycling	Difficult ^[a]	Facile
8. Variability of electronic and steric properties of catalysts	Possible	Not possible
9. Mechanistic understanding	Plausible under random conditions	Extremely complex

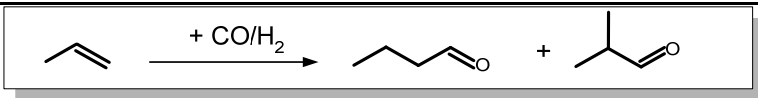
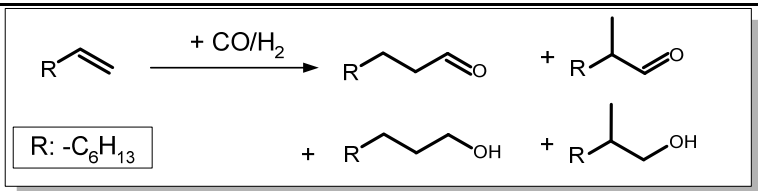
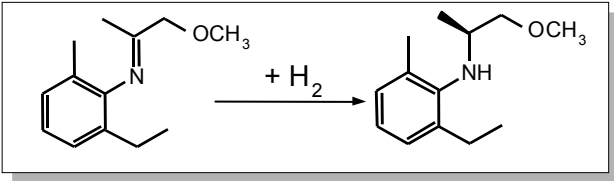
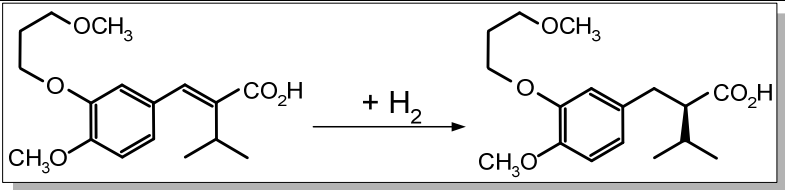
[a] Separating the catalyst components from the product is often straightforward, however, the catalyst loses its activity and/or activity.

Heterogeneous catalysis is the most widely applied in the production of bulk chemicals due to easy recycling possibilities of solid insoluble catalysts. Homogeneous catalysts, including organometallic compounds, enzymes, and organic catalysts are present in the same phase as the reactants. Therefore, homogeneous catalysts are inherently more difficult to separate from the reaction product. Often homogeneous catalysts deactivate during the reaction and the subsequent separation from the product (for example by distillation). This hinders their commercial application, because a homogeneous catalyst can not be easily regenerated. An advantage, which homogeneous catalysts have over their heterogeneous counterparts, is that they are more adaptable to the reaction environment. The properties of homogeneous transition metal catalysts can be changed considerably by altering of the ligands attached to the metal center. Consequently, for a number of reactions homogeneous catalysts possess better activity and selectivity than heterogeneous catalysts. In Table 3 examples of industrial application of homogeneous catalysis are given.

The application of supercritical carbon dioxide, scCO_2 , in particular as a reaction medium in heterogeneously and homogeneously catalyzed reactions has gained increasing interest.^[5,11] In particular, because the performance of both homogeneous and heterogeneous catalysts can be enhanced in a SCF application. Homogeneous catalysis can profit from the high solubility of gases in SCFs. The good mass transfer properties of SCFs reduce diffusion limitations in and around heterogeneous catalyst particles.

On the other hand, the application of common homogeneous catalysts developed for the use in organic solvents is limited in supercritical carbon dioxide because of their low solubility.^[16] The well-known Wilkinson catalyst for hydrogenation, $[\text{RhCl}(\text{PPh}_3)_3]$, has been found to be insoluble in scCO_2 up to 10 MPa and 50 °C.^[17] However, it has been found that attaching ligands modified with perfluoroalkyl groups to the catalytically active metal centre enhances the solubility such that common catalysts become applicable in scCO_2 .^[18-20] Also, the limited solubility of homogeneous catalysts can be exploited to overcome the traditional drawback of homogeneous catalysis. For this purpose, scCO_2 can be used as an extraction medium to separate the reaction product from the homogeneous catalyst. Carbon dioxide then serves as an anti-solvent, the catalyst precipitates while the reaction product dissolves in the carbon dioxide.^[21,22]

Table 3. Examples of homogeneous catalyzed reactions on a commercial scale.

hydroformylation of propene ^[15,23-25]	
	
Catalyst precursor	[HRhCO(P(3-NaSO ₃ C ₆ H ₄) ₃) ₃] or [HRhCO(PPh ₃) ₃]
Application	butanol as solvent, butylacrylate as monomer for polymerization, 2-ethylhexanol as intermediate for plasticizer production
hydroformylation of long-chain alkenes ^[15,18,19,21,23]	
	
Catalyst precursor	[Co ₂ (CO) ₈] or [Co ₂ (CO) ₆ (P(C _n H _{n+1}) ₃) ₂] (n=2-4)
Application	linear alcohols for detergents, alcohols for plasticizers
enantioselective hydrogenation of an enamine ^[26]	
	
Catalyst precursor	[Ir(cod)Cl] ₂ ^[a] and “Josiphos4” as the phosphine ligand
Application	precursor of the herbicide (S)-metolachlor (Dual Magnum®)
enantioselective hydrogenation of an α-isopropylcinnamic acid derivative ^[27]	
	
Catalyst precursor	[Rh(cod) ₂] ^[a] BF ₄ and “3,3'-dimethyl-PipPhos” mixed with tri-m-tolylphosphine as the ligands.
Application	precursor of blood pressure-lowering agent aliskiren TM

[a] “cod” stands for cyclooctadiene.

Recycling of homogeneous catalysts

Besides the development of more active and selective homogeneous catalysts a significant part of the research efforts is directed to improve the recycling of the catalyst. For the development of economically viable and environmentally more sustainable processes, the costly tailor-made catalysts have to be able to be recovered and recycled.^[28] Furthermore, for most applications traces of catalyst in a end product are often highly undesirable.

The strategies to facilitate separation of homogeneous catalysts can roughly be divided in three different categories, see Table 4.^[6] A significant number of examples mentioned in Table 4 involve the use of CO₂ to induce phase separation after reaction. In the examples where reaction and separation have been integrated in a single unit step, CO₂ has been exploited to enhance the mass transfer of reactants and products in the case where insoluble “heterogenized” catalysts have been used. In the integrated reaction and separation examples where a “biphasic” approach was used, the use of CO₂ improved the mass transfer and solubility of gaseous reactants in, for example, the ionic liquid or polyethylene glycol phase.^[29]

Using a separate liquid phase to contain the catalyst, the so-called “biphasic approach”, is applied on an industrial scale, with the Ruhrchemie/Rhône-Poulenc oxo-process and the Shell Higher Olefin Process as examples. However, inherent to the use of auxiliary solvents one has to consider undesired side reactions, contamination of the product with the auxiliary solvent, and possible mass transfer limitations as a result of an additional phase boundary.

Membrane technology for the immobilization of a homogeneous catalyst

Separations using membranes have gained importance as an alternative to conventional separation techniques like distillation and extraction. Separation by a membrane is based on the difference of transport rate of the components in the feed mixture across the membrane. In Figure 2 an overview is given of the most widely used membrane processes, together with the approximate range of the size of the components to be separated.^[30,31] Membranes are most commonly prepared from organic polymeric materials. However, the application of organic polymeric membranes is restricted to moderate temperatures and pressures. Additionally, the type of feed can have a significant effect on the membrane performance as a result of various effects, including sorption and swelling.^[30]

Table 4. Examples of homogeneous catalyst separation routes, with the focus on hydroformylation and hydrogenation reactions.^[a]

Catalyst phase/support	Product phase	Separation method	Refs.
Category 1. separation after reaction with catalyst work-up			
	organic	chemical conversion of the catalyst followed by extraction, BASF hydroformylation process, Ruhrchemie oxo-process.	[15,23]
Category 2. separation after reaction without catalyst work-up			
scCO ₂ ^[a] / soluble polymeric supports	scCO ₂	phase separation by change in P and/or T, or membrane separation	[32,33]
scCO ₂	scCO ₂	phase separation by change in P and/or T	[19,21,34]
organic	scCO ₂	phase separation induced by CO ₂ and change in P and/or T	[22]
organic/fluorous	organic	phase separation induced by fluorous solvent and change in P and/or T	[35-38]
aqueous	organic	decantation	[24]
organic soluble	organic	magnetic field	[39]
inorganic/organic support			
aqueous with additives	organic	decantation	[40,41]
soluble/insoluble support in an aqueous phase (SAPC)	organic	decantation	[42-44]
aqueous with additives	scCO ₂		[45]
ionic liquid	organic	decantation	[8,46]
organic	organic		[47]
Category 3. Integration of separation and reaction without catalyst work-up			
heterogeneous polymeric support	scCO ₂	microfiltration/decantation	[48-51]
	organic	microfiltration/decantation	[52]
heterogeneous inorganic support	scCO ₂	microfiltration/decantation	[53]
	organic	microfiltration/decantation	[44]
ionic liquids	scCO ₂	reactive extraction	[54,55]
Supported Liquid Phase Catalysis (SLPC)	organic	reactive extraction	[52,56]
polyethyleneglycol (PEG)	scCO ₂	reactive extraction	[57]
scCO ₂	scCO ₂	nanofiltration	[58,59]
organic	organic	nanofiltration/ultrafiltration	[56,60-66]

^[a] "scCO₂" implies a CO₂ enriched supercritical phase in which the product and possibly unreacted substrates are dissolved.

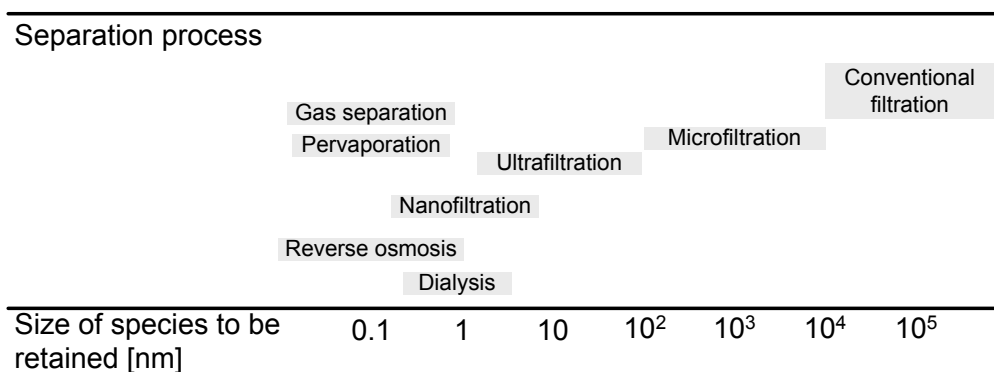


Figure 2. Examples of membrane separation processes.^[30,31]

In applications involving scCO_2 the use of organic polymeric membranes is limited. The swelling and plasticization of polymers occurring in the presence of high pressure CO_2 has a detrimental effect on membrane performance and stability.^[67] Inorganic membranes possess a better structural stability, because swelling or compaction does not occur. Additionally, inorganic membranes have a higher chemical and thermal stability than organic/polymeric membranes.^[30,68] However, the production of ceramic membranes is substantially more costly than the production of polymeric membranes.

During permeation experiments of supercritical carbon dioxide across tubular microporous alumina-supported silica membranes provided by ECN a reasonable flux has been obtained, which was stable for a longer period of time at a temperature of 80 °C and a feed pressure up to 20 MPa.^[69,70] These silica membranes have been used for the retention of a Wilkinson type catalyst in the continuous hydrogenation of 1-butene performed with supercritical carbon dioxide as the solvent.^[58,59] In Figure 3 a schematic representation of this alumina supported silica membrane is depicted.

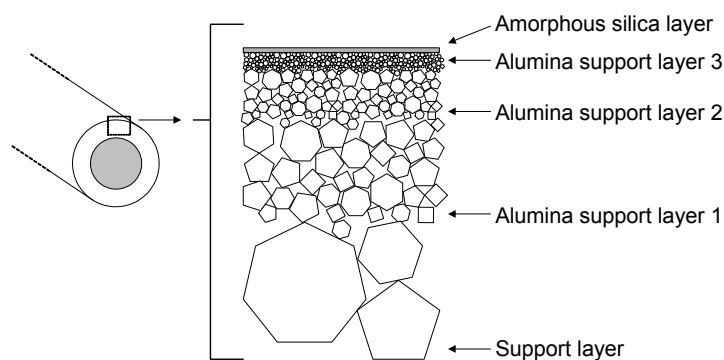


Figure 3. Schematic representation of tubular asymmetric composite ceramic membranes.

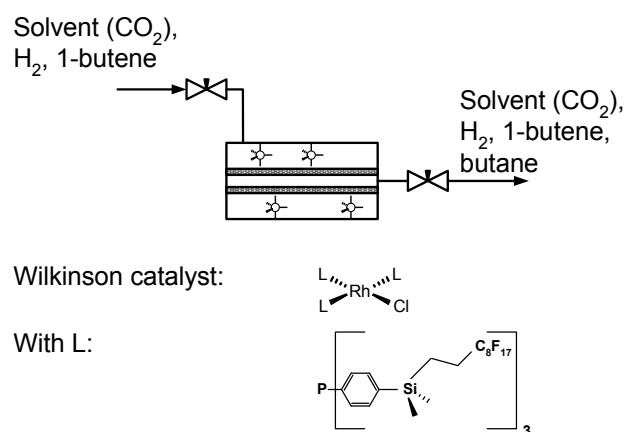


Figure 4. Schematic representation of the tubular membrane reactor and the fluorinated version of the Wilkinson catalyst.

In Figure 4 the membrane configuration and the catalyst used during the hydrogenation are depicted.^[58,59] To enhance the solubility of the hydrogenation catalyst in the supercritical medium, triarylphosphine ligands have been applied, on which perfluoroalkyl chains have been attached. This type of ligands has also been applied in the hydrogenation of 1-octene where the catalyst has been recycled by fluoruous biphasic separation.^[36,71,72]

Outline of this thesis

The aim of this thesis is, first, to evaluate the possible advantages of scCO₂ over organic solvents, which are discussed in the paragraph “Supercritical fluids”. Second, the aim is to evaluate the potential of membrane technology for the retention of homogeneous catalysts for the hydroformylation of alkenes. The hydroformylation of 1-octene has been chosen as the model reaction, because it is a process of industrial relevance.^[73,74] The characteristics of the membrane have to be such that the catalyst and its precursors are sufficiently retained while the product can permeate through the membrane at a high rate for a prolonged period of time under reaction conditions.

The concept of homogeneous hydroformylation of 1-octene in supercritical carbon dioxide using a membrane for the integration of reaction and catalyst separation catalyst, depicted in Figure 5, can have a number of advantages. First of all, applying membrane separation can have a possible improvement in energy efficiency as compared to conventional alkene hydroformylation processes.

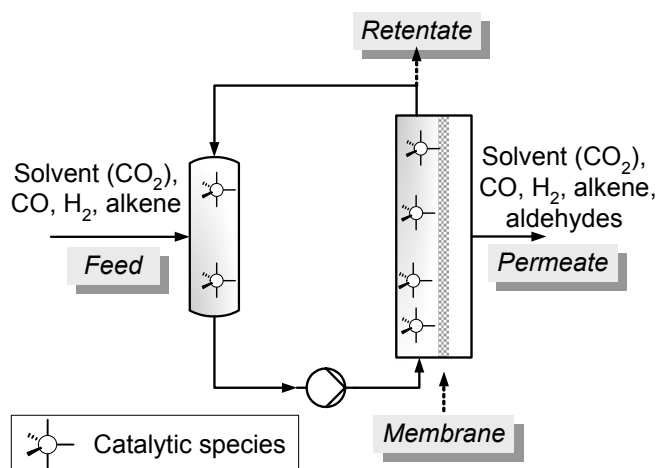


Figure 5. The process concept.

Working with a one-phase supercritical reaction system can improve the catalyst stability and provides good mass transfer. As a result of performing the reaction in a supercritical fluid both pressure and temperature can have a more pronounced effect on the solvent characteristics than when organic solvents would be used. This is an additional aspect that can be used to optimize the reaction conditions. Finally, a membrane reactor configuration allows for a more direct control of the concentration of syngas (equimolar mixture of CO and H₂), which could lead to better catalyst stability and an improved selectivity.

In Chapter 2 an experimental method is described for the batch hydroformylation of 1-octene in supercritical carbon dioxide. A correlation between the change in total pressure and the progress of the reaction is established. In Chapter 3 the dependence of the catalyst activity and selectivity on the reaction parameters like temperature, total pressure, initial reactant concentration, and catalyst precursor concentration, is discussed for the rhodium catalyst hydroformylation of 1-octene in supercritical carbon dioxide. In Chapter 4 a kinetic model for the hydroformylation of 1-octene under supercritical one-phase conditions is evaluated leading to a description of the results presented in Chapter 3. In Chapter 5 a comparison in terms of catalyst activity and selectivity is made between the use of supercritical carbon dioxide, hexane, toluene and perfluoromethylcyclohexane as a solvent. Additionally, monodentate phosphines with varying number of trifluoromethyl substituents have been included in the comparison. In Chapter 6 the cumulative and differential regioselectivity of rhodium catalysts with a varying number of trifluoromethyl substituents has been evaluated using two different “modes of operation”, batch versus semi batch operation. A comparison is

made between results obtained in hexane, scCO₂, and for neat, or “solventless” operation. The permeation of different gases, pure supercritical fluids, and supercritical mixtures through a tubular microporous alumina- supported titania membrane is presented in Chapter 7. Finally, in Chapter 8 results on the continuously operated homogeneously catalyzed hydroformylation in supercritical carbon dioxide performed in a membrane reactor are discussed and directions for further developments are given.

References

- [1] R. Sheldon, *Green Chem.* **2000**, *1*, G1-G4.
- [2] R. A. Sheldon, H. van Bekkum, in *Fine Chemicals through Heterogeneous Catalysis*, (eds. R. A. Sheldon, H. van Bekkum), Wiley-VCH Verlag GmbH, Weinheim, Germany, **2001**, p. 1-12.
- [3] D. Adam, *Nature*, **2000**, *407*, 938-940.
- [4] W. Leitner, *Acc. Chem. Res.* **2002**, *35*, 746-756.
- [5] Jessop, P. G., and Leitner, W. (eds), *Chemical Synthesis using Supercritical Fluids*, 1st ed., Wiley-VCH Verlag GmbH, Weinheim, Germany, **1999**.
- [6] B. Cornils, W. A. Herrmann, I. T. Horváth, W. Leitner, S. Mecking, H. Olivier-Bourbigou, D. Vogt, in *Multiphase Homogeneous Catalysis, Vol 1*, (Eds.: B. Cornils, W. A. Herrmann, I. T. Horváth, W. Leitner, S. Mecking, H. Olivier-Bourbigou, D. Vogt), Wiley-VCH, Weinheim, **2005**, p. 3-23.
- [7] E. J. Beckman, *J. Supercrit. Fluids* **2004**, *28*, 121-191.
- [8] Y. Chauvin, H. Olivier-Bourbigou, in *Multiphase Homogeneous Catalysis, Vol 2*, (Eds.: B. Cornils, W. A. Herrmann, I. T. Horváth, W. Leitner, S. Mecking, H. Olivier-Bourbigou, D. Vogt), Wiley-VCH, Weinheim, **2005**, p. 407-430.
- [9] H. G. Joglekar, I. Rahman, B. D. Kulkarni, *Chem. Eng. Technol.* **2007**, *30*, 819–828.
- [10] S. Angus, B. Armstrong, K. M. de Reuck, *International Thermodynamic Tables of the Fluid State: Carbon Dioxide, Vol. 3*, IUPAC, Pergamon Press, Oxford, **1976**.
- [11] A. Baiker, *Chem. Rev.* **1999**, *99*, 453-473.
- [12] R. Wandeler, A. Baiker, *CaTTech* **2000**, *4*, 128-143.
- [13] E. L. V. Goetheer, *Strategies for Carrier-Mediated Extraction and Reaction in Supercritical Carbon Dioxide*, PhD thesis, Eindhoven, **2002**.
- [14] B. Subramaniam, M. A. McHugh, *Ind. Eng. Chem. Proc. Des. Dev.* **1986**, *25*, 1-12.
- [15] B. Cornils, W. A. Herrmann, in *Applied Homogeneous Catalysis with Organometallic Compounds*, 2nd ed., Vol. 1, (Eds.: B. Cornils, W. A. Herrmann), Wiley-VCH, Weinheim, **2002**, p. 3-15.
- [16] P. G. Jessop, T. Ikariya, R. Noyori, *Chem. Rev.* **1999**, *99*, 475-493.
- [17] U. Kreher, S. Schebesta, D. Walther, *Z. Anorg. Allg. Chem.* **1998**, *624*, 602-612.
- [18] S. Kainz, D. Koch, W. Baumann, W. Leitner, *Angew. Chem. Int. Ed.* **1997**, *15*, 1628-1630.
- [19] D. R. Palo, C. Erkey, *Ind. Eng. Chem. Res.* **1998**, *37*, 4203-4206.
- [20] K.-D. Wagner, N. Dahmen, E. Dinjus, *J. Chem. Eng. Data* **2000**, *45*, 672-677.
- [21] D. Koch, W. Leitner, *J. Am. Chem. Soc.* **1998**, *120*, 13398-13404.
- [22] M. Solinas, J. Jiang, O. Stelzer, W. Leitner, *Angew. Chem. Int. Ed.* **2005**, *44*, 2291-2295.
- [23] M. Beller, B. Cornils, C. D. Frohning, C. W. Kohlpaintner, *J. Mol. Catal. A* **1995**, *104*, 17-85
- [24] C. W. Kohlpaintner, R. W. Fischer, B. Cornils, *Appl. Catal. A* **2001**, *221*, 219-225.
- [25] J. W. Rathke, R. J. Klingler, T. R. Krause, *Organometallics* **1991**, *10*, 1350-1355.
- [26] H.-U. Blaser, B. Pugin, F. Spindler, in *Applied Homogeneous Catalysis with Organometallic Compounds*, 2nd ed., Vol. 2, (Eds.: B. Cornils, W. A. Herrmann), Wiley-VCH, Weinheim, **2002**, p. 1131-1147.

- [27] J. A. F. Boogers, U. Felfer, M. Kotthaus, L. Lefort, G. Steinbauer, A. H. M. de Vries, J. G. de Vries, *Org. Proc. Res. Dev.* **2007**, *11*, 585-591.
- [28] R. T. Baker, S. Kobayashi, W. Leitner, *Adv. Synth. Catal.* **2006**, *348*, 1337-1340.
- [29] D. J. Cole-Hamilton, *Science* **2003**, *299*, 1702-1706.
- [30] M. Mulder, *Principles of Membrane Technology*, 2nd edition, Kluwer Academic Publishers, Dordrecht, **1996**.
- [31] R. W. Baker, *Membrane Technology and Applications*, 2nd edition, John Wiley and Sons, **2004**, p. 1-14.
- [32] Z. K. Lopez-Castillo, R. Flores, I. Kani, J. P. Fackler, Jr., A. Akgerman, *Ind. Eng. Chem. Res.* **2003**, *42*, 3893-3899.
- [33] R. Flores, Z. K. Lopez-Castillo, I. Kani, J. P. Fackler, Jr., A. Akgerman, *Ind. Eng. Chem. Res.* **2003**, *42*, 6720-6729.
- [34] S. Kainz, A. Brinkmann, W. Leitner, A. Pfaltz, *J. Am. Chem. Soc.* **1999**, *121*, 6421-6429.
- [35] I. T. Horváth, G. Kiss, R. A. Cook, J. E. Bond, P. A. Stevens, J. Rábai, E. J. Mozeleski, *J. Am. Chem. Soc.* **1998**, *120*, 3133-3143.
- [36] B. Richter, A. L. Spek, G. van Koten, B.-J. Deelman, *J. Am. Chem. Soc.* **2000**, *122*, 3945-3951.
- [37] D. F. Foster, D. J. Adams, D. Gudmunsen, A. M. Stuart, E. G. Hope, D. J. Cole-Hamilton, *Chem. Commun.* **2002**, 722-723.
- [38] D. J. Adams, J. A. Bennett, D. J. Cole-Hamilton, E. G. Hope, J. Hopewell, J. Kight, P. Pogorzelec, A. M. Stuart, *Dalton Trans.*, **2005**, 3862-3867.
- [39] R. Abu-Reziq, H. Alper, D. Wang, M. L. Post, *J. Am. Chem. Soc.* **2006**, *128*, 5279-5282.
- [40] K. Kunna, C. Müller, J. Loos, D. Vogt, *Angew. Chem. Int. Ed.* **2006**, *45*, 7289-7292.
- [41] F. van Vyve, A. Renken, *Catal. Today* **1999**, *48*, 237-243.
- [42] C. Disser, C. Muennich, *G. Luft, Appl. Catal. A* **2005**, *296*, 201-208.
- [43] M. Bortenschlager, N. Schöllhorn, A. Wittmann, R. Weberskirch, *Chem. Eur. J.* **2007**, *13*, 520-528.
- [44] H. Delmas, U. Jáuregui-Haza, A.-M. Wilhelm, in *Multiphase Homogeneous Catalysis*, Vol. 1, (Eds.: B. Cornils, W. A. Herrmann, I. T. Horváth, W. Leitner, S. Mecking, H. Olivier-Bourbigou, D. Vogt), Wiley-VCH, Weinheim, **2005**, p. 297-304.
- [45] X. Dong, C. Erkey, *ACS Symp. Ser.* **2003**, *860*, 430-443.
- [46] R. P. J. Bronger, S. M. Silva, P. C. J. Kamer, P. W. N. M. van Leeuwen, *Chem. Commun.* **2002**, 3044-3045.
- [47] D. Vogt, in *Multiphase Homogeneous Catalysis*, Vol 1, (Eds.: B. Cornils, W. A. Herrmann, I. T. Horváth, W. Leitner, S. Mecking, H. Olivier-Bourbigou, D. Vogt), Wiley-VCH, Weinheim, **2005**, p. 313-337.
- [48] F. Shibahara, K. Nozaki, T. Hiyama, *J. Am. Chem. Soc.* **2003**, *125*, 8555-8560.
- [49] A. R. Tadd, A. Marteel, M. R. Mason, J. A. Davies, M. A. Abraham, *Ind. Eng. Chem. Res.* **2002**, *41*, 4514-4522.
- [50] O. Hemminger, A. Marteel, M. R. Mason, J. A. Davies, A. R. Tadd, M. A. Abraham, *Green Chem.* **2002**, *4*, 507-512.
- [51] A. R. Tadd, A. Marteel, M. R. Mason, J. A. Davies, M. A. Abraham, *J. Supercrit. Fluids* **2003**, *25*, 183-196.
- [52] P. Panster, S. Wieland, in *Applied Homogeneous Catalysis with Organometallic Compounds*, 2nd ed., Vol. 2, (Eds.: B. Cornils, W. A. Herrmann), Wiley-VCH, Weinheim, **2002**, p. 647-661.
- [53] R. P. J. Bronger, J. P. Bermon, J. N. H. Reek, P. C. J. Kamer, P. W. N. M. van Leeuwen, D. N. Carter, P. Licence, M. Poliakoff, *J. Mol. Catal. A* **2004**, *224*, 145-152.
- [54] P. B. Webb, M. F. Sellin, T. E. Kunene, S. Williamson, A. M. Z. Slawin, D. J. Cole-Hamilton, *J. Am. Chem. Soc.* **2003**, *125*, 15577-15588.
- [55] M. Solinas, A. Pfaltz, P. G. Cozzi, W. Leitner, *J. Am. Chem. Soc.* **2004**, *126*, 16142-16147.
- [56] J. S. Kim, R. Datta, *AIChE J.* **1991**, *37*, 1657-1667.
- [57] D. J. Heldebrant, P. G. Jessop, *J. Am. Chem. Soc.* **2003**, *125*, 5600-5601.

- [58] L. J. P. van den Broeke, E. L. V. Goetheer, A. W. Verkerk, E. de Wolf, B.-J. Deelman, G. van Koten, J. T. F. Keurentjes, *Angew. Chem. Int. Ed.* **2001**, *40*, 4473-4474.
- [59] E. L. V. Goetheer, A. W. Verkerk, L. J. P. van den Broeke, E. de Wolf, B.-J. Deelman, G. van Koten, J. T. F. Keurentjes, *J. Catal.* **2003**, *219*, 126-133.
- [60] N. J. Hovestad, E. B. Eggeling, H. J. Heidebüchel, J. T. B. H. Jastrzebski, U. Kragl, W. Keim, D. Vogt, G. van Koten, *Angew. Chem. Int. Ed.* **1999**, *38*, 1655-1658.
- [61] D. de Groot, E. B. Eggeling, J. C. de Wilde, H. Kooijman, R. J. van Haaren, A. W. van der Made, A. L. Spek, D. Vogt, J. N. H. Reek, P. C. J. Kamer, P. W. N. M. van Leeuwen, *Chem. Commun.* **1999**, 1623-1624.
- [62] U. Kragl, C. Dreisbach, *Angew. Chem. Int. Ed. Engl.* **1996**, *35*, 642-644.
- [63] U. Kragl, C. Dreisbach, in *Applied Homogeneous Catalysis*, 2nd ed., Vol. 2, (Eds.: B. Cornils, W. A. Herrmann), Wiley-VCH, Weinheim, **2002**, p. 941-953.
- [64] J. Sanchez Marcano, in *Multiphase Homogeneous Catalysis*, Vol 1, (Eds.: B. Cornils, W. A. Herrmann, I. T. Horváth, W. Leitner, S. Mecking, H. Olivier-Bourbigou, D. Vogt), Wiley-VCH, Weinheim, **2005**, p. 122-131.
- [65] K. de Smet, S. Aerts, E. Ceulemans, I. F. J. Vankelecom, P. A. Jacobs, *Chem. Commun.* **2001**, 597-598.
- [66] K. de Smet, A. Pleysier, I. F. J. Vankelecom, P. A. Jacobs, *Chem. Eur. J.* **2003**, *9*, 334-338.
- [67] A. Bos, I.G.M. Pünt, M. Wessling, H. Strathmann, *J. Membrane Sci.* **1999**, *155*, 67-78.
- [68] A. J. Burggraaf, L. Cot, in *Fundamentals of Inorganic Membrane Science and Technology*, (eds.: A. J. Burggraaf, L. Cot), Elsevier Science B. V., Amsterdam, **1996**, p. 1-20.
- [69] A. W. Verkerk, E. L. V. Goetheer, L. J. P. van den Broeke, J. T. F. Keurentjes, *Langmuir* **2002**, *18*, 6807-6812.
- [70] V. E. Patil, J. Meeuwissen, L. J.P. van den Broeke, J. T. F. Keurentjes, *J. Supercrit. Fluids* **2006**, *37*, 367-374.
- [71] B. Richter, B.-J. Deelman, G. van Koten, *J. Mol. Catal. A* **1999**, *145*, 317-321.
- [72] B. Richter, E. de Wolf, G. van Koten, B.-J. Deelman, *J. Org. Chem.* **2000**, *13*, 3885-3893.
- [73] C. D. Frohning, C. W. Kohlpaintner, H.-W. Bohnen, in *Applied Homogeneous Catalysis*, 2nd ed., Vol. 1, (Eds.: B. Cornils, W. A. Herrmann), Wiley-VCH, Weinheim, **2002**, p. 31-103.
- [74] The products of 1-octene hydroformylation are hydrogenated to the corresponding alcohols. These alcohols (nonanol, 2-methyloctanol, 2-ethylheptanol, and 2-propylhexanol) are used as a starting material together with phthalic anhydride or 1,2-cyclohexanedicarboxylic anhydride in an esterification reaction to obtain the corresponding diesters, which are commercially available as plasticizers for PVC. See for example: B. L. Wadley, *J. Vinyl Additive Tech.* **2003**, *4*, 172-176.

Chapter 2

Evaluation of pressure and correlation to reaction rates during homogeneously catalyzed hydroformylation in supercritical carbon dioxide

Abstract

For the hydroformylation of 1-octene in supercritical carbon dioxide the relationship between the change in pressure and the change in reaction mixture composition as a function of time has been investigated. The activity and selectivity has been studied for the catalyst based on tris(3,5-bis(trifluoromethyl)phenyl)phosphine and rhodium(I) dicarbonyl acetylacetonate. The influence of the ligand to rhodium ratio on the hydroformylation has been used to demonstrate how the pressure can be correlated to the conversion and yield. The initial rate of reaction is in good agreement with the initial pressure change in the batch reactor. Up to an aldehyde yield of 80 %, the pressure drop appears to be independent of the reaction rate and selectivity. The highest average reaction rate, $7170 \text{ mol}_{1\text{-octene}} \text{ mol}_{\text{Rh}}^{-1} \text{ h}^{-1}$, has been obtained for a ligand to rhodium ratio of 50 and an initial concentration of 1-octene of 0.5 mol L^{-1} . Both the reaction rate and the selectivity increase when the ligand to rhodium ratio is increased. The Peng-Robinson equation of state has been used to describe the pressure as a function of the concentration of the reactants and products. The calculated pressure corresponds reasonably well with the observed reactor pressure. Following the progress of the reaction by monitoring the pressure is a good alternative to reaction mixture sampling, especially for fast reactions.

Introduction

Hydroformylation of alkenes using homogeneous catalysts has been successfully operated commercially for decades. The catalysts are organometallic complexes of rhodium or cobalt, commonly with phosphines or phosphites as modifying ligands, which are used to convert an alkene, hydrogen, and carbon monoxide into an aldehyde product. Rhodium is generally more active and selective in hydroformylation than cobalt and allows a lower working pressure and temperature.^[1]

The use of supercritical fluids in homogeneously metal catalyzed reactions can offer advantages over commonly applied organic solvents including, a high solubility of reactant gases like hydrogen, carbon monoxide and oxygen, the possibility to create a one phase system resulting in the absence of phase boundaries, and “tunability” of solvent characteristics. Carbon dioxide is most commonly used as a “supercritical solvent” and is regarded as an environmentally benign alternative to organic solvents due to its low toxicity and nonflammability. Furthermore, the use of supercritical fluids provides different possibilities to integrate (or to reduce the number of) reaction and separation steps.^[2,3] However, to follow the progress of reactions in supercritical fluids by sampling requires, in general, careful and time-consuming procedures. Therefore, sampling as a function of reaction time is usually omitted, and the catalyst performance in terms of activity and selectivity is obtained from the product composition after cooling down and depressurizing at the end of the experiment.

For hydroformylations in supercritical carbon dioxide (scCO₂) the pressure will change under isothermal, isochoric conditions as a result of the conversion of the reactants.^[4] Thus, similar to other in situ methods, like UV-vis or infrared spectroscopy^[2], monitoring the pressure can provide on-line information about the reaction. One of the first examples of hydroformylation in performed in carbon dioxide rich supercritical mixtures has been monitored using NMR.^[5] For polymerization reactions performed in the presence of CO₂ the conversion has been determined by measuring the pressure in combination with detailed knowledge of the thermodynamic behavior of the different reactants, products and solvent involved.^[6-8]

Hydroformylation performed in carbon dioxide rich supercritical media has been studied extensively during the past decade^[2d] with the hydroformylation of propene among the earliest examples.^[5a,9] However, in literature little attention has been given to what extent

the development of the pressure during the reaction can give information about the course of the reaction. In this work, the relation between the reaction progress obtained by sampling the reaction mixture and the online measured pressure is investigated for the hydroformylation of 1-octene in $scCO_2$ using an in situ prepared catalyst based on rhodium(I) dicarbonyl acetylacetonate and tris(3,5-bis(trifluoromethyl)phenyl)phosphine. The reaction scheme is depicted in Figure 1.

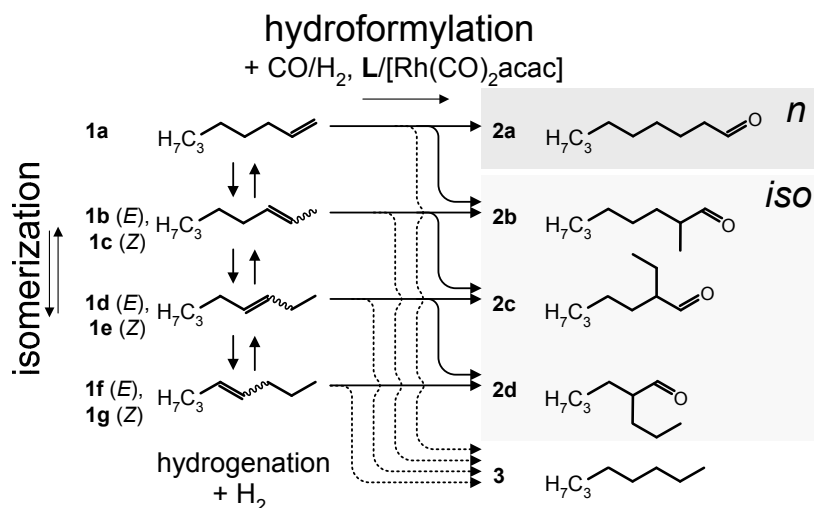


Figure 1. Reaction scheme for the hydroformylation of 1-octene (**1a**), with the two main products *n*-nonanal (**2a**) and 2-methyloctanal (**2b**). The side products are (*E,Z*)-2-octene (**1b**, **1c**), (*E,Z*)-3-octene (**1d**, **1e**), (*E,Z*)-4-octene (**1f**, **1g**), 2-ethylheptanal (**2c**), 2-propylhexanal (**2d**), and *n*-octane (**3**).

The pressure as a function of time will be correlated to the composition of the mixture in two ways. First, the initial reaction rate will be correlated to the (initial) change in pressure by comparing the slope of the yield profile with the slope of the pressure profile. Second, the pressure for a given composition will be calculated using the Peng-Robinson of state (P-R EOS)^[10] and the calculated pressure will be compared to the experimentally determined pressure. Previously the P-R EOS has been used to predict the regioselectivity for the hydroformylation of propene in $scCO_2$.^[11] For the hydroformylation of propene and the allylic epoxidation of trans-2-hexen-1-ol, both with CO_2 as the solvent, the P-R EOS has been used to predict the phase behavior.^[12,13]

Experimental

Materials - Carbon dioxide, carbon monoxide, and hydrogen, grade 5.0, 4.7 and 5.0 respectively, were obtained from Hoekloos (The Netherlands). Prior to use CO_2 was passed

over a Messer Oxisorb filter to remove oxygen and moisture. 1-Octene, **1a**, obtained from Aldrich, was passed over activated alumina, dried with pre-treated molsieves 3A (Aldrich, 4-8 mesh), and stored under argon.

The rhodium precursor, rhodium(I) dicarbonyl acetylacetonate, ($[\text{Rh}(\text{CO})_2\text{acac}]$), was obtained in the form of dark green crystals from Fluka. Tris(3,5-bis-(trifluoromethyl)phenyl)phosphine, Ligand **I**, is a white to light yellow solid and was supplied by Arkema (Vlissingen, The Netherlands). All catalyst precursors were stored under argon and manipulated using Schlenk techniques.

The solvent toluene (Merck, analytical grade), the internal standard *n*-decane (Aldrich, >99% purity) and the substances involved in the reaction, *n*-octane (Aldrich, > 99%), 2-octene (ABCR, mixture of *E* and *Z*, 98%) and nonanal (Fluka, > 95%) used for the GC-analysis were used as received.

High pressure setup - The stainless steel (AISI 316/316L) reactor (custom built Janssen Engineering), depicted in Figure 2, was designed to withstand a maximum working pressure of 60 MPa at a maximum working temperature of 150 °C. Stirring was achieved with a magnetic stirrer head (Premex Minipower) equipped with a Rushton type turbine impeller (Janssen Engineering). Carbon monoxide and hydrogen were dosed through two mass flow controllers (Bronkhorst EL-Flow) independently or together up to a pressure of 9 MPa. CO₂ was fed to the reactor by a syringe pump (Thar Technologies SP300-2, **FP1**); the substrate 1-octene was added with a manual operated syringe pump (Sitec, **FP2**). The pressures of the reactor and the manual syringe pump for reactant feed were monitored with calibrated pressure transducers (Kulite HKM-375, accuracy ± 0.07 MPa). The total reactor volume was composed of the reactor volume (102.7 mL), the tubing connecting the sample volume and the sample pump (1.2 mL), and the variable volume of the sample pump (1.6-5.6 mL, Sitec, **SP**).

The risks involving the use of flammable hydrogen, toxic and flammable carbon monoxide and flammable organic liquids in combination with high pressure were extensively assessed and the appropriate safety measures were taken.

Hydroformylation in scCO₂ - The general procedure for a hydroformylation experiment was started by charging the desired amounts of $[\text{Rh}(\text{CO})_2\text{acac}]$ and the phosphine ligand into the empty reactor and closing the reactor. The reactor volume was then carefully flushed with

argon and subsequently evacuated for three times. Next, the stirring was turned on with a revolution speed of 700 rpm and the desired amount of carbon monoxide and hydrogen gas was fed to the reactor at room temperature. The reactor content was then heated electrically to a temperature of 50 °C and consecutively CO₂ was charged into the reactor at a constant flow up to a pressure of about 26 MPa. These conditions were maintained for at least half an hour before heating further to the desired reaction temperature. In total a period of about 1 h was considered sufficient to allow the active catalyst complexes to be formed in situ from [Rh(CO)₂acac] and **I**. The reaction was started by the addition of the alkene, which was done by opening the valve between the pump and the reactor. A fast pressure equalisation occurred and consecutively the desired volume of **1a** was pumped into the reactor, which as a rule did not take more than 30 s. During reaction the temperature was maintained at 70 ± 0.5 °C.

Three different L:Rh ratios were applied: 4:1, 10:1 and 50:1. These experiments were done in duplicate. One experiment was carried out in which no phosphine ligand was applied. In one of the experiments using L:Rh = 4:1 only one sample was taken after three hours of reaction.

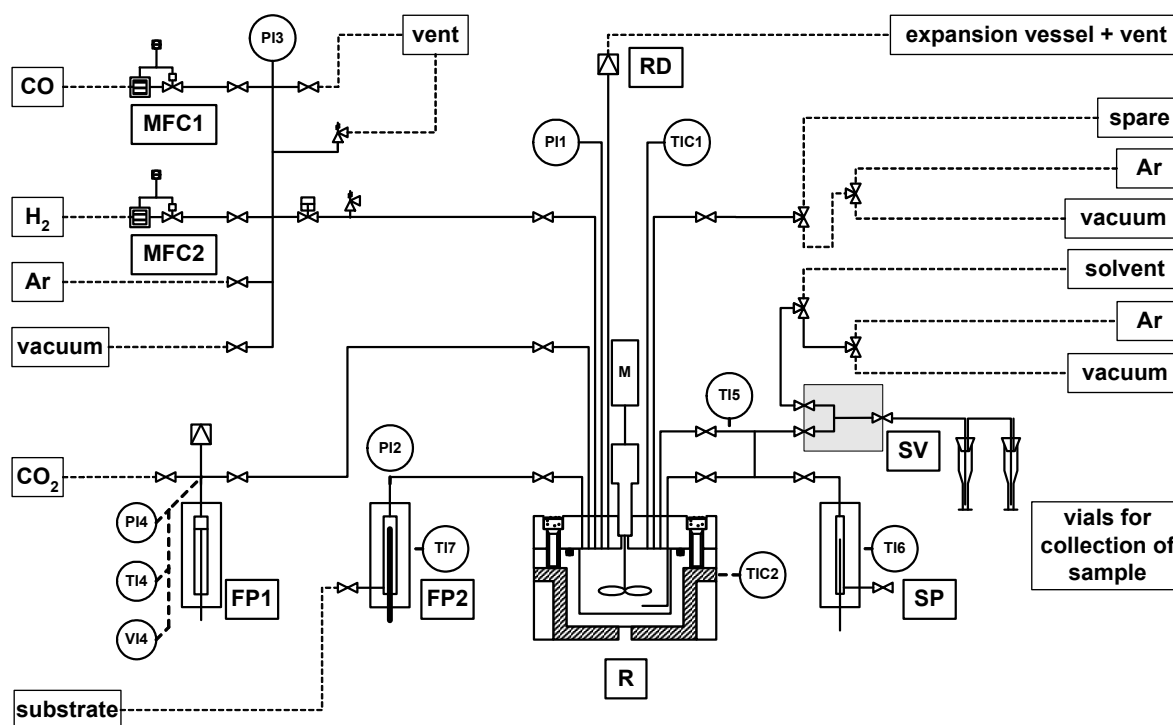


Figure 2. Batch reactor for hydroformylation. **R** reactor, **MFC1** mass flow controller for carbon monoxide, **MFC2** mass flow controller for hydrogen, **FP1** pump for liquid carbon dioxide, **FP2** pump for liquid reactant, **SP** sampling pump, **RD** rupture disc assembly, **SV** sample volume, **TI** temperature indicator, **TIC** temperature indicator controller, **VI** volume indicator, **PI** pressure indicator.

Sampling during batch reaction in supercritical carbon dioxide - First the contents of the tubing connecting the sample volume (SV) and reactor (R) was rinsed with a small volume high-pressure syringe pump (SP). Then the sample volume (0.182 mL), which did not have additional heating, was filled. The content of the sample volume was then carefully bubbled through a vial with a solution of *n*-decane in toluene and afterwards rinsed with additional toluene solution to collect **1a** and its reaction products quantitatively. Subsequently, the sample volume was dried by alternately applying an argon flow and vacuum. The minimum time of taking a sample and preparing for a next one was in the order of 10 min. A reaction time of three hours was considered, then the mixture was rapidly cooled to a temperature of about 25 °C, the gases and liquid carbon dioxide were vented and the remaining liquids consisting of reaction products and catalyst were collected. Sampling was done from either the top or bottom of the reactor and this was also used to verify that the reaction mixture was a homogeneous supercritical phase.

Analysis and calibration - The samples were analyzed off-line using a Fisons Instruments gas chromatograph with a flame ionization detector (GC-FID) equipped with a Restek Rtx-5 column (fused silica, length 30 m, internal diameter 0.53 mm) with helium as the carrier gas. Calibration was done for **1a**, **1b**, **1c**, **3** and **2a**, the sensitivity coefficients for the other octene and aldehyde isomers were taken to be equal to those of **1a** and **2a**, respectively.

The density of **1a** as a function of pressure was determined using the substrate pump **FP2** of which the total volume (the sum of the “dead” and “swept” volume) was known to be 36.2 mL. Each turn of the spindle corresponded to 0.6 mL volume change. When the pump was completely filled with **1a** the pressure of this system was determined as a function of the volume at room temperature. The density of **1a** showed a linear dependency on pressure within the range of pressures applied. The slope of this line was $7.51 \times 10^{-4} \pm 0.52 \times 10^{-4} \text{ g mL}^{-1} \text{ MPa}^{-1}$ ($\pm 7.2\%$) with 95% confidence. The value of this slope was used to determine the mass of **1a** injected into the reactor.

Estimation of the binary interaction parameter for a CO₂ - nonanal mixture - First, the density of **2a** as a function of pressure was determined using the substrate pump **FP2** in a similar manner as for **1a**. The density of **2a** also showed a linear dependency within the pressure. The slope of the line was $6.74 \times 10^{-4} \pm 0.33 \times 10^{-4} \text{ g mL}^{-1} \text{ MPa}^{-1}$ ($\pm 4.8\%$) with 95 % confidence. Subsequently, at a fixed concentration of carbon dioxide (14.7 mol L⁻¹) the pressure in the

reactor was determined as a function of the amount of added **2a**, up to a concentration of 0.549 mol L⁻¹. The observed pressure was compared to the pressure calculated with the P-R EOS.^[10] It was observed that the P-R EOS predicted a higher pressure than was measured. At a CO₂ concentration of 14.7 mol L⁻¹ a pressure of 21.2 MPa was calculated while a pressure of 19.7 MPa was measured. This comparison resulted in a value of 0.07 for the binary interaction parameter. For the different concentrations of **2a** (0.223, 0.387, 0.549 mol L⁻¹), the predicted total pressures had on average a deviation of about 1.5 MPa from the experimentally determined pressure.

Reaction parameters - To obtain normalized concentration profiles for **1a** and its reaction products, each concentration obtained by GC analysis was divided by the sum of all obtained concentrations:

$$[i]_n = \frac{[i]}{\sum [i]} \quad (1)$$

where $i = \mathbf{1a-1g}$, $\mathbf{2a-2d}$ and $\mathbf{3}$, and the subscript n refers to the normalized values.

The activity and selectivity of the different catalytic complexes was expressed in one of the following parameters. The definitions used were based on Westerterp et al.^[14] The conversion, X , was given by:

$$X = \frac{[\mathbf{1a}]_{n,0} - [\mathbf{1a}]_n}{[\mathbf{1a}]_{n,0}} \times 100\% \quad \text{with } [\mathbf{1a}]_{n,0} = 1 \quad (2)$$

The overall selectivity, S_j , towards a product j was defined as:

$$S_j = \frac{[j]_n}{[\mathbf{1a}]_{n,0} - [\mathbf{1a}]_n} \times 100\% \quad (3)$$

where $j = \mathbf{1b-1g}$, $\mathbf{2a-2d}$ and $\mathbf{3}$.

The overall yield, Y_k , for a product k was then:

$$Y_k = \frac{[k]_n}{[\mathbf{1a}]_{n,0}} \times 100\% \quad (4)$$

Y_{ald} indicated the aldehyde yield. The substrate to catalyst ratio, S/C , was calculated as follows:

$$\frac{S}{C} = \frac{m_{1a} \cdot MW_{Rh}}{m_{Rh} \cdot MW_{1a}} \quad (5)$$

with m_{1a} the mass of **1a** injected, MW_{1a} the molar mass of **1a**, and m_{Rh} and MW_{Rh} the mass conveyed to the reactor and the molar mass of the rhodium precursor, respectively.

The turn-over-number based on the conversion of **1a**, TON_{1a} , was calculated as follows:

$$TON_{1a} = \frac{S}{C} \cdot X \quad (6)$$

The “initial” turn-over-frequency based on the conversion of **1a**, TOF_{1a} , was calculated by multiplying S/C with the slope of a line fitted through the conversion data points up to a conversion where there was a linear trend (typically up to a conversion of 0.6). In a similar manner an initial turn-over-frequency was defined for the formation of aldehydes, TOF_{ald} .

The *n:iso* ratio was obtained by dividing the concentration of linear aldehyde product by the sum of the concentrations of the branched aldehyde products:

$$n : iso = \frac{[2a]_n}{[2b]_n + [2c]_n + [2d]_n} \quad (7)$$

The term *n:iso* ratio is used throughout this thesis. In literature often also the symbols l:b, l/b, n/i, or n/b are used to indicate the ratio of linear (normal) aldehyde over branched (isomeric aldehydes).

To establish a relation between the initial pressure drop and the initial reaction rate the following parameters are defined. The first parameter, $\Delta p/\Delta X$, is based on the conversion and is calculated as follows:

$$\frac{\Delta p}{\Delta X} = \frac{\Delta p}{\Delta t} \cdot \frac{\Delta t}{\Delta X} = \frac{\Delta p}{\Delta t} \cdot \frac{S}{C} \cdot \frac{1}{TOF_{1a}} \quad (8)$$

The parameter based on the yield of aldehydes is indicated by $\Delta p/\Delta Y_{ald}$ and is calculated as follows:

$$\frac{\Delta p}{\Delta Y} = \frac{\Delta p}{\Delta t} \cdot \frac{\Delta t}{\Delta Y_{ald}} = \frac{\Delta p}{\Delta t} \cdot \frac{S}{C} \cdot \frac{1}{TOF_{ald}} \quad (9)$$

The Peng-Robinson equation of state is defined as follows:

$$p = \frac{RT}{V - b} - \frac{a(T)}{V(V + b) + b(V - b)} \quad (10)$$

with p the pressure, R the gas constant, and V the molar volume. The parameters a and b are determined using the mixing rules:

$$a = \sum_i \sum_j a_{ij} x_i x_j, \text{ with } a_{ij} = (1 - k_{ij}) \sqrt{a_i a_j} \quad (11)$$

$$b = \sum_i b_i x_i \quad (12)$$

where a_i and b_i are pure component properties and k_{ij} is the binary interaction parameter.

Matlab (version 6.1, release 12.1) was used for all the data manipulation, the calculations of reaction parameters, and the calculations with the P-R EOS. No specific Matlab modules were used, the use of Matlab allowed for a convenient manipulation of the large pressure data sets.

Results and discussion

To gain insight in the relation between the pressure and the reaction progress obtained by sampling the hydroformylation of **1a** was performed for a constant initial reactant and solvent concentration using the ligand tris(3,5-bis(trifluoromethyl)phenyl)phosphine (**I**) and rhodium(I) dicarbonyl acetylacetonate as the catalyst precursors. The ligand to rhodium ratio (L:Rh) was varied and its influence on the rate and selectivity of the reaction investigated. Reaction conditions and the main results are given in Table 1.

We will first discuss the pressure and composition profiles of the hydroformylation reaction. We will then switch to the experiments where different L:Rh ratios were used to demonstrate how the change in pressure could be used to evaluate the reaction progress.

Table 1. Overview of experimental conditions and aldehyde selectivity.

Exp. entry ^[a]	n_{1a} [mmol]	S/C	L:Rh	$[\text{CO}_2]$ ^[b] [mol L ⁻¹]	S_{ald} ^[c,d,e] [%]	S_{2a} ^[c] [%]	$n:iso$ ^[c]
1	54.3	2020	0	14.8	96.5	54.8	1.31
2	55.2	2020 (1.7 %)	4.03 (2.2 %)	15.1	98.5	66.5 (1.2 %)	2.07 (3.3 %)
3	55.0	2100	4.15	14.7	98.5	67.2	2.14
4	55.3	2030 (1.2 %)	10.0 (1.3 %)	14.9 (1.3 %)	98.8	70.8	2.53
5	54.2	1990 (1.4 %)	49.9	14.7	98.8	75.5	3.25

^[a] Reaction conditions $[\text{CO}]_0 = [\text{H}_2]_0 = 1.0 \text{ mol L}^{-1}$, $T = 70 \text{ }^\circ\text{C}$. The values shown for experiment entries 2, 4 and 5 the are the averages of two experiments. The values in between brackets indicate the deviation from the average. Deviations smaller than 1 % are not indicated.

^[b] Calculated from the pressure, temperature, volume in the liquid CO_2 pump (**FP1**). The density of liquid was calculated using the Benedict-Webb-Rubin equation of state.

^[c] After approximately 3 hours of reaction.

^[d] The conversion (X) rounded to the nearest decimal was 99.4 % after 3 hours of reaction in all cases.

^[e] For entry 1 the overall selectivity for **3** (S_3) was 1.4 %, for the remaining entries S_3 was smaller than 1 %.

Hydroformylation in scCO₂ - For a representative experiment, the pressure and temperature in the reactor and the pressure of the substrate injection pump, **FP2** in Figure 2, during charging of the reactor and the reaction are plotted as a function of time in Figure 3. Based on literature the concentrations of reactants and CO₂ are chosen such that a one-phase system should be present at least at the start of the reaction.^[15] The total concentrations based on analysis of the samples (taken from either the top or the bottom of the reactor) are within 20 % deviation of the initial concentration of **1a** applied. This suggests that the reaction mixture is a one-phase system throughout the course of the reaction considering that the sampling volume is not heated, which could account for the deviation. However, the existence of a two-phase system (which then should be a “highly expanded” liquid/supercritical reaction mixture and a CO₂/CO/H₂ rich phase) can not be ruled out, because of the absence of windows in the reactor for a visual confirmation.

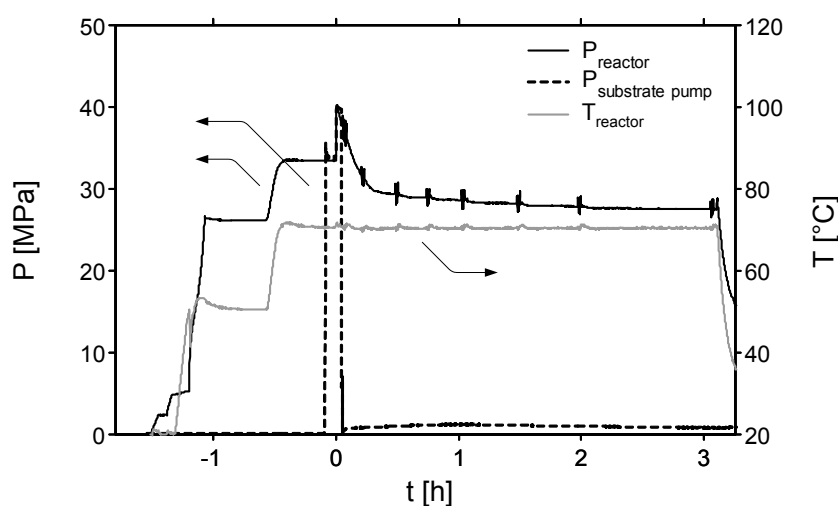


Figure 3. Overview of pressure and temperature as a function of time for an experiment entry 5 (with $[\mathbf{1a}]_0 = 0.5 \text{ mol L}^{-1}$, $[\text{CO}]_0 = [\text{H}_2]_0 = 1 \text{ mol L}^{-1}$, $[\text{CO}_2] = 14.8 \text{ mol L}^{-1}$, $[\text{Rh}] = 2.52 \times 10^{-4} \text{ mol L}^{-1}$, and $[\mathbf{I}] = 1.25 \times 10^{-2} \text{ mol L}^{-1}$).

Before the addition to the reactor, **1a** in the feed pump (**FP2**) is compressed to a pressure just above the pressure present in the reactor. This is represented by the dashed line in Figure 3. When the valve between **FP2** and the reactor is opened to add **1a**, a pressure equalisation takes place. This is marked as $t = 0 \text{ h}$. The total procedure to perform the experiment takes about 5 hours, where the preparation takes about 2 hours. The main advantages of the setup used here are the facile procedure to charge the reactor with catalyst, reactant, and solvent, the well-defined moment of the start of the reaction, and the well-

defined moment of taking a sample. As a result of the charging procedure the preformed catalyst species are in equilibrium with the phosphine ligand, carbon monoxide and hydrogen before the reaction with alkene takes place. Upon injection of **1a** the reaction starts immediately.

It can be seen in Figure 3 that the addition of **1a** ($t = 0$ h) has only a small effect on the temperature but results in a steep pressure increase from about 33 to 40 MPa. The reaction temperature reaches a maximum of only 71.6 °C just after the addition of **1a**, which is caused by the fast pressure increase and the start of the reaction (Entry 5 in Table 1 and Figure 3). The pressure decreases relatively fast during the first hour of reaction and then levels off. The total pressure drop, after three hours of reaction, including sampling is approximately 12 MPa. The time of the start of the reaction is especially relevant to know in the case of fast reactions. For one of the runs, entry 5, the first sample has been taken after 5.5 min and already a conversion of 36.3% has been determined. This corresponds to a TOF_{1a} of about $7800 \text{ mol}_{1a} \text{ mol}_{Rh}^{-1} \text{ h}^{-1}$. This means that an inaccuracy of about 1 min in charging of the reactor and therefore in the starting time of the reaction results in a variation of the TOF of about 20 %.

The influence of sampling - In Figure 4 a comparison is made of the pressure profile for an experiment with and without sampling, entries 2 and 3 in Table 1, respectively. The experimental conditions applied are similar for the two experiments. Initially, the pressure profiles were parallel, which indicates a similar reaction rate. The total pressure drop for the experiment with sampling is 12.8 MPa; for the experiment without sampling the pressure drop is 11.6 MPa (including the sample at $t = 3$ h). This means that sampling contributes for about 10 % to the pressure drop. The outcome after 3 h of reaction was the same in terms of conversion, selectivity and *n:iso* ratio, illustrating the good reproducibility of the experiments, see Table 1. In the following, we have neglected pressure drop as a result of sampling when we determine the slope of pressure-time curves, because the reaction itself has a considerably larger contribution to pressure drop than sampling in the first hour of reaction.

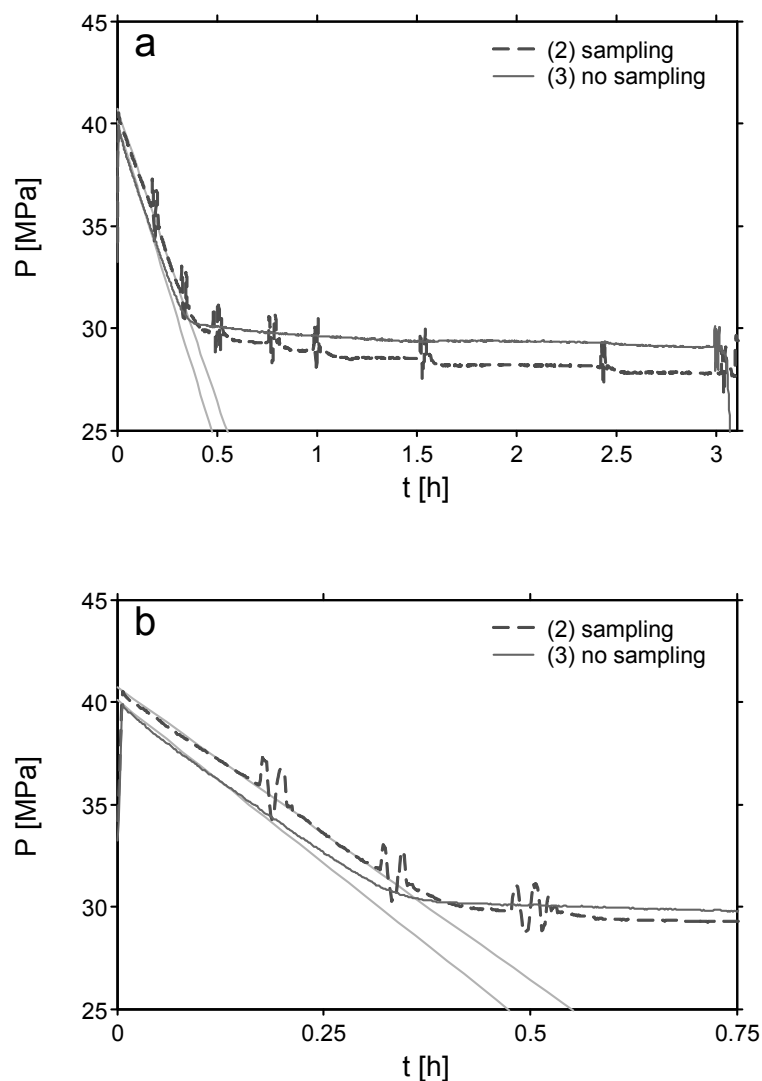


Figure 4. Pressure profiles for the situation with (entry 2) and without sampling (entry 3). See Table 1 for the conditions. a) Pressure as function of time for the whole reaction; b) Close up of the initial stage of the pressure as a function of time with $t = 0 - 0.75$ h. The grey lines are tangent lines corresponding to the slopes of the curves in the initial stage of the reaction.

Effect of ligand to rhodium ratio ($L:Rh$) - In Figure 5 the progress of the yield of aldehydes in time, as measured by GC, is depicted for experiments with four different amounts of ligand **I**. “No ligand” in Figure 5 applies to the case in which no ligand was used. In general, the selectivity for the linear aldehyde product increases with an increase in concentration of monodentate triphenylphosphine, up to a certain value and then remains constant.^[16-18] Furthermore, for the triphenylphosphine-Rh catalyst usually a decrease in activity is observed when the $L:Rh$ ratio is increased. In this case, increasing the ligand to rhodium ratio results in a clear increase of the initial aldehyde formation rate and an increase in regioselectivity in

terms of *n:iso* ratio. This demonstrates clearly the advantage of using phosphine-modified catalysts. Increasing the L:Rh ratio from 10:1 to 50:1 gives an increase in aldehyde production rate that is less pronounced. The profiles for L:Rh = 10:1 and L:Rh = 50:1 almost coincide with each other. The change in pressure as a function of time for the four different L:Rh ratios is shown in Figure 6.

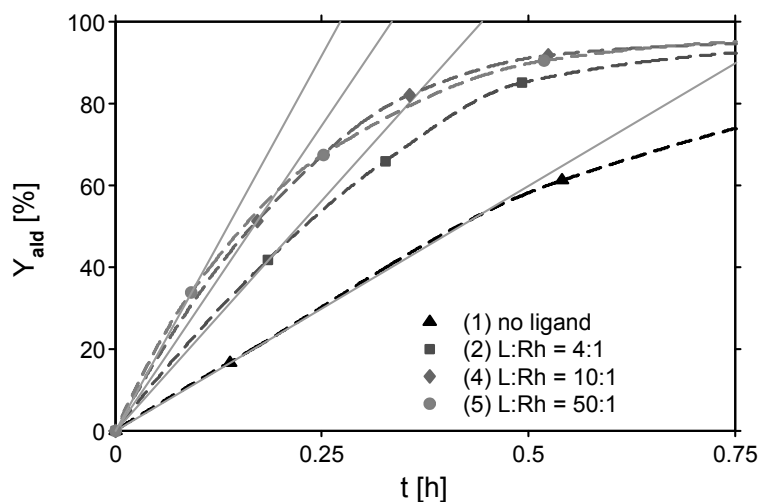


Figure 5. Yield of aldehydes, Y_{ald} , as a function of time for different L:Rh ratios (L:Rh = 0:1 (“no ligand”), 4:1, 10:1 and 50:1). See table 1 for the conditions. The grey lines are tangent lines corresponding to the slopes of the curves in the initial stage of the reaction. For clarity duplicate experiments are not indicated.

The overall selectivity for the aldehydes differs only slightly when the overall outcome of the reaction after 3 h is considered. These results are summarized in Table 1. For entries 1, 2, 4, and 5 the yield of aldehydes is similar after 3 h of reaction. The similar aldehyde yield is also reflected in the comparable pressure drop for each of the four experiments, which can be seen in Figure 6a. A confirmation that the reaction for a L:Rh = 50:1 is indeed faster than for a L:Rh = 10:1 can be observed in Figure 6b. In the initial stage of the reaction the pressure decreases faster in the case where L:Rh = 50:1 than for the case where L:Rh = 10:1.

As given in Table 1, for the hydroformylation of **1a** with I-Rh, an increase in the ligand to rhodium ratio from 0 to 50 resulted in an increase of the averaged value for the overall selectivity for **2a**, the *n:iso* ratio, and the initial reaction rate (TOF_{1a}) from 55.2 to 75.7%, 1.31 to 3.25, and 2830 to 7170 $\text{mol}_{1a} \text{mol}_{Rh}^{-1} \text{h}^{-1}$, respectively.

The dependence of the reaction rate on the L:Rh ratio observed for the **I**-Rh catalyst is remarkably different from the results reported in literature on the hydroformylation of linear alkenes with the well-known triphenylphosphine-Rh catalyst system.^[16,18,19]

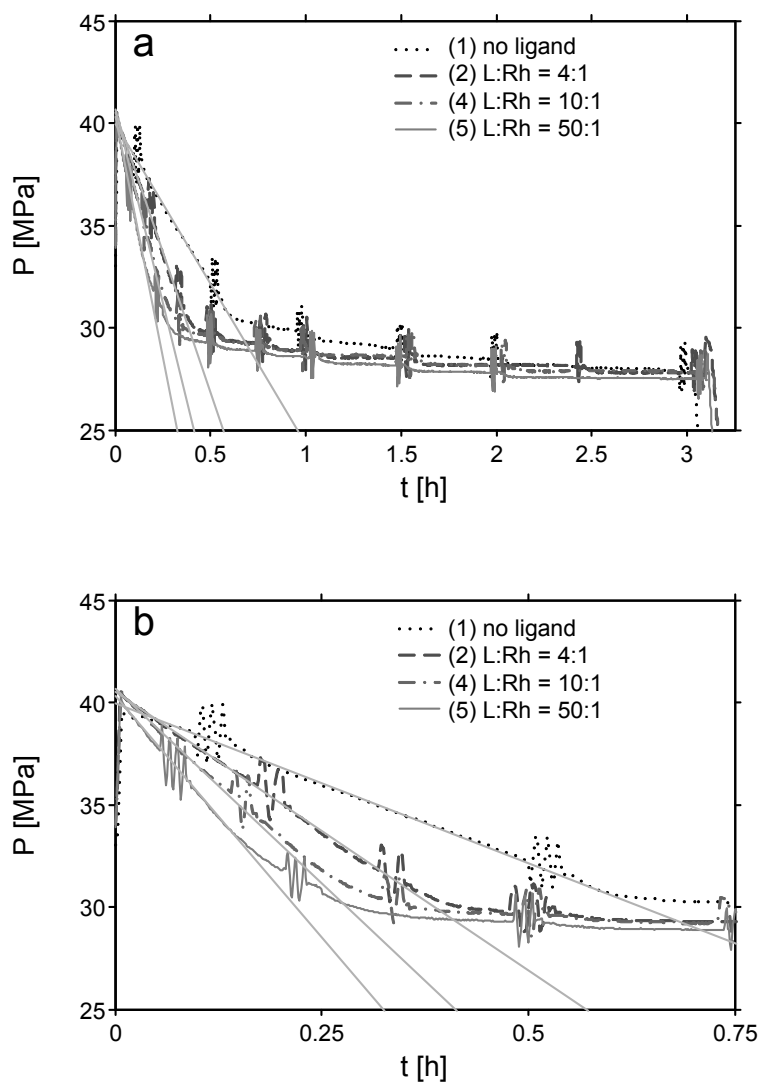


Figure 6. Pressure profiles as a function of the time for different L:Rh ratios (L:Rh = 0:1 (“no ligand”), 4:1, 10:1 and 50:1). See Table 1 for the conditions. a) Pressure as a function of time for the whole period of reaction; b) Close up of the initial stage for the pressure as function of time with $t = 0 - 0.75$ h. The grey lines are tangent lines corresponding to the slopes of the curves in the initial stage of the reaction. For clarity duplicate experiments are not indicated.

In our studies a significant increase in reaction rate is observed when the L:Rh is increased from 4:1 to 50:1. Davis and Erkey observed a slight decrease in reaction rate for the hydroformylation of **1a** in $scCO_2$ using the **I**-Rh catalyst at 50 °C when they increased the ratio L:Rh.^[19] The final *n:iso* ratios are somewhat lower than those obtained by Erkey and co-

workers^[19], which can be attributed to the higher reaction temperature applied.^[1] In our work, the increase in reaction rate is combined with an enhancement of selectivity. A possible explanation for this phenomenon can be given when a part of the involved equilibria of the different complexes, **C1** to **C4**, are considered as depicted in Figure 7. It has been observed by Haji and Erkey that in the presence of an equimolar mixture of syngas (CO/H₂) **C1** dissociates to yield mainly **C2**, **C3**, and the dimer [RhCOL₂]₂.^[20] They did not observe **C1** under those conditions. Also at 70 °C it can be assumed that some **C4** will be formed, certainly, because we applied a higher concentration of CO than Haji and Erkey used in their work.^[20] The intermediates **C2** and **C4** can be considered to be the starting species in the so-called dissociative catalytic hydroformylation cycle.^[21] The use of **I** leads to a considerably faster hydroformylation than the use of the rhodium precursor alone. The increase in regioselectivity and reaction rate could then be explained by a shift from a relatively lower concentration of intermediate **C2** (and relatively larger concentration of **C4**) at the lower **I** concentration to a relatively higher concentration of **C2** at a higher **I** concentration, while the concentration of **C1** (inactive in hydroformylation) remains negligible. In the case of triphenylphosphine (PPh₃) a higher concentration of intermediate **C2** than intermediate **C4** induces a higher selectivity.^[21] For [HRh(CO)_n(PPh₃)_{4-n}] (n= 1,2) type of catalysts it is known that an excess of triphenylphosphine leads to the formation of [HRhCO(PPh₃)₃], which is not active in hydroformylation. For **I** it is plausible that a higher concentration of **C2** also can give rise to a higher reaction rate.

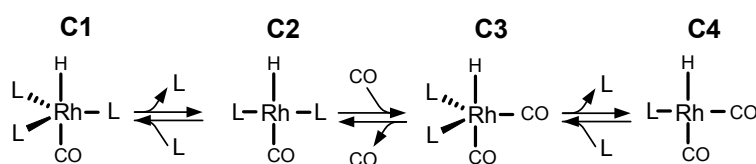


Figure 7. A part of the equilibria of the organometallic species present in solution. L is the **I** ligand coordinated with the phosphorous to rhodium metal centre.

In Figure 8 the normalized concentrations as a function of time are given. As can be seen, the use of [Rh(CO)₂acac] with ligand **I** facilitates an effective and fast hydroformylation. In the first hour of reaction a small amount of **1a** isomers are formed and these isomers are also hydroformylated. At higher conversion the concentration of **2a** does not increase anymore but the concentrations of **2b**, **2c**, and **2d** increase as the total concentration of **1a** isomers decrease. It should be noted that the symbols at time zero do not represent an

actual measurement, but are based on the initial amount of reactants present in the reactor assuming zero conversion.

Erkey and co-workers^[19] and Arai and co-workers^[22] have reported on hydroformylation reactions carried out using the catalyst based on $[\text{Rh}(\text{CO})_2\text{acac}]$ with ligand **I**. For CO_2 rich “supercritical” systems it is evident that with this catalyst higher hydroformylation rates have been observed compared to the reaction rates observed for other rhodium catalysts with phosphines as ligands.^[23-32]

With regard to the high activity of the catalyst used in this work, employing ligand **I**, at 70 °C it can also be stated that experimental method presented in this work, i.e. our the method of initiating the reaction, provides convenient means to obtain accurate kinetic reaction data. The high activity of the catalyst is mainly due the electron withdrawing effect of the trifluoromethyl groups.^[25,27,33,34] When hexane is used as the reaction medium the catalyst also induces a high hydroformylation rate and a selectivity similar to that observed for the reaction in CO_2 .^[35]

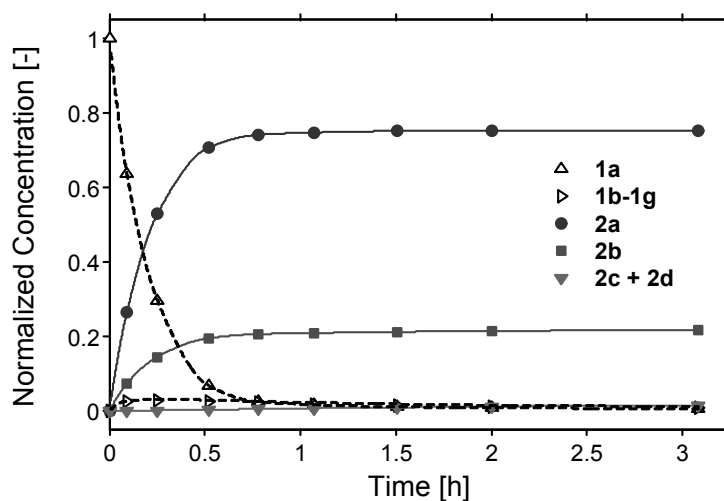


Figure 8. Normalized concentration profile at the reaction conditions given in Table 1, entry 5. The normalized concentration of **3** after 3 h reaction was less than 0.01.

Pressure data to determine the reaction rate - If the evolution of the pressure (Figure 3) is compared with the progress of the reaction (Figure 8) it can be seen that the two profiles show the same behavior. To evaluate this in more detail, the change in pressure has been compared with the initial reaction rate by dividing the pressure drop rate ($\Delta p/\Delta t$) by the reaction rates

based on the conversion of **1a** ($\Delta X/\Delta t$) and by the formation of aldehydes ($\Delta Y_{\text{ald}}/\Delta t$). The results for these two quantities $\Delta p/\Delta X$ and $\Delta p/\Delta Y_{\text{ald}}$ are given in Table 2.

Table 2. Initial rates of reaction and pressure change. The corresponding experimental conditions for entries 1-5 are stated in Table 1.

entry ^[a]	$\Delta p/\Delta t$ ^[b] [MPa h ⁻¹]	Intercept y-axis ^[b,c] [MPa]	P_{max} [MPa]	$P_{3\text{h}}$ [MPa]	TOF _{1a} ^[d] [e]	TOF _{ald} ^[d] [f]	$\Delta p/\Delta X$ ^[g] [MPa]	$\Delta p/\Delta Y_{\text{ald}}$ ^[h] [MPa]
1	-15.6	39.9	39.6	28.1	2.83	2.42	-11.2	-13.1
2	-29.8 (9%)	40.7	40.6	28.0	4.87 (4%)	4.47 (4%)	-12.4 (7%)	-13.5 (7%)
3	-30.1	39.9	39.9	28.3				
4	-32.3 (17%)	40.5	40.4	27.8	5.65 (6%)	5.29 (7%)	-11.6 (3%)	-12.3 (3%)
5	-47.2	40.0	39.9	27.6	7.17 (8%)	6.63 (9%)	-13.2 (10%)	-14.3 (10%)

[a] The values shown for experiment 2, 4 and 5 are the averages of two experiments. The values in between brackets indicate the deviation from the average. Deviations smaller than 1 % are not indicated.

[b] The initial slope is determined by fitting a linear equation through the pressure versus time starting at t_{max} till $t = 0.3$ h for the slower reactions (entry 1) and till $t = 0.15$ h for the faster reaction (entries 2, 4 and 5). The pressure data where the pressure fluctuates as a result of sampling took place have been excluded.

[c] The average value of the intercept is 40.3 MPa.

[d] For entry 1 data points up to a conversion of 40 % have been taken into account. For entries 2, 4 and 5 data points up to a conversion of 60 % have been used.

[e] [$10^3 \text{ mol}_{1a} \text{ mol}_{\text{Rh}}^{-1} \text{ h}^{-1}$]

[f] [$10^3 \text{ mol}_{\text{ald}} \text{ mol}_{\text{Rh}}^{-1} \text{ h}^{-1}$]

[g] The average value of $\Delta p/\Delta X$ is -12.1 MPa, see equation (8).

[h] The average value of $\Delta p/\Delta Y_{\text{ald}}$ is -13.3 MPa, see equation (9).

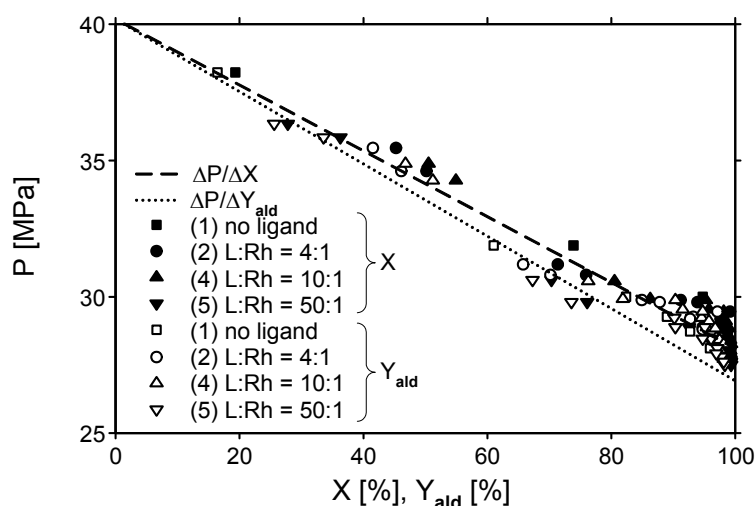


Figure 9. Pressure as a function of the conversion, X , and yield of aldehydes, Y_{ald} , for entries 1, 2 and 4, 5.

In Table 2 also the maximum pressure, P_{\max} (pressure after addition of **1a**), the pressure after three hours of reaction, P_{3h} , and the initial pressure drop for the various experiments are given. For experiments 1 to 5, excluding experiment 3 where the yield has only been determined at the end of the experiment, the ratio $\Delta p/\Delta Y_{\text{ald}}$ is fairly constant. The $\Delta p/\Delta X$ values are lower than $\Delta p/\Delta Y_{\text{ald}}$ values. This can be explained by the fact that **1a** is also converted into a certain amount of octene isomers. It can be expected that the formation of octene isomers, in which no carbon monoxide or hydrogen is consumed, has a negligible effect on the pressure. By applying **I** the formation of octene isomers is suppressed as compared to the case where only $[\text{Rh}(\text{CO})_2\text{acac}]$ is used as the catalyst precursor.

The pressure as a function of conversion and the pressure as a function of yield are visualized in Figure 9. The results for the pressure versus conversion or aldehyde yield show a more or less linear behavior up to a conversion of 80 %. Two lines, one with the average of the values of $\Delta p/\Delta X$ as the slope and the other with the average of the values of $\Delta p/\Delta Y_{\text{ald}}$ as the slope, both starting in 40.2 MPa at $X = Y_{\text{ald}} = 0$, are also plotted. The lines give a good description of the pressure as the function of conversion and yield up to 80% for all the experiments. So, for the same initial conditions the pressure is mainly determined by the aldehyde yield, and seems independent of the catalyst activity or chemoselectivity (without considering hydrogenation). This can be explained by assuming that the **1a** isomers have a similar contribution to the total pressure as **1a**. The same seems to apply for the isomers of **2a**. The pressure at the end of the reaction is quite similar for all cases, see Table 2, P_{3h} ranges from 27.6 to 28.3 MPa. On the other hand there is a difference in regioselectivity, see Table 1, $n:\text{iso}$ ranges from 1.31 to 3.25. This implies that the interaction of the **1a** isomers with one of the other components in the reaction mixture can be described by the same set of binary interaction parameters. The same holds for **2a** and its isomers.

In the cases presented here hydrogenation, the conversion of hydrogen and **1a** to **3**, is negligible (see Table 1). As a result hydrogenation will have a negligible influence on (the change of) the total pressure during reaction. To our knowledge limited thermodynamic literature data exist on binary systems like carbon dioxide - **1a** (or one of the other **1a** isomers) or carbon dioxide - nonanal (or other **2a** isomers). Jiang et al. performed a study on the phase behavior of mixtures present during the hydroformylation of 1-hexene in carbon dioxide.^[36] However, they did not take into account the formation of 1-hexene isomers, hexane, or heptanal isomers. Ke et al. performed a study of the phase behavior of during the

hydroformylation of propene in carbon dioxide.^[12] In that case isomerization of the alkene did not play a role. They used the P-R EOS to predict the critical points of the reaction mixtures. For the two aldehyde products (butanal and methylpropanal) they only took into account the binary interaction parameters with carbon dioxide and not the binary interaction parameters resulting from the binary systems with the reactants.

It can be concluded that the change in pressure is a good measure for the rate of aldehyde formation, and that in this case both $\Delta p/\Delta Y_{ald}$ and $\Delta p/\Delta X$ appear to be independent of catalytic activity and selectivity. It is noted that this approach is only applicable to assess the activity of catalysts, which have a high chemoselectivity at fixed initial concentrations of reactants and solvent.

Modeling the pressure data - In order to evaluate the catalyst activity and chemoselectivity in more detail also the measured reactor pressure is compared to the pressure calculated by using the measured composition of the mixture in the standard P-R EOS.^[10] By this means the contribution of the solvent (CO₂), the various reactants (**1a**, H₂ and CO), intermediate products (**1a** isomers) and final products (aldehydes and **3**) to the reactor pressure is taken into account. It must be noted that during our hydroformylation experiments only small amounts of **3** were formed, see Table 1. However, for the sake of completeness we have considered **3** in our calculations also because information on the interaction of CO₂ and **3** is available [37]. The concentration of catalyst is low (Rh concentration of 0.25×10^{-4} mol L⁻¹ with a maximum ligand concentration of 1.25×10^{-2} mol L⁻¹) as compared the concentration of the reactants, so the influence of the catalyst and excess ligand is not taken into account.

Several assumptions have been made to reduce the number of binary parameters required to calculate the pressure. The reaction mixture is considered as a one-phase high-pressure gas/supercritical system. The classical mixing rules have been used to calculate the parameters a_{ij} and b_{ij} , based on the binary interaction parameter, k_{ij} . The **1a** isomers are represented by **1a** and the aldehyde isomers are represented by **2a**. This reduces the number of mixture components to 6, which requires a total of 15 binary interaction parameters. Subsequently, the pressure of the reaction mixture is calculated using 6 binary interaction parameters. Only the interaction between the reactants and products and CO₂ and the interaction between CO and H₂ are taken into account, all the other interactions involving the reactants and products are neglected. The binary parameter of the CO₂ - aldehydes system is

estimated from measurements of the pressure of CO₂ - **2a** mixtures as described in the experimental section. The binary parameter of CO₂ - **1a** isomers is chosen such that it gives the best representation of the initial pressure of the experiments. This value, however, is rather high implicating a non-ideal system. The values used for the binary k_{ij} parameters are given in Table 3.

Table 3. Binary interaction parameters used to predict the pressure using the P-R EOS.

	CO	H ₂	CO ₂	1a-1g	3	2a-2d
CO	0					
H ₂	0.0919 ^[a]	0				
CO ₂	-0.155 ^[b]	-0.1622 ^[a]	0			
1a-1g	0	0	0.2	0		
3	0	0	0.1241 ^[c]	0	0	
2a-2d	0	0	0.07	0	0	0

^[a] These values are taken from the Aspen Plus database (version 2004.1).

^[b] Value from literature [12].

^[c] Value from literature [37].

In Figure 10 the pressure during reaction is plotted versus time for experiments entry 1 and entry 5. Also, the pressure calculated using the P-R EOS is shown. The calculated pressures show good agreement with the experimental values, considering that a minimum number of binary parameters have been taken into account. Good agreement has been obtained for the situation where the chemoselectivity is relatively low, entry 1, as well as for the situation where the chemoselectivity is relatively high, entry 5.

In Figure 11 the calculated pressures are compared to the experimental pressure in a parity plot using all the pressure data from the seven different experiments (entry 1 and 2 runs for entries 2, 4, and 5 in Table 2). It can be seen that there is a reasonable agreement over the whole pressure range between the calculated pressure and the pressure during the hydroformylation experiments. If the concentration of **3** in the calculations would be excluded a very similar graph would be obtained. It should be noted that the P-R EOS is generally used to predict vapor-liquid equilibria at a broad range of pressures but there is still not a thorough understanding how well cubic EOS like the P-R EOS can predict the phase behavior and volumetric properties involving mixtures of supercritical components.^[38] Furthermore, Valderrama^[38] also points out that in general more than one binary interaction parameter has to be used to obtain more accurate results when predicting thermodynamic properties of mixtures involving supercritical components. So, in that light we can not expect here an optimal description when one interaction parameter is used to describe each binary system.

Despite the assumptions, the results of Figures 10 and 11 indicate that in principle the P-R EOS can describe the pressure as a function of composition for a given temperature. This means that in combination with a kinetic model and knowledge about the various interactions between reactant, products, and solvent the catalytic activity and chemoselectivity can be derived from only the pressure data.

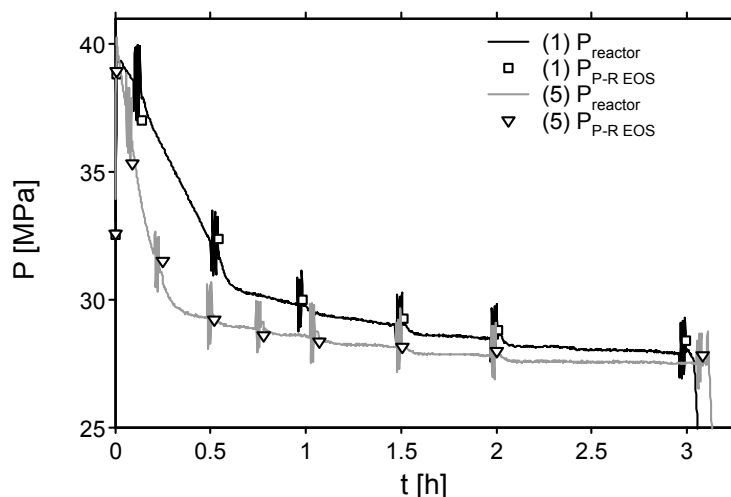


Figure 10. Pressure as a function of time, comparison between calculated and measured pressure.

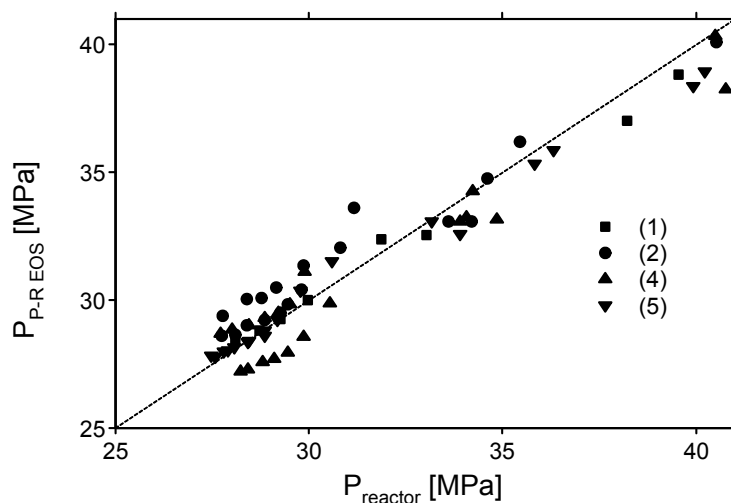


Figure 11. Calculated pressure, $P_{P-R\text{ EOS}}$, versus the reactor pressure, P_{reactor} , measured during hydroformylation experiments.

Erkey and co-workers have reported on an expression for the reaction rate of the hydroformylation of **1a** in scCO_2 using a rhodium catalyst with trifluoromethyl substituted

triarylphosphine ligands.^[19,26] The kinetic models they proposed are valid at a temperature of 50 °C and do not take into account isomerization. The rate expressions they proposed can serve as a good starting point for the development of a kinetic model in which also isomerization is taken into account. Information on the regioselectivity is difficult to deduce from the pressure data, because the thermodynamic properties of the aldehyde products are very similar.

Clearly for hydroformylation systems with a high regioselectivity this approach can even be more valuable, because the thermodynamic properties will be determined by only one of the aldehyde products. Typically, for such selective catalysts preferentially linear aldehydes are formed.^[39]

Conclusions

An experimental method has been presented, which provides well-defined reaction conditions for the homogeneously catalyzed hydroformylation of 1-octene. A good match between the pressure drop and the initial reaction rate has been found for the hydroformylation of 1-octene in scCO₂. A relationship is established between the initial pressure drop and the initial reaction rate in terms of $\Delta p/\Delta X$ and $\Delta p/\Delta Y_{\text{ald}}$. Especially, in the case of fast reactions the ability to follow the pressure as a function time provides a good alternative to determine the initial reaction rate since at high pressures it is difficult to take samples at a high frequency.

The increase of reaction rate with the L:Rh ratio for the hydroformylation in scCO₂ at the conditions applied here is different from the general trend reported in literature in which the reaction rate decreases with increasing L:Rh ratio.

The pressure calculated by using reactor temperature, composition and binary parameters in the Peng-Robinson EOS is in agreement with experimentally determined reactor pressures. This broadens the use of pressure and temperature measurements of single-phase high-pressure batch reactions to establish the composition of a reaction mixture and initial reaction rates. Sampling of the reaction mixture will be the main method to obtain information on the regioselectivity of the hydroformylation.

It can be concluded that the methodology using only pressure data, in combination with thermodynamics and reaction kinetics, can be used to screen catalysts for their performance in homogeneously catalyzed hydroformylation reactions in supercritical fluids. Further studies

have to be carried out to establish whether the Peng-Robinson EOS is the best equation of state to describe the density of this reaction mixture at high pressure.

References

- [1] C. D. Frohning, C. W. Kohlpaintner, H.-W. Bohnen, in *Applied Homogeneous Catalysis with Organometallic Compounds*, 2nd ed., Vol. 1, (Eds.: B. Cornils, W. A. Herrmann), Wiley-VCH, Weinheim, **2002**, p. 31-103.
- [2] a) P. G. Jessop, W. Leitner (eds.), *Chemical Synthesis Using Supercritical Fluids*, Wiley-VCH, Weinheim, **1999**; b) P. G. Jessop, T. Ikariya, R. Noyori, *Chem. Rev.* **1999**, *99*, 475-493; c) E. J. Beckman, *J. Supercrit. Fluids* **2004**, *28*, 121-191; d) S. Bektesevic, A. M. Kleman, A. E. Marteel-Parrish, M. A. Abraham, *J. Supercrit. Fluids* **2006**, *38*, 232-241; e) P. G. Jessop, *J. Supercrit. Fluids* **2006**, *38*, 211-231; f) R. S. Oakes, A. A. Clifford, C. M. Rayner, *J. Chem. Soc., Perkin Trans. 1* **2001**, 917-941; g) C. C. Tzschucke, C. Markert, W. Bannwarth, S. Roller, *Angew. Chem. Int. Ed.* **2002**, *41*, 3964-4000; h) D. Prajapati, M. Gohain, *Tetrahedron* **2004**, *60*, 815-833; i) S. Liu, J. Xiao, *J. Mol. Catal. A* **2007**, *270*, 1-43; j) C. M. Rayner, *Org. Proc. Res. Dev.* **2007**, *11*, 121-132.
- [3] examples of integration of reaction and separation: a) M. F. Sellin, P. B. Webb, D. J. Cole-Hamilton, *Chem. Commun.* **2001**, 781-782; b) P. B. Webb, T. E. Kunene, D. J. Cole-Hamilton, *Green Chem.* **2005**, *7*, 373-379.
- [4] For an example of a pressure profile during hydroformylation: F. Patcas, C. Maniut, C. Ionescu, S. Pitter, E. Dinjus, *Appl. Catal. B* **2007**, *70*, 630-636.
- [5] a) J. W. Rathke, R. J. Klingler, T. R. Krause, *Organometallics* **1991**, *10*, 1350-1355; b) M. J. Chen, R. J. Klingler, J. W. Rathke, K. W. Kramarz, *Organometallics* **2004**, *23*, 2701-2707.
- [6] T. J. de Vries, M. F. Kemmere, J. T. F. Keurentjes, *Macromolecules* **2004**, *37*, 4241-4246.
- [7] M. van Schilt, M. Kemmere, J. Keurentjes, *Catal. Today* **2006**, *115*, 162-169.
- [8] P. A. Mueller, G. Storti, M. Morbidelli, *Chem. Eng. Sci.* **2005**, *60*, 1911-1925.
- [9] Y. Guo, A. Akgerman, *Ind. Eng. Chem. Res.* **1997**, *36*, 4581-4585.
- [10] D.-Y. Peng, D. B. Robinson, *Ind. Eng. Chem. Fundam.* **1976**, *15*, 59-64.
- [11] Y. Guo, A. Akgerman, *J. Supercrit. Fluids* **1999**, *15*, 63-71.
- [12] J. Ke, B. Han, M. W. George, H. Yan, M. Poliakov, *J. Am. Chem. Soc.* **2001**, *123*, 3661-3670.
- [13] B. A. Stradi, J. P. Kohn, M. A. Stadtherr, J. F. Brennecke, *J. Supercrit. Fluids* **1998**, *12*, 109-122.
- [14] K. R. Westerterp, W. P. M. van Swaaij, A. A. C. M. Beenackers, *Chemical Reactor Design and Operation*, John Wiley & Sons, Chichester, 2nd ed., **1984**.
- [15] D. R. Palo, C. Erkey, *Ind. Eng. Chem. Res.* **1998**, *37*, 4203-4206.
- [16] K. L. Olivier, F. B. Booth, *Hydrocarbon Process* **1970**, *49(4)*, 112-114.
- [17] R. M. Deshpande, B. M. Bhanage, S. S. Divekar, R. V. Chaudari, *J. Mol. Catal.* **1993**, *78*, L37-L40.
- [18] P. Cavalieri d'Oro, L. Raimondi, G. Pagani, G. Montrasi, G. Gregorio, A. Andreetta, *Chim. Ind.* **1980**, *62*, 572-579.
- [19] T. Davis, C. Erkey, *Ind. Eng. Chem. Res.* **2000**, *39*, 3671-3678.
- [20] S. Haji, C. Erkey, *Tetrahedron* **2002**, *58*, 3929-3941.
- [21] P. W. N. M. van Leeuwen, in *Homogeneous Catalysis: Understanding the Art*, Kluwer Academic Publishers, **2004**, pp. 139-174.
- [22] S.-I. Fujita, S. Fujisawa, B. M. Bhanage, M. Arai, *Tetrahedron Lett.* **2004**, *45*, 1307-1310.
- [23] S. Kainz, D. Koch, W. Baumann, W. Leitner, *Angew. Chem. Int. Ed.* **1997**, *15*, 1628-1630.
- [24] D. Koch, W. Leitner, *J. Am. Chem. Soc.* **1998**, *120*, 13398-13404.
- [25] D. R. Palo, C. Erkey, *Organometallics* **2000**, *19*, 81-86.
- [26] D. R. Palo, C. Erkey, *Ind. Eng. Chem. Res.* **1999**, *38*, 3786-3792.

- [27] A. M. Banet Osuna, W. Chen, E. G. Hope, R. D. W. Kemmitt, D. R. Paige, A. M. Stuart, J. Xiao, L. Xu, *J. Chem. Soc., Dalton Trans.* **2000**, 4052-4055.
- [28] M. Giménez-Pedrós, A. Aghmiz, N. Ruiz, A. M. Masdeu-Bultó, *Eur. J. Inorg. Chem.* **2006**, 1067-1075.
- [29] I. Bach, D. J. Cole-Hamilton, *Chem. Commun.* **1998**, 1463-1464.
- [30] M. Giménez-Pedrós, A. M. Masdeu-Bultó, J. Bayardon, D. Sinou, *Catal. Lett.* **2006**, *107*, 205-208.
- [31] A. R. Tadd, A. Marteel, M. R. Mason, J. A. Davies, M. A. Abraham, *Ind. Eng. Chem. Res.* **2002**, *41*, 4514-4522
- [32] Z. K. Lopez-Castillo, R. Flores, I. Kani,, J. P. Fackler Jr., A. Akgerman, *Ind. Eng. Chem. Res.* **2003**, *42*, 3893-3899.
- [33] W. R. Moser, C. J. Papile, D. A. Brannon, R. A. Duwell, *J. Mol. Catal.* *41* (1987) 271-292.
- [34] C. P. Casey, E. L. Paulsen, E. W. Beuttenmueller, B. R. Proft, L. M. Petrovich, B. A. Matter, D. R. Powell, *J. Am. Chem. Soc.* **1997**, *119*, 11817-11825.
- [35] a) Chapter 5 and 6; b) A. C. J. Koeken, M. C. A. van Vliet, L. J. P. van den Broeke, B.-J. Deelman, J. T. F. Keurentjes, *Adv. Synth. Catal.* **2006**, *348*, 1553-1559.
- [36] T. Jiang, Z. Hou, B. Han, L. Gao, Z. Liu, J. He, G. Yang, *Fluid Phase Equilib.* **2004**, *215*, 85-89.
- [37] R. Jiménez-Gallegos, L. A. Galicia-Luna, O. Elizalde-Solis, *J. Chem. Eng. Data* **2006**, *51*, 1624-1628.
- [38] J. O. Valderrama, *Ind. Eng. Chem. Res.* **2003**, *42*, 1603-1618.
- [39] for example: N. J. Meehan, A. J. Sandee, J. N. H. Reek, P. C. J. Kamer, P. W. N. M. van Leeuwen, M. Poliakoff, *Chem. Commun.* **2000**, 1497-1498.

Chapter 3

Chemoselectivity and regioselectivity of 1-octene hydroformylation in supercritical carbon dioxide

Abstract

The activity, chemoselectivity, and regioselectivity of the hydroformylation of 1-octene, catalyzed by a supercritical carbon dioxide soluble catalyst have been evaluated. The effect of total pressure, temperature, concentration of reactants, and concentration of catalyst precursors, rhodium(I) dicarbonyl acetylacetonate and tris(3,5-bis(trifluoromethyl)phenyl)phosphine, has been studied. With an increase in temperature the initial rate of aldehyde formation and the rate of 1-octene isomerization both increase. As a consequence, a lower regioselectivity is obtained at higher temperatures. By applying a lower CO₂ amount, which implies a lower total pressure, a higher regioselectivity towards the linear product nonanal has been obtained. At a temperature of 70 °C and a ligand to rhodium ratio of 4 the catalyst has sufficient activity towards hydroformylation of internal octenes, which results in a decrease of the regioselectivity in the high conversion and high yield range. The use of tris(3,5-bis(trifluoromethyl)phenyl)phosphine as the ligand in the hydroformylation of 1-octene results in a reaction rate and regioselectivity higher than obtained for the unmodified or the triphenylphosphine modified rhodium catalyst.

Introduction

Hydroformylation of alkenes using homogeneous catalysts is applied on a commercial scale to produce aldehyde intermediates for the production of detergents, plasticizers, and solvents. The applied catalysts are organometallic complexes of rhodium or cobalt, commonly with phosphines or phosphites as modifying ligands.^[1] In order to reuse the catalyst, separation steps like distillation or extraction are required, which generally have a detrimental effect on catalyst activity and selectivity. The Ruhrchemie/Rhône-Poulenc (RCH/RP) hydroformylation process is a well-known example where, by means of an aqueous phase, the reaction and the separation step of the homogeneous rhodium catalyst are integrated.^[2] However, this approach is limited to the hydroformylation of short-chain alkenes, because long-chain alkenes are too sparingly soluble in water to obtain acceptable space-time yields.

Supercritical fluids have received considerable attention as alternative solvents for the hydroformylation on long-chain alkenes, including 1-octene.^[3] Carbon dioxide is of particular interest since it has accessible critical properties, is nonflammable, and has low toxicity. Furthermore, by using carbon dioxide one-phase reaction systems can be created, in which optimal use can be made of the characteristics of a supercritical fluid. This includes the absence of phase boundaries, the high diffusivity of the different species, and the high solubility of gaseous reactants.

One of the restrictions of applying supercritical carbon dioxide, scCO_2 , as a solvent is the limited solubility of common homogeneous catalysts. For Wilkinson type hydroformylation and hydrogenation catalysts this drawback has been overcome by attaching perfluoroalkyl groups to the para or meta positions of the triphenylphosphine ligands.^[4-7] The “tunability” of the supercritical solvent properties by relatively small changes in temperature and pressure allows the precipitation and reuse of these fluorinated catalysts.^[4,5]

The solvent in which the hydroformylation is performed can have a significant effect on the activity or selectivity of the reaction.^[7-9] The properties of scCO_2 are pressure and temperature dependent, whereas the properties of organic solvents are much less affected by temperature or pressure. In this respect scCO_2 differs from conventional organic solvents, however, no clear picture exists of how carbon dioxide can affect the kinetics of hydroformylation reactions. Erkey and co-workers applied a constant total initial pressure constant, and when the reactant concentration was varied the CO_2 concentration was varied simultaneously.^[10,11] Davis and Erkey studied the influence of reactant and ligand

concentration on the hydroformylation of 1-octene at temperatures of 40 , 45 , and 50 °C at a constant total pressure.^[10] In this manner, the possible effect of total pressure on the reaction kinetics was avoided. According to the observations of Palo and Erkey for the hydroformylation of 1-octene in scCO₂ the total pressure had no influence on the reaction rate or selectivity.^[11] However, Sellin et al. reported that the CO₂ concentration had a clear effect on the regioselectivity of the hydroformylation of 1-hexene, carried out at 100 °C in a CO₂ enriched reaction mixture.^[12]

Here we present a detailed study on the influence of the concentration of the reactants, and the concentration of the catalyst precursors, rhodium(I) dicarbonyl acetylacetonate and tris(3,5-bis(trifluoromethyl)phenyl)phosphine, on the reaction rate and selectivity of the hydroformylation of 1-octene carried out in scCO₂ (Figure 1 and Figure 2). The concentration of **1a**, **1a** isomers, and the aldehyde products have been obtained as a function of time for hydroformylations carried out at temperatures in the range of 40 to 80 °C, and up to pressures of about 50 MPa. During the various experiments the carbon dioxide concentration has been kept constant in order to achieve a comparable effect of CO₂ on the reaction kinetics per experiment. This implies that the initial total pressure needs to be adapted to the initial reactant concentration.

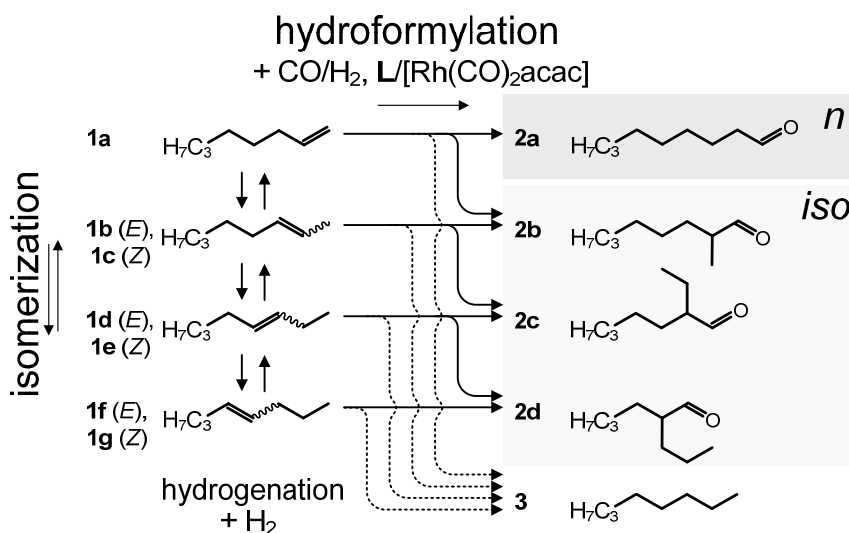


Figure 1. Reaction scheme for the hydroformylation of 1-octene (**1a**), with the two main products nonanal (**2a**) and 2-methyloctanal (**2b**). The side products are (*E,Z*)-2-octene (**1b**, **1c**), (*E,Z*)-3-octene (**1d**, **1e**), (*E,Z*)-4-octene (**1f**, **1g**), 2-ethylheptanal (**2c**), 2-propylhexanal (**2d**), and *n*-octane (**3**).

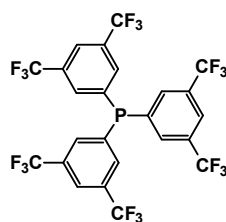


Figure 2. Ligand structure: tris(3,5-bis(trifluoromethyl)phenyl)phosphine (**I**).

Experimental

Materials - Carbon dioxide, carbon monoxide, and hydrogen, grade 5.0, 4.7, and 5.0, respectively, were obtained from Hoekloos (The Netherlands). Prior to use CO₂ was passed over a Messer Oxisorb filter to remove oxygen and moisture. 1-Octene, **1a**, obtained from Aldrich, was passed over activated alumina, dried with pre-treated molsieves 3A (Aldrich, 4-8 mesh), and stored under argon.

The rhodium precursor, rhodium(I) dicarbonyl acetylacetonate, ([Rh(CO)₂acac]), was obtained as dark green crystals from Fluka. Ligand **I**, tris(3,5-bis(trifluoromethyl)phenyl)phosphine, is a white to light yellow solid and was supplied by Arkema (Vlissingen, The Netherlands). Triphenylphosphine was obtained from Aldrich. All catalyst precursors were stored under argon and manipulated using Schlenk techniques.

The solvent toluene (Merck, analytical grade), the internal standard *n*-decane (Aldrich, >99% purity) and the substances involved in the reaction, *n*-octane (Aldrich, > 99%), 2-octene (ABCR, mixture of E and Z, 98%), and nonanal (Fluka, > 95%) used for the GC-analysis were used as received.

Hydroformylation in scCO₂ - The general procedure for a hydroformylation experiment was started by charging the desired amounts of [Rh(CO)₂acac] and the phosphine ligand into the empty reactor and subsequently closing the reactor. The details of the high-pressure batch reactor setup are described in Chapter 2. The reactor volume was carefully flushed with argon and subsequently evacuated for three times. Next, the stirring was turned on with a stirring rate of 700 rpm and the desired amount of carbon monoxide and hydrogen gas was fed to the reactor at room temperature. The reactor content was heated to a temperature of 50 °C, and consecutively CO₂ was charged into the reactor at a constant flow typically up to a total pressure such that about 14.5 mol L⁻¹ CO₂ was present. In the case when 1 mol L⁻¹ of CO, 1 mol L⁻¹ of H₂, and 14.5 mol L⁻¹ of CO₂ was applied this corresponded to about 26 MPa total

pressure at 50 °C. When the CO and H₂ concentration were varied, the total reactor pressure required to achieve a CO₂ concentration of 14.5 mol L⁻¹ at 50 °C was estimated using the Peng-Robinson equation of state and the input parameters as stated in Chapter 2. Then, these conditions were maintained for at least half an hour before heating further to the desired reaction temperature. In total a period of about 1 h was considered sufficient to allow the active catalyst complexes to be formed in-situ from the [Rh(CO)₂acac] and **I**. The reaction was started by the addition of the **1a**, which was done by opening the valve between the pump and the reactor. A fast pressure equalisation occurred and consecutively the desired volume of **1a** was pumped into the reactor, which as a rule did not take more than 30 s. While pumping **1a** the reactor temperature increased as a result of a fast pressure increase and the start of the reaction. The maximum temperature increase observed upon injection of **1a** was 3 °C for entry 20 (Table 1). The temperature usually stabilized within 15 min. During the remainder of reaction the reactor temperature was maintained within a deviation of less than 1 °C from the desired temperature.

Samples were withdrawn from the high-pressure mixture. The content of the sample volume was carefully bubbled through a vial with a solution of *n*-decane in toluene and afterwards rinsed with additional toluene solution to collect **1a** and its reaction products quantitatively. Subsequently, the sample volume was dried by alternately applying an argon flow and vacuum. The minimum time of taking a sample and preparing for a next one was in the order of 10 min. A reaction time of three hours was considered, after which the mixture was rapidly cooled, the gases were vented and the remaining liquids consisting of reaction products and catalyst were collected.

Sampling was done from either the top or bottom of the reactor, and this was also used to verify that the reaction mixture was always a homogeneous supercritical phase. To ensure that the reactor was cleaned properly, blank reaction runs were performed regularly at reaction conditions. The concentration of catalyst precursors were chosen such that catalytic complexes would dissolve completely for the conditions applied here.^[10]

In Table 1 the different experiments are specified in terms of the amount of reactants used. The concentrations used in the various experiments were obtained by using the reactor volume of 0.1076 L. For entry 19 this was not applicable because a two-phase system was present.

Analysis and calibration - The samples were analyzed off-line using a Fisons Instruments GC-FID equipped with a Restek Rtx-5 column (fused silica, length 30 m, internal diameter 0.53 mm) with helium as the carrier gas. Calibration was done for **1a**, **1b**, **1c**, **3** and **2a**, the sensitivity coefficients for the other octene and aldehyde isomers were taken to be equal to those of **1a** and **2a**, respectively.

Reaction parameters - To obtain normalized concentration profiles for **1a** and its reaction products, each concentration obtained by GC analysis was divided by the sum of all obtained concentrations:

$$[i]_n = \frac{[i]}{\sum [i]} \quad (1)$$

where $i = \mathbf{1a-1g}$, $\mathbf{2a-2d}$ and $\mathbf{3}$, and the subscript n refers to the normalized values.

The activity and selectivity of the different catalytic complexes was expressed in one of the following parameters. The definitions used were based on Westerterp et al.^[13] The conversion, X , was given by:

$$X = \frac{[\mathbf{1a}]_{n,0} - [\mathbf{1a}]_n}{[\mathbf{1a}]_{n,0}} \times 100\% \quad \text{with } [\mathbf{1a}]_{n,0} = 1 \quad (2)$$

The overall selectivity, S_j , towards a product j was defined as:

$$S_j = \frac{[j]_n}{[\mathbf{1a}]_{n,0} - [\mathbf{1a}]_n} \times 100\% \quad (3)$$

where $j = \mathbf{1b-1g}$, $\mathbf{2a-2d}$ and $\mathbf{3}$.

The overall yield, Y_k , for a product k was then:

$$Y_k = \frac{[k]_n}{[\mathbf{1a}]_{n,0}} \times 100\% \quad (4)$$

The substrate to catalyst ratio, S/C , was calculated as follows:

$$\frac{S}{C} = \frac{m_{\mathbf{1a}} \cdot MW_{Rh}}{m_{Rh} \cdot MW_{\mathbf{1a}}} \quad (5)$$

with $m_{\mathbf{1a}}$ the mass of **1a** injected, $MW_{\mathbf{1a}}$ the molar mass of **1a**, and m_{Rh} and MW_{Rh} the mass conveyed to the reactor and the molar mass of the rhodium precursor, respectively.

The turn-over-number based on the conversion of **1a**, $TON_{\mathbf{1a}}$, was calculated as follows:

$$TON_{\mathbf{1a}} = \frac{S}{C} \cdot X \quad (6)$$

The “initial” overall rate of reaction for component R_p (with $p=1\mathbf{a}$, $2\mathbf{a}$, $2\mathbf{a}-2\mathbf{d}$) was calculated by multiplying the initial amount of $1\mathbf{a}$ in mol, $n_{1\mathbf{a},0}$, with the slope of a line fitted through the conversion or yield data points up to a conversion where there was a linear trend (typically up to a conversion of 60 %). A distinction is made between the linear aldehyde product, $2\mathbf{a}$, and total amount of aldehydes, $2\mathbf{a}-2\mathbf{d}$, abbreviated as “ald”.

The *n:iso* ratio was obtained by dividing the concentration of linear aldehyde product by the sum of the concentrations of the branched aldehyde products:

$$n : iso = \frac{[2\mathbf{a}]_n}{[2\mathbf{b}]_n + [2\mathbf{c}]_n + [2\mathbf{d}]_n} \quad (7)$$

Reproducibility – For a number of experiments the results were an average of two experiments: entries 8-10, and 21 in Table 1. For example, for entry 10 the values for the initial reaction rate, $R_{1\mathbf{a},0}$, $R_{\text{ald},0}$, and $R_{2\mathbf{a},0}$, obtained for the two separate experiments showed each a deviation from the average value of about 9 %. For the other duplicate experiments smaller deviations for $R_{1\mathbf{a},0}$, $R_{\text{ald},0}$, and $R_{2\mathbf{a},0}$ than for entry 10 were observed. For the reaction parameters, including X , *n:iso*, $S_{2\mathbf{a}}$, and S_{ald} , a deviation from the average value of less than 3% was obtained. The maximum deviation obtained for $S_{1\mathbf{b}-1\mathbf{g}}$ and S_3 was between 0 and 30 %. This was acceptable because the values of these parameters were small, and had, therefore, a lower significance.

Results and discussion

The results on chemo- and regioselectivity will be discussed as a function of the reaction parameters like temperature, concentration of reactants, and catalyst precursors. In Table 1 the conditions and main results of hydroformylation of $1\mathbf{a}$ in a CO_2 enriched supercritical one-phase system are given.

The conditions for entry 8 have been taken as reference conditions, i.e. $T = 70\text{ }^\circ\text{C}$, $L:\text{Rh} = 4:1$, $[\text{CO}]_0 = 1\text{ mol L}^{-1}$, $[\text{H}_2]_0 = 1\text{ mol L}^{-1}$, and $[1\mathbf{a}]_0 = 0.5\text{ mol L}^{-1}$. All the other experiments have been performed by varying only one condition at a time as compared to entry 8. At a temperature of $70\text{ }^\circ\text{C}$ the influence of the (initial) concentration of reactants and catalyst precursors, as well as the solvent concentration has been investigated. At a $L:\text{Rh}$ of 4:1 the reaction temperature has been varied from 40 to $80\text{ }^\circ\text{C}$.

Table 1. Overview of experimental conditions and main results

entry ^[a]	T [°C]	P _{max} ^[b] [MPa]	n _{CO2} [mol]	n _{CO} [10 ⁻³ mol]	n _{H2} [10 ⁻³ mol]	n _{1a} [10 ⁻³ mol]	n _{Rh} [10 ⁻⁶ mol]	L:Rh	R _{1a,0} [c]	R _{ald} , [d]	R _{2a,0} , [e]	TOF _{1a,0} [f]	X ^[g] [%]	n:iso ^[g] [-]	S _{2a} ^[g] [%]	S _{ald} ^[g] [%]	S _{1b-1g} ^[g] [%]	S ₃ ^[g] [%]
1	40	27.4	1.6	108	108	54.5	26.3	4.1	2.7	2.6	1.9	0.36	53.4	2.9	71.9	97.0	2.4	0.5
2	50	31.4	1.6	109	108	54.5	27.2	3.9	7.1	6.8	5.0	0.94	97.6	2.6	71.1	98.3	1.4	0.3
3 ^[h]	50	30.9	1.6	108	108	54.2	27.2	10	7.7	7.3	5.6	1.0	97.6	3.2	75.1	98.6	1.2	0.2
4	50	32.1	1.6	108	108	54.6	27.1	50	8.4	7.8	6.2	1.1	96.3	3.9	77.7	97.7	1.7	0.7
5 ^[h]	60	36.2	1.6	107	107	54.7	27.2	4.0	18	16	12	2.3	99.0	2.4	69.6	98.9	0.6	0.4
6	60	34.9	1.6	108	108	54.7	27.2	10	20	19	15	2.7	99.4	2.9	73.7	99.0	0.7	0.3
7	70	39.7	1.6	109	108	54.3	26.8	0	21	18	13	2.8	99.4	1.3	54.8	96.5	2.1	1.4
8 ^[k]	70	40.6	1.6	107	107	55.2	27.3	4.0	37	34	25	4.9	99.4	2.1	66.5	98.5	0.9	0.5
9 ^[k]	70	40.7	1.6	105	108	55.3	27.2	10	46	42	32	6.0	99.4	2.5	70.8	98.8	0.8	0.4
10 ^[k]	70	40.2	1.6	108	108	54.2	27.2	50	54	50	39	7.2	99.4	3.2	75.5	98.8	0.8	0.3
11	70	39.0	1.6	81	108	54.4	27.7	3.9	48	44	33	6.2	99.7	2.3	68.3	97.7	1.5	0.9
12	70	44.5	1.6	162	111	55.0	29.3	3.7	29	27	19	3.6	99.8	1.9	64.8	98.8	0.7	0.5
13	70	38.2	1.6	109	86	55.0	26.6	4.0	29	26	19	4.0	99.9	2.1	65.6	96.7	2.2	1.1
14	70	44.0	1.6	109	166	54.7	26.6	4.0	78	68	49	11	99.9	2.1	67.6	99.1	0.3	0.7
15	70	34.5	1.6	109	110	12.1	27.3	3.9	30	27	19	4.0	99.9	2.0	65.5	97.8	1.5	0.7
16	70	52.3	1.6	109	110	109	26.6	4.0	48	43	32	6.5	99.5	2.6	63.4	87.7	10.2	2.1
17	70	40.2	1.6	108	111	55.4	13.8	4.0	20	18	12	5.2	≈100	1.9	64.4	97.8	1.4	0.8
18	70	39.5	1.6	109	109	54.8	52.5	4.1	93	79	58	6.4	99.9	2.3	68.3	98.5	0.9	0.6
19 ^[l]	70	24.0	1.2	109	108	54.9	26.7	50	60	56	45	8.1	99.8	3.8	78.3	99.0	0.7	0.2
20	70	30.5	1.4	108	109	54.7	28.3	48	54	51	40	6.9	99.5	3.4	76.6	99.0	0.7	0.3
21 ^[k]	80	44.8	1.6	108	107	54.9	27.8	4.0	52	45	33	6.7	99.4	2.0	65.2	97.2	1.8	1
22 ^[m]	70	39.6	1.6	109	108	55.5	26.6	52	2.2	2.0	1.6	0.30	30.0	3.3	75.0	97.5	1.5	1

^[a] General conditions: V_{reactor} = 0.1076 L, stirrer speed = 700 rpm. ^[b] Maximum reactor pressure reached upon injection of **1a**. ^[c] [10⁻⁶ mol_{1a} s⁻¹]. ^[d] [10⁻⁶ mol_{ald} s⁻¹]. ^[e] [10⁻⁶ mol_{2a} s⁻¹]. ^[f] [10³ mol_{1a} mol_{Rh} h⁻¹]. ^[g] Values after approximately three hours of reaction. ^[h] Catalyst preformation was done on the previous day. Conditions: 2 MPa (at 20 °C) 1:1 syngas, in CO₂ at a total pressure of 18 MPa and 50 °C for one hour at 700 rpm stirrer rate. After careful depressurization the catalyst was stored overnight under argon atmosphere. The different procedure did not result in significantly different reaction kinetics. ^[k] Duplicate experiments. ^[l] Two phase reaction system. ^[m] Experiment similar to entry 10 using triphenylphosphine as the ligand.

Finally, the effect of excess ligand, L:Rh ratio, has been studied as a function of the temperature at 50, 60, and 70 °C, respectively. Also, experiments have been carried out in which no phosphine (unmodified catalyst) has been applied or where triphenylphosphine (PPh₃) has been applied.

Influence of CO₂ – The density of scCO₂ can vary significantly with changes in pressure, whereas the density of liquid solvents is only slightly affected by the pressure. To study the effect of density three different amounts of CO₂ have been applied, ranging from 1.2 to 1.6 mol (entries 10, 19, and 20 in Table 1). The selectivity towards aldehydes and the *n:iso* ratio are plotted as a function of Y_{ald} instead of the conversion for reasons of clarity. It has been demonstrated in Chapter 2 that with the catalyst based on [Rh(CO)₂acac] and **I** a significant isomerization rate can be observed. Therefore, it can occur that the conversion is close to 100 %, while Y_{ald} is still increasing as a result of the hydroformylation of internal octenes (**1b-1g**). As can be seen in Figure 3a, the chemoselectivity towards aldehydes, S_{ald}, as a function of the yield of aldehydes, Y_{ald}, is similar in all three cases. The regioselectivity expressed in terms of the *n:iso* ratio, depicted in Figure 3b, shows a clear dependence on the amount of CO₂. For the lowest amount of CO₂ the highest *n:iso* ratio has been observed. In the case that 1.2 mol of CO₂ has been used, a two-phase reaction mixture has been observed during the reaction. Significantly higher total concentrations (concentrations which are more than 20 % higher than the concentration expected based on the amount of **1a** injected) have been determined by GC-analysis of samples taken from the bottom. This could be the reason for the different value of S_{ald} observed for entry 19 at a Y_{ald} value of about 70 % as compared the S_{ald} values obtained when using the higher CO₂ densities (entries 10 and 20). This result, where there is an effect of the amount of CO₂ on the regioselectivity, has prompted us to carry out the experiments at a fixed amount of CO₂ rather than at a fixed initial total pressure.

The dependence of the regioselectivity on the amount of CO₂ has not been reported before for the hydroformylation of **1a** with a fluorous Rh-based catalyst.^[5,10,14,15] Apparently, the temperature of 70 °C applied here, possibly in combination with the high ligand concentration, leads to a reaction system which is more susceptible to the CO₂ concentration. In the case of the hydroformylation of 1-hexene in the presence of a Rh-catalyst at 100 °C in a CO₂ enriched reaction mixture, the regioselectivity was also influenced by the CO₂ concentration; the *n:iso* ratio also increased with a decrease in CO₂ concentration, although the effect was smaller.^[12]

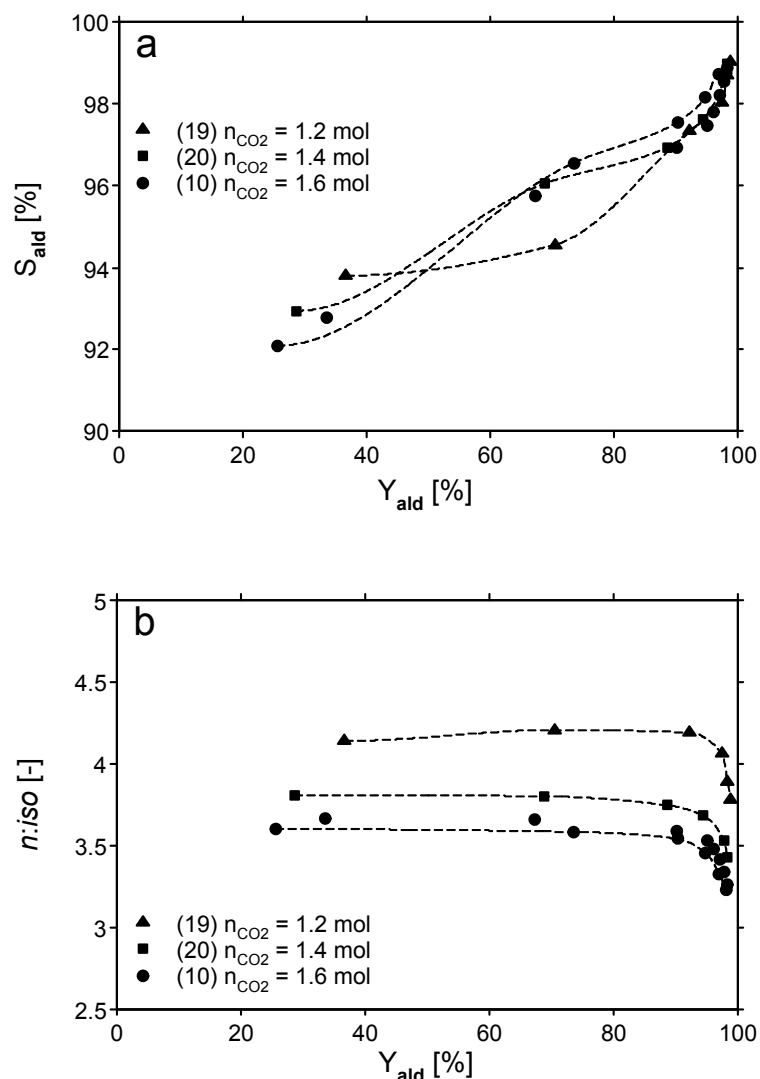


Figure 3. a) The overall selectivity towards aldehydes, S_{ald} , as a function of the yield of aldehydes, Y_{ald} ; b) The $n:iso$ ratio as a function of Y_{ald} .

For propene hydroformylation with a Co-catalyst Guo and Akgerman also reported a strong dependence of the regioselectivity on the CO₂ concentration.^[16]

In the case of reactions in supercritical fluids it is known that the pressure, or concentration, can have several thermodynamic effects. First of all, the pressure can influence the reaction rate constant of elementary reaction steps, based on transition-state theory.^[17,18] In the catalytic cycle of the hydroformylation reaction several organometallic reaction intermediates are involved, which implies that at least as many elementary reaction steps have to be taken into account. Guo and Akgerman have presented an alternative approach for the

hydroformylation of propene. The reaction kinetics is based on an empirical model for the overall reaction towards the linear and branched aldehyde products.^[19]

Another thermodynamic effect is that the fugacity (f)[‡],^[20] of the reactants carbon monoxide and hydrogen increases with an increase in CO₂ concentration. At the reaction temperature of 70 °C, the fugacity of carbon monoxide and hydrogen has a stronger dependence on the CO₂ concentration than the fugacity of **1a**. For the concentration used in the reference experiment, entry 8, the fugacity coefficient for CO and H₂ as a function of the concentration of CO₂ increase from 1 to 1.5 (f_{CO} : from 2.9 to 4.3 MPa) and from 1 to 3.2 (f_{H_2} : from 2.9 to 9.3 MPa), respectively. This corresponds to starting with an equimolar CO-H₂ mixture, with a concentration of 1 mol L⁻¹ for each species, and adding CO₂ to a final concentration of 14.5 mol L⁻¹. These values for the fugacity are based on calculations with the Peng-Robinson equation of state. A simultaneous increase in the fugacity of carbon monoxide and hydrogen will probably not have a substantial effect on the overall reaction rate, as carbon monoxide has a negative reaction order and hydrogen a positive one.^[1] However, when it is assumed that the catalyst species and excess ligand have a constant fugacity as a function of CO₂ pressure, the decrease in regioselectivity can be explained by the increase in fugacity of carbon monoxide. An increase in carbon monoxide concentration leads to catalytic species, which are less selective towards the formation of the linear product.^[21]

A further possible explanation for the decrease in regioselectivity at a higher CO₂ concentration is that the phosphine ligand can be oxidized through a reaction with CO₂.^[22] Furthermore, water and oxygen can also oxidize the phosphine ligand.^[22] Although the high purity grade CO₂ is further purified before use, traces of water and oxygen can still be present in the CO₂. As higher concentrations of CO₂ are used, higher concentrations of these impurities can be present during catalyst preparation and reaction.

Influence of temperature – In Figure 4a the selectivity towards aldehydes is shown as a function of aldehyde yield, for temperatures ranging from 40 to 80 °C and a L:Rh ratio of 4:1. Also, the results for an experiment at 70 °C without ligand are shown. For the cases with **I**, the values for S_{ald} increase with a decrease in temperature. For the case where no ligand is applied (entry 7), the value of S_{ald} first decreases and then starts to increase at a Y_{ald} value of 60 %, while for the ligand modified catalyst S_{ald} increases over the whole Y_{ald} range.

[‡] The fugacity of a gas represents the effective pressure of a gas. The fugacity of a species i , f_i , is related to the partial pressure of i , p_i , in the following way: $f_i = \phi_i \times p_i$. ϕ_i is the (dimensionless) fugacity coefficient.

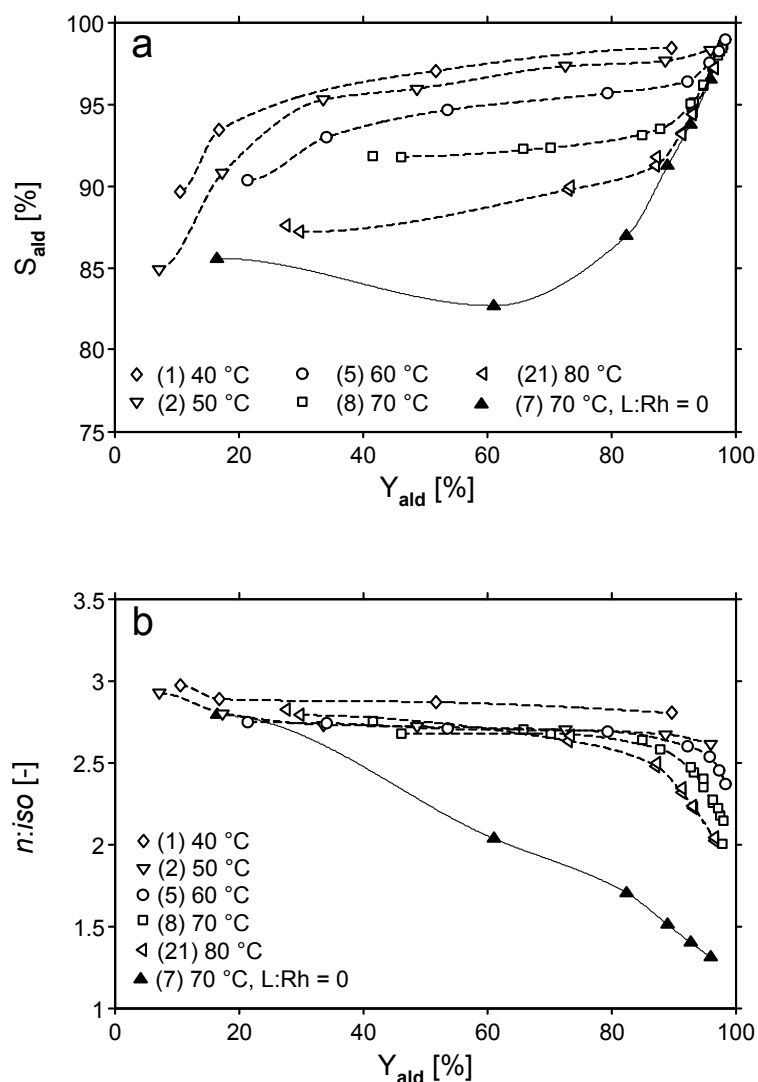


Figure 4. a) The overall selectivity towards aldehydes, S_{ald} , as a function of the yield of aldehydes, Y_{ald} ; b) The $n:iso$ ratio as a function of Y_{ald} .

At an aldehyde yield, below 20 %, the values for S_{ald} seem to start at about 85 %, independently of the temperature. For the case where no ligand has been used the lowest values for S_{ald} have been obtained, up to a Y_{ald} of 80 %. For the high yield range, the S_{ald} converges to the same value.

The difference between S_{ald} for different temperatures is caused by a difference in isomerization rate. A higher reaction temperature results in a higher rate of isomerization of **1a**, which is the main side reaction. This is common for the triphenylphosphine modified rhodium catalyst.^[1] The increase in isomerization rate has also been observed for phosphite modified rhodium catalysts.^[23] The fact that the isomerization rate increases with temperature

can also be deduced from the initial rates given in Table 1. The difference between $R_{1a,0}$ and $R_{ald,0}$ represents the initial rate of isomerization of **1a**. The hydrogenation activity is substantially smaller than the isomerization activity, which is confirmed by the small fraction of octane obtained at the end of most of the reactions. It should be noted that from the dependence of the selectivity for the aldehydes on the (aldehyde) yield the selectivity for the octene isomers can be derived as hydrogenation only takes place to a small extent. The overall selectivity towards the internal octenes, **1b** to **1g**, is given by $1-S_{ald}$.

In Figure 4b the *n:iso* ratio as a function of Y_{ald} is shown, for temperatures in the range of 40 °C to 80 °C. The octene isomers formed in the initial stage of the reaction are also hydroformylated, as is illustrated by the increase in S_{ald} and the simultaneous decrease of the *n:iso* ratio for values of Y_{ald} above 80 %. It is seen that there is only a small effect of the temperature on the *n:iso* ratio. The *n:iso* ratio for a temperature of 40 °C is slightly higher than the results obtained at a higher temperature. In the temperature range from 50 °C to 80 °C the *n:iso* ratio has approximately the same value for a Y_{ald} value of 20 to 70 %.

Furthermore, with an increase in reaction temperature the *n:iso* ratio starts to decrease at a lower value for the aldehyde yield. The final value for the *n:iso* ratio observed at a yield above 95 % (i.e. after three hours of reaction), decreases with an increase in temperature (see also Table 1). For the case where no ligand is applied the regioselectivity decreases steadily as a function of Y_{ald} , while the initial regioselectivity is similar to the cases where **I** has been used. The use of the “fluorous” ligand, **I**, is advantageous because both selectivity and activity of the catalyst are improved.

Influence of ligand – In Figure 5a values for S_{ald} are depicted as a function of Y_{ald} at L:Rh values of 10:1 and 50:1 at a temperature of 50, 60, and 70 °C, respectively. For the results shown in Figure 5a it can be concluded that for a L:Rh higher than 10:1 there is only a moderate effect of the temperature on S_{ald} as a function of Y_{ald} . The difference between the results presented in Figure 4a and Figure 5a are caused by a difference in isomerization activity. At a low L:Rh ratio the isomerization activity appears to be slightly higher and seems to be more susceptible to the temperature.

In Figure 5b results are shown for the *n:iso* ratio as a function of Y_{ald} corresponding to the experiments with a L:Rh of 10:1 and 50:1. It is known that an excess of triphenylphosphine (PPh₃) ligand improves the selectivity of a rhodium based catalyst.^[1] At a high L:Rh and 50 °C, the highest *n:iso* ratio is obtained.

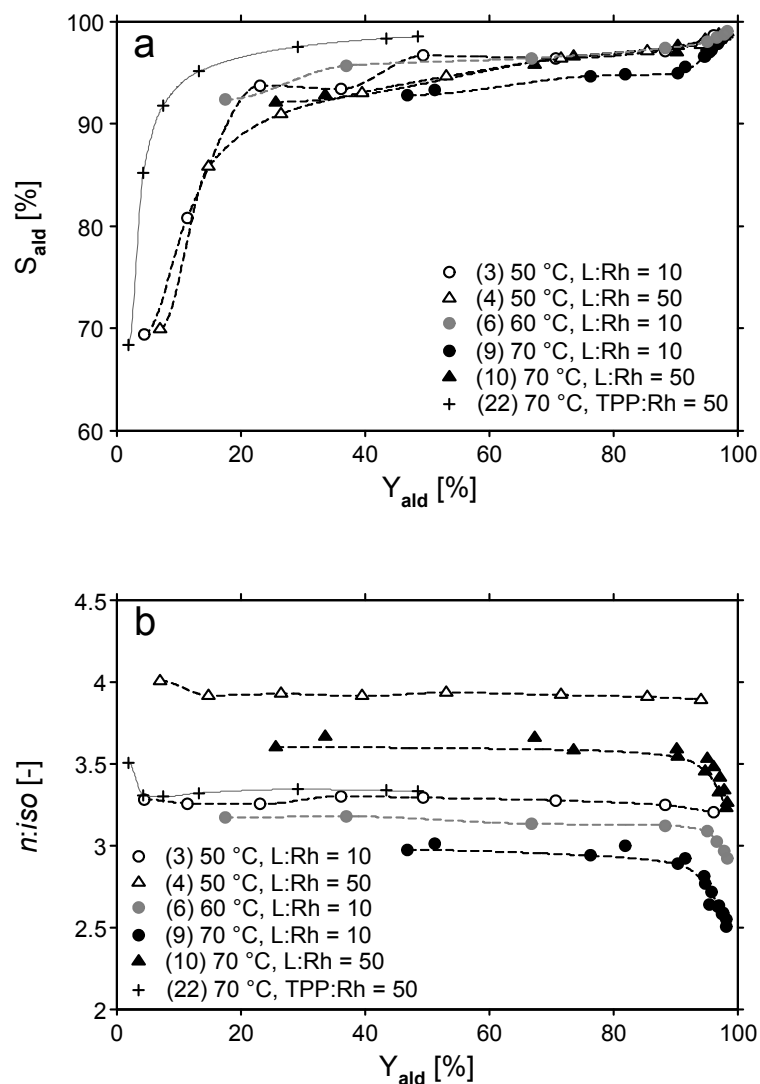


Figure 5. a) The overall selectivity towards aldehydes, S_{ald} , as a function of the yield of aldehydes, Y_{ald} ; b) The $n:iso$ ratio as a function of Y_{ald} .

For the three experiments at 50 °C, i.e. with a L:Rh of 4:1 (see Figure 4b), 10:1, and 50:1, a constant $n:iso$ ratio is observed, where the $n:iso$ ratio increases with an increase in L:Rh ratio. The fact that at 50 °C the $n:iso$ ratio is constant is a result of the low isomerization activity irrespective of the L:Rh ratio. These results obtained at 50 °C are in agreement with the results reported by Davis and Erkey.^[10] At the higher temperatures, 60 °C to 80 °C, the $n:iso$ ratio decreases in the high yield range, as a result of the hydroformylation of internal octenes.

In the temperature range of 50 °C to 70 °C it can be observed (Figure 5b) that the regioselectivity increases with an increase in ligand concentration. On the other hand, the activity of the catalyst does not decrease, or even increases (Table 1). With respect to this, the

well-known PPh₃ based rhodium catalyst has a significantly different behavior. The activity of the catalyst decreases substantially with an increasing excess PPh₃ concentration.^[21,24-27] For the catalytic system based on [Rh(CO)₂acac] and a bulky phosphite increasing the phosphite-Rh ratio also does not result in a decrease in hydroformylation rate.^[23] From Figure 5a it follows that the results for S_{ald} for the hydroformylation using PPh₃ are clearly higher than for the catalytic system with the fluorous **I**. However, at similar conditions, the regioselectivity in terms of *n:iso* ratio, and the initial rates are substantially higher for the **I**-Rh catalyst than for the PPh₃-Rh catalyst, as can be deduced from Table 1 and Figure 5b.

It should be noted that it has not been confirmed that the PPh₃-Rh catalyst, at the conditions studied here, is completely dissolved in the supercritical reaction system. However, it is known that triphenylphosphines with electron withdrawing substituents like the trifluoromethyl group generally give rise to a more active catalyst than the parent PPh₃. Therefore, the difference in activity is plausible. For further discussion on this topic the reader is referred to Chapters 5 and 6.

Influence of hydrogen and carbon monoxide concentration – Starting from the reference reaction condition corresponding to entry 8, the initial concentration of carbon monoxide and hydrogen have been varied while keeping the concentration of the other components constant. In Figure 6a the results for S_{ald} as a function of the initial concentration of carbon monoxide and hydrogen are shown. From a comparison of the results given in Figure 6a it can be concluded that applying a high carbon monoxide concentration results in the highest aldehyde selectivity over a broad yield range. An increase in the concentration of carbon monoxide results in a decrease of hydroformylation activity and regioselectivity. A similar behavior has been reported by van Leeuwen and co-workers for the bulky phosphite modified rhodium catalyzed hydroformylation of **1a**.^[23] For an initial concentration of 0.75 mol L⁻¹ (entry 11) of carbon monoxide the *n:iso* ratio remains constant at about 2.9 in the yield range of 20 to 80 %. When the hydrogen concentration is varied no clear effect on S_{ald} can be discerned. Compared to the results obtained at the reference reaction conditions (entry 8), both at a lower and at a higher initial hydrogen concentration a lower S_{ald} is observed.

As can be seen in Figure 6b there is also no pronounced effect of the hydrogen concentration on the regioselectivity. However, the hydrogen concentration has a very significant effect on the reaction rate. A higher concentration of hydrogen results in faster

reaction; for the highest initial hydrogen concentration, 1.54 mol L^{-1} , a TOF of $11 \times 10^3 \text{ mol}_{1a} \text{ mol}_{Rh}^{-1} \text{ h}^{-1}$ has been observed (entry 14).

Influence of 1a and catalyst concentration – In Figure 7a the effect of the initial concentration of **1a** and the effect of the catalyst concentration on S_{ald} is shown, while in Figure 7b the effect of the initial concentration of **1a** and the effect of the catalyst concentration on the *n:iso* ratio is shown.

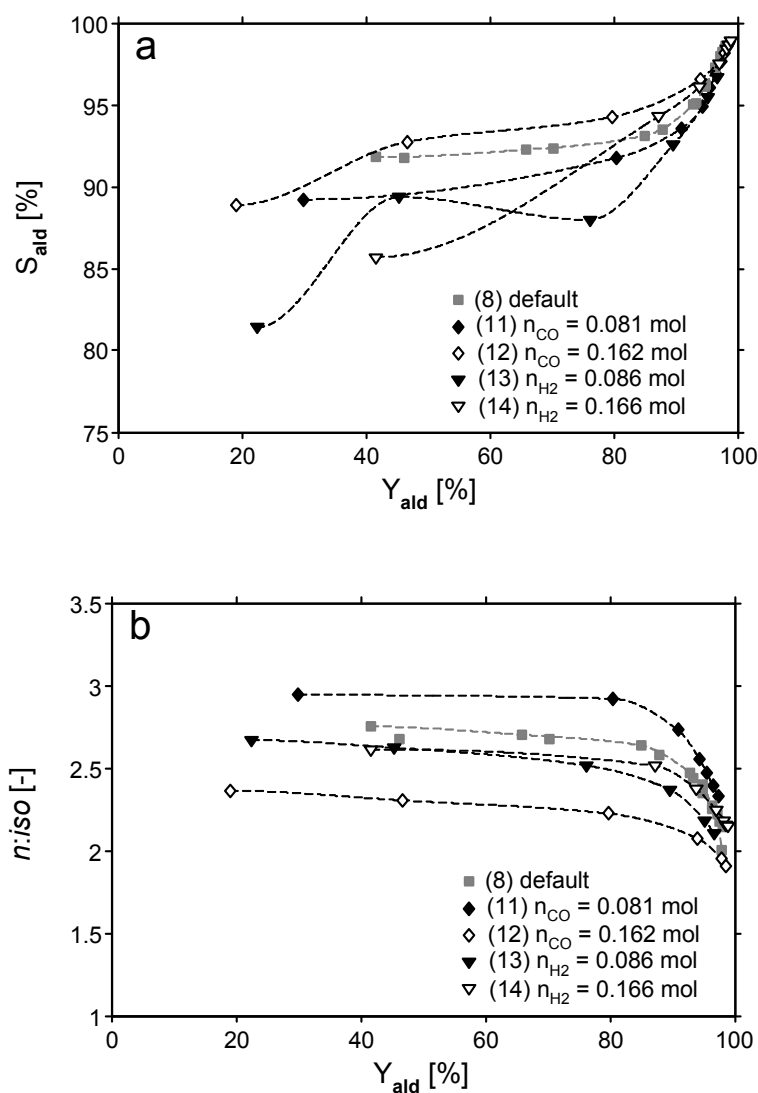


Figure 6. a) The overall selectivity towards aldehydes, S_{ald} , as a function of the yield of aldehydes when the initial concentration of carbon monoxide and hydrogen is varied; b) S_{ald} as a function of Y_{ald} for the case when the initial concentration of **1a** and catalyst is varied.

For an initial **1a** concentration of 1.0 mol L^{-1} (entry 16), and in the lower yield range, the values for Y_{ald} are comparable to the results obtained for the experiment with an initial **1a**

concentration of 0.5 mol L^{-1} (entry 8). However, at high yield ($> 60 \%$) isomerization of **1a** becomes more important because of the low concentration of hydrogen and carbon monoxide, as compared to case with an initial **1a** concentration of 0.11 mol L^{-1} (entry 15). As a result of the lower carbon monoxide concentration, at an aldehyde yield above 50% , the regioselectivity observed in the experiment corresponding with entry 16 ($n_{1a} = 109 \text{ mmol}$) is higher than the regioselectivity corresponding with entry 15 ($n_{1a} = 12.1 \text{ mmol}$).

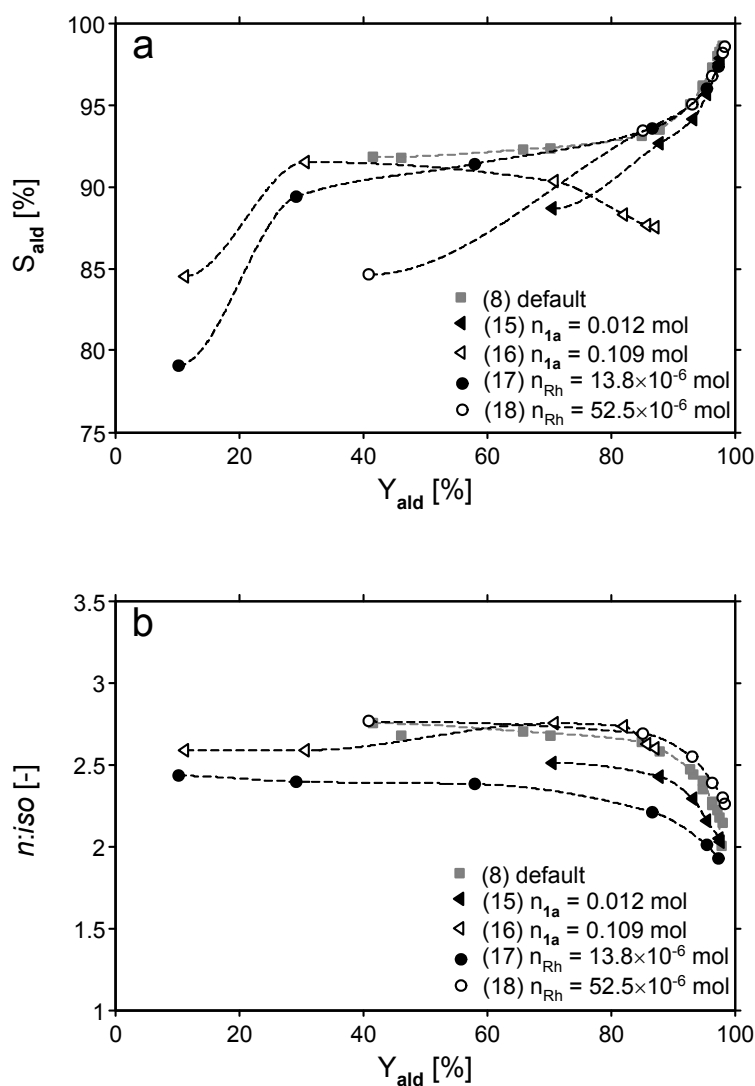


Figure 7. a) the $n:iso$ as a function of Y_{ald} when the initial concentration of carbon monoxide and hydrogen is varied; b) $n:iso$ as a function of Y_{ald} for the case when the initial concentration of **1a** and catalyst is varied.

This means that a variation in the **1a** concentration has a smaller effect on the reaction rate, as compared to a variation the hydrogen concentration (Table 1).

At a catalyst concentration of 1.28×10^{-4} mol L⁻¹ (entry 17) the overall selectivity for the aldehydes is similar to that of the reference concentration of 2.54×10^{-4} mol L⁻¹ (entry 8). At a catalyst concentration of 4.88×10^{-4} mol L⁻¹ (entry 18) the *n:iso* ratio is similar to that of the reference concentration of 2.54×10^{-4} mol L⁻¹ (entry 8). The linear dependence of the reaction rate on the Rh concentration in combination with the improvement of regioselectivity with an increase in ligand concentration can be seen as a confirmation that the catalyst and its precursors are dissolved completely under the conditions applied here.

When the experiments where the reactant and catalyst concentration have been varied (Figures 6 and 7) are compared with the experiments where the temperature has been varied (Figure 4) the same behavior for the regioselectivity as a function of the yield has been observed. Above a yield of about 80 % the *n:iso* shows in all cases a decreasing trend. This behavior for the *n:iso* ratio is mainly caused by the hydroformylation of 2-octene. Additionally, the *n:iso* ratio also decreases at a high aldehyde yield because small quantities of **2c** and **2d** are formed, which can only be the result of the hydroformylation of 3-octene (and possibly 4-octene). It is noted that for entry 16 at a high aldehyde yield this phenomenon is not observed. At a low concentration of hydrogen and carbon monoxide hydroformylation is suppressed and isomerization of the octenes becomes the main reaction.

Conclusions

With respect to the observed reaction rates it can be concluded that carbon monoxide and hydrogen have a clear effect. The effect of **1a** on the reaction rate is less pronounced. The reaction rates increase linearly with increasing concentration of rhodium at a L:Rh of 4:1. A slight increase in reaction rate has been observed when the ligand to rhodium ratio is increased, which is in contrast with the behavior of the well-known HRhCO(PPh₃)₃ catalyst. It appears that for the reaction using the Rh-catalyst based on tris(3,5-bis(trifluoromethyl)phenyl)phosphine the influence of hydrogen, carbon monoxide, and ligand concentration on the activity and selectivity is similar as for the case where a catalyst based on [Rh(CO)₂acac] and a bulky phosphite is used.

Applying a lower CO₂ concentration results in an improvement of regioselectivity but no pronounced change in reaction rate. The regioselectivity is improved when the concentration of catalyst precursors is increased. Increasing the L:Rh ratio enhances the regioselectivity. Compared to the other reactants, carbon monoxide has the most significant

effect on the regioselectivity. Increasing the reaction temperature results in clear increase in the formation rate of aldehydes and 1-octene isomers and in a lower chemo- and regioselectivity. The rhodium catalyst modified with tris(3,5-bis(trifluoromethyl)phenyl)-phosphine has a significantly better activity and regioselectivity as compared to the unmodified or the PPh₃ modified rhodium catalyst.

References

- [1] C. D. Frohning, C. W. Kohlpaintner, H.-W. Bohnen, in *Applied Homogeneous Catalysis with Organometallic Compounds*, 2nd ed., Vol. 1, (Eds.: B. Cornils, W. A. Herrmann), Wiley-VCH, Weinheim, **2002**, p. 31-103.
- [2] C. W. Kohlpaintner, R. W. Fischer, B. Cornils, *Appl. Catal. A* **2001**, *221*, 219-225.
- [3] a) S. Bektsev, A. M. Kleman, A. E. Marteel-Parrish, M. A. Abraham, *J. Supercrit. Fluids* **2006**, *38*, 232-241; b) P. G. Jessop, *J. Supercrit. Fluids* **2006**, *38*, 211-231; c) P. G. Jessop, T. Ikariya, R. Noyori, *Chem. Rev.* **1999**, *99*, 475-493.
- [4] S. Kainz, D. Koch, W. Baumann, W. Leitner, *Angew. Chem. Int. Ed.* **1997**, *15*, 1628-1630.
- [5] D. R. Palo, C. Erkey, *Ind. Eng. Chem. Res.* **1998**, *37*, 4203-4206.
- [6] a) L. J. P. van den Broeke, E. L. V. Goetheer, A. W. Verkerk, E. de Wolf, B.-J. Deelman, G. van Koten, J. T. F. Keurentjes, *Angew. Chem. Int. Ed.* **2001**, *40*, 4473-4474; b) E. L. V. Goetheer, A. W. Verkerk, L. J. P. van den Broeke, E. de Wolf, B.-J. Deelman, G. van Koten, J. T. F. Keurentjes, *J. Catal.* **2003**, *219*, 126-133.
- [7] A. C. J. Koeken, M. C. A. van Vliet, L. J. P. van den Broeke, B.-J. Deelman, J. T. F. Keurentjes, *Adv. Synth. Catal.* **2006**, *348*, 1553-1559.
- [8] Chapter 5 of this thesis.
- [9] S. S. Divekar, B. M. Bhanage, R. M. Deshpande, R. V. Gholap, R. V. Chaudhari, *J. Mol. Catal.* **1994**, *91*, L1-L6.
- [10] T. Davis, C. Erkey, *Ind. Eng. Chem. Res.* **2000**, *39*, 3671-3678.
- [11] D. R. Palo, C. Erkey, *Ind. Eng. Chem. Res.* **1999**, *38*, 2163-2165.
- [12] M. F. Sellin, Ingrid Bach, J. M. Webster, F. Montilla, V. Rosa, T. Avilés, M. Poliakov, D. J. Cole-Hamilton, *J. Chem. Soc. Dalton Trans.*, **2002**, *24*, 4569-4576.
- [13] K. R. Westerterp, W. P. M. van Swaaij, A. A. C. M. Beenackers, *Chemical Reactor Design and Operation*, John Wiley & Sons, Chichester, 2nd edition, **1984**.
- [14] D. R. Palo, C. Erkey, *Organometallics* **2000**, *19*, 81-86.
- [15] A. M. Banet Osuna, W. Chen, E. G. Hope, R. D. W. Kemmitt, D. R. Paige, A. M. Stuart, J. Xiao, L. Xu, *J. Chem. Soc. Dalton Trans.* **2000**, *22*, 4052-4055.
- [16] Y. Guo, A. Akgerman, *Ind. Eng. Chem. Res.* **1997**, *36*, 4581-4585.
- [17] C. B. Roberts, J. E. Chateauneuf, J. F. Brennecke, *J. Am. Chem. Soc.* **1992**, *114*, 8455-8463.
- [18] P. E. Savage, S. Gopalan, T. I. Mizan, C. J. Martino, E. E. Brock, *AIChE J.* **1995**, *41*, 1723-1779.
- [19] Y. Guo, A. Akgerman, *J. Supercrit. Fluids* **1999**, *15*, 63-71.
- [20] J. M. Smith, H. C. Van Ness, M. M. Abbott, *Introduction to Chemical Engineering Thermodynamics*, McGraw-Hill, 5th ed., New York, **1996**, p. 315-365.
- [21] P. Cavalieri d'Oro, L. Raimondi, G. Pagani, G. Montrasi, G. Gregorio, A. Andretta, *Chim. Ind.* **1980**, *62*, 572-579.
- [22] P. W. N. M. van Leeuwen, *Appl. Catal. A* **2001**, *212*, 61-81.
- [23] A. van Rooy, E. N. Orij, P. C. J. Kamer, P. W. N. M. van Leeuwen, *Organometallics* **1995**, *14*, 34-43.
- [24] K. L. Olivier, F. B. Booth, *Hydrocarbon Process.* **1970**, *4*, 112-114.

- [25] P. W. N. M. van Leeuwen, in *Homogeneous Catalysis: Understanding the Art*, Kluwer Academic Publishers, **2004**, Dordrecht, p. 139-174.
- [26] C. K. Brown, G. Wilkinson, *J. Chem. Soc. A* **1970**, *17*, 2753-2764.
- [27] G. Kiss, E. J. Mozeleski, K.C. Nadler, E. van Driessche, C. de Roover, *J. Mol. Catal. A* **1999**, *138*, 155-176.

Chapter 4

Modeling of the kinetics of 1-octene hydroformylation in supercritical carbon dioxide

Abstract

The activity, chemoselectivity, and regioselectivity of the hydroformylation of 1-octene, catalyzed by a supercritical carbon dioxide soluble catalyst have been evaluated. The concentration of reactants, the concentration of catalyst precursors, rhodium(I) dicarbonyl acetylacetonate and tris(3,5-bis(trifluoromethyl)phenyl)phosphine, and temperature has been varied. A kinetic model has been developed, which describes the obtained experimental results. Besides hydroformylation, the kinetic model incorporates isomerization and hydrogenation as side reactions. The catalyst shows a significant isomerization activity while hydrogenation activity is negligible. From the kinetic model a first order dependence on hydrogen and catalyst concentration has been obtained, whereas the dependence on the carbon monoxide concentration can be approximated by negative second order. The obtained kinetics resembles “type II” hydroformylation kinetics. Increasing the ligand to rhodium ratio results in a significant increase in regioselectivity while the catalytic activity shows a small increase. At a temperature of 70 °C and for a ligand to rhodium ratio of 48 a selectivity for nonanal of 70.4% with a *n:iso* ratio of 3.4 and a turn-over-frequency in the order of $12 \times 10^3 \text{ mol}_{1\text{-octene}} \text{ mol}_{\text{Rh}}^{-1} \text{ h}^{-1}$ has been obtained.

Introduction

Supercritical fluids have received considerable attention as alternative solvents for the hydroformylation of long-chain alkenes, including 1-octene.^[1] Carbon dioxide is of particular interest since it has accessible critical properties, is nonflammable, and has a low toxicity. Furthermore, by using carbon dioxide as the solvent a one-phase reaction system can be created, in which optimal use can be made of the characteristics of a supercritical fluid. This includes the absence of phase boundaries, the high diffusivity of the different species, and the high solubility of gaseous reactants.

One of the restrictions of applying supercritical carbon dioxide, scCO₂, as a solvent is the limited solubility of common homogeneous catalysts in this medium. For Wilkinson type hydroformylation and hydrogenation catalysts this drawback has been overcome by attaching perfluoroalkyl groups to the para or meta positions of the triphenylphosphine ligands.^[2-6] The “tunability” of the supercritical solvent properties by relatively small changes in temperature and pressure allows the precipitation and reuse of these fluorinated catalysts.^[2,3]

Davis and Erkey studied the influence of reactant and ligand concentration on the hydroformylation of 1-octene at temperatures of 40 and 50 °C at a constant total pressure.^[7] When the initial concentration of reactant was varied, the CO₂ concentration was changed simultaneously in order to obtain the same initial total pressure. By this means the thermodynamic effect of total pressure was similar for each of their experiments. This effect that absolute pressure can have on the reaction rate constant of an elementary reaction is based on the transition state theory.^[8] In several studies it has been observed that in particular the regioselectivity is affected by CO₂ pressure.^[9-11] However, it is not proven that this phenomenon is a result of a thermodynamic effect related to the absolute pressure. Other effects of CO₂ on the Rh-catalyzed hydroformylation reaction could be caused by chemical interaction of CO₂ with Rh^[12] or oxidation of the phosphine ligand by CO₂ or impurities.^[13]

Here we present a detailed description of the reaction kinetics of the hydroformylation of 1-octene carried out in scCO₂ (Figure 1). Based on the “chemical” effects CO₂ might have on the catalysis, keeping the concentration of CO₂ constant instead of the total pressure would also be logical. In our approach for all hydroformylation experiments the carbon dioxide concentration is the same, in the order of 14.5 mol L⁻¹, to achieve a similar effect of CO₂ on the catalysis in each experiment. As a consequence, when the concentration of the reactants was varied the initial total pressure varied.

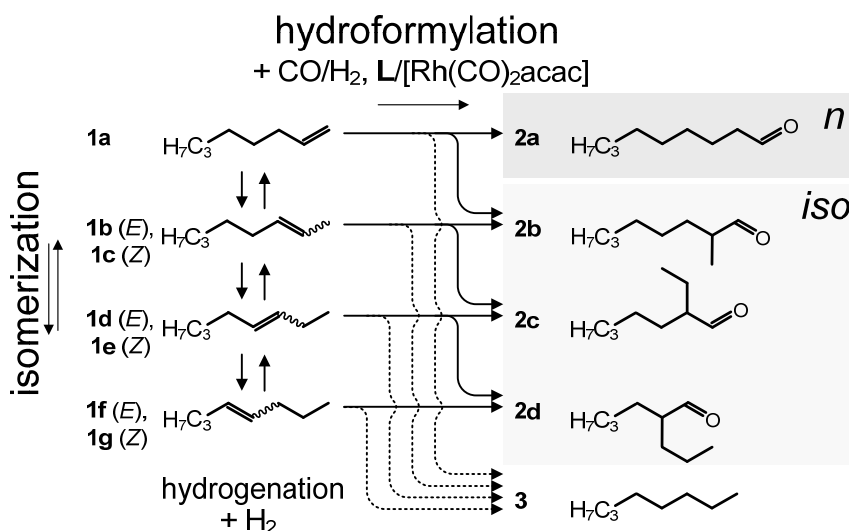


Figure 1. Reaction scheme for the hydroformylation of 1-octene (**1a**), with the two main products nonanal (**2a**) and 2-methyloctanal (**2b**). The side products are (*E,Z*)-2-octene (**1b**, **1c**), (*E,Z*)-3-octene (**1d**, **1e**), (*E,Z*)-4-octene (**1f**, **1g**), 2-ethylheptanal (**2c**), 2-propylhexanal (**2d**), and n-octane (**3**).

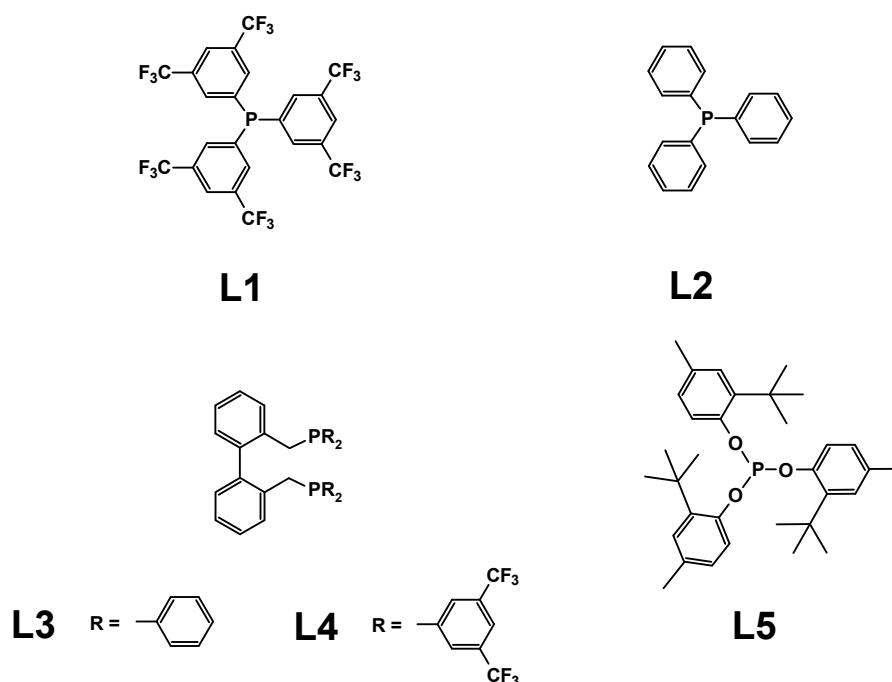


Figure 2. Tris(3,5-bis(trifluoromethyl)phenyl)phosphine (**L1**); triphenylphosphine (**L2**); 2,2'-bis-((diphenylphosphino)methyl)-1,1'-biphenyl (BISBI; **L3**); 2,2'-Bis{[bis-{3,5-di(trifluoromethyl)phenyl}phosphino)methyl]-1,1'-biphenyl, (BISBI-(3,5-CF₃), **L4**); tris(2-tertbutyl-4-methylphenyl)phosphite (**L5**).

To evaluate the kinetic model the effect of the concentration of the reactants, hydrogen, carbon monoxide, and 1-octene, and the concentration of the catalyst precursors, rhodium(I) dicarbonyl acetylacetonate and tris(3,5-bis(trifluoromethyl)phenyl)phosphine (**L1** in Figure 2), has been investigated. In particular, the kinetic model is used to describe the change in the observed reaction rates and selectivity as a function of the concentration of reactants and catalyst precursors. The concentration of **1a**, **1a** isomers, and the aldehyde products have been obtained as a function of time for hydroformylations carried out at temperatures in the range of 40 to 80 °C, and up to pressures of about 50 MPa.

Hydroformylation and isomerization mechanism - In Figure 3 the generally accepted mechanism of hydroformylation is depicted. It is based on the reaction mechanisms suggested by Wilkinson and co-workers for the starting compound $\text{HRhCO}(\text{PPh}_3)_3$ ^[14], and by Heck based on the starting compound $\text{HCo}(\text{CO})_4$ ^[15]. The so-called faster dissociative pathway with sequence **C2a-C3a-C4a-C5a-C6a-C7a**, as opposed to the slow associative pathway through sequence **C2a-C2b-C3b-C5a-C6a-C7a**, has been generally accepted as the main route for the hydroformylation of alkenes. L represents the triphenylphosphine ligand (**L2** in Figure 2) coordinated by a metal-phosphorous bond. Starting from **C1** or **C2b**, the first step is the dissociation of L or CO, respectively, to form the very reactive intermediate **C2a**. An alkene coordinates then to **C2a** and this results in complex **C3a**. Through migratory insertion of the alkene into the Rh-H bond complex **C4a** is formed. Subsequently, CO coordinates to **C4a**, which results in **C5a**. The second migration of CO into the Rh-alkyl bond then can take place to form **C6a**. Then oxidative addition of hydrogen takes place to form **C7a** followed by reductive elimination resulting in the aldehyde product and the intermediate **C2a**. **C2a** undergoes then a fast coordination with either L, CO, or alkene to form again **C1**, **C2b**, or **C3a**, respectively. This is still a “simplified” scheme, for a more detailed discussion the reader is referred to references [16,17] and references therein.

Besides the formation of linear aldehydes from primary linear alkenes, a certain amount of branched aldehydes is formed. The mechanism of the most important formation routes of branched aldehydes is depicted in Figure 4. The insertion of the alkene can also occur such that, out of **C3a**, **C4c** is formed.^[18] **C4c** leads to the formation of, for example, 2-methyloctanal when 1-octene is the alkene. Through hydrogen-elimination **C4c** is converted into **C3c**. Dissociation of the alkene from **C3c** then yields the internal alkene. The internal alkene in turn can coordinate with **C2a** resulting in further isomerization or hydroformylation.

Accordingly, for **1a** these mechanisms result in the products presented in Figure 1. Another side reaction, which is presented in Figure 4 is the hydrogenation reaction. When oxidative addition of hydrogen occurs to species **C4a**, **C4d** is formed that through reductive elimination results in an alkane.^[19] Hydrogenation can also occur through species **C4c**.

Catalyst selectivity - The use of triphenylphosphine has a positive influence on the selectivity of the hydroformylation catalyst towards the linear aldehyde product, which is the desired product in most of the applications.^[9,17] To obtain the optimum selectivity towards the linear product, the occurrence of intermediate **C2a** has to be maximized. This is achieved by applying a high **L2** concentration in combination with a low carbon monoxide concentration. Applying a high **L2** concentration also implies an increase in concentration of inactive **C1**, which can decelerate the reaction. At a low **L2** concentration and a high carbon monoxide concentration other species can be formed, which are also active for hydroformylation. The intermediate **C2c** (Figure 5) is an example of a species that is formed under these conditions and is also active in hydroformylation. Hydroformylation through **C2c** is less selective, because there is less steric hindrance around the metal centre resulting in a larger portion of the **C4c** type intermediate.

The stereochemistry around the metal centre is another aspect that can influence the selectivity. The species **C2b** gives rise to the highest selectivity for the linear product, but **C2b** is in equilibrium with a number of other species (Figure 5). **C2b**, with two phosphine ligands in the equatorial position, is in equilibrium with its isomer **C2d**, with one ligand in equatorial position and one ligand in the apical position, but these isomers give rise to differences in selectivity, because of the difference in coordination of the ligands to the metal centre. The development of diphosphines, which coordinated mainly in the “bisequatorial” manner, such that only a “**C2a** type” intermediate takes part in the catalysis, was an important breakthrough in the search for more selective hydroformylation catalysts.^[16,17,20] Rhodium catalysts with diphosphines coordinated in the bisequatorial position give rise to high linear to branched ratios.^[21,22] **L3** and **L4** (Figure 2) are two examples of such diphosphines.

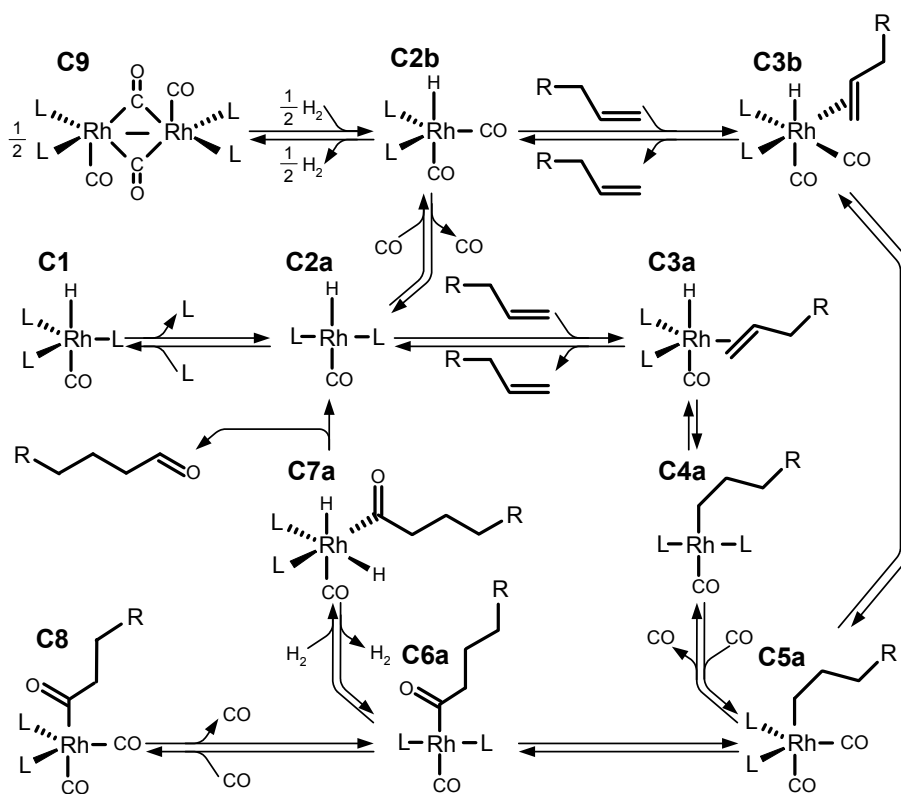


Figure 3. The generally accepted mechanism of the rhodium-catalyzed hydroformylation reaction. R is $-C_5H_{11}$ for 1-octene.

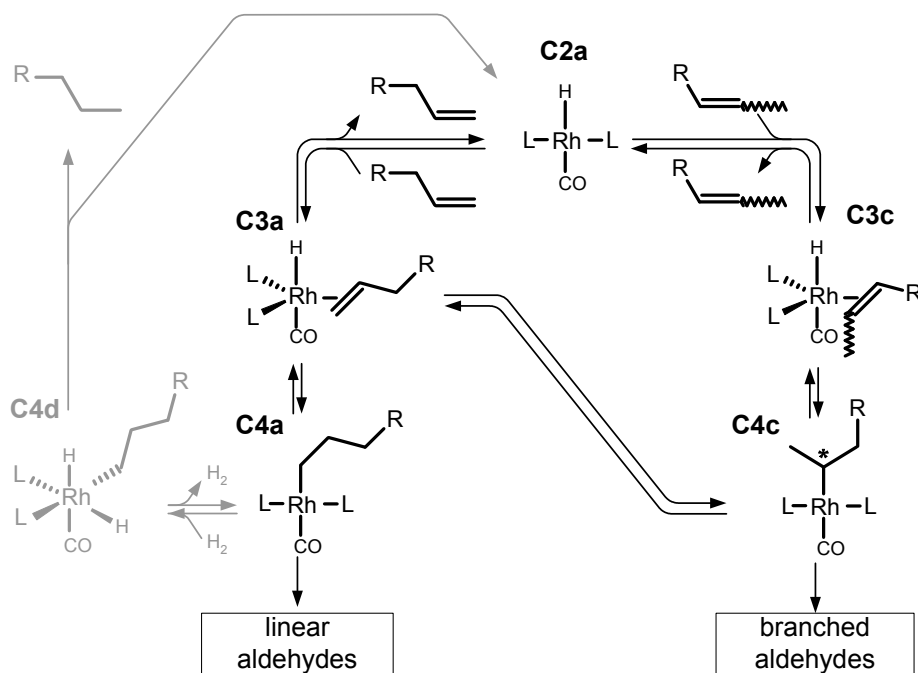


Figure 4. A simplified version of the mechanism of the formation of branched aldehydes, alkene isomerization and alkene hydrogenation. R is $-C_5H_{11}$ for 1-octene.

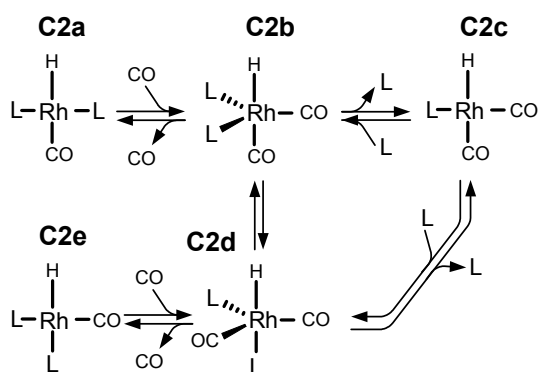


Figure 5. Equilibria between different catalytic species.

Catalyst activity - In the mechanism given in Figure 3 the dissociative pathway yields the highest activity. From this mechanism the effect of reactant concentration and concentration of the catalyst precursors can be anticipated. In particular, variation in CO or ligand concentration will have a significant effect on the presence of active intermediates. Starting with **C2a**, an increase in the ligand or CO concentration leads to more **C1** or more **C2b**, respectively. Additionally, an increase in CO concentration will lead to more **C8**, which is in equilibrium with **C6a**. The species **C1**, **C2b**, and **C8** are saturated complexes, and are therefore “inactive” species in terms of catalytic activity. As a consequence, an increase in ligand or CO concentration will lead to a lower activity, also because of a decrease in concentration of the reactive **C2a** and **C6a** intermediates.

The influence of electron withdrawing substituents - It is well-established that triphenylphosphines with electron withdrawing substituents on the aryl ring, like the trifluoromethyl group, lead to a faster catalytic reaction as compared to the well-known triphenylphosphine (**L2**).^[6,17,23-26] A similar behavior has been found for diphosphines, **L4** is more active than **L3**.^[27,28] Additionally, by applying trifluoromethyl-substituted phosphines, like **L1** or **L4**, the regioselectivity towards the linear product is enhanced when a linear alkene is applied as the reactant.

Rate equations - A number of empirical models for the reaction rate of the hydroformylation with Rh-catalysts have been proposed.^[16] Van Leeuwen and co-workers discussed two types of rate equations, I and II, as starting point for the modeling of the reaction kinetics.^[17,29,30]

$$R_1 = \frac{p_1 [\text{alkene}][\text{Rh}]}{p_2 + [\text{Ligand}]} \quad (1)$$

$$R_{II} = \frac{p_3 [H_2] [Rh]}{p_4 + [CO]} \quad (2)$$

where p_1 to p_4 are constants.

It should be noted that the kinetic expressions for homogeneous catalysis are based on the concentrations of the reactants in the, usually liquid, reaction phase (where also the catalyst is present). The generally accepted rate equation is R_I , for which alkene coordination or the insertion of the alkene into the Rh-H bond can be considered to be the rate-determining step, i.e. the sequence **C2a-C3a-C4a**. Type I kinetics is associated with Rh-catalysts modified with **L2**. Type II kinetics, which is considered less common, corresponds best to the kinetics observed for Rh-catalysts with CO and bulky phosphites, like **L5** in Figure 2. For type II kinetics the rate-determining step is considered to be the oxidative addition of hydrogen, i.e. the sequence **C6a-C7a**.

Deshpande and Chaudhari have proposed a kinetic expression for the hydroformylation of 1-hexene with $HRhCO(L2)_3$ as the catalyst precursor.^[31]

$$R = \frac{p_5 [CO] [H_2] [alkene] [Rh]}{(1 + p_6 [CO])^{p_7} (1 + p_8 [alkene])^{p_9}} \quad (3)$$

with p_5 to p_9 constants.

Davis and Erkey postulated an expression for the rate of disappearance of **1a** using the catalyst precursor $HRhCO(L1)_3$.^[7]

$$R = \frac{0.588 [H_2]^{0.83} [alkene]^{0.40} [Rh]^{0.94}}{1 + 0.98 [CO]^{1.61}} \quad (4)$$

It is noted that for this equation R is in $\text{mol L}^{-1} \text{s}^{-1}$. This rate equation is valid in the temperature range of 40 - 50 °C. For a temperature below 50 °C isomerization activity is low, and as a consequence isomerization as a side reaction is not taken into account.^[7,9]

Experimental

Materials - Carbon dioxide, carbon monoxide, and hydrogen, grade 5.0, 4.7, and 5.0, respectively, were obtained from Hoekloos (The Netherlands). Prior to use CO_2 was passed over a Messer Oxisorb filter to remove oxygen and moisture. 1-Octene, **1a**, obtained from Aldrich, was passed over activated alumina, dried with pre-treated molsieves 3A (Aldrich, 4-8 mesh), and stored under argon.

The rhodium precursor, rhodium(I) dicarbonyl acetylacetonate, ([Rh(CO)₂acac]), was obtained as dark green crystals from Fluka. Ligand **L1**, tris(3,5-bis(trifluoromethyl)phenyl)-phosphine, is a white to light yellow solid and was supplied by Arkema (Vlissingen, The Netherlands). All catalyst precursors were stored under argon and manipulated using Schlenk techniques.

The solvent toluene (Merck, analytical grade), the internal standard *n*-decane (Aldrich, >99% purity) and the substances involved in the reaction, *n*-octane (Aldrich, > 99%), 2-octene (ABCR, mixture of E and Z, 98%), and nonanal (Fluka, > 95%) used for the GC-analysis were used as received.

Hydroformylation in scCO₂ - The general procedure for a hydroformylation experiment was started by charging the desired amounts of [Rh(CO)₂acac] and the fluorinated phosphine ligand into the empty reactor and subsequently closing the reactor. The details of the high-pressure batch reactor setup are described in Chapter 2. The reactor volume was carefully flushed with argon and subsequently evacuated for three times. Next, the stirring was turned on with a stirring rate of 700 rpm and the desired amount of carbon monoxide and hydrogen gas was fed to the reactor at room temperature. The reactor content was heated to a temperature of 50 °C, and consecutively CO₂ was charged into the reactor at a constant flow typically up to a total pressure such that about 14.5 mol L⁻¹ CO₂ was present. In the case when 1 mol L⁻¹ of CO, 1 mol L⁻¹ of H₂, and 14.5 mol L⁻¹ of CO₂ was applied this corresponded to about 26 MPa total pressure at 50 °C. When the CO and H₂ concentration were varied, the total reactor pressure required to achieve a CO₂ concentration of 14.5 mol L⁻¹ at 50 °C was estimated using the Peng-Robinson equation of state and the input parameters as stated in Chapter 2. Then, these conditions were maintained for at least half an hour before heating further to the desired reaction temperature. In total a period of about 1 h was considered to allow the active catalyst complexes to be formed in situ from the [Rh(CO)₂acac] and **L1**. The reaction was started by the addition of the **1a**, which was done by opening the valve between the pump and the reactor. A fast pressure equalisation occurred and consecutively the desired volume of **1a** was pumped into the reactor, which as a rule did not take more than 30 s. While pumping **1a** the reactor temperature increased as a result of a fast pressure increase and the start of the reaction. The temperature usually stabilized within 15 min. During the remainder of reaction the reactor temperature was maintained within a deviation of less than 1 °C from the desired temperature.

Samples were withdrawn from the high-pressure mixture. The content of the sample volume was carefully bubbled through a vial with a solution of *n*-decane in toluene and afterwards rinsed with additional toluene solution to collect **1a** and its reaction products quantitatively. Subsequently, the sample volume was dried by alternately applying an argon flow and vacuum. The minimum time of taking a sample and preparing for a next one was in the order of 10 min. A reaction time of three hours was considered, after which the mixture was rapidly cooled, the gases were vented and the remaining liquids consisting of reaction products and catalyst were collected.

Sampling was done from either the top or bottom of the reactor, and this was also used to verify that the reaction mixture was always a homogeneous supercritical phase. To ensure that the reactor was cleaned properly, blank reaction runs were performed regularly at reaction conditions. The concentration of catalyst precursors were chosen such that catalytic complexes would dissolve completely for the conditions applied here.

In Table 1 the different experiments are specified in terms of the amount of reactants used. The concentrations used in the various experiments were obtained by using the reactor volume of 0.1076 L.

Analysis and calibration - The samples were analyzed off-line using a Fisons Instruments GC-FID equipped with a Restek Rtx-5 column (fused silica, length 30 m, internal diameter 0.53 mm) with helium as the carrier gas. Calibration was done for **1a**, **1b**, **1c**, **3** and **2a**, the sensitivity coefficients for the other octene and aldehyde isomers were taken to be equal to those of **1a** and **2a**, respectively.

Reaction parameters - To obtain normalized concentration profiles for **1a** and its reaction products, each concentration obtained by GC analysis was divided by the sum of all obtained concentrations:

$$[i]_n = \frac{[i]}{\sum [i]} \quad (5)$$

where $i = \mathbf{1a-1g}$, $\mathbf{2a-2d}$ and $\mathbf{3}$, and the subscript n refers to the normalized values.

The activity and selectivity of the different catalytic complexes was expressed in one of the following parameters. The definitions used were based on Westerterp et al.^[32] The conversion, X , was given by:

$$X = \frac{[\mathbf{1a}]_{n,0} - [\mathbf{1a}]_n}{[\mathbf{1a}]_{n,0}} \times 100\% \text{ with } [\mathbf{1a}]_{n,0} = 1 \quad (6)$$

The overall selectivity, S_j , towards a product j was defined as:

$$S_j = \frac{[j]_n}{[\mathbf{1a}]_{n,0} - [\mathbf{1a}]_n} \times 100\% \quad (7)$$

where $j = \mathbf{1b-1g}$, $\mathbf{2a-2d}$ and $\mathbf{3}$.

The overall yield, Y_k , for a product k was then:

$$Y_k = \frac{[k]_n}{[\mathbf{1a}]_{n,0}} \times 100\% \quad (8)$$

The substrate to catalyst ratio, S/C , was calculated as follows:

$$\frac{S}{C} = \frac{m_{\mathbf{1a}} \cdot MW_{Rh}}{m_{Rh} \cdot MW_{\mathbf{1a}}} \quad (9)$$

with $m_{\mathbf{1a}}$ the mass of $\mathbf{1a}$ injected, $MW_{\mathbf{1a}}$ the molar mass of $\mathbf{1a}$, and m_{Rh} and MW_{Rh} the mass conveyed to the reactor and the molar mass of the rhodium precursor, respectively.

The turn-over-number based on the conversion of $\mathbf{1a}$, $TON_{\mathbf{1a}}$, was calculated as follows:

$$TON_{\mathbf{1a}} = \frac{S}{C} \cdot X \quad (10)$$

The “initial” overall rate of reaction for component R_p (with $p=\mathbf{1a}$, $\mathbf{2a}$, $\mathbf{2a-2d}$) was calculated by multiplying the initial amount of $\mathbf{1a}$ in mol, $n_{\mathbf{1a},0}$, with the slope of a line fitted through the conversion or yield data points up to a conversion where there was a linear trend (typically up to a conversion of 0.6). A distinction is made between the linear aldehyde product, $\mathbf{2a}$, and total amount of aldehydes, $\mathbf{2a-2d}$, abbreviated as “ald”.

The n : iso ratio was obtained by dividing the concentration of linear aldehyde product by the sum of the concentrations of the branched aldehyde products:

$$n : iso = \frac{[\mathbf{2a}]_n}{[\mathbf{2b}]_n + [\mathbf{2c}]_n + [\mathbf{2d}]_n} \quad (11)$$

Kinetic model

For the construction of a kinetic model for the hydroformylation of $\mathbf{1a}$, the reactants and products shown in Figure 1 were grouped in **A** (carbon monoxide), **B** (hydrogen), **Rh** (rhodium precursor), **D** ($\mathbf{1a}$), **E** ($\mathbf{1b-1g}$), **F** ($\mathbf{2a}$), **G** ($\mathbf{2b-2d}$) and **H** ($\mathbf{3}$). The main components of group **E** and **G** are $\mathbf{1b}$ and $\mathbf{1c}$, and $\mathbf{2b}$, respectively. The other isomers, $\mathbf{1d}$ to $\mathbf{1g}$, were also

present but in very small amounts. As a result, it was difficult to obtain an accurate description of the isomerization of, for example, **1b** and **1c** towards **1d** and **1e**. Therefore, to simplify the model the according isomers were lumped in one group.

The concentration profiles of carbon monoxide and hydrogen were determined from their initial concentration and the stoichiometry of the reactions. Furthermore, from the results for the chemo- and regioselectivity reported in chapter 3 it was obvious that isomerization of **1a** had to be incorporated as a side reaction. Hydrogenation of the octenes was also taken into account in the model as a possible reaction step. However, it was noted that concentration of *n*-octane found in the experiments usually was considerably smaller than the sum of the concentration of octene isomers. The reaction network is illustrated in Figure 6. The model allows a description of the *n*:*iso* ratio, because the formation of linear (**F**) and branched aldehydes (**G**) are considered separately.

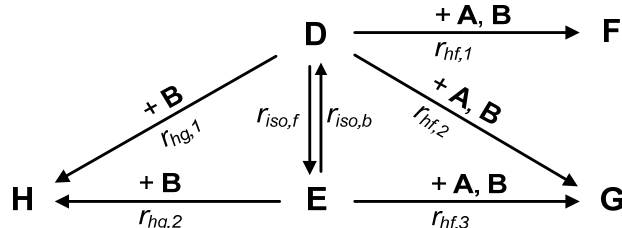


Figure 6. Reaction network. The rate expressions $r_{hf,1}$, $r_{hf,2}$, $r_{hf,3}$, $r_{iso,f}$, $r_{iso,b}$, $r_{hg,1}$, and $r_{hg,2}$ are defined in equations 12 to 18.

The empirical rate equation for the hydroformylation reaction was adapted from [31]. Additionally, the influence of the ligand concentration was taken into account. As illustrated in chapter 3 an increase in ligand concentration had a moderately positive effect on the reaction rate and the selectivity, but no pronounced effect on the isomerization rate of **1a**. The concentration of rhodium and ligand were considered to be constant during the reaction. Based on the nomenclature for the reaction rate constants, k_i , given in Figure 6, the following set of equations is proposed:

$$r_{hf,n} = \frac{k_{hf,n} [A][B]^\beta [D][Rh]^\delta (1 + K_{L,n} [L])}{(1 + K_{A,n} [A])^\alpha (1 + K_D [D])^\gamma}, \quad n = 1, 2. \quad (12, 13)$$

$$r_{hf,3} = \frac{k_{hf,3} [A][B]^\beta [E][Rh]^\delta}{(1 + K_{A,3} [A])^\alpha (1 + K_D [E])^\gamma (1 + K_{L,3} [L])} \quad (14)$$

The isomerization reactions were regarded as first order in rhodium (**Rh**) and octene (**D** or **E**):

$$r_{iso,f} = k_{iso,f} [\mathbf{D}][\mathbf{Rh}] \quad (15)$$

$$r_{iso,b} = k_{iso,b} [\mathbf{E}][\mathbf{Rh}] \quad (16)$$

The kinetics of the hydrogenation reactions were approximated by a first order reaction in hydrogen (**B**), octene (**D** or **E**) and rhodium (**Rh**):^[33]

$$r_{hg,1} = k_{hg,1} [\mathbf{B}][\mathbf{D}][\mathbf{Rh}] \quad (17)$$

$$r_{hg,2} = k_{hg,2} [\mathbf{B}][\mathbf{E}][\mathbf{Rh}] \quad (18)$$

where the subscripts hf, iso, and hg refer to hydroformylation, isomerization, and hydrogenation, respectively.

The mass balances for the reactants and products are given by:

$$\frac{d[\mathbf{A}]}{dt} = -r_{hf,1} - r_{hf,2} - r_{hf,3} \quad (19)$$

$$\frac{d[\mathbf{B}]}{dt} = -r_{hf,1} - r_{hf,2} - r_{hf,3} - r_{hg,1} - r_{hg,2} \quad (20)$$

$$\frac{d[\mathbf{D}]}{dt} = -r_{hf,1} - r_{hf,2} - r_{hg,1} - r_{iso,f} + r_{iso,b} \quad (21)$$

$$\frac{d[\mathbf{E}]}{dt} = -r_{hf,3} - r_{hg,2} + r_{iso,f} - r_{iso,b} \quad (22)$$

$$\frac{d[\mathbf{F}]}{dt} = r_{hf,1} \quad (23)$$

$$\frac{d[\mathbf{G}]}{dt} = r_{hf,2} + r_{hf,3} \quad (24)$$

$$\frac{d[\mathbf{H}]}{dt} = r_{hg,1} + r_{hg,2} \quad (25)$$

$$\frac{d[\mathbf{Rh}]}{dt} = \frac{d[\mathbf{L1}]}{dt} = 0 \quad (26)$$

For the input values of the model, first the concentrations obtained with GC analysis (in mol L⁻¹) were normalized, see equation 5. Subsequently, the normalized concentrations were multiplied with the initial concentration based on the amount of **1a** injected and the volume of the reactor. This was done to cancel out the effect of scattering in the total concentration obtained by GC-analysis.

For all computations Matlab software was used. The mass balances were integrated numerically using the ODE solver “ode23tb.m”. This solver uses an implicit Runge-Kutta formula, with a trapezoidal rule step and a second stage that is a backward differentiation

formula (TR-BDF2). The sum of squares (SSQ) was minimized using the script 'lsqnonlin.m'. This function uses a trust-region reflective Newton method to calculate the optimal set of parameters associated with the minimum value of SSQ.

The SSQ was minimized for the experiments at 70 °C in which 1.6 mol of CO₂ and ligand was applied. This corresponded to entries 4 to 17 in Table 1, which corresponded to 17 experiments where a total of 114 samples were taken as a function of time. The SSQ was the sum of 798 values as there were 7 concentration values ([A] to [H]) evaluated.

Results and discussion

In Table 1 the conditions and main results of hydroformylation of **1a** in a CO₂- enriched supercritical one-phase system are shown. At a temperature of 70 °C the influence of (initial) concentration of reactants, catalyst precursors, and solvent has been investigated. At a L:Rh of 4 the reaction temperature has been varied from 40 to 80 °C.

Evaluation of the kinetic model - The parameter values yielding the minimum SSQ, the so-called residual sum of squares (RSS), with a value of 0.1552 mol² L⁻², are given in Table 2. From the confidence intervals in Table 2 it can be deduced that the significance of the hydrogenation of octenes and the isomerization of internal octenes (**1b** to **1g**) towards **1a** is small. The value of K_{L,3} implies that there is a strong influence of ligand concentration on the hydroformylation of the internal alkenes. The values calculated for K_{L,1}, K_{L,2} and K_{L,3} are in agreement with the observation that an increase in ligand concentration enhances the regioselectivity towards **2a**.

The hydroformylation of **1a** appears to be first order in catalyst and hydrogen concentration based on the values of β and δ , respectively. Carbon monoxide has a negative reaction order of approximately 2 at high concentration. The reaction order of carbon monoxide in the hydroformylation of internal octenes is positive as the value of K_{A,3} is zero. The influence of octene concentration is more subtle; at high concentration octene appears to have a reaction order closer to zero.

Table 1. Overview of experimental conditions and main results

entry ^[a]	T [°C]	P _{max} ^[b] [MPa]	n _{CO2} [mol]	n _{CO} [10 ⁻³ mol]	n _{H2} [10 ⁻³ mol]	n _{Ia} [10 ⁻³ mol]	n _{Rh} [10 ⁻⁶ mol]	L:Rh	R _{Ia,0} [c]	R _{ald,0} [d]	R _{2a,0} [e]	TOF _{Ia,0} [f]	X ^[g] [%]	n:iso ^[g] [-]	S _{2a} ^[g] [%]	S _{ald} ^[g] [%]	S _{Ib- Ic} ^[g] [%]	S ₃ ^[g] [%]
1	40	27.4	1.6	108	108	54.5	26.3	4.1	2.7	2.6	1.9	0.36	53.4	2.9	71.9	97.0	2.4	0.5
2	50	31.4	1.6	109	108	54.5	27.2	3.9	7.1	6.8	5.0	0.94	97.6	2.6	71.1	98.3	1.4	0.3
3 ^[h]	60	36.2	1.6	107	107	54.7	27.2	4.0	18	16	12	2.3	99.0	2.4	69.6	98.9	0.6	0.4
4 ^[k]	70	40.6	1.6	107	107	55.2	27.3	4.0	37	34	25	4.9	99.4	2.1	66.5	98.5	0.9	0.5
5 ^[k]	70	40.7	1.6	105	108	55.3	27.2	10	46	42	32	6.0	99.4	2.5	70.8	98.8	0.8	0.4
6 ^[k]	70	40.2	1.6	108	108	54.2	27.2	50	54	50	39	7.2	99.4	3.2	75.5	98.8	0.8	0.3
7	70	39.0	1.6	81	108	54.4	27.7	3.9	48	44	33	6.2	99.7	2.3	68.3	97.7	1.5	0.9
8	70	44.5	1.6	162	111	55.0	29.3	3.7	29	27	19	3.6	99.8	1.9	64.8	98.8	0.7	0.5
9	70	38.2	1.6	109	86	55.0	26.6	4.0	29	26	19	4.0	99.9	2.1	65.6	96.7	2.2	1.1
10	70	44.0	1.6	109	166	54.7	26.6	4.0	78	68	49	11	99.9	2.1	67.6	99.1	0.3	0.7
11	70	34.5	1.6	109	110	12.1	27.3	3.9	30	27	19	4.0	99.9	2.0	65.5	97.8	1.5	0.7
12	70	52.3	1.6	109	110	109	26.6	4.0	48	43	32	6.5	99.5	2.6	63.4	87.7	10.2	2.1
13	70	40.2	1.6	108	111	55.4	13.8	4.0	20	18	12	5.2	≈100	1.9	64.4	97.8	1.4	0.8
14	70	40.2	1.6	109	110	55.1	13.8	7.5	21	19	13	5.4	99.9	2.2	67.3	97.9	1.2	0.8
15	70	39.5	1.6	109	109	54.8	52.5	4.1	93	79	58	6.4	99.9	2.3	68.3	98.5	0.9	0.6
16	70	50.8	1.6	108	108	105	28.1	48	92	73	56	12	99.1	3.4	70.4	91.1	6.6	2.4
17	70	50.2	1.6	108	108	105	53.8	50	147	132	105	9.8	99.2	3.3	69.6	90.5	6.1	3.3
18 ^[k]	80	44.8	1.6	108	107	54.9	27.8	4.0	52	45	33	6.7	99.4	2.0	65.2	97.2	1.8	1

^[a] General conditions: V_{reactor} = 0.1076 L, stirrer speed = 700 rpm. ^[b] Maximum reactor pressure reached upon injection of **1a**. ^[c] [10⁻⁶ mol_{Ia} s⁻¹]. ^[d] [10⁻⁶ mol_{ald} s⁻¹]. ^[e] [10⁻⁶ mol_{2a} s⁻¹]. ^[f] [10³ mol_{Ia} mol_{Rh} h⁻¹]. ^[g] Values after approximately three hours of reaction. ^[h] Catalyst preformation was done on the previous day. Conditions: 2 MPa (at 20 °C) 1:1 syngas, in CO₂ at a total pressure of 18 MPa and 50 °C for one hour at 700 rpm stirrer rate. After careful depressurization the catalyst was stored overnight under argon atmosphere. The different procedure did not result in significant different reaction kinetics. ^[k] Duplicate experiments.

Table 2. Overview of parameter values obtained from a fit of the equations for the reaction rate, equations 12 to 18, to the experimentally determined concentrations.

Parameter	Value	95% confidence region		Unit
		lower	upper	
$k_{hf,1}$	118	76	159	$L^{1+\beta+\delta} \text{mol}^{-1-\beta-\delta} \text{s}^{-1}$
$k_{hf,2}$	50.0	28.4	71.7	$L^{1+\beta+\delta} \text{mol}^{-1-\beta-\delta} \text{s}^{-1}$
$k_{hf,3}$	2.60	1.23	3.97	$L^{1+\beta+\delta} \text{mol}^{-1-\beta-\delta} \text{s}^{-1}$
$K_{A,1}$	2.11	1.53	2.70	$L \text{mol}^{-1}$
$K_{A,2}$	2.41	1.68	3.14	$L \text{mol}^{-1}$
$K_{A,3}$	0	-0.2	0.2	$L \text{mol}^{-1}$
K_D	0.95	0.37	1.54	$L \text{mol}^{-1}$
$K_{L,1}$	33.0	30.0	36.0	$L \text{mol}^{-1}$
$K_{L,2}$	12.2	7.9	16.5	$L \text{mol}^{-1}$
$K_{L,3}$	60.7	8.4	113.1	$L \text{mol}^{-1}$
α	3.26	2.92	3.60	-
β	1.05	0.99	1.11	-
γ	2.20	1.25	3.14	-
δ	0.929	0.896	0.962	-
$k_{iso,f}$	0.494	0.455	0.534	$L \text{mol}^{-1} \text{s}^{-1}$
$k_{iso,b}$	0	-0.04	0.04	$L \text{mol}^{-1} \text{s}^{-1}$
$k_{hg,1}$	0.027	0.019	0.035	$L^2 \text{mol}^{-2} \text{s}^{-1}$
$k_{hg,2}$	0.318	0.203	0.432	$L^2 \text{mol}^{-2} \text{s}^{-1}$

In Figure 7a the residual errors of **D** and **E** are shown as function of aldehyde yield, and in Figure 7b the residual errors of **F** and **G** are shown. As the concentrations of **D** and **F** are higher than those of **E** and **G** the corresponding residual errors are also higher. Except for a residual error of 0.1 mol L^{-1} for **D** at Y_{ald} of 0.3 most of the residual errors are between -0.05 and 0.05 mol L^{-1} . In the range of Y_{ald} from 0 to 0.8 the largest residuals are observed for **D**. In Figure 7b it is shown that the residual errors at a high aldehyde yield are within the range 0.03 mol L^{-1} to 0.03 mol L^{-1} . The residual errors of **D**, **E**, **F**, and **G**, show no clear dependence on the aldehyde yield, which indicates that there is no systematic error and that the model gives a good representation of the experimental data.

In Figure 8 a parity plot is used to compare the experimentally determined initial reaction rates ($R_{1a,0}$, $R_{ald,0}$, $R_{2a,0}$ in Table 1) to the initial rates calculated with the model using the same “linearized” approach as used for the experimental data. The initial rates calculated with the kinetic model agree well with the experimentally determined rates. However, for high values of the reaction rates, $R_{i,0}$ above $60 \times 10^{-6} \text{ mol s}^{-1}$, the values seem to be less well predicted. This is probably a result of the sampling frequency applied during the experiments. For very fast reactions only 1 or 2 samples can be taken in the conversion range up to 60%, and this means that the initial rate can be based on the first sample only.

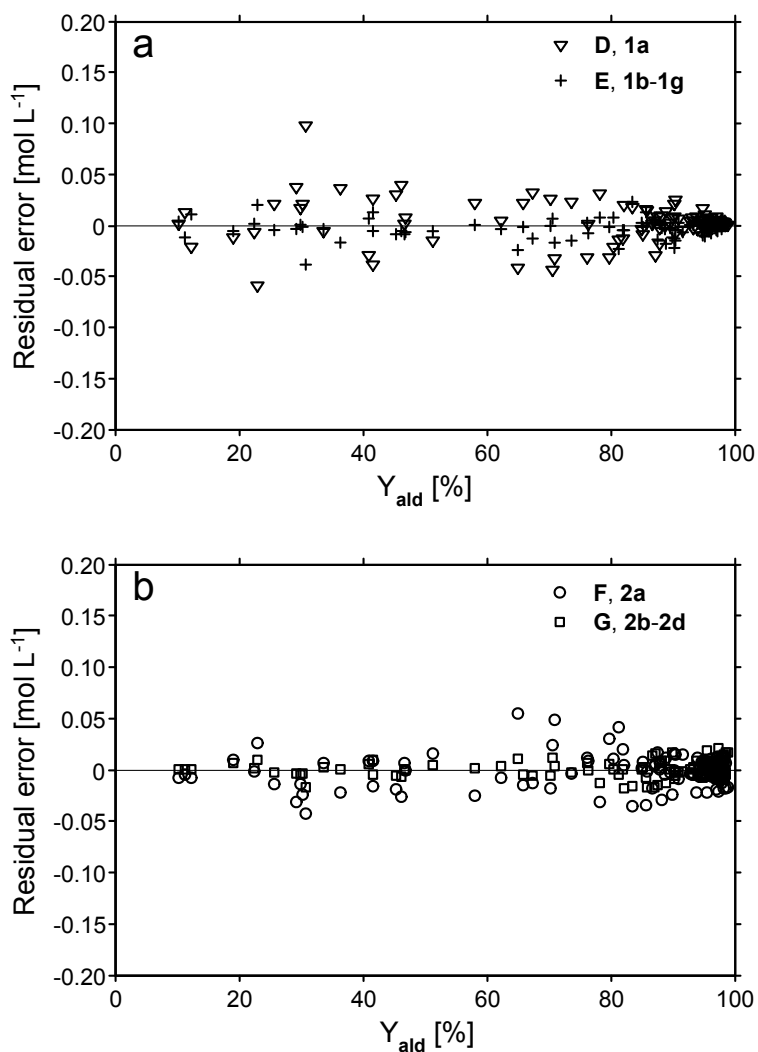


Figure 7. a) The residual errors for **D** and **E**; b) the residual errors for **F** and **G**.

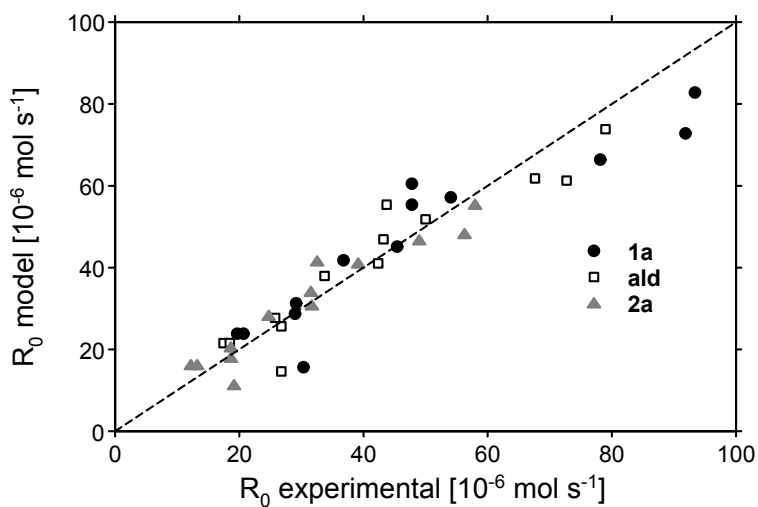


Figure 8. Comparison of the experimental initial rate and the rate predicted by the kinetic model for entry 4 -17.

Concentration profiles – In Figure 9a, 9b, and 9c concentration profiles are given for the experiments in which the initial carbon monoxide concentration has been varied. The lines represent the results obtained with the model. It can be seen in Figure 9a and 9b that the kinetic model represents the conversion of **1a** and the appearance of the **1a** isomers. The model gives a good description of the influence of carbon monoxide on the regioselectivity as well as can be seen in Figure 9c, because the concentration as a function of time of **2a** (**F**) and **2b-2d** (**G**) is represented correctly.

Activation energy - When it is assumed that the reaction orders (α , β , γ , and δ) do not change with temperature, there are 14 temperature dependent parameters. To obtain the temperature dependence of these 14 parameters the influence of the concentration of carbon monoxide, **1a**, and catalyst precursors has to be measured at different temperatures. As a consequence, the set of experiments summarized in Table 1 does not provide sufficient data to determine the temperature dependence of $K_{A,1}$ to $K_{A,3}$, K_D , and $K_{L,1}$, to $K_{L,3}$.

An estimate for the activation energy of the formation of **2a** and the formation of branched aldehydes, **2b-2d**, can be made by using the following empirical rate equations as proposed by Heil and co-workers for the catalyst $\text{Rh}_4(\text{CO})_{12}$.^[34]

$$R_{2a,0} = \frac{d[\mathbf{2a}]}{dt} = k_{\text{app},1} [\mathbf{1a}]_0 [\mathbf{Rh}]_0 \frac{[\text{H}_2]_0}{[\text{CO}]_0} \quad (27)$$

$$R_{2b-2d,0} = \frac{d[\mathbf{2b-2d}]}{dt} = k_{\text{app},1} [\mathbf{1a}]_0 [\mathbf{Rh}]_0 \frac{[\text{H}_2]_0}{[\text{CO}]_0} \quad (28)$$

where:

$$k_{\text{app},i} = k_{0,i} e^{\frac{-E_{\text{act},i}}{RT}}, \quad i = 1 \text{ for } R_{2a,0}, \quad i = 2 \text{ for } R_{2b-2d,0} \quad (29)$$

As can be seen in Figure 10, the result at $3.4 \times 10^4 \text{ K mol}^{-1} \text{ J}^{-1}$, which corresponds to the reaction temperature of 80 °C, deviates from the results found for 40 to 70 °C. The estimated activation energies, with 95% confidence levels, are $76 \pm 6 \text{ kJ/mol}$ for the formation of **2a** and $79 \pm 14 \text{ kJ/mol}$ for the formation of **2b-2d**, in the temperature range of 40 °C to 70 °C. These values agree well with what has been observed for Rh-catalyzed hydroformylation of ethene, propene, and **1a**.^[7,35,36]

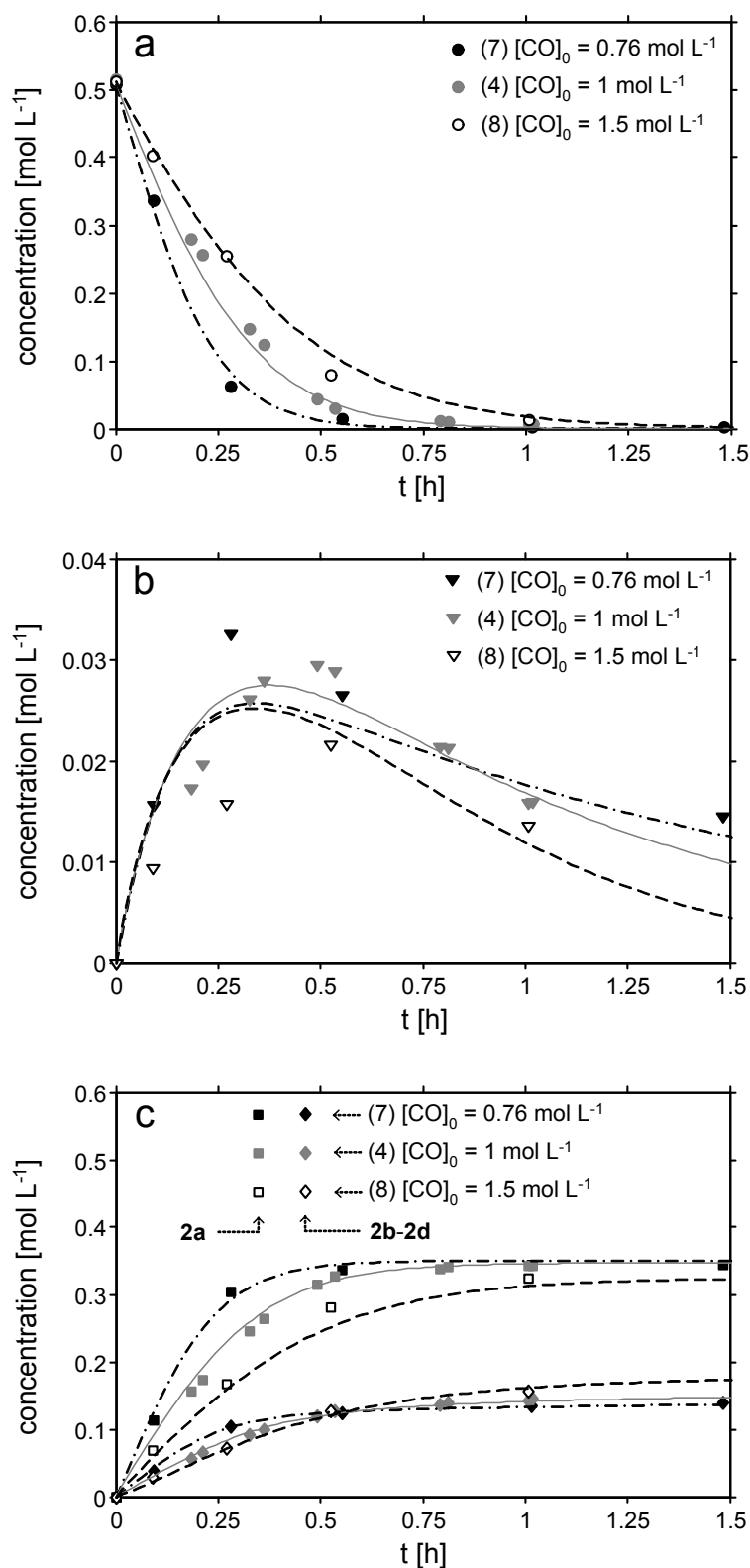


Figure 9. Comparison of the experimentally obtained concentration profile of **1a** (a), **1b-1g** (b), **2a** (c) and **2b-2d** (c) indicated by markers and the model concentration profiles indicated by the lines: $[CO]_0 = 0.76 \text{ mol L}^{-1}$ - - - -, $[CO]_0 = 1 \text{ mol L}^{-1}$ ———, $[CO]_0 = 1.5 \text{ mol L}^{-1}$ - . . . - .

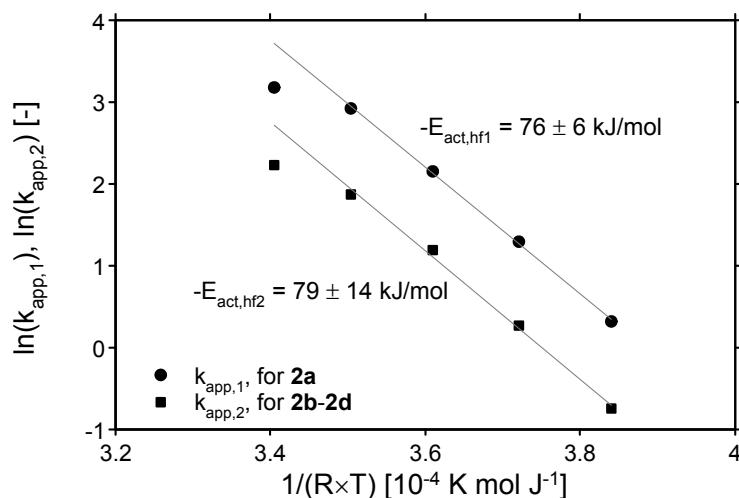


Figure 10. Apparent activation energy for the formation of the linear (**2a**) and branched aldehydes (**2b-2d**).

Comparison of the observed reaction orders with literature - Based on the kinetic parameters given in Table 2 it appears that the kinetics of the **L1**-Rh system shows resemblance with the type II kinetics (equation 2). The reaction rate equations (equations 12 to 14) are approximately first order in hydrogen and catalyst concentration, β and γ close to 1. The reaction rate is approximately second order in carbon monoxide concentration, with the carbon monoxide concentration in the denominator.

Although the **L1**-Rh catalytic system gives rise to kinetics, which appears to have similarity to the kinetics observed for bulky phosphites, there are some subtle differences. The observed rates for the **L1** modified rhodium catalyst applied in scCO_2 are high, however not as high as observed for the bulky phosphite, **L5**, in toluene at 70 °C.^[30] The solvent has a significant effect on the catalysis; use of the **L1**-Rh catalyst in toluene gives rise to a more selective but slower reaction than in scCO_2 .^[5,25] Furthermore, it has been observed by Haji and Erkey that in the presence of hydrogen and carbon monoxide $[\text{HRhCO}(\mathbf{L1})_3]$ is converted to $[\text{HRhCO}(\mathbf{L1})_2]$ and $[\text{HRh}(\text{CO})_2(\mathbf{L1})_2]$ in scCO_2 .^[37] It appears that in solution preferentially two **L1** are coordinated to rhodium, as opposed to the case of **L5**-Rh system where only one phosphite is coordinated to rhodium.^[30]

The observation (Table 1) that the reaction rates increase slightly with an increase in ligand concentration, i.e. an increase in **L1**:Rh ratio, differs from what is observed for **L2**-Rh systems. If it is assumed that **C1** (Figure 3) does not form at temperatures of 50 to 70 °C in

the presence of hydrogen and carbon monoxide in scCO₂, the positive influence of an increasing L:Rh ratio on the regioselectivity and the reaction rate can be explained by a shift in equilibrium from **C2c** towards **C2a** and **C2b**. It is expected that species **C2a** leads to faster hydroformylation than species **C2c**, because coordination of **L1** leads to a more active catalyst as compared to the “unmodified” Rh-catalyst (no ligand).^[9,23]

For the hydroformylation of 1-decene at 70 °C, using [HRhCO(**L2**)₃] as the catalyst precursor and benzene as the solvent, Chaudhari and co-workers found that the experimental data could be described by:^[38]

$$R = \frac{p_{10}[\text{CO}][\text{H}_2]^{1.5}[\text{alkene}][\text{Rh}]^{1.2}}{(1 + p_{11}[\text{CO}])^3(1 + p_{12}[\text{alkene}])} \quad (27)$$

In terms of reaction orders this expression shows a resemblance with the expression obtained here. However, the positive order in hydrogen concentration is in disagreement with the ‘Type I’ kinetics suggested by Van Leeuwen and co-workers for **L2**-Rh.^[17]

According to Van Leeuwen and co-workers the positive order in hydrogen observed for the **L2**-Rh system indicates the presence of Rh dimers (**C9** in Figure 3). At a higher concentration of hydrogen the equilibrium between the dimer **C9** and **C2b** shifts towards **C2b**, resulting in a faster reaction. For the hydroformylations in scCO₂ studied here the concentration of hydrogen present during the preparation of the active catalyst and at the start of the reaction is higher than for most cases described in literature where an organic solvent is used. The fact that a nearly first order dependence of the reaction rate on the rhodium concentration is found supports that the presence of a significant concentration of **C9** in scCO₂ is unlikely.^[39]

It is known that the application of electron-withdrawing ligands, like **L1**, decelerates the oxidative addition of hydrogen, as compared to the use of **L2**.^[17,40] It has been observed for tris(*p*-trifluoromethylphenyl)phosphine that **C5a** is the dominant species in solution, which is probably caused by the faster reaction of **C4a** to **C5a** and **C2b** to **C2a** in combination with slower reaction of **C6a** towards **C7a**.^[24] As **L1** has even more electron withdrawing substituents than tris(*p*-trifluoromethylphenyl)phosphine these effects will be even more pronounced for **L1**. This suggests that the oxidative addition of hydrogen could become the rate-determining step when **L1** is used as the ligand, which is characteristic for type II kinetics, as opposed to the alkene coordination to **C2a** observed for type I kinetics.

The approximate negative second order in carbon monoxide can most likely be explained by an increase in species **C2b** and **C8** (Figure 3) with an increase in carbon monoxide concentration. **C2b** can participate in the so-called associative pathway for hydroformylation (**C2a-C2b-C3b-C5a-C6a-C7a**, Figure 3). However, the associative pathway most likely has a negligible contribution to the overall hydroformylation rate as the dissociative pathway (**C2a-C3a-C4a-C5a-C6a-C7a**, Figure 3) is considerably faster. The “saturated” complex **C8** is an inactive species and an increase in concentration of **C8** can therefore lead to a decrease in the overall reaction rate.

Conclusion

A kinetic model has been developed, which gives a good description of the experimental data for the hydroformylation of 1-octene in scCO₂ at 70 °C. To accurately describe the concentration profiles for the **L1**-Rh catalyst at 70 °C isomerization of **1a** has to be taken into account. The model allows a prediction of regioselectivity as a function of initial concentrations. Such a model for the hydroformylation using **L1**-Rh in scCO₂ has not been described before. The highest activity in terms of TOF_{1a}, $12 \times 10^3 \text{ mol}_{1a} \text{ mol}_{Rh}^{-1} \text{ h}^{-1}$, in combination with a *n:iso* ratio of 3.4 has been observed at a L:Rh of 48, $[1a]_0 = 0.97 \text{ mol L}^{-1}$, $[CO]_0 = [H_2]_0 = 1.0 \text{ mol L}^{-1}$, and S/C = 3750.

An approximate first order dependency of the hydroformylation rate on the hydrogen and catalyst concentration has been found. The obtained rate equation shows resemblance to the rate equation obtained by Davis and Erkey.^[7] The decrease in hydroformylation activity with an increase in ligand concentration, observed for PPh₃-Rh, i.e. **L2**-Rh, systems, appears not to take place for the **L1**-Rh catalyst up to a L:Rh ratio of 50.

References

- [1] a) S. Bektesevic, A. M. Kleman, A. E. Marteel-Parrish, M. A. Abraham, J. Supercrit. Fluids **2006**, *38*, 232-241; b) P. G. Jessop, J. Supercrit. Fluids **2006**, *38*, 211-231; c) P. G. Jessop, T. Ikariya, R. Noyori, Chem. Rev. **1999**, *99*, 475-493.
- [2] S. Kainz, D. Koch, W. Baumann, W. Leitner, Angew. Chem. Int. Ed. **1997**, *15*, 1628-1630.
- [3] D. R. Palo, C. Erkey, Ind. Eng. Chem. Res. **1998**, *37*, 4203-4206.
- [4] a) L. J. P. van den Broeke, E. L. V. Goetheer, A.W. Verkerk, E. deWolf, B.-J. Deelman, G. van Koten, J. T. F. Keurentjes, Angew. Chem. Int. Ed. **2001**, *40*, 4473-4474; b) E. L. V. Goetheer, A.W. Verkerk, L. J. P. van den Broeke, E. de Wolf, B.-J. Deelman, G. van Koten, J. T. F. Keurentjes, J. Catal. **2003**, *219*, 126-133.

- [5] A. C. J. Koeken, M. C. A. van Vliet, L. J. P. van den Broeke, B.-J. Deelman, J. T. F. Keurentjes, *Adv. Synth. Catal.* **2006**, *348*, 1553-1559.
- [6] A. M. Banet Osuna, W. Chen, E. G. Hope, R. D. W. Kemmitt, D. R. Paige, A. M. Stuart, J. Xiao, L. Xu, *J. Chem. Soc. Dalton Trans.* **2000**, *22*, 4052-4055.
- [7] T. Davis, C. Erkey, *Ind. Eng. Chem. Res.* **2000**, *39*, 3671-3678.
- [8] P. E. Savage, S. Gopalan, T. I. Mizan, C. J. Martino, E. E. Brock, *AIChE J.* **1995**, *41*, 1723-1779.
- [9] Chapter 2 and 3 of this thesis.
- [10] M. F. Sellin, Ingrid Bach, J. M. Webster, F. Montilla, V. Rosa, T. Avilés, M. Poliakov, D. J. Cole-Hamilton, *J. Chem. Soc. Dalton Trans.*, **2002**, *24*, 4569-4576.
- [11] Y. Guo, A. Akgerman, *Ind. Eng. Chem. Res.* **1997**, *36*, 4581-4585.
- [12] W. Leitner, E. Dinjus, F. Gaßner, *J. Organomet. Chem.* **1994**, *475*, 257-266.
- [13] P. W. N. M. van Leeuwen, *Appl. Catal. A* **2001**, *212*, 61-81.
- [14] D. Evans, J. A. Osborn, G. Wilkinson, *J. Chem. Soc. A* **1968**, *12*, 3133-3142.
- [15] R. F. Heck, *Acc. Chem. Res.* **1968**, *2*, 10-16.
- [16] C. D. Frohning, C. W. Kohlpaintner, H.-W. Bohnen, in *Applied Homogeneous Catalysis with Organometallic Compounds*, 2nd ed., Vol. 1, (Eds.: B. Cornils, W. A. Herrmann), Wiley-VCH, Weinheim, **2002**, p. 31-103.
- [17] P. W. N. M. van Leeuwen, in *Homogeneous Catalysis: Understanding the Art*, Kluwer Academic Publishers, **2004**, pp. 139-174.
- [18] W. A. Herrmann, M. Prinz, in *Applied Homogeneous Catalysis with Organometallic Compounds*, 2nd ed., Vol. 3, (Eds.: B. Cornils, W. A. Herrmann), Wiley-VCH, Weinheim, **2002**, p. 1119-1130.
- [19] D. Evans, G. Yagupski, G. Wilkinson, *J. Chem. Soc. A* **1968**, *11*, 2660-2665.
- [20] M. Beller, B. Cornils, C. D. Frohning, C. W. Kohlpaintner, *J. Mol. Catal. A* **1995**, *104*, 17-85.
- [21] C. P. Casey, G. T. Whiteker, M. G. Melville, L. M. Petrovich, J. A. Gavney, Jr., D. R. Powell, *J. Am. Chem. Soc.* **1992**, *114*, 5535-5543.
- [22] M. Kranenburg, Y. E. M. van der Burgt, P. C. J. Kamer, P. W. N. M. van Leeuwen, *Organometallics* **1995**, *14*, 3081-3089.
- [23] D. R. Palo, C. Erkey, *Organometallics* **2000**, *19*, 81-86.
- [24] W. R. Moser, C. J. Papile, D. A. Brannon, R. A. Duwell, *J. Mol. Catal.* **1987**, *41*, 291-302.
- [25] Chapter 5 of this thesis.
- [26] Chapter 6 of this thesis.
- [27] C. P. Casey, E. L. Paulsen, E. W. Beuttenmueller, B. R. Proft, L. M. Petrovich, B. A. Matter, D. R. Powell, *J. Am. Chem. Soc.* **1997**, *119*, 11817-11825.
- [28] H. Klein, R. Jackstell, K.-D. Wiese, C. Borgmann, M. Beller, *Angew. Chem. Int. Ed.* **2001**, *40*, 3408-3411.
- [29] S. C. van der Slot, P. C. J. Kamer, P. W. N. M. van Leeuwen, J. A. Iggo, B. T. Heaton, *Organometallics* **2001**, *20*, 430-441.
- [30] A. van Rooy, J. N. H. de Bruijn, K. F. Roobeek, P. C. J. Kamer, P. W. N. M. van Leeuwen, *J. Organomet. Chem.* **1996**, *507*, 69-73.
- [31] R. M. Deshpande, R. V. Chaudhari, *Ind. Eng. Chem. Res.* **1988**, *27*, 1996-2002.
- [32] K. R. Westerterp, W. P. M. van Swaaij, A. A. C. M. Beenackers, *Chemical Reactor Design and Operation*, John Wiley & Sons, Chichester, 2nd ed., **1984**.
- [33] J. A. Osborn, F. H. Jardine, J. F. Young, G. Wilkinson, *J. Chem. Soc. A* **1966**, *12*, 1711-1732.
- [34] B. Heil, L. Markó, *Chem. Ber.* **1968**, *101*, 2209-2214.
- [35] G. Kiss, E. J. Mozeleski, K.C. Nadler, E. van Driessche, C. de Roover, *J. Mol. Catal. A* **1999**, *138*, 155-176.
- [36] P. Cavaliere d'Oro, L. Raimondi, G. Pagani, G. Montrasi, G. Gregorio, A. Andreetta, *Chim. Ind.* **1980**, *62*, 572-579.
- [37] S. Haji, C. Erkey, *Tetrahedron* **2002**, *58*, 3929-3941.
- [38] S. S. Divekar, R. M. Deshpande, R. V. Chaudhari, *Catal. Lett.* **1993**, *21*, 191-200.

- [39] S. C. van der Slot, P. C. J. Kamer, P. W. N. M. van Leeuwen, J. A. Iggo, B. T. Heaton, *Organometallics* **2001**, *20*, 430-441
- [40] A. Buhling, P. C. J. Kamer, P. W. N. M. van Leeuwen, *J. Mol. Catal. A* **1995**, *98*, 69-80.

Chapter 5

Hydroformylation of 1-octene in supercritical carbon dioxide and organic solvents using trifluoromethyl substituted triphenylphosphine ligands^{*,**}

Abstract

Two different in situ prepared catalysts generated from $[\text{Rh}(\text{CO})_2\text{acac}]$ and trifluoromethyl-substituted triphenylphosphine ligands have been evaluated for their activity and selectivity in hydroformylation of 1-octene. The solvents used were supercritical carbon dioxide, hexane, toluene, and perfluoromethylcyclohexane. The highest value for the turn-over-frequency, $9820 \text{ mol}_{1\text{-octene}} \text{ mol}_{\text{Rh}}^{-1} \text{ h}^{-1}$, has been obtained in supercritical carbon dioxide using ligand $\text{P}(\text{C}_6\text{H}_3\text{-3,5}-(\text{CF}_3)_2)_3$. For both supercritical carbon dioxide and hexane employing ligand $\text{P}(\text{C}_6\text{H}_4\text{-3-CF}_3)_3$, a selectivity towards the linear aldehyde product, nonanal, and an *n:iso* ratio of 79.3 % and 4.6-4.8 have been obtained, respectively. These values are significantly higher than that obtained with triphenylphosphine as ligand (selectivity for nonanal: 74-76%, *n:iso*: 3.1-3.3). An increase in the number of trifluoromethyl substituents on the triphenylphosphine ligand results in an increase in 1-octene conversion rate, an increase in the *n:iso* ratio and a decrease in the overall selectivity towards aldehydes. In terms of turn-over-frequency and selectivity the three ligands give comparable results in supercritical carbon dioxide and hexane. This leads to the conclusion that the properties of supercritical carbon dioxide as a solvent for hydroformylation can be better compared with those of hexane rather than with those of toluene.

* This Chapter is based on the article: A. C. J. Koeken, M. C. A. van Vliet, L. J. P. van den Broeke, B.-J. Deelman, J. T. F. Keurentjes, *Adv. Synth. Catal.* **2006**, 348, 1553-1559.

** The methods and results of the hydroformylation in the organic solvents have been obtained by courtesy of M. C. A. van Vliet and B.-J. Deelman.

Introduction

Supercritical carbon dioxide, scCO_2 , has been established as an environmentally benign alternative to organic solvents in the field of homogeneous catalysis.^[1] In terms of production volume, hydroformylation is one of the most important examples of homogeneous catalysis applied on an industrial scale.

Commercial hydroformylation processes are commonly carried out in a gas-liquid system or in a gas-liquid-liquid system. Rigorous mixing of the phases is required to reduce or prevent mass transfer limitations. The Ruhrchemie/Rhône-Poulenc (RCH/RP) hydroformylation process, in which propene is converted to butanal using a phosphine modified rhodium catalyst, is an example of homogeneous catalysis in a gas-liquid-liquid system.^[2] In this process, the sulfonated phosphine renders the catalyst preferentially soluble in the aqueous phase, facilitating easy catalyst separation and recovery through liquid-liquid phase separation. By this means one of the major disadvantages of homogeneous catalysis, which is the difficult recovery of the catalyst, is overcome.

Research into hydroformylation reactions has focused on ligand design to make the catalyst complex more selective, more active, or better separable from the product.^[3] To facilitate catalyst separation phosphine ligands have been covalently attached to a support, such that the catalyst complexes form a separate solid^[4-8] or liquid^[9] phase, which can be recovered by filtration or decantation, respectively. Another strategy is to design ligands that dissolve in an aqueous^[2], fluoruous^[10-13], or ionic^[14,15] solvent that is immiscible with the organic phase containing the product.

The RCH/RP process is limited to the conversion of short chain alkenes, such as propene and 1-butene, because the solubility of longer chain alkenes in water is too low to realize an acceptable reaction rate.^[16] Currently, industrial hydroformylation of long chain alkenes, including 1-octene, is carried out using a cobalt catalyst. Although the cobalt-based processes have been optimized over the years, relatively harsh conditions, typically 30 MPa and 175 °C for the Exxon process, are required to keep the catalyst active and stable, while the activity and selectivity for linear aldehyde formation are lower than in rhodium-catalyzed hydroformylation.^[2] Employing a rhodium catalyst and scCO_2 as the reaction medium could be advantageous for the hydroformylation of long chain alkenes when combined with a facile recovery of the expensive rhodium catalyst. It has been shown that a homogeneous catalyst can be recovered using a microporous ceramic membrane in combination with scCO_2 as the

reaction medium.^[17,18] The use of scCO₂ has the additional advantage that it reduces mass transfer limitations, resulting in a more efficient use of reactor volume at elevated process pressure. Moreover, the development in the synthesis of bulky phosphites and disphosphines has led to improved activity and regio- or stereoselectivity for rhodium catalyzed hydroformylation reactions.^[19]

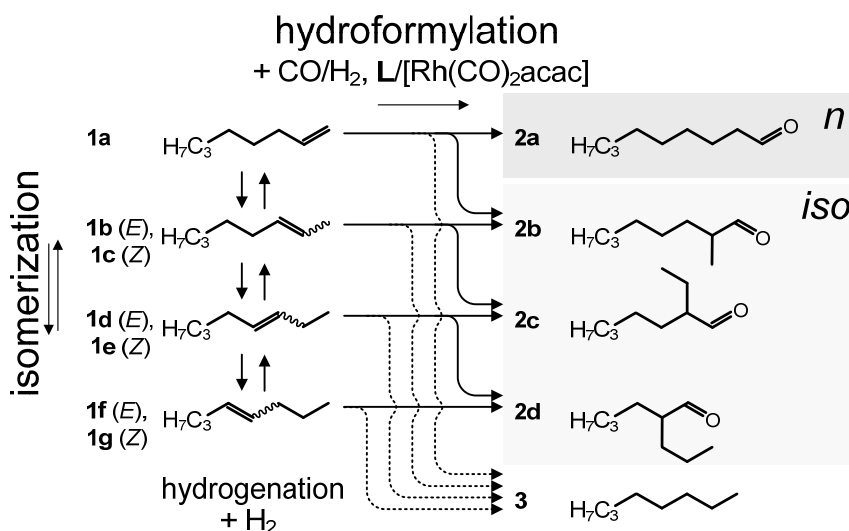


Figure 1. Reaction scheme for the hydroformylation of 1-octene (**1a**), with the two main products nonanal (**2a**) and 2-methyloctanal (**2b**). The side products are (*E,Z*)-2-octene (**1b**, **1c**), (*E,Z*)-3-octene (**1d**, **1e**), (*E,Z*)-4-octene (**1f**, **1g**), 2-ethylheptanal (**2c**), 2-propylhexanal (**2d**), and *n*-octane (**3**). **L** is the phosphine ligand.

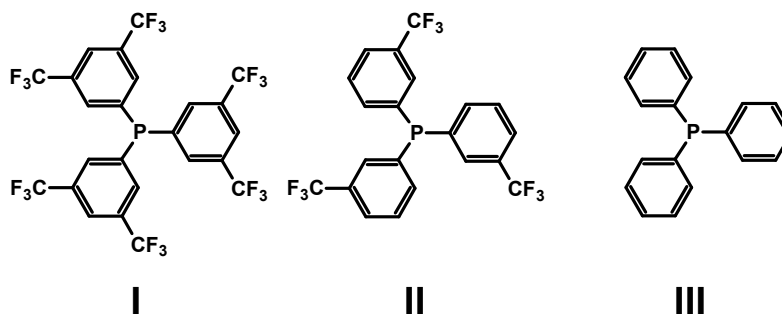


Figure 2. The three triphenylphosphine analogs used: tris(bis-3,5-(trifluoromethyl)phenyl)phosphine (**I**), tris(3-trifluoromethylphenyl)phosphine (**II**) and triphenylphosphine (**III**).

A number of researchers have illustrated the potential of scCO₂ as an alternative reaction medium for the hydroformylation long chain alkenes, such as 1-octene.^[20-22] Besides the requirement of a good selectivity and activity, it is important that the catalyst is also sufficiently soluble in the supercritical mixture.^[20] Generally, it is concluded that the hydroformylation rates in scCO₂ are comparable or even exceed the rates observed in organic

solvents. It has been demonstrated that the attachment of perfluoroalkyl substituents on a ligand improves the solubility in $scCO_2$ considerably.^[20,23] Additionally, the attachment of perfluoroalkyl substituents on the aryl rings of triphenylphosphine has led to an improved catalytic activity.^[24,25]

In terms of activity and selectivity the comparison between an organic solvent and $scCO_2$ as a reaction medium for hydroformylations has only been made to a limited extent. In general, toluene is used to benchmark the performance in $scCO_2$.^[22,26] In this chapter the hydroformylation of 1-octene (**1a**), see Figure 1, is evaluated for four different solvents, including $scCO_2$, *n*-hexane, toluene, and perfluoromethylcyclohexane. Also, the effect of ligand modification is addressed. Beside triphenylphosphine, two different monodentate triarylphosphine analogs with trifluoromethyl substituents on the meta positions were used. The chemical structures of the three phosphines used are shown in Figure 2.

Experimental Section

Materials - Ligand **I** and **II** were supplied by Arkema (Vlissingen). Ligand **III** was purchased from Aldrich. Rhodium(I) dicarbonyl acetylacetonate ($[Rh(CO)_2acac]$) was obtained from Fluka. The ligands and $[Rh(CO)_2acac]$ were stored under argon. **1a** was purchased from Aldrich, dried over molsieves and stored under argon.

ScCO₂ hydroformylation procedure - The general procedure for a hydroformylation experiment started with conveying $54.8 \pm 0.6 \mu\text{mol}$ of $[Rh(CO)_2acac]$ and $27.5 \pm 0.6 \text{ mmol}$ of fluorinated phosphine ligand into the reactor. After closing the reactor, which is described in more detail in Chapter 2, the reactor volume was carefully flushed with argon and evacuated three times. Next, the stirrer was turned on with a revolution speed of 700 rpm and the desired amount of carbon monoxide and hydrogen gas were fed to the reactor at room temperature. A total pressure of 4.9 MPa was used to obtain a concentration of 1 mol L^{-1} for both CO and H₂. The reactor content was then heated to a temperature of 50 °C and subsequently CO₂ was pumped into the reactor to a pressure of 26 MPa. These conditions were maintained for at least half an hour before heating further to the desired reaction temperature. An hour in total, 30 min at 50 °C and 30 min at 70 °C, was considered sufficient to allow the active catalyst complexes to be formed in situ from the $[Rh(CO)_2acac]$ precursor and the different fluorinated ligands. The **1a** in the feed pump was then compressed to a pressure just above the pressure

present in the reactor. Subsequently, the reaction was initiated by opening the valve between pump and reactor, causing a fast pressure equalisation, and by consecutively pumping the desired volume of **1a** into the reactor, which as a rule did not take more than 30 s. Initially, high pressure samples were taken every 10-30 min. At higher conversions the sampling frequency was reduced to 1 per h. The content of the sample volume was carefully bubbled through a vial with a solution of *n*-decane in toluene, and after depressurization the sample volume was rinsed with additional toluene solution to collect **1a** and its reaction products quantitatively. Subsequently the sample volume was dried by alternately applying an argon flow and vacuum. A reaction time of 3 h was observed.

Organic solvent hydroformylation procedure - [Rh(CO)₂acac] (12.5 μmol; S/C=2000; 1 mL stock solution in toluene) and ligand (0.625 mmol; 50 eq.) were mixed in 10 mL of degassed toluene and stirred for 0.5 h at 67 °C under an atmosphere of 0.8 MPa syngas. Then **1a** and *n*-decane (25 + 5.5 mmol; 5.0 mL of a standard mixture) were added via a short column of alumina, followed by degassed toluene (10 mL). The mixture was pressurized with 1 MPa of 1:1 synthesis gas and stirred at 70 °C. Additional syngas was added to maintain the pressure at 1 ± 0.1 MPa. Samples were taken at regular intervals. Conversions and selectivity were determined after a reaction time of 3 h. The TOF was determined based on a sample taken after approximately 15 min.

For experiments with hexane or perfluoromethylcyclohexane (pfmch) as solvent a slightly different procedure was followed. [Rh(CO)₂acac] (12.5 μmol; S/C=2000; 1 mL stock solution in methyltertbutylether) and ligand (0.625 mmol; 50 eq.) were mixed in 5 mL of degassed Et₂O and stirred for 0.5 h at 70 °C under an atmosphere of 8 bars syngas. Volatiles were removed under vacuum and then **1a** and *n*-decane (25 + 5.5 mmol; 5.0 mL of a standard mixture) were added via a short column of alumina, followed by degassed hexane or pfmch (20 mL). The remainder of the experiments was carried out following the procedure applied using toluene as the solvent.

Analysis - The samples were analyzed offline using a Fisons Instruments GC-FID equipped with a Restek Rtx-5 column (fused silica, length 30 m, internal diameter 0.53 mm) where helium was the carrier gas. Calibration was done for **1a**, **1b**, **1c**, **3** and **2a**, the sensitivity coefficients for the other octene and aldehyde isomers were taken to be equal to those of **1a** and **2a**, respectively.

Results and discussion

First, the hydroformylation in supercritical carbon dioxide is discussed. In all the experiments a high ligand to rhodium ratio was used, in the order of 50:1, which approaches conditions used on an industrial scale. A high ligand to rhodium ratio usually results in an increase in the selectivity towards the linear product.^[2] Also, we chose a relatively high reaction temperature of 70 °C to ensure a high catalytic activity. Most results reported for the hydroformylation of **1a** in scCO₂ were obtained at temperatures lower than 70 °C.^[21,22] In Table 1 an overview is given of the experimental reaction conditions for the case scCO₂ or an organic solvent is used.

Table 1. Overview of experimental conditions.

	Symbol	Unit	ScCO ₂	Organic solvent
Reactor temperature	T	[°C]	70	70
Reactor pressure	P	[MPa]	50 ^[a]	1
Reactor volume	V	[mL]	107.6	100
Mode of operation			batch	semi-batch
Amount solvent ^[b]		[mL]	87 ^[c]	21 ^[d]
Amount 1a ^[b]		[mmol]	105	25.0
Amount syngas ^[e]	P _{CO/H₂}	[MPa]	4.9 ^[f]	1.0
Amount [Rh(CO) ₂ acac] ^[b]	Rh	[μmol]	54.8	12.5
Ligand ^[b]	L	[mmol]	2.75	0.625

^[a] Maximum pressure reached after injection of **1a**.

^[b] Average value.

^[c] At 20 °C and 6.0 MPa.

^[d] 20 mL solvent plus 1.07 mL (5.5 mmol) *n*-decane as internal standard.

^[e] Molar ratio CO:H₂ = 1:1.

^[f] At 20 °C. This pressure corresponds with 110 mmol of syngas

The batch reactors used did not allow for a visual inspection of the mixture during the catalyst pre-formation or the catalytic reaction. Prior to the reaction in scCO₂, the catalyst complex was formed in situ from [Rh(CO)₂acac] and one of the phosphine analogues in the presence of CO, H₂ and CO₂ (under the conditions as stated in Table 1). The reaction was started upon addition of **1a**. We employed a CO₂ density of 0.63 g mL⁻¹, which was higher than the density used by Koch and Leitner, who observed a one-phase mixture.^[22] Furthermore, employing a higher density and a higher temperature at the same concentration of solvent and reactants increases the likelihood that a one-phase mixture is present during the progress of the reaction.^[27] The maximum initial total pressure obtained after addition of **1a** was ca 50 MPa. This corresponds to a total reaction mixture density of approximately 0.78 g mL⁻¹. The total concentration (the sum of **1a** and its reaction products, excluding CO and H₂, as measured by off-line GC) became constant after approximately 20 minutes and then did not

on average deviate more than 12 % from the initial concentration based on the amount of **1a** added to the reactor vessel. Furthermore, the homogeneity of the reaction mixture was confirmed by taking samples at different locations, i.e. the top and bottom, of the reactor. Considering these arguments it is likely that during the reactions there is a one-phase reaction system.

The normalized concentrations of the main reactant and products as a function of time for the experiment conducted in scCO₂ with **I** as the ligand are depicted in Figure 3a. In Figure 3b the normalized concentrations of the remaining octene isomers, aldehyde isomers, and octane are given. The catalyst derived from **I** gave rise to a significant amount of isomers of **1a**, resulting in a maximum concentration of about 6 % and 5.5 % for **1b** and **1c** after approximately 0.5 h of reaction, respectively. It can be seen that after almost complete conversion of **1a** the concentration of **2a** remains constant. However, as a result of the hydroformylation of **1b** and **1c** the concentrations of **2b** and **2c** still increase. After 2 h the hydroformylation product **2d** also starts to appear.

In Figure 4 the conversion of **1a** is plotted as a function of time for the reaction in scCO₂ for the different catalytic systems. No noticeable induction time has been observed at the sampling frequency used. Therefore, the slope of the conversion profile, the straight lines in Figure 4, is a measure of the initial activity. Although **III** is significantly less soluble in scCO₂ than **I** or **II**, a reasonable activity is observed for this ligand. A TOF of 470 mol_{1a} mol_{Rh}⁻¹ h⁻¹ is obtained. The number of trifluoromethyl groups per ligand follows the order: **I** > **II** > **III**. Figure 4 shows that the activity of the corresponding catalytic system follows the same sequence. The highest activity, a TOF of 9820 mol_{1a} mol_{Rh}⁻¹ h⁻¹, was observed for the catalyst derived from **I**.

In Figure 5 the overall selectivity towards aldehydes is given as a function of time. Davis and Erkey have reported a minimum overall selectivity of 95% towards aldehydes at a TOF of ca 1400 mol_{1a} mol_{Rh}⁻¹ h⁻¹ by applying **I**, with L:Rh = 3:1, at a temperature of 50 °C at similar reactant concentrations.^[28] We obtained an overall selectivity of 90.5 % towards aldehydes at a TOF of 9820 mol_{1a} mol_{Rh}⁻¹ h⁻¹. This difference can be explained by the higher temperature applied in our experiments, which leads to more isomerization of **1a**.^[2] The catalyst derived from **I** shows activity for the hydroformylation of internal alkenes, **1b** and **1c**. This has also been observed in a study on the hydroformylation of dienes where the same catalyst was used.^[26]

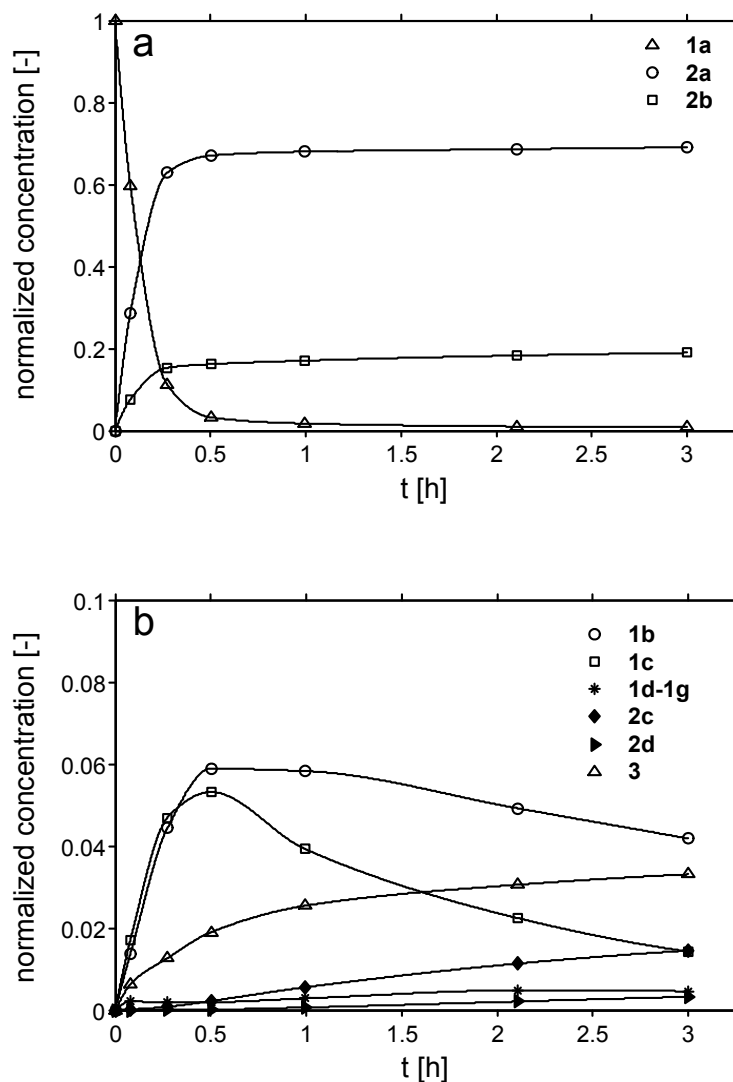


Figure 3. a) Normalized concentrations of the main reactant and products; b) normalized concentrations of isomers as a function of time for the experiment with ligand I. Experimental conditions: $T = 70\text{ }^{\circ}\text{C}$, $[\mathbf{1a}]_0 = 0.98\text{ mol L}^{-1}$, $[\mathbf{1a}]_0:[\text{Rh}] = 2.0 \times 10^3$, $[\text{CO}_2] = 14.5\text{ mol L}^{-1}$, $[\text{CO}]_0 = [\text{H}_2]_0 = 1\text{ mol L}^{-1}$.

To be able to make a comparison with the results in scCO_2 , the three ligands have also been used to prepare the catalysts in situ for the hydroformylation of **1a** in the organic solvents toluene, hexane, and the fluorinated solvent perfluoromethylcyclohexane (pfmch). In this case the reactions were performed under a constant syngas pressure (molar ratio $\text{H}_2:\text{CO} = 1:1$) of 1.0 MPa, whereas during the reactions in scCO_2 no additional syngas was added (4.9 MPa initial syngas pressure, a near stoichiometric amount).

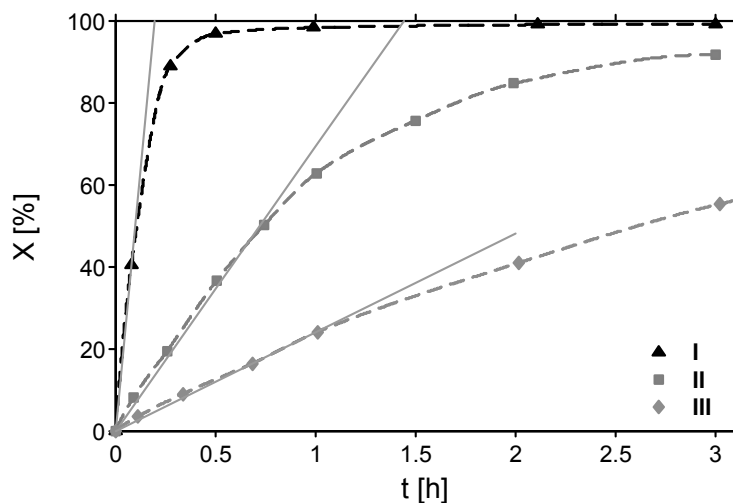


Figure 4. Conversion of **1a**, X, as a function of time using **I**, **II**, and **III** with a L:Rh ratio of 50:1. The markers indicate the times at which samples were taken. Experimental conditions: T = 70 °C, $[\mathbf{1a}]_0 = 0.974 \pm 0.005 \text{ mol L}^{-1}$, $[\mathbf{1a}]_0:[\text{Rh}] = 2.0 \cdot 10^3$, $[\text{CO}_2] = 14.3 \pm 0.2 \text{ mol L}^{-1}$, $[\text{CO}]_0 = [\text{H}_2]_0 = 1 \text{ mol L}^{-1}$. The grey lines are tangent lines corresponding to the slopes of the curves in the initial stage of the reaction.

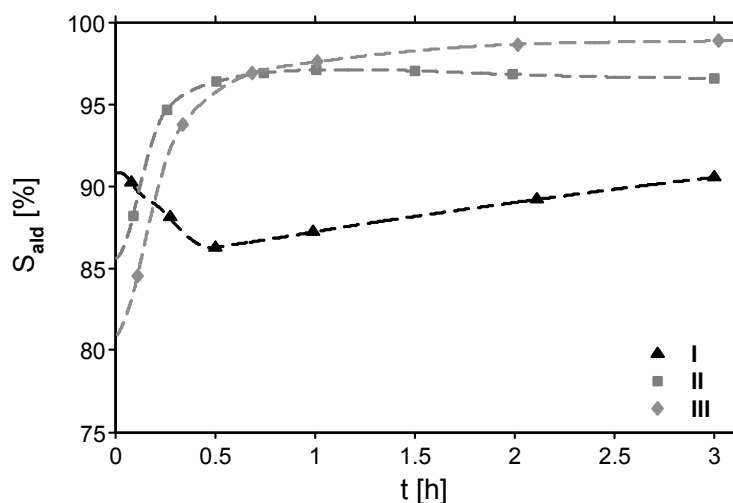


Figure 5. The overall selectivity for aldehydes, S_{ald} , as a function of time using **I**, **II**, and **III** with a L:Rh ratio of 50:1. The markers indicate the times at which samples were taken. Experimental conditions: T = 70 °C, $[\mathbf{1a}]_0 = 0.974 \pm 0.005 \text{ mol L}^{-1}$, $[\mathbf{1a}]_0:[\text{Rh}] = 2.0 \cdot 10^3$, $[\text{CO}_2] = 14.3 \pm 0.2 \text{ mol L}^{-1}$, $[\text{CO}]_0 = [\text{H}_2]_0 = 1 \text{ mol L}^{-1}$.

In Table 2 a detailed comparison is made of the reaction rates and selectivity obtained for the three catalyst systems in the four solvents. Additionally, results are given for experiments in toluene where a L:Rh ratio of 100 was used.

For the hydroformylation in scCO_2 the parent phosphine, triphenylphosphine **III**, offers a better total aldehyde selectivity than **I** or **II**, but this is at the cost of a lower activity and, when compared to **II**, a lower *n:iso* ratio resulting in less linear aldehyde. For **I** the total aldehyde selectivity “drops” in the early phases of the reaction only to recover slowly over the course of the reaction. This is caused by the formation of isomers of **1a** and subsequent hydroformylation of these isomers to aldehydes. The observed trend for the activity as a function of the number of trifluoromethyl substituents could be a result of differences in solubility of the different ligands. It can be expected that the solubility increases with the number of trifluoromethyl groups on the ligand. For **III** a solubility of 0.101 mol L^{-1} in pure carbon dioxide at 25.2 MPa and 57 °C was reported.^[23] However, the presence of carbon monoxide and hydrogen could have an opposite anti-solvent effect. The amount of phosphine applied corresponds to a concentration of 0.025 mol L^{-1} assuming total solubility. This value is four times lower than the reported solubility value; this implies that **III** is most likely completely dissolved under the conditions applied. The addition of **1a** will probably improve the solubility of the ligand and its corresponding complex due to co-solvent effects. The observation that there is no, or very little, induction time is another indication that the catalyst is completely dissolved before the addition of **1a**. Therefore, it is concluded that the observed reaction rates represent the real activity of the catalyst. Furthermore, comparable activities with the same dependence on the ligand used were found in hexane, supporting this conclusion.

The dependence of the activity on the number of fluorine atoms in the phosphines corresponds with results obtained by Palo and Erkey (50 °C, L:Rh = 3:1, P = 27.3 MPa) but absolute activities were significantly lower under these conditions ($\text{TOF} = 500\text{-}900 \text{ mol}_{1\text{a}} \text{ mol}_{\text{Rh}}^{-1} \text{ h}^{-1}$) mainly as a result of the lower temperature they applied.^[24] Also, they obtained moderate *n:iso* ratios in the range 3.0-3.3 for **I**, **II**, and $\text{P}(\text{C}_6\text{H}_4\text{-4-CF}_3)_3$ while the concentration of rhodium was comparable to that in our experiments. This can be attributed to the lower ligand to rhodium ratio they applied. The optimum in *n:iso* ratio obtained for **II**, both in scCO_2 (*n:iso* = 4.6) and organic solvent (*n:iso* = 4.0-4.8) can be considered remarkable because Palo and Erkey have not observed such a clear difference in regioselectivity between **I** and **II**. This indicates that the regioselectivity of the reaction becomes more sensitive to variation in perfluoralkylation at higher L:Rh ratios, while the higher activity obtained with fluorinated phosphines is essentially maintained.

Few results have been reported on the use of **III** as a ligand for homogeneous hydroformylation catalysts in scCO₂ because of its limited solubility and poor activity. Sellins and co-workers have used **III** for the hydroformylation of **1a** in scCO₂ at 100 °C using Rh₂(OAc)₄ as the metal precursor with L:Rh = 3.3.^[29] They obtained a low activity, (TOF = 104 mol_{aldehyde} mol_{Rh}⁻¹ h⁻¹) but a comparable *n:iso* ratio of 3.4 and a slightly lower selectivity towards aldehydes at a conversion of 39.6 %. The observed differences in activity and selectivity are probably a result of the higher temperature and the lower initial pressure used than in our experiments. This could have resulted in a lower solubility for **III** and its corresponding catalyst complex. Kainz et al have reported a conversion of 26 % and a *n:iso* ratio of 3.5 after 19 h for the hydroformylation of **1a** with a concentration of 0.48 mol L⁻¹ at 60 °C using **III** and [Rh(hfacac)(η⁴-C₈H₁₂)] with a 6:1 ratio.^[20] The density of the mixture applied there was approximately 0.75 g mL⁻¹, which is similar to the density applied in our case. The experimental conditions we applied, a high density combined with a relatively high temperature, can account for the higher activity of **III**/[Rh(CO)₂acac] observed as compared to these previous reported values.

From Table 2 it follows that, despite the experimental differences, the results obtained in scCO₂ and the organic solvents hexane and toluene are comparable, while the fluoros solvent pfmch gives rise to inferior results. Clearly, the three catalysts systems employed are not fluoros enough to completely dissolve in pfmch. For **I**/[Rh(CO)₂acac] the highest TOFs are observed in scCO₂ and hexane. For **II**/[Rh(CO)₂acac] and **III**/[Rh(CO)₂acac] the activity order scCO₂ < hexane < toluene and scCO₂ < hexane ≈ toluene, respectively, is observed. The trends in *n:iso* ratio as well as the total aldehyde selectivity are essentially reproduced in all 4 solvent systems. The highest selectivity towards **2a** is always obtained with **II** in scCO₂ and hexane. It can be seen in Table 2 that in toluene this high selectivity with **II**/[Rh(CO)₂acac] can only be reached when the amount of ligand is increased to a L:Rh ratio of 100. For the total selectivity towards the aldehydes, **2a-2d**, **III** gives the best result. The formation of octene isomers and their successive hydroformylation has an unfavorable effect on the *n:iso* ratio. For the different solvents, scCO₂, hexane, and toluene, similar trends in activity and selectivity are observed, indicating that the extent and location of trifluoromethylation, rather than difference in solubility are responsible for the variations observed.

Another effect of the number of trifluoromethyl substituents can be distinguished when the TOFs for **I**, **II**, and **III** obtained in toluene at a L:Rh of 50:1 (entry 4-6) are compared with

those obtained at a L:Rh of 100:1 (7-9). The phenomenon of a constant (or increasing) activity with increasing L:Rh observed for **I** applied in scCO₂, see Chapter 3 and 4, is also observed for **I** in toluene. For **II** and **III** increasing the L:Rh ratio is coupled with a decrease in the initial activity.

Table 2. Comparison of the results obtained with different ligands and solvents.

Entry	Solvent	L	[1a] ₀	[1a] ₀ : [Rh]	L:Rh	TOF ^[a]	X ^[b]	<i>n:iso</i> ^[b,c]	S ^[b,d]			
			[mol L ⁻¹]	[10 ³]		[a]	[%]		2a	2a-2d	1b-1g	3
									[%]	[%]	[%]	[%]
1	scCO ₂	I	0.98	2.0	50	9.82	99.2	3.33	69.6	90.5	6.1	3.3
2	scCO ₂	II	0.97	1.9	50	1.33	91.7	4.59	79.3	96.6	2.9	< 1
3	scCO ₂	III	0.97	2.0	51	0.47	55.3	3.33	76.0	98.8	< 1	< 1
4	toluene	I	0.96	2.0	50	5.90	98.1	3.7	71.5	90.6	7.5	1.9
5	toluene	II	0.96	2.0	50	3.66	97.9	4.0	76.0	95.1	4.2	< 1
6	toluene	III	0.96	2.0	50	1.15	93.1	2.8	73.7	98.6	< 1	< 1
7	toluene	I	1.0	2.0	100	5.90	98	4.5	75	91	7	1
8	toluene	II	1.0	2.0	100	1.70	97	5.3	80	95	4	< 1
9	toluene	III	1.0	2.0	100	0.90	89	3.1	74	97	2	< 1
10	hexane	I	1.0	2.0	50	8.96	98.7	3.9	74.4	93.7	5.3	1.0
11	hexane	II	1.0	2.0	50	1.80	98.9	4.8	79.3	95.7	4.1	< 1
12	hexane	III	1.0	2.0	50	1.12	90.6	3.1	74.0	98.0	1.5	< 1
13	pfmch	I	1.0	2.0	50	0.55	91.5	2.4	28.9	41.1	53.6	5.2
14	pfmch	II	1.0	2.0	50	1.20	99.3	3.2	72.2	94.7	4.6	< 1
15	pfmch	III	1.0	2.0	50	< 0.04	9.2	1.5	9.5	15.7	84.3	nd ^[e]

^[a] The initial turn-over-frequency, TOF, is given by the product of the slope of the linear fit and the (initial) substrate to catalyst ratio. The unit is [10³ mol_{1a} mol_{Rh}⁻¹ h⁻¹].

^[b] Conversion (X), the *n:iso* ratio, and the selectivity (S) shown here are at approximately 3 h of reaction.

^[c] $n:iso = [2a]/([2b]+[2c]+[2d])$.

^[d] The overall selectivity for a product(s) at a certain time: $S_i(t) = [i](t)/\{[1a]_0 - [1a](t)\}$, where *i* = **1b-1d**, **2a-2d**, and **3**.

^[e] **3** signal overlaps with **1a** signal.

The hydroformylation in scCO₂ was performed batch-wise, while for the organic solvents the reaction was performed semi-batch. As can be derived from the results obtained in CO₂ and hexane in Table 2 the difference in the mode of operation has a relatively small effect on the overall outcome of the reaction in terms of activity. The fact that the syngas pressure on the reaction rate is almost zeroth order seems to be a plausible explanation for this phenomenon.^[2] Furthermore, the effect of the partial pressure of hydrogen and carbon monoxide are opposite, and it is to be expected that for an equimolar syngas mixture the partial pressure effects will cancel each other out.

Conclusion

From the different results the following can be concluded in terms of the effect of the solvent and the effect of the ligand. The activity increases up to one order of magnitude with the number of electron withdrawing trifluoromethyl substituents attached to the meta positions on the aryl rings for scCO₂, hexane and toluene in the order **I** > **II** > **III**. The highest activity was found for **I**, using scCO₂. Similar ligand-dependent trends in activity and selectivity were observed for the hydroformylation in scCO₂, toluene and hexane, with the results in hexane matching closest those obtained in scCO₂.

The catalyst **II**/[Rh(CO)₂acac] gives the best compromise between activity and selectivity towards the linear aldehyde. Conditions were found, using hexane and scCO₂ as a reaction medium, where **II**/[Rh(CO)₂acac] gives a 2.5 fold higher activity and a 5% higher selectivity for the linear aldehyde than **III**/[Rh(CO)₂acac]. A similar selectivity for **2a** with **II**/[Rh(CO)₂acac] can also be reached using the solvent toluene. However, this required a much higher L:Rh ratio of 100. The combined selectivity towards the aldehydes (linear and branched as well as other isomers) in scCO₂, hexane, and toluene follow the order: **III** > **II** > **I**. The higher 1-alkene isomerization activity of the catalyst systems resulting from ligands **I** and **II** is responsible for this effect. The difference in experimental procedure for scCO₂ and the organic solvents has a small effect on the overall performance of the hydroformylation of **1a**. This leads to the general conclusion that hexane, rather than toluene, best matches the solvent properties of scCO₂ in the context of hydroformylation catalysis.

References

- [1] P. G. Jessop, T. Ikariya, R. Noyori, *Chem. Rev.* **1999**, *99*, 475-493.
- [2] C. D. Frohning, C. W. Kohlpaintner, H.-W. Bohnen, in *Applied Homogeneous Catalysis*, 2nd ed., Vol. 1 (Ed.: B. Cornils, W. A. Herrmann, Wiley-VCH, Weinheim, **2002**, pp. 31-103.
- [3] D. J. Cole-Hamilton, *Science* **2003**, *299*, 1702-1706.
- [4] N. J. Meehan, M. Poliakoff, A. J. Sandee, J. N. H. Reek, P. C. J. Kamer, P. W. N. M. van Leeuwen, *Chem. Commun.* **2000**, 1497-1498.
- [5] A. J. Sandee, J. N. H. Reek, P. C. J. Kamer, P. W. N. M. van Leeuwen, *J. Am. Chem. Soc.* **2001**, *123*, 8468-8476.
- [6] S. Bektesevic, T. Tack, m. R. Mason, M. A. Abraham, *Ind. Eng. Chem. Res.* **2005**, *44*, 4973-4981.
- [7] I. Kani, R. Flores, J. P. Fackler, Jr., A. Akgerman, *J. Supercrit. Fluids* **2004**, *31*, 287-294.
- [8] F. Shibahara, K. Nozaki, T. Hiyama, *J. Am. Chem. Soc.* **2003**, *125*, 8555-8560.
- [9] M. Solinas, J. Jiang, O. Stelzer, W. Leitner, *Angew. Chem. Int. Ed.* **2005**, *44*, 2291-2295.
- [10] B. Richter, A. L. Spek, G. van Koten, B.-J. Deelman, *J. Am. Chem. Soc.* **2000**, *122*, 3945-3951.

- [11] D. J. Adams, J. A. Bennett, D. J. Cole-Hamilton, E. G. Hope, J. Hopewell, J. Kight, P. Pogorzelec, A. M. Stuart, *Dalton Trans.* **2005**, 3862-3867.
- [12] D. F. Foster, D. Gudmunsen, D. J. Adams, A. M. Stuart, E. G. Hope, D. J. Cole-Hamilton, G. P. Schwarz, P. Pogorzelec, *Tetrahedron* **2002**, *58*, 3901-3910.
- [13] A. Aghmiz, C. Claver, A. M. Masdeu-Bultó, D. Maillard, D. Sinou, *J. Mol. Catal. A*, **2004**, *208*, 97-101.
- [14] P. B. Webb, M. F. Sellin, T. E. Kunene, S. Williamson, A. M. Z. Slawin, D. J. Cole-Hamilton, *J. Am. Chem. Soc.* **2003**, *125*, 15577-15588.
- [15] M. Solinas, A. Pfaltz, P. G. Cozzi, W. Leitner, *J. Am. Chem. Soc.* **2004**, *126*, 16142-16147.
- [16] B. Cornils, in *Multiphase Homogeneous Catalysis*, Vol 1, (Eds.: B. Cornils, W. A. Herrmann, I. T. Horváth, W. Leitner, S. Mecking, H. Olivier-Bourbigou, D. Vogt), Wiley-VCH, Weinheim, **2005**, p. 27-39.
- [17] L. J. P. van den Broeke, E. L. V. Goetheer, A. W. Verkerk, E. de Wolf, B.-J. Deelman, G. van Koten, J. T. F. Keurentjes, *Angew. Chem. Int. Ed.* **2001**, *40*, 4473-4474.
- [18] E. L. V. Goetheer, A. W. Verkerk, L. J. P. van den Broeke, E. de Wolf, B.-J. Deelman, G. van Koten, J. T. F. Keurentjes, *J. Catal.* **2003**, *219*, 126-133.
- [19] M. Beller, B. Cornils, C. D. Frohning, C. W. Kohlpainter, *J. Mol. Catal. A* **1995**, *104*, 17-85.
- [20] S. Kainz, D. Koch, W. Baumann, W. Leitner, *Angew. Chem. Int. Ed.* **1997**, *15*, 1628-1630.
- [21] D. R. Palo, C. Erkey, *Ind. Eng. Chem. Res.* **1998**, *37*, 4203-4206.
- [22] D. Koch, W. Leitner, *J. Am. Chem. Soc.* **1998**, *120*, 13398-13404.
- [23] K.-D. Wagner, N. Dahmen, E. Dinjus, *J. Chem. Eng. Data* **2000**, *45*, 672-677.
- [24] W. R. Moser, C. J. Papile, D. A. Brannon, R. A. Duwell, *J. Mol. Catal.* **1987**, *41*, 271-292.
- [25] D. R. Palo, C. Erkey, *Organometallics* **2000**, *19*, 81-86.
- [26] S.-I. Fujita, S. Fujisawa, B. M. Bhanage, Y. Ikushima, M. Arai, *Eur. J. Org. Chem.* **2004**, 2881-2887.
- [27] J. Ke, B. Han, M. W. George, H. Yan, M. Poliakoff, *J. Am. Chem. Soc.* **2001**, *123*, 3661-3670.
- [28] T. Davis, C. Erkey, *Ind. Eng. Chem. Res.* **2000**, *39*, 3671-3678.
- [29] M. F. Sellin, I. Bach, J. M. Webster, F. Montilla, V. Rosa, T. Avilés, M. Poliakoff, D. J. Cole-Hamilton, *J. Chem. Soc. Dalton Trans.* **2002**, 4569-4576.

Chapter 6

Selectivity of rhodium catalyzed hydroformylation of 1-octene during batch and semi-batch operation using trifluoromethyl substituted ligands *

Abstract

The regioselectivity of catalysts generated in situ from rhodium(I) dicarbonyl acetylacetonate and trifluoromethyl substituted triphenylphosphine ligands has been evaluated during the hydroformylation of 1-octene. The influence of batch or semi-batch operation, the solvent, and the number of trifluoromethyl substituents has been investigated. During semi-batch operation in hexane a constant syngas pressure results in a constant regioselectivity over a broad conversion range for catalysts based on bis(3,5-bis(trifluoromethyl)phenyl)phenylphosphine and tris(3-trifluoromethylphenyl)phosphine. During batch operation in a supercritical CO₂-rich system the differential *n:iso* ratio increases from approximately 4 to a value of 12-16 and 6-8 at about 90–95 % conversion for bis(3,5-bis(trifluoromethyl)phenyl)phenylphosphine and tris(3-trifluoromethylphenyl)phosphine, respectively. Hydroformylation in neat 1-octene is faster than in a supercritical CO₂-rich one-phase system, with a similar overall selectivity as observed in the supercritical case. The hydroformylation and isomerization activity, regioselectivity, and selectivity towards nonanal decreases with the basicity of the ligand. The catalyst based on tris(3,5-bis(trifluoromethyl)phenyl)phosphine shows the highest activity but with a similar or lower selectivity for nonanal than triphenylphosphine. The results provide further directions for the development of ligands that are especially designed for the separation of homogeneous catalysts in continuously operated hydroformylation in scCO₂.

* This chapter is based on a manuscript accepted for publication in Adv. Synth. Catal., “Selectivity of rhodium catalyzed hydroformylation of 1-octene during batch and semi-batch operation using trifluoromethyl substituted ligands” by A. C. J. Koeken, M. C. A. van Vliet, L. J. P. van den Broeke, B.-J. Deelman, J. T. F. Keurentjes.

Introduction

The hydroformylation of alkenes is an important example of homogeneous catalysis on an industrial scale.^[1] Organometallic complexes of rhodium have proven to be the most active and selective catalysts in hydroformylation. In the hydroformylation of propene a water-soluble rhodium catalyst is used, facilitating an easy separation from the organic product phase.^[1,2] However, water-soluble catalysts have only limited application in the hydroformylation of long-chain alkenes as the low solubility of long-chain alkenes in water will result in relatively low reaction rates.^[2] Research dealing with hydroformylation of long-chain alkenes, therefore, focuses on alternative solvents in conjunction with the development of ligands and additives to make rhodium catalysts more active and selective and easier to separate from the product.^[3] Perfluorinated solvents^[4], ionic liquids^[5], water in combination with a phase transfer agent^[6], PEGs^[7], and supercritical fluids^[8] are regarded as promising alternative solvents, which can facilitate catalyst separation.^[9-12] Another approach to catalyst recycling is the attachment of ligands to soluble or insoluble macromolecular supports, which can be separated by filtration or decantation.^[13,14] The development of for example, diphosphines^[15], diphosphites^[16], diphosphines by self-assembly^[17], and tetraphosphines^[18], has led to rhodium catalyzed hydroformylation of long-chain alkenes with a very good regioselectivity for the linear aldehyde product.

The advantages of the application of carbon dioxide to create a one-phase supercritical reaction mixture include the absence of phase boundaries, high diffusivity of the different species, and high solubility of carbon monoxide and hydrogen.^[8] However, the solubility of common homogeneous catalysts in scCO₂ is limited.^[19] This can be seen as an advantage in view of the possibility to separate the catalyst, because CO₂ has been applied as an anti-solvent in order to precipitate and recycle the catalyst.^[20] In order to influence and improve the solubility of Wilkinson type hydroformylation catalysts in CO₂-rich reaction environments, perfluorinated groups or “tails” can be attached to the triphenylphosphine ligands.^[21,22] Besides the improvement of catalyst solubility in scCO₂ or fluorinated systems, phosphine ligands with perfluoroalkyl groups also significantly influence the hydroformylation catalysis.^[23-25]

In chapter 5 it was shown that for the rhodium catalyzed hydroformylation of 1-octene the influence of the trifluoromethyl substituents on the phosphine on the activity and overall selectivity is about the same when scCO₂^[26], hexane or toluene are applied as solvent. In this

comparison it was observed that the (final) ratio of linear over branched aldehydes (*n:iso* ratio) was almost always comparable although the experimental conditions, like pressure and concentration of the syngas, were considerably different.

In this chapter a closer look is taken at the cumulative (or overall or integral) selectivity and the differential (or intrinsic) selectivity in the application of in situ prepared catalysts generated from $[\text{Rh}(\text{CO})_2\text{acac}]$ and three trifluoromethyl substituted triphenylphosphine ligands or the triphenylphosphine ligand (Figure 1) in the hydroformylation of 1-octene (**1a**) (Figure 2).

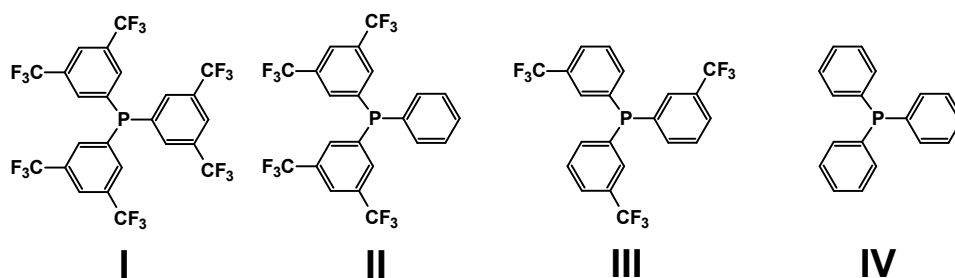


Figure 1. Ligands used in the rhodium catalyzed hydroformylation: tris(3,5-bis(trifluoromethyl)phenyl)phosphine (**I**), bis(3,5-bis(trifluoromethyl)phenyl)phenylphosphine (**II**), tris(3-trifluoromethylphenyl)phosphine (**III**), triphenylphosphine (**IV**). In the text, the catalytic complexes $\text{L}/[\text{Rh}(\text{CO})_2\text{acac}]$ (acac: acetylacetonate) are indicated by the ligand only.

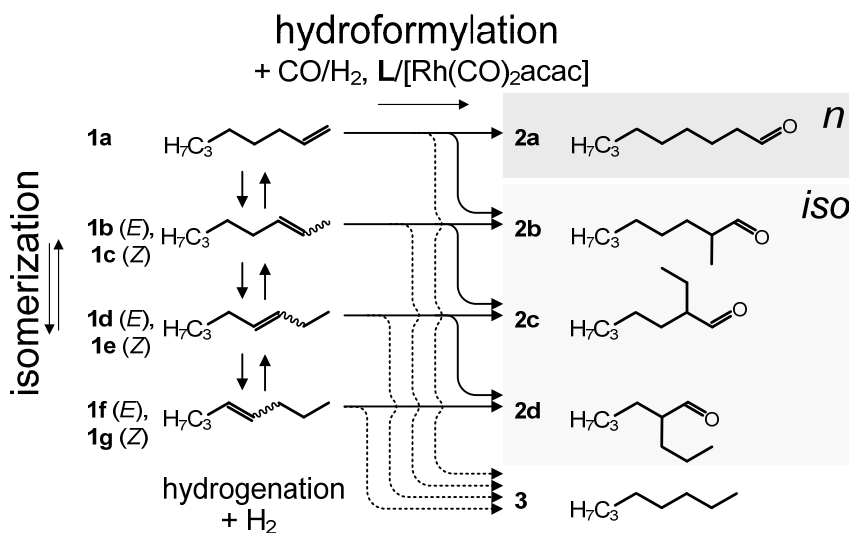


Figure 2. Reaction scheme for the hydroformylation of 1-octene (**1a**), with the two main products nonanal (**2a**) and 2-methyloctanal (**2b**). The side products are (*E,Z*)-2-octene (**1b**, **1c**), (*E,Z*)-3-octene (**1d**, **1e**), (*E,Z*)-4-octene (**1f**, **1g**), 2-ethylheptanal (**2c**), 2-propylhexanal (**2d**), and *n*-octane (**3**). **L** is the phosphine ligand.

In particular, the use of **II** and **III** has been evaluated in four situations: batch and semi-batch with hexane as solvent, batch with scCO_2 as solvent, and solventless (neat **1a**). A high ligand

to rhodium ratio, L:Rh = 50:1, is applied, which approaches industrial conditions. An enhanced regioselectivity towards the linear product can be expected at higher ligand concentration.^[1,27] The differential selectivity indicates to what extent 1-octene is converted into the desired products at some moment in the batch reactor. For commercial hydroformylation processes predominantly CSTRs or loop reactors are being used.^[28] For these continuously operated processes with these type of reactor configurations the overall selectivity is equal to the differential selectivity.^[28]

Experimental

Materials - Ligand **I**, **II** and **III** were supplied by Arkema (Vlissingen). Ligand **IV** was purchased from Aldrich. Rhodium(I) dicarbonyl acetylacetonate ($[\text{Rh}(\text{CO})_2\text{acac}]$) was obtained from Fluka. The ligands and $[\text{Rh}(\text{CO})_2\text{acac}]$ were stored under argon. **1a** was purchased from Aldrich, passed over a column of activated alumina (Brockmann I, Sigma – Aldrich) dried over molsieves and stored under argon. Hydrogen grade 5.0, carbon monoxide 4.7 and carbon dioxide grade 5.0 were purchased from Hoekloos. Prior to use carbon dioxide was passed over a Messer Oxisorb filter to remove oxygen and moisture. Analytical grade hexane was obtained from Merck and dried over molsieves and stored under argon. Toluene (analytical grade, Merck) and decane (99% purity, Aldrich) used to prepare the samples for GC analysis were used as received.

Hydroformylation in $sc\text{CO}_2$ - The procedure for the hydroformylation in CO_2 was described in chapter 5.

*Hydroformylation in neat **1a*** - The conditions during catalyst pre-formation for the experiments without solvent were the same as in the experiments with CO_2 as the solvent. After the pre-formation time of approximately one hour the reactor was cooled rapidly to room temperature and the gases were carefully vented. The catalyst and excess ligand remained in the reactor and were stored overnight under argon atmosphere. After evacuating the reactor, carbon monoxide and hydrogen were fed to the reactor up to 4.9 MPa at room temperature after the stirrer speed was set to 1400 rpm. Then the reactor was heated up to 70 °C. When the reactor temperature was stabilized, **1a** was pressurized to a pressure just above reactor pressure and subsequently the desired volume was injected into the reactor within 30 s. This marked the start of the reaction. The samples taken from the liquid phase were

immediately diluted with a solution of 0.01 mol L⁻¹ of decane in toluene and cooled to room temperature.

Hydroformylation in hexane - The experimental procedure was started by conveying the desired amounts of catalyst (on average 26.0 μmol [Rh(CO)₂acac] and 1.31 mmol ligand) into the reactor. The reactor was closed and alternately evacuated and rinsed with argon three times. The reactor was evacuated and the desired amount of hexane was injected at room temperature. Then carbon monoxide and hydrogen were fed to the reactor up to 4.3 MPa. The stirrer was turned at a revolution rate of 1400 rpm and the pressure typically dropped to a pressure of 3.6 MPa. After stirring at 50 °C for half an hour the reactor was heated and kept for another half hour at 70 °C before injecting **1a** in a similar manner described for the scCO₂ and the neat experiments. In the semi-batch experiments the pressure was kept constant at 4.7 ± 0.2 MPa. Samples were taken from the liquid phase and treated in a similar way as in the neat experiments.

Analysis - The samples were analyzed offline on the same day as the reaction was conducted using a Fisons Instruments GC-FID equipped with a Restek Rtx-5 column (fused silica, length 30 m, internal diameter 0.53 mm) with helium as the carrier gas. Calibration was done for **1a**, **1b**, **1c**, **3** and **2a**, the sensitivity coefficients for the other octene and aldehyde isomers were taken to be equal to those of **1a** and **2a**, respectively.

Reaction parameters - To obtain consistent concentration profiles for **1a** and its reaction products, each concentration obtained by GC analysis was normalized to the sum of all obtained concentrations:

$$[i]_n = \frac{[i]}{\sum [i]} \quad (1)$$

where $i = \mathbf{1a-1g}$, $\mathbf{2a-2d}$ and **3**, and the subscript n refers to the normalized values. The activity and selectivity of the different catalytic complexes was expressed in one of the following parameters. The conversion, X , was given by:

$$X = \frac{[\mathbf{1a}]_{n,0} - [\mathbf{1a}]_n}{[\mathbf{1a}]_{n,0}} \times 100\% \quad (2)$$

with $[\mathbf{1a}]_{n,0} = 1$.

The (overall or cumulative) n :*iso* ratio was calculated as follows:

$$n : iso = \frac{[2a]}{[2b] + [2c] + [2d]} \quad (3)$$

The overall selectivity, S_j , towards a product i was defined as:

$$S_j = \frac{[j]_n}{\{[1a]_{n,0} - [1a]_n\}} \times 100\% \quad (4)$$

where $j = 1b-1g, 2a-2d$ and **3**.

The differential $n:iso$ ratio was calculated as follows:

$$\text{differential } n : iso_k = \frac{n : iso_{\text{sample}_{k+1}} - n : iso_{\text{sample}_k}}{X_{\text{sample}_{k+1}} - X_{\text{sample}_k}} \quad (5)$$

where k goes from 1 to the total number of samples taken during an experiment minus 1.

The differential selectivity Σ_p for product p was determined by:

$$\Sigma_{p,k} = \frac{S_{p,\text{sample}_{k+1}} - S_{p,\text{sample}_k}}{X_{\text{sample}_{k+1}} - X_{\text{sample}_k}} \times 100\% \quad (6)$$

with $p = 1b-1g, 2a-2d$ and **3**.

Σ_p was only evaluated for **2a** and the sum of the branched aldehydes **2b** to **2d**. The differential parameters were evaluated as a function of conversion. The conversion values corresponding to differential parameter values were calculated as follows:

$$X_k = \frac{(X_{\text{sample}_{k+1}} + X_{\text{sample}_k})}{2} \quad (7)$$

The overall yield for a product q was:

$$Y_q = \frac{[q]_n}{[1a]_{n,0}} \times 100\% \quad (8)$$

where $q = 1b-1g, 2a-2d$ and **3**.

The substrate to catalyst ratio S/C was calculated as follows:

$$\frac{S}{C} = \frac{m_{1a} \cdot MW_{Rh}}{m_{Rh} \cdot MW_{1a}} \quad (9)$$

with m_{1a} the mass of **1a** injected, MW_{1a} the molar mass of **1a**, and m_{Rh} and MW_{Rh} the mass conveyed to the reactor and the molar mass of the rhodium precursor, respectively.

The turn-over-number based on the conversion of **1a**, TON_{1a} , was calculated as follows:

$$TON_{1a} = \frac{S}{C} \cdot X \quad (10)$$

The “initial” Turn-Over-Frequency based on either **1a**, **2a**, or aldehydes (**2a-2d** also abbreviated as “ald”) was calculated by multiplying $n_{1a,0}$ (initial amount of **1a** in mol) with the slope of a line fitted through the conversion, Y_{2a} or Y_{ald} data points up to a conversion where there was a linear trend (typically up to a conversion of 60 %).

Results and discussion

Concentration profile - For **III** (Figure 1) it has been observed that during the reaction the aldehyde selectivity decreased because of a slow buildup of **1a** isomers (see also chapter 5). For ligand **II** a similar behavior is observed (Figure 3). After approximately 1 hour of reaction the concentration of **2a** still increases slowly, while the concentration of **2b** to **2d** remains constant, which implies that the selectivity of the catalyst changes during the reaction. The experimental conditions and main results for the 12 cases discussed in this chapter are summarized in Table 1.

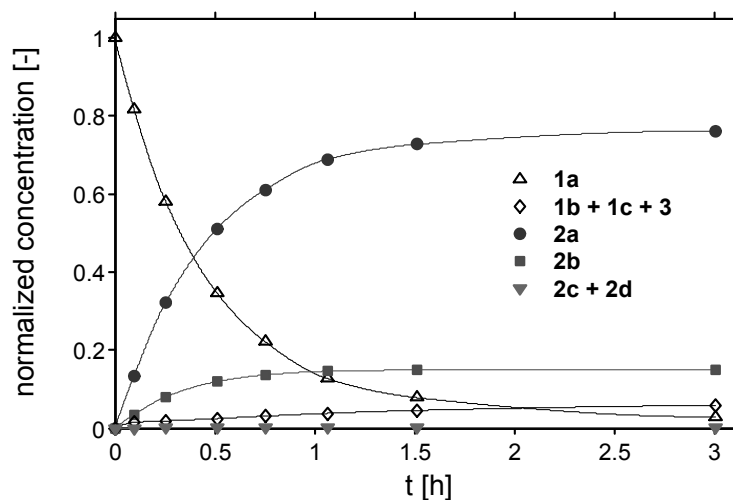


Figure 3. Normalized concentration profile of the hydroformylation of **1a** in CO₂ using **II**. The reaction conditions are given in Table 1, entry 6.

Cumulative n:iso ratio - To investigate whether there is a change in regioselectivity, in particular a change in *n:iso* ratio, as a result of the mode of operation, **II** and **III** have been applied in batch and semi-batch with respect to syngas and using hexane as the solvent (Figure 4). During semi-batch operation a constant *n:iso* ratio over a broad conversion range is observed, while during batch operation the *n:iso* ratio increases clearly with an increase in conversion.

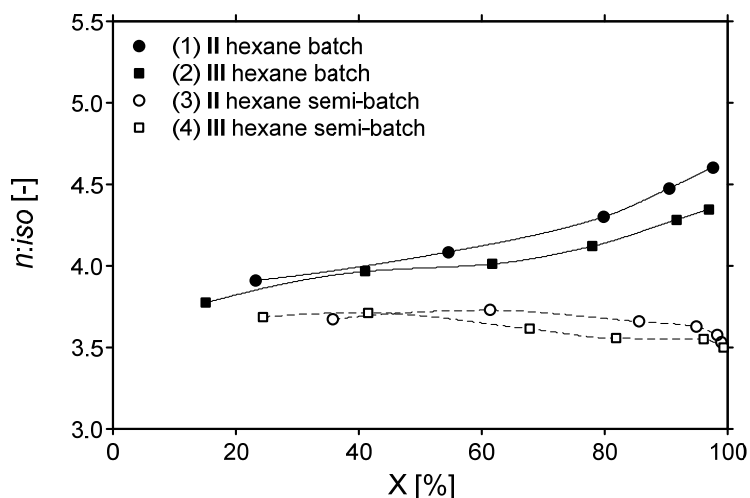


Figure 4. The *n:iso* ratio as a function of conversion (*X*) for the experiments with ligand **II** and **III** in hexane for the batch and semi-batch case (entry 1 to 4 in Table 1).

Table 1. Summary of conditions and results.

Entry	Solvent ^[a]	L	<i>n</i> _{1a} [mmol]	<i>n</i> _{CO:H₂} [mmol]	<i>P</i> _{max} ^[b] [MPa]	TOF _{1a} ^[c] [d]	TOF _{ald} ^[c] [e]	<i>X</i> ^[f] [%]	<i>S</i> _{ald} [%]	<i>S</i> _{2a} [%]	<i>S</i> _{1b-1g} [%]	<i>n:iso</i> [-]
1	hexane ^[g]	II	49.8	49.9:49.2	4.5	3.04	2.89	97.7	95.4	78.4	4.1	4.60
2	hexane ^[g]	III	49.9	51.6:50.8	4.6	1.79	1.69	97.0	96.8	78.7	2.7	4.34
3	hexane ^[g]	II	49.7	[h]	5.0	3.10	3.01	99.0	98.4	76.6	1.0	3.52
4	hexane ^[g]	III	49.9	[h]	4.6	2.07	2.02	99.4	98.8	76.8	1.0	3.50
5	CO ₂	I	105	108:108	50.1	9.82	8.87	99.2	90.5	69.6	6.1	3.33
6	CO ₂	II	105	109:109	49.5	3.29	3.13	97.2	94.0	78.4	5.1	5.02
7	CO ₂	III	105	109:109	49.6	1.33	1.28	91.7	96.6	79.3	2.9	4.59
8 ^[k]	CO ₂	IV	107	108:109	51.0	0.463	0.455	93.0	99.0	77.1	0.1	3.53
9	Neat	I	104	104:103	6.5	15.4 ^[l]	14.3 ^[l]	98.7	94.3	77.8	4.5	4.71
10	Neat	II	100	104:105	6.5	7.38	6.79	99.9	94.7	79.8	4.6	5.37
11	Neat	III	100	104:105	6.5	3.50	3.16	99.8	96.7	79.1	2.7	4.48
12	Neat	IV	100	104:105	6.5	1.03	1.00	95.9	98.3	75.8	1.1	3.38

^[a] General applied conditions: *T* = 70 °C, *S/C* = 2.0 × 10³ mol_{1a} mol_{Rh}⁻¹. For entry 1-4 and 9-12: *V*_{reactor} = 0.103 L; for entry 5-8: *V*_{reactor} = 0.108 L.

^[b] Maximum pressure reached upon injection of **1a**.

^[c] Obtained from multiplying *S/C* with the slope of a linear fit through conversion (TOF_{1a}) or yield (TOF_{ald}) data up to a conversion of 60 % (40 % for **IV**).

^[d] [10³ mol_{1a} mol_{Rh}⁻¹ h⁻¹]

^[e] [10³ mol_{aldehydes} mol_{Rh}⁻¹ h⁻¹]

^[f] Conversion (*X*), selectivity for aldehydes (*S*_{ald}), selectivity for nonanal (*S*_{2a}), selectivity for isomers of **1a** (*S*_{1b-1g}) and the *n:iso* after 3 hours of reaction.

^[g] Amount of hexane used for entry 1: 44.7 mL; entry 2: 42.8 mL; entry 3: 47.2 mL; entry 4: 43.9 mL.

^[h] semi-batch, CO:H₂ = 1.00:1.00.

^[k] Results after 9 h reaction.

^[l] The TOF_{ald} was determined from the pressure change in the first 5 minutes of reaction. TOF_{1a} and TOF_{2a} are estimated based on TOF_{ald} and the composition of the first sample taken after 12 min.

The initial activity of **III** in hexane is similar for the batch case (entry 2), semi-batch case (entry 4) and for the case where a lower syngas pressure has been applied (as reported in Chapter 5). The same holds for **II** even when taking into account the reaction in scCO₂ (entry 6). It appears that the finding that the reaction rate is only slightly dependent on the concentration of CO/H₂ (1:1) as reported by Cavalieri d'Oro et al.^[29] for the hydroformylation of propene with [HRhCO(**IV**)₃] as the pre-catalyst also holds for **II** and **III**.

To study the influence of solvent on the selectivity in more detail, the *n:iso* ratio as a function of conversion has been obtained using **I** to **IV** in a one-phase supercritical system (Figure 5a) or in neat **1a** (Figure 5b), both in batch. The results for the *n:iso* ratio obtained for the neat experiments show more or less the same dependence on the conversion as the results obtained in scCO₂. For **II** and **III** a clear increase is observed in the *n:iso* ratio as the reaction progresses. The increase in *n:iso* ratio is more pronounced for the supercritical batch system than for the two-phase hexane batch system. For **IV** in CO₂, the *n:iso* ratio is more or less constant as function of the conversion up to a conversion of 80 % but then also starts to increase at higher conversion. For **I**, which is the most active catalyst in this comparison, a small increase in the *n:iso* ratio is observed up to a conversion of approximately 90 % when scCO₂ is used. At high conversion, a decrease in *n:iso* ratio is observed. Initially, **I** gives rise to a substantial amount of **1a** isomerization. Moreover, **I** has sufficient activity towards the hydroformylation of internal alkenes (**1b** to **1g**), and as a result the *n:iso* ratio drops at a high **1a** conversion because of the production of **2b** to **2d** through hydroformylation of **1a** isomers. It is noted that for neat conditions the highest values for the *n:iso* ratio have been obtained. Additionally, the rhodium catalysts modified with **I**, **II**, or **III** are very active in the “solventless” hydroformylation of **1a**.

The final outcome of the reaction in terms of *n:iso* ratio observed for neat **1a** is roughly the same when compared to the reaction in scCO₂ except for **I** (entry 5 and 9). However, the *n:iso* as a function of conversion for the neat experiments appears to increase linearly while in CO₂ the *n:iso* ratio increases in an exponential manner. The large difference between the observed overall *n:iso* ratio for **I** can possibly be explained by the fact that the reaction is very fast and solubility of H₂ and CO is low in neat **1a** and aldehydes. Possibly, as a result of mass transfer limitations the concentration of CO in the liquid phase is at a minimum and this favors the formation of linear aldehydes.^[30]

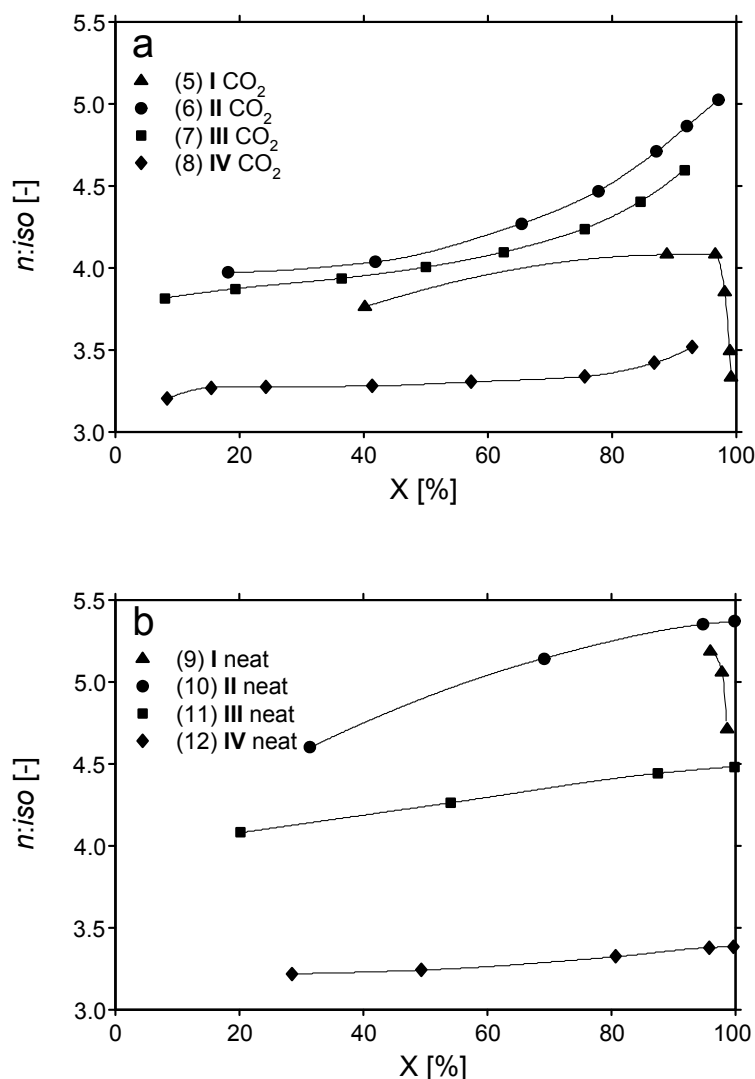


Figure 5. a) Ratio of linear to branched product, $n:iso$, ratio as a function of conversion for the experiments with ligand **I** to **IV** in the one-phase supercritical CO₂; b) $n:iso$ ratio as a function of conversion for the experiments with ligand **I** to **IV** in neat **1a**. It should be noted that in particular for **I** to **III** in neat **1a** a minimum amount of samples were taken to minimize the effect of sampling on the reaction.

Catalytic activity versus selectivity - Based on the TOF values (Table 1) the hydroformylation in neat **1a** is about 1.5 to 2 times faster, as compared to reaction rates obtained in the other solvents. This can probably be attributed to a higher local concentration of catalyst in the liquid **1a** phase in combination with the highest concentration of **1a** possible. The activity of the rhodium complex clearly increases when a triarylphosphine is applied with a greater number of trifluoromethyl substituents. Both in CO₂ and in neat **1a** the initial TOF values observed for ligand increase in the order: **I** > **II** > **III** > **IV**. As can be deduced from Table 1

by comparing TOF_{1a} and TOF_{ald} , the initial rate of isomerization and hydrogenation of **1a** towards the isomers **1b** to **1g** and **3**, respectively, also increases for the ligand in the order: **I** > **II** > **III** > **IV**. The regioselectivity in terms of *n:iso* ratio, however, increases in the order **II** > **III** > **I** \approx **IV**. The difference in regioselectivity of **I**, **II**, and **III** observed in CO₂ becomes most pronounced at a conversion above 60 %.

It has been demonstrated by Moser et al. that the (hydroformylation and isomerization) activity and the regioselectivity in terms of *n:iso* ratio of the catalyst generated from rhodium and a para substituted triarylphosphine (PAR₃) increases with a decreasing basicity of the phosphine ligand.^[31] The basicity of the phosphine ligand decreases by attaching trifluoromethyl substituents on the aryl ring of a triarylphosphine.^[23] Moreover, for monodentate triarylphosphines it is expected that electron-withdrawing groups induce a higher fraction of the diequatorial coordinated [HCO(alkene)Rh(PAR₃)₂] intermediate responsible for a higher selectivity towards the linear aldehyde.^[27,32,33] Additionally, the electron-withdrawing groups present in this diequatorial intermediate should lead to an even higher selectivity towards the linear aldehyde, which was demonstrated by Casey et al for the diphosphines BISBI and T-BDCP^[32] Indeed, a similar dependence as observed by Moser et al.^[31] of the regioselectivity (*n:iso*) and activity on the basicity of the ligand is observed here when the ligands **II** to **IV** are considered, see Table 1. The results obtained with **I**, however, deviate from the behavior described by Moser et al.,^[31] because for **I** a lower regioselectivity is observed than for **II** (in neat **1a**) and **III** (in CO₂ and neat **1a**). Furthermore, in the application of **II** to **IV** in scCO₂ the regioselectivity (*n:iso*) is not clearly coupled with the overall selectivity for **2a** (*n*-aldehyde selectivity, S_{2a}, in Table 1) as observed by Casey et al. for the bidentate phosphines.^[32] The *n*-aldehyde selectivity increases in the order **I** < **IV** < **II** < **III** in scCO₂. Palo and Erkey also tested **I** and **III** in the rhodium catalyzed hydroformylation of **1a** in scCO₂, but they did not observe a significant increase in *n:iso* ratio with an increase in basicity of ligands.^[23] Probably the reaction conditions they applied (T = 50 °C and L:Rh = 3:1) can account for this. This clear deviation of **I** from the expected dependence of the catalytic behavior on the number of electron-withdrawing substituents in the series **I** to **IV**, which is independent of the solvent has not been established before.

Differential n:iso ratio - An increase in (cumulative or overall) *n:iso* ratio with an increase in conversion implies that as the reaction proceeds the catalyst converts **1a** with an increasing

differential *n:iso* ratio. In Figure 6a and Figure 6b a comparison is made between the differential *n:iso* ratio, calculated from the cumulative *n:iso* ratio, obtained with **II** and **III**, respectively. Additionally, the differential *n:iso* obtained with **IV** in CO₂ is shown in Figure 6b. From this comparison the influence of the operating conditions, a one-phase supercritical batch system, a two-phase batch system, and a two-phase system semi-batch system, becomes clear. For all cases where an additional solvent is used, the differential *n:iso* ratio is initially about 3.7 and increases continuously with increasing conversion. For the batch case with **II** and **III** in CO₂ and hexane the increase in differential *n:iso* becomes more pronounced at a conversion of above 50 %. For **IV** in CO₂ the increase in differential ratio becomes more apparent above a conversion of 70 %. The highest value for the differential *n:iso* ratio is obtained for **II** in scCO₂; the differential *n:iso* ratio increases to a value of approximately 14–16. In hexane, the differential *n:iso* increases less sharply, the highest value obtained is 6–6.5. For the semi-batch experiment performed in hexane the differential *n:iso* ratio is constant up to a conversion of about 90 % and then drops to a value of about 2.5, as a result of the hydroformylation of internal octenes. For neat **1a** and using **II** the maximum differential *n:iso* ratio observed is about 6.0 at a conversion around 82 %. For **III** a similar behavior is observed; the highest differential *n:iso* ratio obtained is about 8–9 and 5–6 for scCO₂ and hexane, respectively.

Screening of new hydroformylation catalysts is predominantly done at “low” pressures and semi-batch with respect to the gaseous reactants. Usually, during semi-batch hydroformylation, using rhodium catalysts in the presence of excess phosphine ligand, a constant or a decrease in *n:iso* ratio has been observed for a variety of solvents.^[29,34,35] For hydroformylation with **IV** applying a lower CO partial pressure results in a higher regioselectivity, i.e. a higher *n:iso* ratio, at the cost of a lower chemoselectivity, i.e. a higher degree of hydrogenation and/or isomerization.^[27,29,30]

For supercritical conditions it is more convenient to work batch-wise. To keep the concentration of syngas constant in a supercritical reaction mixture requires a dosing mechanism that delivers syngas at high pressures. Moreover, the pressure of the supercritical mixture not only changes as a result of the conversion of syngas but also as a result of a different interaction between **1a** and CO₂ as compared to the interaction between the aldehydes and CO₂ as illustrated in Chapter 2. Although it seems plausible based on results presented above, remarkably, no change in selectivity during the reaction has been reported

before in the batch hydroformylation of **1a**.^[23,36-38] Only in the case when tri[3-(1H,1H,2H,2H-perfluorooctyl)phenyl]phosphite is used, a clear increase in *n*:*iso* ratio as function of the conversion was observed.^[36]

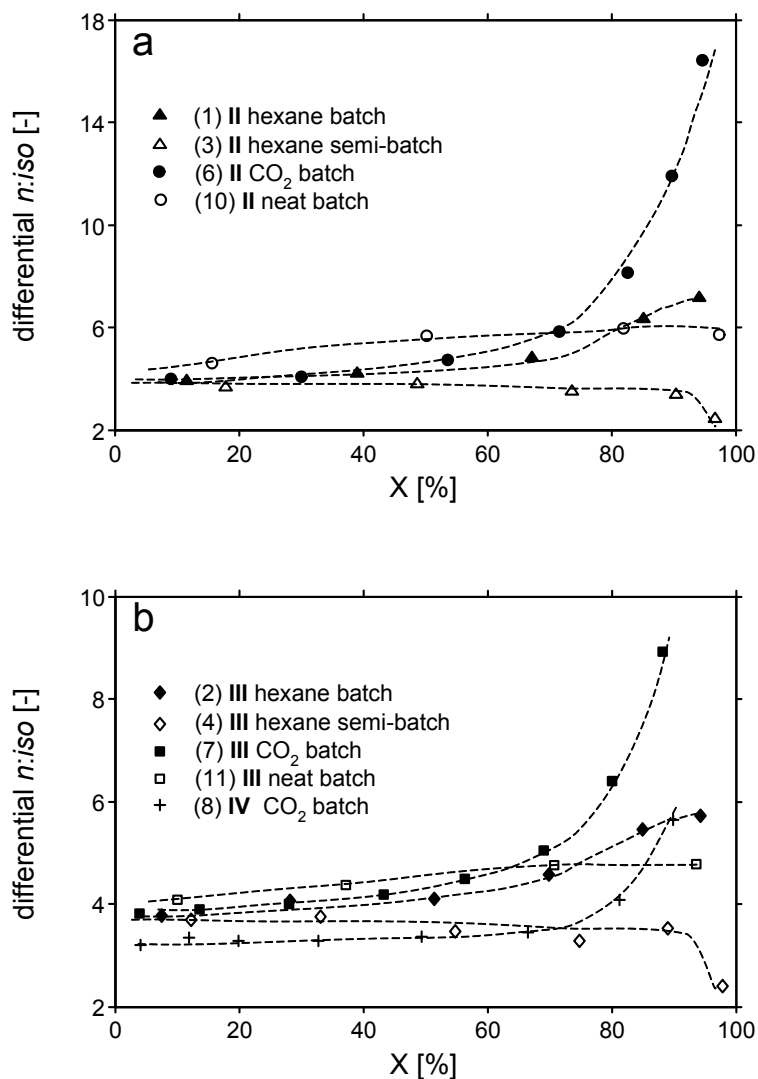


Figure 6. a) Differential *n*:*iso* ratio as a function of conversion for **II** (entries 1, 3, 6, and 10). b) Differential *n*:*iso* ratio as a function of conversion for **III** (entries 2, 4, 7, and 11). The dashed lines indicate the trend.

In the application of the triphenylphosphine analogues tris[4-(1H,1H,2H,2H-perfluorooctyl)phenyl]phosphine or tris[3-(1H,1H,2H,2H-perfluorooctyl)phenyl]phosphine in the rhodium catalyzed hydroformylation of **1a** in *sc*CO₂ Koch et al.^[36] observed a constant *n*:*iso* ratio of about 5.5. In this case, the electron withdrawing effect of the perfluoroalkyl group on the phosphorous is counteracted by the ethyl “spacers” between the perfluoroalkyl

group and the aryl ring. The electron density on the phosphorous of these phosphines with perfluoroalkyl chains is similar to that of triphenylphosphine. So, the *n:iso* ratio obtained with **IV** in scCO₂ (Figure 5a) is in good agreement with the observations by Koch et al.^[36] The difference in regioselectivity can probably be attributed to the steric effects caused by the perfluoroalkyl substituents. Finally, the catalytic activity we observed (entry 8 in Table 1) is close to the activity of 430 mol_{ald} mol_{Rh}⁻¹ h⁻¹ reported by Koch et al. for tris[4-(1H,1H,2H,2H-perfluorooctyl)phenyl]phosphine at 65 °C.

Based on the differential *n:iso* of entry 2 and 4 as a function of conversion the similar overall *n:iso* found in Chapter 5 when applying **III** during batch operation in scCO₂ (*n:iso* (3 h) = 4.6) or during semi-batch operation in hexane (*n:iso* (3 h) = 4.8) can be explained. The syngas pressure applied in the semi-batch experiment using hexane as the solvent was 1 MPa. This syngas pressure corresponds to the pressure at about 80% conversion in the case of entry 10. The value of 5 for the differential *n:iso* ratio observed at 80 % conversion is close to the value of 4.8 for the overall *n:iso* observed previously.

Differential selectivity - By plotting the differential selectivity towards nonanal, Σ_{2a} , and towards the nonanal isomers, Σ_{2b-2d} , as a function of the conversion, the reason for the increase in the differential *n:iso* ratio becomes clear. In Figure 7a the differential selectivity obtained with **II** in CO₂ and hexane, batch and semi-batch, are compared. For the supercritical system (entry 6), the selectivity towards the linear aldehyde product is more or less constant up to a conversion of 90 %, while Σ_{2b-2d} decreases from 18.5 % at 9 % conversion to 4 % at approximately 95 % conversion. For the batch hydroformylation in hexane (entry 1) a similar but more moderate behavior is observed. For the semi-batch case (entry 3), Σ_{2a} decreases and Σ_{2b-2d} increases slightly. Above 90 % conversion Σ_{2a} decreases by about 10%, and Σ_{2b-2d} increases by about 20%, which is reflected in the lower differential *n:iso* ratio. For **IV** in CO₂, both Σ_{2a} and Σ_{2b-2d} remain constant, in the conversion range of 5% to about 70%, above 70 % Σ_{2a} increase to a value of about 80 % and Σ_{2b-2d} decreases to a value of about 15 %.

For the catalyst **III** a similar but more moderate behavior of Σ_{2a} and Σ_{2b-2d} as a function of conversion is observed than for **II** (Figure 7b). In the batch experiments in CO₂ and hexane Σ_{2a} only increases up to values of 85 % at about 90 % conversion. However, in the conversion range of 80 to 95 % the differential *n:iso* ratio is somewhat lower than for **II**, because Σ_{2b-2d} does not decrease as much as for **II**.

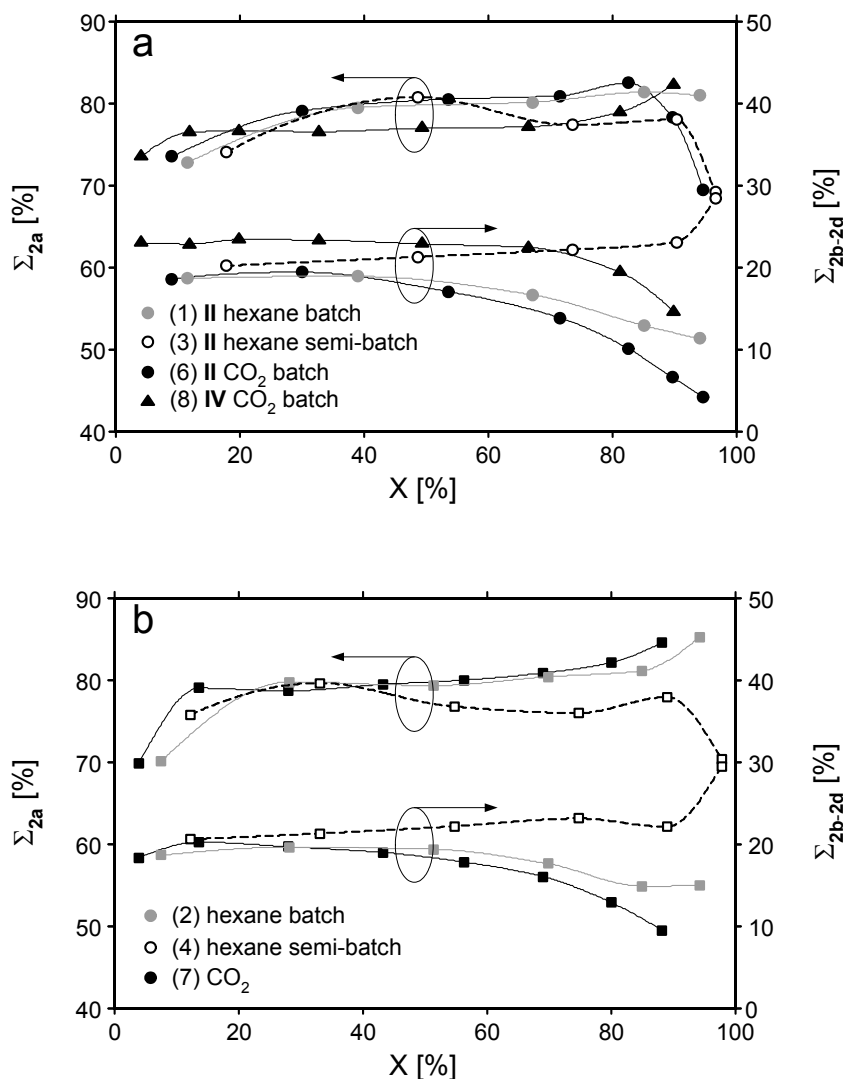


Figure 7. a) Differential selectivity for **2a** (nonanal), Σ_{2a} , and the differential selectivity towards the branched aldehydes, Σ_{2b-2d} , 2-methyloctanal (**2b**), 2-ethylheptanal (**2c**) and 2-propylhexanal (**2d**) using **II** as a function of conversion for entries 1, 3 and 6; b) Differential selectivity using **III** as a function of conversion for entries 2, 4 and 7.

It seems that **III** maintains a higher chemoselectivity towards aldehydes than **II** at low CO partial pressure. For the semi-batch case (entry 4), Σ_{2a} and Σ_{2b-2d} remain more or less constant up to a conversion of about 90 %. Above 90 % conversion a similar behavior as for **II** is observed, Σ_{2a} decreases to 70 % while Σ_{2b-2d} increases to about 30 %.

Conclusion

By following the reaction in time it was observed that a low CO partial pressure induces a higher differential *n:iso* ratio for **II** and **III** than expected based on the overall *n:iso* ratio, especially in scCO₂ (Figure 5 and 6). This appears to be caused by a slower hydroformylation of **1a** to the branched aldehyde. For **IV** in scCO₂ this phenomenon also takes place but in a more moderate manner at a lower CO concentration.

The hydroformylation and isomerization activity increases with the number of trifluoromethyl substituents and decreasing basicity of the ligand in the order: **I** < **II** < **III** < **IV**. When the catalysts **II** to **IV** are considered, also the regioselectivity (*n:iso*) increases with the number of electron-withdrawing trifluoromethyl groups. The regioselectivity and selectivity for **2a** obtained with **I** is similar or lower to that obtained with **IV**.

From the various results it can be derived that if the hydroformylation of **1a** could be operated continuously using **II** a *n:iso* ratio of about 12-16 can be obtained. The preferred conditions are a one-phase CO₂ enriched mixture at a low CO partial pressure (for entry 6 approximately 0.3–0.6 MPa). As can be deduced from Figure 7a, this will be at the expense of a lower overall aldehyde selectivity (*n + iso*) as the selectivity towards isomerization products **1b** and **1c** will be higher.

The improved results obtained in scCO₂ and the effect of different substitution patterns on the ligands provide directions for further development of ligands that are especially designed for the separation of homogeneous catalysts in continuously operated hydroformylation in scCO₂.

References

- [1] C. D. Frohning, C. W. Kohlpaintner, H.-W. Bohnen, in *Applied Homogeneous Catalysis*, 2nd ed., Vol. 1 (Ed.: B. Cornils, W. A. Herrmann), Wiley-VCH, Weinheim, **2002**, pp. 31-103.
- [2] a) C. W. Kohlpaintner, R. W. Fischer, B. Cornils, *Appl. Catal. A* **2001**, *221*, 219-225.; b) B. Cornils, in *Multiphase Homogeneous Catalysis*, Vol 1, (Eds.: B. Cornils, W. A. Herrmann, I. T. Horváth, W. Leinter, S. Mecking, H. Olivier-Bourbigou, D. Vogt), Wiley-VCH, Weinheim, **2005**, p. 27-39.
- [3] D. J. Cole-Hamilton, *Science* **2003**, *299*, 1702-1706.
- [4] a) I. T. Horváth, G. Kiss, R. A. Cook, J. E. Bond, P. A. Stevens, J. Rábai, E. J. Mozeleski, *J. Am. Chem. Soc.* **1998**, *120*, 3133-3143; b) B. Richter, A. L. Spek, G. van Koten, B.-J. Deelman, *J. Am. Chem. Soc.* **2000**, *122*, 3945-3951
- [5] P. B. Webb, M. F. Sellin, T. E. Kunene, S. Williamson, A. M. Z. Slawin, D. J. Cole-Hamilton, *J. Am. Chem. Soc.* **2003**, *125*, 15577-15588.
- [6] K. Kunna, C. Müller, J. Loos, D. Vogt, *Angew. Chem., Int. Ed.* **2006**, *45*, 7289-7292.

- [7] D. J. Heldebrant, P. G. Jessop, *J. Am. Chem. Soc.* **2003**, *125*, 5600-5601.
- [8] a) P. G. Jessop, W. Leitner (Eds.), *Chemical Synthesis Using Supercritical Fluids*, Wiley-VCH, Weinheim, **1999**, pp. 1-13; b) E. J. Beckman, *J. Supercrit. Fluids* **2004**, *28*, 121-191
- [9] B. Cornils, W. A. Herrmann, I. T. Horváth, W. Leitner, S. Mecking, H. Olivier-Bourbigou, D. Vogt, in *Multiphase Homogeneous Catalysis, Vol 1*, (Eds.: B. Cornils, W. A. Herrmann, I. T. Horváth, W. Leitner, S. Mecking, H. Olivier-Bourbigou, D. Vogt), Wiley-VCH, Weinheim, **2005**, p. 3-23.
- [10] R. A. Sheldon, *Green Chem.* **2005**, *7*, 267-278.
- [11] J. M. DeSimone, *Science* **2002**, *297*, 799-802.
- [12] D. E. Bergbreiter, S. D. Sung, *Adv. Synth. Catal.* **2006**, *348*, 1352-1366.
- [13] A. Corma, H. Garcia, *Adv. Synth. Catal.* **2006**, *348*, 1391-1412. b) B. M. L. Dooos, I. F. J. Vankelecom, P. A. Jacobs, *Adv. Synth. Catal.* **2006**, *348*, 1413-1446.
- [14] for example a) R. P. J. Bronger, J. P. Bermon, J. N. H. Reek, P. C. J. Kamer, P. W. N. M. van Leeuwen, D. N. Carter, P. Licence, M. Poliakoff, *J. Mol. Catal. A* **2004**, *224*, 145-152; b) F. Shibahara, K. Nozaki, T. Hiyama, *J. Am. Chem. Soc.* **2003**, *125*, 8555-8560.
- [15] for example: a) T. J. Devon, G. W. Philips, T. A. Puckette, J. L. Stavinoha, J. J. Vanderbilt (to Eastman Kodak) U.S. Patent 4.694.109, **1987**; b) M. Kranenburg, Y. E. M. van der Burgt, P. C. J. Kamer, P. W. N. M. van Leeuwen, K. Goubitz, J. Fraanje, *Organometallics* **1995**, *14*, 3081-3089; c) H. Klein, R. Jackstell, K.-D. Wiese, C. Borgmann, M. Beller, *Angew. Chem. Int. Ed.* **2001**, *40*, 3408-3410.
- [16] for example: E. Billig, A.G. Abatjoglou, D.R. Bryant (to Union Carbide Corp.), *Eur. Pat. Appl. EP 0.213639*, **1987**.
- [17] for example: a) B. Breit, W. Seiche, *J. Am. Chem. Soc.* **2003**, *125*, 6608-6609; b) B. Breit, W. Seiche, *Angew. Chem. Int. Ed.* **2005**, *44*, 1640-1643.
- [18] Y. Yan, X. Zhang, X. Zhanga, *Adv. Synth. Catal.* **2007**, *349*, 1582-1586.
- [19] P. G. Jessop, T. Ikariya, R. Noyori, *Chem. Rev.* **1999**, *99*, 475-493.
- [20] M. Solinas, J. Jiang, O. Stelzer, W. Leitner, *Angew. Chem. Int. Ed.* **2005**, *44*, 2291-2295.
- [21] S. Kainz, D. Koch, W. Baumann, W. Leitner, *Angew. Chem. Int. Ed.* **1997**, *15*, 1628-1630.
- [22] D. R. Palo, C. Erkey, *Ind. Eng. Chem. Res.* **1998**, *37*, 4203-4206.
- [23] D. R. Palo, C. Erkey, *Organometallics* **2000**, *19*, 81-86.
- [24] D. J. Adams, J. A. Bennett, D. J. Cole-Hamilton, E. G. Hope, J. Hopewell, J. Kight, P. Pogorzelec, A. M. Stuart, *Dalton Trans.*, **2005**, 3862-3867.
- [25] a) A. C. J. Koeken, M. C. A. van Vliet, L. J. P. van den Broeke, B.-J. Deelman, J. T. F. Keurentjes, *Adv. Synth. Catal.* **2006**, *348*, 1553-1559; b) Chapter 5.
- [26] "Applying scCO₂ as a solvent" implies that the reaction mixture, reactants, products and CO₂, were in a supercritical one-phase state.
- [27] P. W. N. M. van Leeuwen, in *Homogeneous Catalysis: Understanding the Art*, Kluwer Academic Publishers, **2004**, pp. 139-174.
- [28] K. R. Westerterp, W. P. M. van Swaaij, A. A. C. M. Beenackers, *Chemical Reactor Design and Operation*, John Wiley & Sons, Chichester, 2nd ed., **1984**, p. 83-87.
- [29] P. Cavaliere d'Oro, L. Raimondi, G. Pagani, G. Montrasi, G. Gregorio, A. Andreetta, *Chim. Ind.* **1980**, *62*, 572-579.
- [30] K. L. Olivier, F. B. Booth, *Hydrocarbon Process.* **1970**, *4*, 112-114.
- [31] W. R. Moser, C. J. Papile, D. A. Brannon, R. A. Duwell, *J. Mol. Catal.* **1987**, *41*, 271-292.
- [32] C. P. Casey, E. L. Paulsen, E. W. Beuttenmueller, B. R. Proft, L. M. Petrovich, B. A. Matter, D. R. Powell, *J. Am. Chem. Soc.* **1997**, *119*, 11817-11825.
- [33] Chapter 4.
- [34] S. S. Divekar, B. M. Bhanage, R. M. Deshpande, R. V. Gholap, R. V. Chaudhari, *J. Mol. Catal.* **1994**, *91*, L1-L6.
- [35] H. H. Y. Ünveren, R. Schomäcker, *Catal. Lett.* **2006**, *110*, 195-201.
- [36] D. Koch, W. Leitner, *J. Am. Chem. Soc.* **1998**, *120*, 13398-13404.
- [37] D. R. Palo, C. Erkey, *Ind. Eng. Chem. Res.* **1999**, *38*, 2163-2165.

[38] T. Davis, C. Erkey, *Ind. Eng. Chem. Res.* **2000**, *39*, 3671-3678.

Chapter 7

Permeation of gases and supercritical fluids through a supported microporous titania membrane

Abstract

A tubular alumina supported microporous titania membrane has been characterized by studying the permeation of pure substances and mixtures at subcritical and supercritical conditions. At a feed pressure of 0.5 MPa the main transport mechanism for helium across the membrane is gas translation diffusion. For nitrogen and sulfurhexafluoride surface diffusion is the main transport mechanism. For carbon dioxide a combination of the two mechanisms, surface diffusion and gas translation diffusion, is observed. The permeation of supercritical carbon dioxide and sulfurhexafluoride at supercritical conditions at 50 °C up to feed pressures of 20 and 8 MPa, respectively, is best described by the viscous flow model. Using the viscous flow model about the same value for the “mobility” constant, which describes membrane characteristics, has been calculated for carbon dioxide and sulfurhexafluoride. The addition of the solutes hexane and octane to a carbon dioxide rich supercritical fluid has a minor influence on the permeance of carbon dioxide through the membrane and the membrane does not retain them. The behavior of the permeance of supercritical carbon dioxide observed for the titania membrane is similar to the behavior observed for microporous alumina supported silica membranes.

Introduction

Supercritical fluids exhibit interesting properties like high diffusivity of solutes, tunable solvent properties by altering pressure or temperature, and high solubility of permanent gases. Consequently, supercritical fluids are interesting as a solvent in reaction and extraction applications.^[1,2] In particular, carbon dioxide is an appealing “supercritical” solvent, because it has an accessible supercritical temperature and pressure, a low toxicity, and is nonflammable.

The facile separation of carbon dioxide and an organic (reaction) product just by simple depressurization can be seen as an advantage. However, a substantial amount of energy is required to compress carbon dioxide to elevated pressure.^[1] So, depressurization should be minimized. Membrane separation, in particular nanofiltration, is a promising technology to regenerate or purify supercritical carbon dioxide with a minimum energy loss.^[3,4] Nanofiltration has also the potential to provide a solution to the difficult separation of a homogeneous catalyst from a reaction product; large enough catalytic complexes will be retained by the membrane.^[5,6] The advantage is that the catalyst generally remains in its most active form when using membrane separation at reaction conditions.

A good and predictable performance of the membrane exposed to reaction conditions is a prerequisite for practical applications. Polymeric membranes are the most widely applied type of membranes.^[7] However, in applications involving supercritical carbon dioxide the use of polymeric membranes is limited. The swelling and plasticization of polymers occurring in the presence of high pressure carbon dioxide has a detrimental effect on membrane performance and stability.^[8] Also, the thermal stability of polymeric membranes can be insufficient for application at temperatures corresponding to reaction conditions. Ceramic membranes do have the capability to be used under more demanding conditions. For example, above the critical temperature and pressure of carbon dioxide, 31 °C and 7.4 MPa, alumina supported silica membranes appear to have promising and predictable characteristics.^[4,9] However, the possibility to tune the pore diameter using a selective layer based on titania, typically in the range 0.5 to 1.5 nm, is a clear advantage for the retention of a homogeneous catalyst in combination with a high flux of reaction products and solvent through the membrane.^[10] Another possible advantage of titania over silica is that in the presence of water the microporous, i.e a pore diameter smaller than 2 nm, titania membranes have a good

stability whereas silica membranes have a limited stability.^[11] In this respect, it is to be expected that microporous alumina supported titania membranes show a better stability.^[12]

There is a limited amount of literature on the performance of these ceramic membranes in terms of flux of a supercritical fluid mixture consisting of carbon dioxide and a solute of moderate molecular weight, like *n*-hexane or *n*-octane. Knowledge on the permeation behavior of such solutions is a prerequisite in view of the application of these membranes in the retention of homogeneous catalysts under one-phase supercritical reaction conditions. Here, an alumina supported microporous titania membrane is characterized by permeation of pure substances in the gaseous or supercritical state. Subsequently, the permeation of a supercritical solution of hexane or octane in carbon dioxide is investigated at 50 °C and pressures up to 20 MPa. Additionally, results on the retention of triphenylphosphine oxide, an analogue of triphenylphosphine, which is applied as a ligand in rhodium catalyzed hydroformylation, are presented.

Mass transfer mechanisms – In general three different mechanisms can describe mass transport across a porous membrane.

The first mechanism is based on a combination of surface diffusion and gas translation, which applies to microporous membranes with a pore diameter below 2 nm. For a temperature between 300 and 500 K, it has been found that for a silicalite-1 zeolite membrane with a pore size of 0.55 nm, surface diffusion and gas translation diffusion are the two main mechanisms for mass transport at a feed pressure of 0.101 MPa.^[13] Typically, as a function of temperature the flux of CO₂ first decreases, has a minimum, and then increases. The decreasing behavior observed for the permeance is a result of a decrease in the amount adsorbed with an increase in temperature, whereas the increase in the permeance is the result of an increase in gas translation diffusion with an increase in temperature.

For surface diffusion the driving force across the membrane is the difference in the degree of adsorption (surface occupancy) of the permeating species at the feed side and permeate side of the membrane:

$$N_{sd} = -\varepsilon\rho D_{sd}(q) \frac{\partial q}{\partial x} \quad (1)$$

where *q* is the amount adsorbed, ε the porosity, and ρ the density of the selective membrane layer. The diffusion coefficient is given by:

$$D(q) = D_{sd,0}(q)e^{\frac{-E_{s,D}}{RT}} \quad (2)$$

It can be expected that at high pressure the surface diffusion plays a only a minor role, because adsorption in microporous materials is described by a so-called type I isotherm. This type of adsorption can be described by a Langmuir isotherm:^[14]

$$\frac{q}{q_{sat}} = \frac{bP}{1 + bP} \quad (3)$$

with P the pressure and b a temperature-dependent parameter.

At high pressures and a relatively small pressure difference across the membrane, the amount adsorbed at the feed side will be about the same as the amount adsorbed on the permeate side. As a result, there is no driving force for surface diffusion, see equation 1. Furthermore, the amount adsorbed at a fixed pressure decreases with increasing temperature, the so-called isobar. This means that at high enough temperatures only gas translation diffusion will take place, which for an ideal gas can be expressed as:

$$N_{gt} = \frac{\varepsilon D_{gt}}{RTL} \Delta P \quad (4)$$

in which the diffusion coefficient is given by:

$$D_{gt} = \frac{\lambda}{z} \sqrt{\frac{8RT}{\pi M_i}} e^{\frac{-E_{GT}}{RT}} \quad (5)$$

The second mechanism is known as Knudsen transport, which predominantly takes place in mesoporous or macroporous membrane structures. These are membranes with a pore diameter between 2 and 5 nm, and the Knudsen flow is expressed as:

$$N_{Kn} = -\frac{2r}{3} \sqrt{\frac{8RT}{\pi M_i}} \frac{\partial C_i}{\partial x} \quad (6)$$

For an ideal gas equation 6 can be rewritten as:

$$N = -\frac{2r}{3RTL} \sqrt{\frac{8RT}{\pi M_i}} \Delta P \quad (7)$$

Based on values for the pore diameter of the titania membranes, it is to be expected that Knudsen transport has a negligible contribution to the mass transport of supercritical carbon dioxide.

The third mechanism is based on viscous flow. It has been suggested that the transport of supercritical carbon dioxide across a microporous silica membrane is mainly governed by viscous flow.^[4] Viscous flow is described by Darcy's law and can be expressed as:

$$\frac{F_{v,i}}{A} = -\frac{B_i}{\mu_i} \frac{\partial P}{\partial x} \quad (8)$$

where $F_{v,i}$ is the volumetric flow rate of a component i perpendicular to a surface with area A . B_i is a structure parameter, P the pressure, and μ_i the dynamic viscosity. The flux, $N_{v,i}$, is then given by:

$$N_{v,i} = -\frac{B_i}{\mu_i} \frac{\rho_i}{M_i} \frac{\partial P}{\partial x} \quad (9)$$

with ρ_i the density and M_i the molecular mass.

At higher feed pressures the term ρ_i/μ_i can be considered independent of pressure for small pressure differences across the membrane and then from equation 9 the following expression for convective flow through the pores can be found:

$$N_{v,i} = \frac{B_i}{M_i L} \frac{\rho_{f,i}}{\mu_{f,i}} \Delta P \quad (10)$$

$$K_i = \frac{B_i}{L} = \frac{\epsilon_i}{\tau} \frac{r^2}{8L} = \frac{N_{v,i} M_i \mu_{f,i}}{\Delta P \rho_{f,i}} \quad (11)$$

When a temperature near the critical temperature of the permeating species is applied the dependence of ρ_i and μ_i should be taken into account. This is demonstrated for CO_2 and SF_6 , by studying the variation in pressure, which is given by:

$$DF_{VF} = -\frac{1}{M_i \Delta P} \int_{P_f}^{P_f - \Delta P} \frac{\rho_i}{\mu_i} dP \quad (12)$$

In Figure 1a and Figure 1b this "driving force", DF_{VF} , is plotted as a function of feed pressure, P_f , for different pressure differences, ΔP , across the membrane. For small pressure differences the maximum in the DF_{VF} coincides with the maximum in ratio of the density to the dynamic viscosity. For a pressure difference larger than 0.1 MPa the maximum in DF_{VF} shifts to higher pressures.

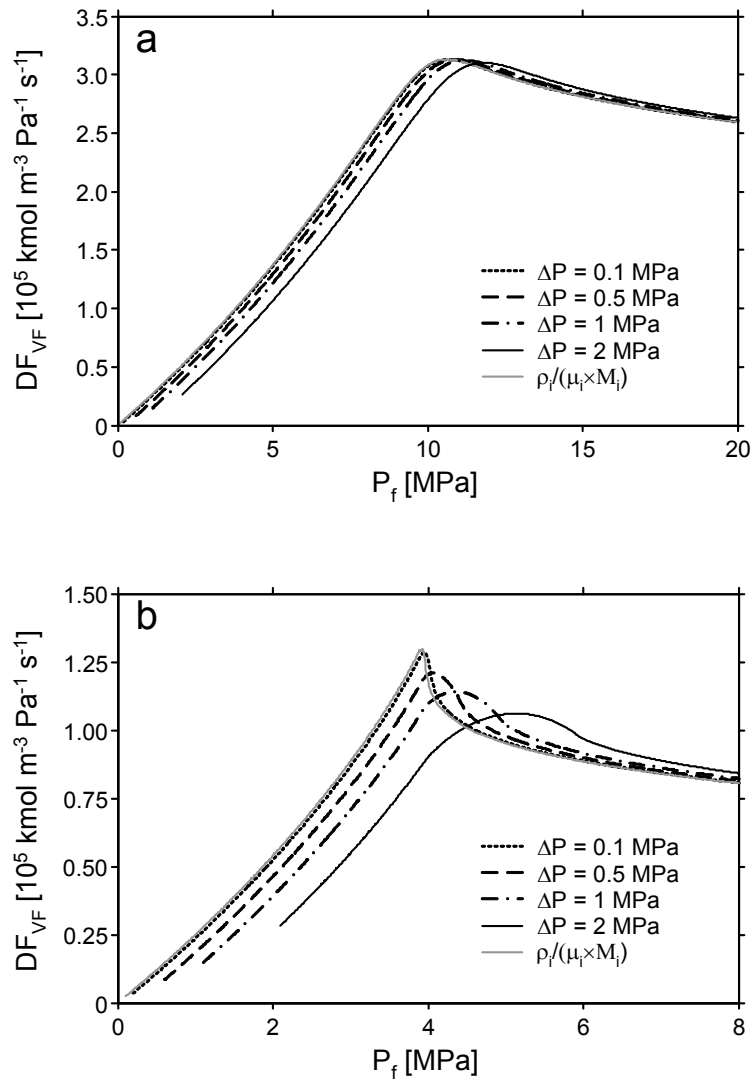


Figure 1. DF_{VF} as a function of feed pressure and pressure difference across the membrane for CO_2 at 50°C (a)^[15] and for SF_6 at 48°C (b).^[16]

Finally, a convenient quantity to describe the mass transport across a microporous membrane is the permeance, Π , which is given by:

$$\Pi = \frac{N}{\Delta P} \quad (13)$$

Experimental

Materials - Carbon dioxide, sulfurhexafluoride, helium, and nitrogen, grade 5.0, 2.8, 5.0 and 5.0, respectively, were obtained from Hoekloos (The Netherlands). Prior to use CO_2 was passed over a Messer Oxisorb filter to remove oxygen and moisture. *n*-Hexane (Merck,

analytical grade), *n*-octane (Aldrich, > 99%) and toluene (Merck, analytical grade) were dried with pre-treated molsieves 3A (Aldrich, 4-8 mesh), and stored under argon. For GC-analysis, the solvent toluene (Merck, analytical grade), and the internal standard *n*-decane (Aldrich, >99% purity) were used as received. Triphenylphosphine oxide and hexadecane were obtained from Fluka and Aldrich, respectively. A selection of the main properties of the substances used for the permeation experiments is given in Table 1. The main characteristics of the tubular alumina supported titania membrane are given in Table 2.

Table 1. Properties of the materials used in permeation experiments.^[15,17]

substance	T _b [°C]	T _c [°C]	P _c [MPa]	M _w [g mol ⁻¹]	d _{kinetic} [nm]
carbon dioxide		31.0	7.38	44.01	0.33
helium		-268	0.229	4.00	0.26
<i>n</i> -hexane	68.7	234.4	3.02	86.18	0.45 ^[a]
nitrogen		-147	0.340	28.01	0.36
<i>n</i> -octane	125.5	295.7	2.49	114.23	0.45 ^[a]
sulphur hexafluoride		45.4	3.76	146.05	0.55
toluene	110.6	319.8	4.1	92.14	0.66 ^[a]
triphenylphosphine oxide	360			278.29	

^[a] Estimated from [18].

Table 2. Characteristics membrane provided by ECN.

average Kelvin diameter of pores determined by permporometry	< 1×10 ⁻⁹ m
thickness selective titania layer	(1-2)×10 ⁻⁷ m
molecular weight cut-off of PEGs dissolved in water	< 600 D
outer diameter	0.014 m
effective length	0.11 m

High pressure membrane set-up - The setup, depicted in Figure 1, was designed such that it would be possible to feed gas, liquid, or a supercritical mixture up to pressures of 30 MPa. The membrane module (in house custom built) could be heated up to 200 °C by means of a digital controller (Labview software, **TIC**). **TIC1** also allowed for a temperature setpoint program. By this means the membrane module could be heated slowly in order to minimize thermal stresses on the membrane. Membrane sealing was achieved with O-rings. The tubing was traced and the temperature of the tracing is controlled digitally by **TIC2** (Labview software). The maximum allowable working temperature of the pressure difference transmitter (Endress+Hauser Deltabar PMD75, **ΔPI**) and the manual backpressure controller

(Tescom, **BPC**) was 75 °C. The pressure generator (Sitec, **PG**) had a working volume of 0.30 L and could be heated up to a temperature of 100 °C by using a thermostatic bath, in order to pump supercritical mixture to the membrane. The volume of the retention side, excluding **PG**, was 0.057 L and the volume of the permeation side till the sample point, **SP**, was estimated to be 0.019 L.

Permeation of pure substances - The experimental procedure was started by heating the set-up to the desired working temperature. The transport of gaseous species was measured by having **V1**, **BV5**, **V3**, **V5**, and **V6** open while the other valves were closed. The feed pressure was kept constant and the backpressure controller allowed for the control of the trans-membrane pressure.

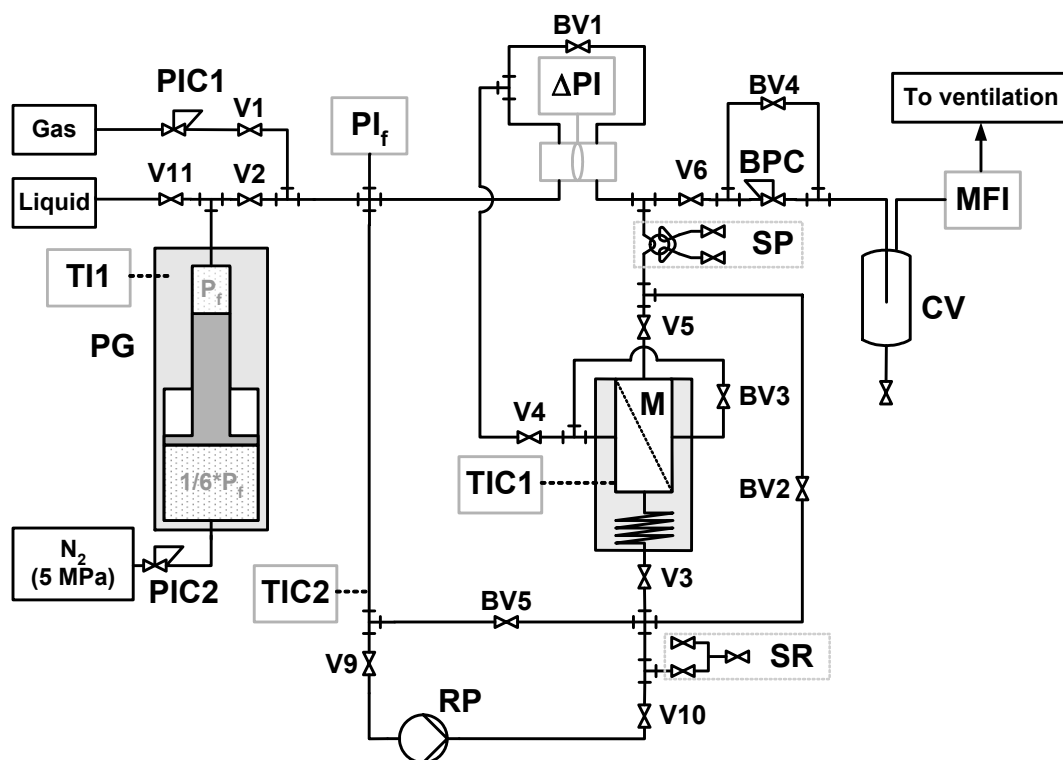


Figure 2. **PIC1** pressure reducing valve (0-1.5 MPa), **PIC2** digital pressure indicator controller (0.1-5 MPa), **BPC** backpressure controller (0.1-40 MPa), **PI_f** feed pressure indicator, **ΔPI** Pressure difference indicator, **TIC1** temperature indicator controller membrane module, **TIC2** temperature indicator controller tracing, **TI1** temperature indicator of **PG** pressure generator, **SP** sampling point permeate, **SR** sampling point retentate, **V** valve, **BV** bypass valve, **CV** collection vessel, **MFI** mass flow indicator, **M** membrane module imbedded in a heating mantle.

For the measurement at supercritical conditions the complete setup, including **PG**, was first filled with CO₂ or SF₆ at the desired feed pressure, while **V2**, **BV1**, **BV5**, **V3**, **V5**, **V6** and

V11, were open and the remaining valves were closed. Then **V11** was closed and the pressure of the set-up was further adjusted with **PG**. The nitrogen pressure in the low-pressure section of **PG** was regulated with **PIC2** (Bronkhorst). By regulating the pressure in the low pressure between 0.1 and 5 MPa, the working pressure of the pressure generator could be regulated between 0.6 and 30 MPa accordingly. Subsequently, the bypass valve, **BV1**, was closed and **BPC** was adjusted carefully in order to generate a pressure difference across the membrane, usually, in the range of 0.3 to 1 MPa. When the permeate stream passed the **BPC** it was expanded to atmospheric pressure. In order to maintain a stable pressure difference the **BPC** was also heated. The outgoing flow was measured using a mass flow meter, **MFI**. In the case of a small flow also a soap bubble flow meter could be applied. The position of the piston of the pressure generator was measured in order to determine the feed flow rate.

Permeation of supercritical solutions - After the complete set-up had reached the desired operating temperature, first the organic liquid, hexane or octane, was pumped into **PG** and subsequently CO₂ was charged in the **PG** up to the desired working pressure. Then a part of the content of the **PG** was used to charge the remaining part of the setup, while **V2**, **BV5**, **V3**, **BV3**, **V5**, and **BV1** were open and the other valves were closed. The recirculation pump (Sitec, **RP**) was turned on in order to minimize the presence of stagnant fluid in the system and to achieve further mixing. Recirculating the supercritical fluid through the retentate side as well as the permeate side was done for a period of about 0.5 to 1 h.

Before permeation was started, **V4** was opened and **BV1** and **BV3** were closed. In this way the circulation was restricted to the retentate/feed side of the membrane. Besides the above-mentioned aspects, the circulation also minimized the possible occurrence of concentration polarization at the retentate side of the membrane. Then **BPC** was adjusted carefully in order to generate a pressure difference across the membrane. Samples could be taken from the retentate and permeate side in order to determine the concentration of the dissolved species. The mass transfer rate across the membrane could be monitored by measuring the volume pumped by **PG** and by measuring the flow rate through **MFI**.

Permeation/retention measurements of triphenylphosphine oxide - The procedure for measuring the retention of triphenylphosphine oxide was performed in a similar way as for the permeation of supercritical solutions. However, at the start of the experiment the permeate

side was filled with pure toluene. Additionally, the permeate was collected (just after valve **V5**) at atmospheric pressure.

Analysis and calibration - The samples were analyzed off-line using a Fisons Instruments GF-FID equipped with a Restek Rtx-5 column (fused silica, length 30 m, internal diameter 0.53 mm) with helium as the carrier gas. Calibration was done for hexane and octane against *n*-decane as an internal standard and toluene as the solvent. Calibration for triphenylphosphine oxide was done against hexadecane as a standard with toluene as the solvent. The samples were diluted with the appropriate amount of corresponding internal standard solution.

Membrane treatment - Prior to permeation measurements the membrane was kept under nitrogen or helium flow at a temperature of 200 °C to remove adsorbed water. In between experiments with supercritical mixtures of CO₂ and *n*-hexane or *n*-octane, adsorbed species were removed by rinsing with supercritical carbon dioxide and helium at 50 °C. Depressurization from high pressure, after measurements with CO₂ or SF₆, was done carefully overnight.

Results and discussion

First the permeation of pure substances at low feed pressure will be discussed. Next the permeation of pure CO₂ and SF₆ at supercritical conditions will be presented. Finally, results on the permeation on supercritical mixtures will be given and discussed.

Permeation of pure gases - In Figure 3 the permeance across the titania membrane of He, N₂, CO₂, and SF₆ is given as a function of temperature. For the different gaseous species, a different behavior is observed. The permeance of helium increases over the whole temperature range. For N₂ and SF₆ the permeance decreases with an increase in temperature. For CO₂ the permeance first decreases and then increases slightly. The behavior for He indicates an activated process corresponding to gas translation diffusion.^[9,13] For N₂ and SF₆ the decreasing behavior implicates that surface diffusion is the main transport mechanism for these two substances for the temperature range applied here. The permeance of CO₂ is a combination of these two transport mechanisms. At temperatures above 100 °C, the permeance appears to increase with increasing temperature, which implicates an activated

transport mechanism. The decreasing behavior, observed at lower temperatures, is a result of surface diffusion.

The temperature dependence of the permeance for the different species shows resemblance with what has previously been observed for a microporous supported silica membrane.^[9] The values for the helium permeance observed here are somewhat lower than observed for the silica membrane. The CO₂ and the SF₆ permeance, however, are a factor of 2 to 3 higher than for the silica membrane.^[19] Most likely this difference is a result of the stronger adsorption of CO₂ and SF₆ on titania as compared to silica.

Permeation of supercritical CO₂ and SF₆ – In Figure 4 the permeance of CO₂ is given as a function of feed pressure at 50 °C. Additionally, results for the CO₂ permeation across a silica membrane [8][8] are given for comparison. The permeance increases with feed pressure up to 6.5×10^{-8} mol m⁻² Pa⁻¹ s⁻¹ at a feed pressure of about 12 MPa. The influence of the pressure difference is small. The value at 12 MPa for a pressure difference of about 1 MPa deviates from the other data for this pressure difference. The line in Figure 4 represents the result of the viscous flow model. The factor K_i for CO₂ was calculated using equation 11 and the permeance values at 20 MPa feed pressure. It can be seen that the viscous flow model describes the feed pressure dependence in the permeance reasonably well. At feed pressures below 6 MPa the permeance values are higher than the model prediction. This probably can be explained by the occurrence of surface diffusion as a transport mechanism at lower pressure.^[4]

The CO₂ permeance observed for the microporous silica membrane is somewhat lower than the permeance observed for the titania membrane. The value for K_i found for the silica membrane is 2.0×10^{-16} m taking the permeance value at 18 MPa. It appears that this type of pressure dependence of the permeance on the feed pressure is characteristic for these microporous alumina supported membranes.^[4,9] Also for organic polymeric membranes a similar behavior has been observed.^[4,20,21] The permeance values for the polymeric membranes are higher than those observed for the ceramic membranes.

In Figure 5 the permeance of SF₆ is shown as a function of feed pressure. A similar behavior of the SF₆ permeance as a function of feed pressure is observed as for CO₂ permeance. Furthermore, there seems to be a more clear effect of pressure difference on the permeance. Between 2 and 5 MPa the permeance decreases with increasing the pressure difference. This behavior can be explained by taking into account the pressure dependency of

the density and viscosity, as illustrated in Figure 1b. Again, the viscous flow model appears to give a reasonable description of the permeance as a function of feed pressure. The value calculated for K_i is 2.5×10^{-16} m, based on the permeance values at a feed pressure of 8 MPa.

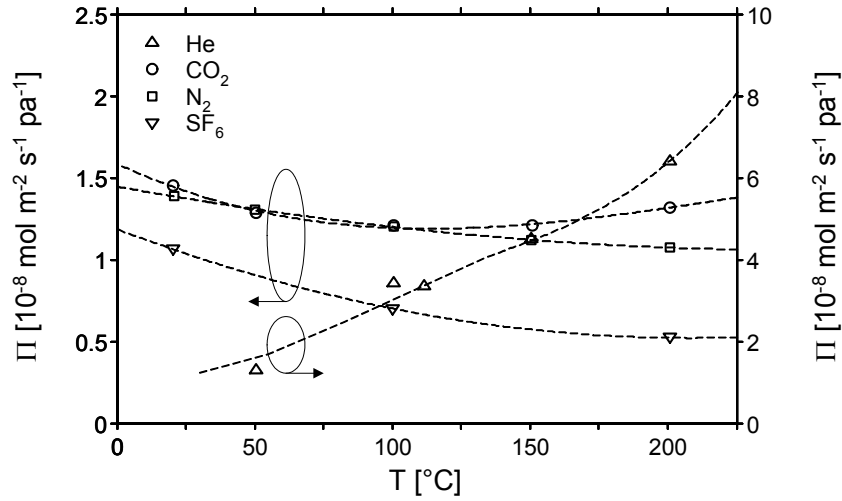


Figure 3. Permeance as a function of temperature for helium, carbon dioxide, nitrogen, and sulfur hexafluoride with a feed pressure of 0.5 MPa and a pressure difference of 0.3 MPa across the membrane at steady state. The dashed lines are a guide to the eye.

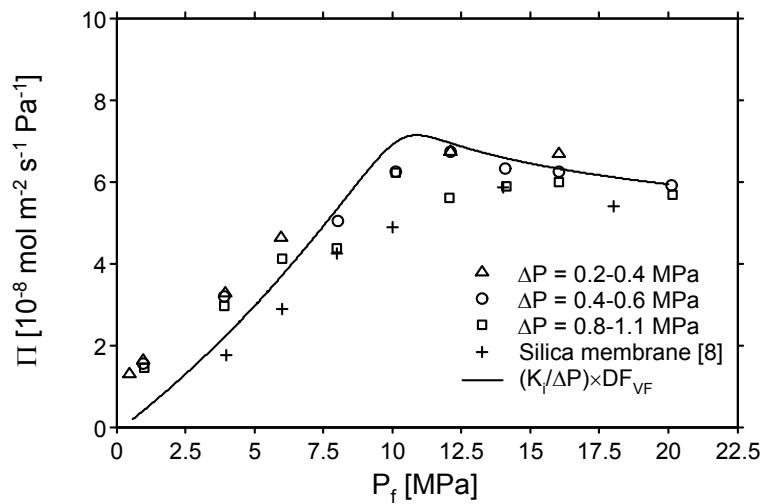


Figure 4. Permeance as a function of feed pressure for carbon dioxide with average pressure differences of 0.3, 0.5, and 1 MPa across the membrane at steady state. The line is calculated for a pressure difference of 0.5 MPa and K_i for CO_2 has a value of 2.3×10^{-16} m.

As shown in Table 1 the kinetic diameter of SF_6 is 0.55 nm. In Figure 6 the pore diameter, d_p , of the membrane is given as a function of porosity, based on equation 11 and a value of

2.3×10^{-16} m for K_i . With a porosity of 0.01, which is a value assumed in [4] for a microporous silica membrane, a pore diameter of 0.54 nm can be calculated. This suggests that the titania membrane has a pore size distribution between 0.5 and 1 nm.

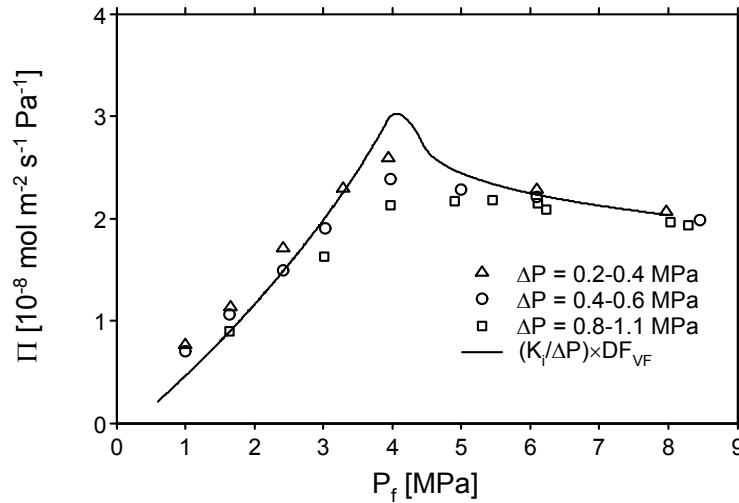


Figure 5. Permeance as a function of feed pressure for sulfur hexafluoride with pressure average differences of 0.3, 0.5, and 1 MPa across the membrane at steady state. The line is calculated for a pressure difference of 0.5 MPa and K_i for SF_6 has a value of 2.5×10^{-16} m.

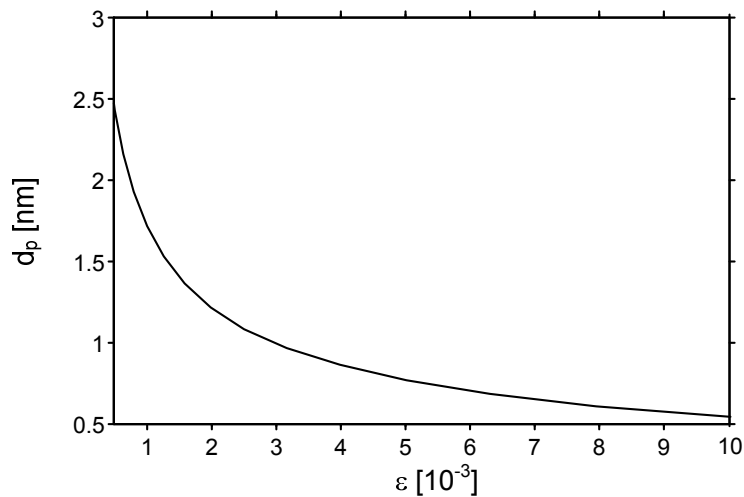


Figure 6. Pore diameter, d_p , as a function of porosity, ϵ , calculated with equation 11 for $K_i = 2.3 \times 10^{-16}$ m, $\tau = 2$, $L = 2 \times 10^{-7}$ m.

Permeation of CO_2 enriched supercritical solutions of alkanes – In Table 3 results are shown for the permeation of supercritical mixtures of hexane in carbon dioxide. C_i and C_s are the concentrations of solute and solvent in the feed pump, **PG**, respectively. $C_{R,av}$ and $C_{P,av}$ are the

averages of the concentrations of solute observed at the retentate and the concentrations observed at the permeate side, respectively, during a period of 4 to 6 hours indicated by t . $C_{R,e}$ and $C_{P,e}$ are the final concentrations of solute observed at the retentate and permeate side, respectively. Π is the permeance based on the flow measured by **MFI**. It has been assumed that the measured gas flow has the same characteristics of a gas flow of pure carbon dioxide. $F_{v,pump}$ is de volume flow of high pressure mixture at 50 °C measured with **PG**.

Table 3. Experimental conditions and main results for the permeation of hexane dissolved in carbon dioxide at 50 °C.

entry	C_i [a]	C_s [a]	P_f [MPa]	ΔP_{av} [MPa]	t [h]	$C_{R,av}$ [a]	$C_{P,av}$ [a]	$C_{R,e}$ [a]	$C_{P,e}$ [a]	Π [b]	$F_{v,pump}$ [mL min ⁻¹]
3	0.086	15	15.3	0.49	5.5	0.013	0.019	0.020	0.017	6.1	0.53
4	0.47	14	15.4	0.52	5.8	0.22	0.17	0.50	0.42	5.8	0.56
5	0.57	14	15.3	0.97	3.6	0.37	0.43	0.60	0.59	5.4	0.92
6	0.51	14	15.3	0.96	4.5	0.38	0.34	0.49	0.44	5.4	0.90

[a] mol L⁻¹

[b] 10⁻⁸ mol m⁻² Pa⁻¹ s⁻¹

It should be noted that for all experiments with supercritical mixtures a systematic deviation between the concentration expected to be present in the pump and the retentate concentration has been observed. Although the supercritical mixture is generated a day before an experiment, the time of about 17 h is apparently not enough to obtain a homogeneous supercritical mixture. The pressure, temperature and concentration of hexane or octane applied here should ensure a one-phase supercritical system. The mole fraction of CO₂ is above 0.96 in all cases.^[22] The measured concentrations give the best description of the concentration of solute at the retentate and permeate side of the membrane. Furthermore, it should be noted that in the cases where the final concentration of retentate and permeate is higher than the average of all the samples measured during the experiment, the concentration of the solute at both the retentate and permeate side shows an increase in time. This is an indication that the mixture has not been equilibrated long enough, and that during the experiments there has been a concentration gradient in the pump.

When the concentration of the retentate and permeate side are compared (Table 3), it can be seen that in most cases the retentate concentration is slightly higher than the permeate concentration. The permeance is slightly lower than observed for pure carbon dioxide. The results indicate that there is little rejection of hexane.

In Table 4 the results for the permeation of supercritical mixtures of carbon dioxide and octane are given. The difference between retentate and permeate concentration is small.

Regarding entries 1, 2, 7, and 8, the permeance values decrease with a higher concentration of octane and higher pressure difference. Again, the small difference between retentate and permeate concentration indicates a negligible rejection of octane under these conditions.

Table 4. Experimental conditions and main results for the permeation of octane dissolved in carbon dioxide at 50 °C.

entry	C_i [a]	C_s [a]	P_f [MPa]	ΔP_{av} [MPa]	t [h]	$C_{R,av}$ [a]	$C_{P,av}$ [a]	$C_{R,e}$ [a]	$C_{P,e}$ [a]	Π [b]	$F_{v,pump}$ [mL min ⁻¹]
1	0.10	16	15.4	0.45	4.7	0.046	0.040	0.047	0.040	5.7	0.46
2	0.24	15	15.4	0.51	7.6	0.13	0.13	0.16	0.15	5.7	0.49
7	0.52	14	15.3	0.94	4.3	0.43	0.43	0.54	0.53	5.0	0.75
8	0.57	15	15.4	0.94	3.9	0.30	0.31	0.30	0.30	5.2	0.82
9	0.25	17	20.3	0.98	3.8	0.14	0.15	0.14	0.14	4.6	0.78
13	0.57	14	15.4	0.99	5.3	0.23	0.20	0.62	0.49	3.0	0.52
14	0.28	-	15.4	0.99	4.6	0.18	0.18	0.18	0.17	3.2	0.55

[a] mol L⁻¹

[b] 10⁻⁸ mol m⁻² Pa⁻¹ s⁻¹

It should be noted that the experiments corresponding to entry 13 and 14 have been performed after the rejection experiments with triphenylphosphine oxide dissolved in toluene.

Table 5 shows the results of the retention experiments of triphenylphosphine oxide. Entry 10 and 11 is one experiment conducted during two days, during which no steady state has been reached. The concentration at the permeate side appears to increase to the concentration measured at the retention side. These results indicate a limited retention of triphenylphosphine oxide by the titania membrane. It is unclear why the measured concentration of triphenylphosphine oxide is about a factor 2 smaller than the feed concentration. A possible explanation could be that triphenylphosphine oxide or the toluene adsorbs strongly to the membrane. This could also be an additional reason for the lower value for the CO₂ permeance observed after exposure to toluene, see entry 13 and 14 (Table 4).

Table 5. Experimental conditions and main results for the permeation of triphenylphosphine oxide dissolved in toluene at 50 °C.

entry	C_i [a]	C_s [a]	P_f [MPa]	ΔP_{av} [MPa]	t [h]	$C_{R,av}$ [a]	$C_{P,av}$ [a]	$C_{R,e}$ [a]	$C_{P,e}$ [a]	Π [b]	$F_{v,pump}$ [mL min ⁻¹]
10	0.002	9	1.1	1.0	3.5	0.0011	0.0002	0.0009	0.0004	0.3 ^[c]	0.095
11	0.002	9	1.1	1.0	6.5	0.0011	0.0006	0.001	0.0008	0.4 ^[c]	0.14

[a] mol L⁻¹

[b] 10⁻⁸ mol m⁻² Pa⁻¹ s⁻¹

[c] based on $F_{v,pump}$

In Figure 7 the permeance of CO₂ is plotted as a function of the concentration of solute measured at the retention side. For both hexane and octane as a solute, the measured

permeance appears to decrease with an increase in concentration. For octane this effect seems to be more pronounced than for hexane, which probably can be attributed to the higher molecular mass of octane. In Figure 8 the volumetric feed flow obtained for hexane and octane dissolved in scCO₂ is given as a function of the pressure difference across the membrane. For both hexane and octane the flow appears to show a linear dependence on the transmembrane pressure.

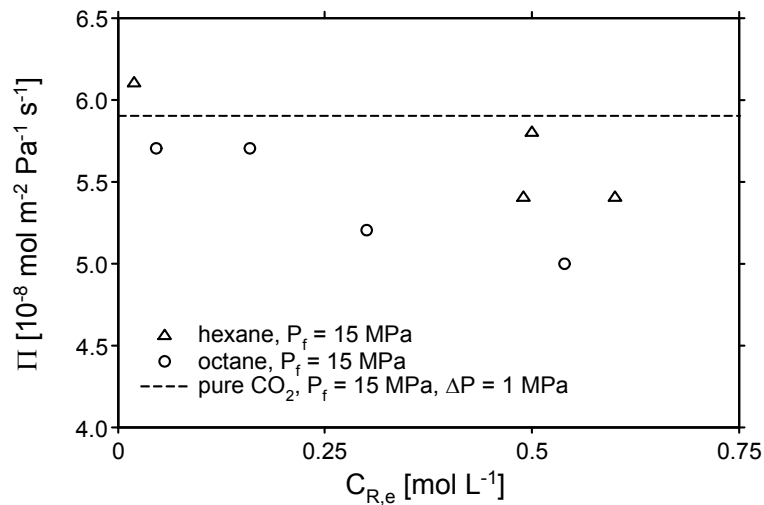


Figure 7. Permeance as a function of the observed retentate concentration for the solutes hexane and octane at a feed pressure 15 MPa.

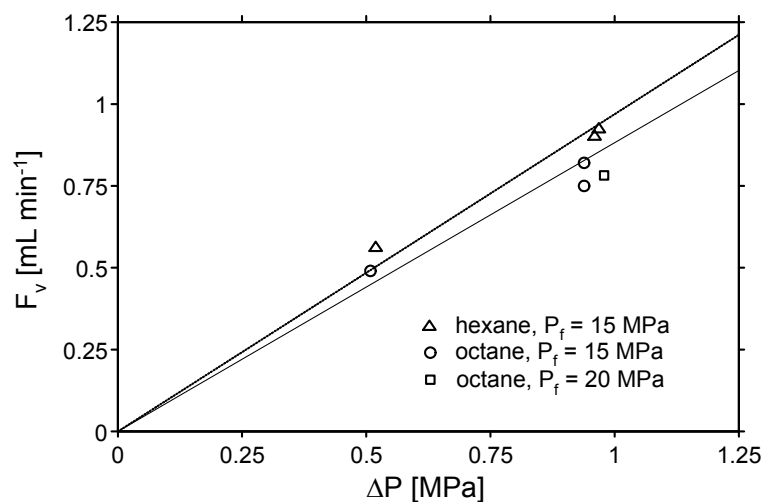


Figure 8. The volumetric flow at 50 °C versus pressure difference for the solutes hexane and octane. The lines are a guide to the eye.

Based on the results for the permeation of octane dissolved in CO₂ and the limited retention of triphenylphosphine oxide it is to be expected that for the current titania membrane the hydroformylation product nonanal will permeate through the membrane. Furthermore, complete retention of fluoros monodentate ligands, presented in Chapter 2 to 6, by using the titania membrane studied here cannot be expected.

Conclusion

An alumina supported titania membrane has been characterized by permeation experiments with pure substances at low and high feed pressures. The temperature dependence of the permeance of helium, carbon dioxide, nitrogen and sulfur hexafluoride at a pressure of 0.5 MPa suggest mass transport across the membrane by surface diffusion and activated gas translation diffusion through the micropores. The observed permeance as a function of feed pressure for both carbon dioxide and sulfur hexafluoride can be described using the viscous flow model. The membrane shows a negligible rejection of the solutes hexane, octane dissolved in a CO₂ rich supercritical medium, and of triphenylphosphine oxide dissolved in toluene. The application of a solution of triphenylphosphine oxide in toluene as the feed, resulted in a decrease in the permeance of CO₂ across the membrane, from about 6×10^{-8} mol m⁻² Pa⁻¹ s⁻¹ to about 3×10^{-8} mol m⁻² Pa⁻¹ s⁻¹.

It should be noted that only one titania membrane has been used for all the measurements. The dependence of the permeation of carbon dioxide across the titania membrane on the feed pressure is similar to what has been previously observed for microporous alumina supported silica membranes. The current titania membrane shows a reasonable stability over a period of operation of about at least 6 months in varying conditions.

References

- [1] P. G. Jessop, W. Leitner (Eds.), *Chemical Synthesis Using Supercritical Fluids*, Wiley-VCH, Weinheim, **1999**, p. 1-13.
- [2] M. A. McHugh, V. J. Krukonis, *Supercritical Fluid Extraction*, Butterworth-Heinemann, Boston, **1994**, p. 1-26.
- [3] S. Sarrade, C. Guizard, G. M. Rios, *Desalination* **2002**, *144*, 137-142.
- [4] V. E. Patil, J. Meeuwissen, L. J. P. van den Broeke, J. T. F. Keurentjes, *J. Supercrit. Fluids* **2006**, *37*, 367-374.
- [5] L. J. P. van den Broeke, E. L. V. Goetheer, A. W. Verkerk, E. de Wolf, B.-J. Deelman, G. van Koten, J. T. F. Keurentjes, *Angew. Chem. Int. Ed.* **2001**, *40*, 4473-4474.

- [6] K. de Smet, S. Aerts, E. Ceulemans, I. F. J. Vankelecom, P. A. Jacobs, *Chem. Commun.* **2001**, 597-598.
- [7] R. W. Baker, *Membrane Technology and Applications*, John Wiley and Sons, Ltd, Chichester, **2004**, p. 1-14.
- [8] A. Bos, I. G. M. Pünt, M. Wessling, H. Strathmann, *J. Membrane Sci.* **1999**, *155*, 67-78.
- [9] A. W. Verkerk, E. L. V. Goetheer, L. J. P. van den Broeke, J. T. F. Keurentjes, *Langmuir* **2002**, *18*, 6807-6812.
- [10] J. Sekulić, J. E. ten Elshof, D. H. A. Blank, *Adv. Mater.* **2004**, *16*, 1547-1550.
- [11] J. Campaniello, C. W. R. Engelen, W. G. Haije, P. P. A. C. Pex, J. F. Vente, *Chem. Commun.* **2004**, 834-835.
- [12] T. van Gestel, C. Vandecasteele, A. Buekenhoudt, C. Dotremont, J. Luyten, B. van der Bruggen, G. Maes, *J. Membrane Sci.* **2003**, *214*, 21-29.
- [13] W. J. W. Bakker, L. J. P. van den Broeke, F. Kapteijn, J. A. Moulijn, *AIChE J.* **1997**, *43*, 2203-2214.
- [14] W. Zhu, J. M. van de Graaf, L. J. P. van den Broeke, F. Kapteijn, J. A. Moulijn, *Ind. Eng. Chem. Res.* **1998**, *37*, 1934-1942.
- [15] <http://webbook.nist.gov/chemistry/>
- [16] J. Wilhelm, D. Seibt, E. Bich, E. Vogel, E. Hassel, *J. Chem. Eng. Data* **2005**, *50*, 896-906.
- [17] M. B. Rao, R. G. Jenkins, *Carbon* **1987**, *25*, 445-446.
- [18] C. E. Webster, R. S. Drago, M. C. Zerner, *J. Am. Chem. Soc.* **1998**, *120*, 5509-5516.
- [19] A. W. Verkerk, in *Application of silica membranes in separation and hybrid reactor systems*, PhD thesis, Eindhoven University of Technology, Eindhoven, **2003**, p.37-59.
- [20] S. Sarrade, G.M. Rios, M. Carlés, *J. Membrane Sci.* **1996**, *114*, 81-91.
- [21] V. E. Patil, L. J. P. van den Broeke, F. F. Vercauteren, J. T. F. Keurentjes, *J. Membrane Sci.* **2006**, *271*, 77-85.
- [22] E.-J. Choi, S.-D. Yeo, *J. Chem. Eng. Data* **1998**, *43*, 714-716.

Chapter 8

Integration of reaction and separation at supercritical conditions using a titania membrane

Abstract

Several aspects relevant for the development of a continuous process suited for hydroformylation in supercritical carbon dioxide with catalyst retention by a ceramic membrane have been studied. From a study of the reaction kinetics, it can be concluded that using carbon dioxide as a solvent can improve catalyst activity and selectivity. The permeation characteristics of supercritical mixtures across a microporous titania have been evaluated. In this chapter preliminary results for the continuous homogeneously catalyzed hydroformylation integrated with membrane separation are presented. The results obtained throughout this thesis are put into perspective and directions for further research and recommendations for improvement are given.

Introduction

In the previous chapters the applicability of carbon dioxide in the rhodium-catalyzed hydroformylation of 1-octene has been demonstrated. An experimental procedure for the hydroformylation of 1-octene in supercritical carbon dioxide has been presented, which allows a facile operation and reproducible initial reaction conditions. Furthermore, the relevance of pressure measurement during reaction has been illustrated, for which a correlation has been established between pressure and conversion. The influence of the reaction parameters like temperature, solvent concentration (total initial reactor pressure), reactant concentration, catalyst concentration, and the ligand to rhodium ratio on the activity and selectivity of the reaction has been studied. A kinetic model of the hydroformylation in a homogenous carbon dioxide rich one-phase system has been formulated and has been evaluated for its description of the experimentally obtained concentration profiles. A comparison has been made between the solvents carbon dioxide, hexane, toluene, and perfluoromethylcyclohexane. In this comparison also different catalysts have been used. The comparison has focused on the differential regioselectivity observed during batch and semi batch operation. Additionally, results on “solventless” hydroformylation have been presented. It has been demonstrated that the permeation characteristics of high-pressure supercritical fluids across a microporous titania membrane can be described by a viscous flow model. A good impression is obtained about the optimal conditions for a continuous hydroformylation process carried out in supercritical carbon dioxide.

In this chapter a continuous hydroformylation reaction is discussed. A set up has been developed and used that closely matches the characteristics of the proposed membrane reactor concept depicted in Figure 1. Moreover, some relevant aspects for the further development of continuously operated homogeneously catalyzed reactions in supercritical fluids are discussed in this chapter.

Membrane reactor for homogeneous hydroformylation:

Experimental

Materials and analysis – The same sampling, materials handling, and analysis methods were used as described in Chapters 2 to 7. The same membrane, for which the permeation results were presented in Chapter 7, was applied here.

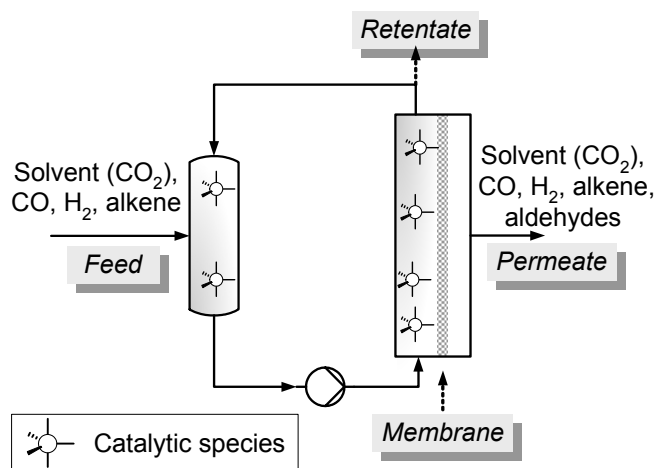


Figure 1. Schematic representation of the membrane reactor.

High pressure membrane reactor setup - The setup described in Chapter 7 was modified to allow addition of the catalyst precursors, formation of the catalyst, release of catalyst at the retentate side of membrane setup at high pressure, and visual inspection of the mixture during reaction. The setup is depicted in Figure 2. The temperature controlled high-pressure optical cell with a volume of 15 mL (Sitec) could be charged independently from the rest of the setup with the desired amounts of syngas and carbon dioxide up to pressures of 30 MPa. The total retentate/reactor volume, including **HPOC**, was 0.072 L.

Procedure - The conditions applied for the continuous reaction are given in Table 1 and have been chosen such that a considerable regioselectivity can be expected. The reactant concentrations have been chosen relatively low in order to simulate the conditions applied during the membrane permeation experiments. An excess of syngas with respect to 1-octene has been used in order to have sufficient stabilization of the catalyst in the case of complete conversion. Furthermore, an excess of hydrogen with respect to carbon monoxide has been applied to promote a high reaction rate.

The experiment, which was performed during five consecutive days, was started by charging **PG** with 1-octene, carbon monoxide, hydrogen, and finally carbon dioxide up to a pressure of 22 MPa at a temperature of 50 °C. The mixture in **PG** was allowed to equilibrate overnight. Then the membrane section, **HPOC** excluded, was charged with the reactants and solvent corresponding to the concentrations given in Table 1. The circulation was turned on to achieve a good distribution and mixing of the reactants and solvent throughout the whole setup, excluding **PG** and **HPOC**, for a period of 1 h.

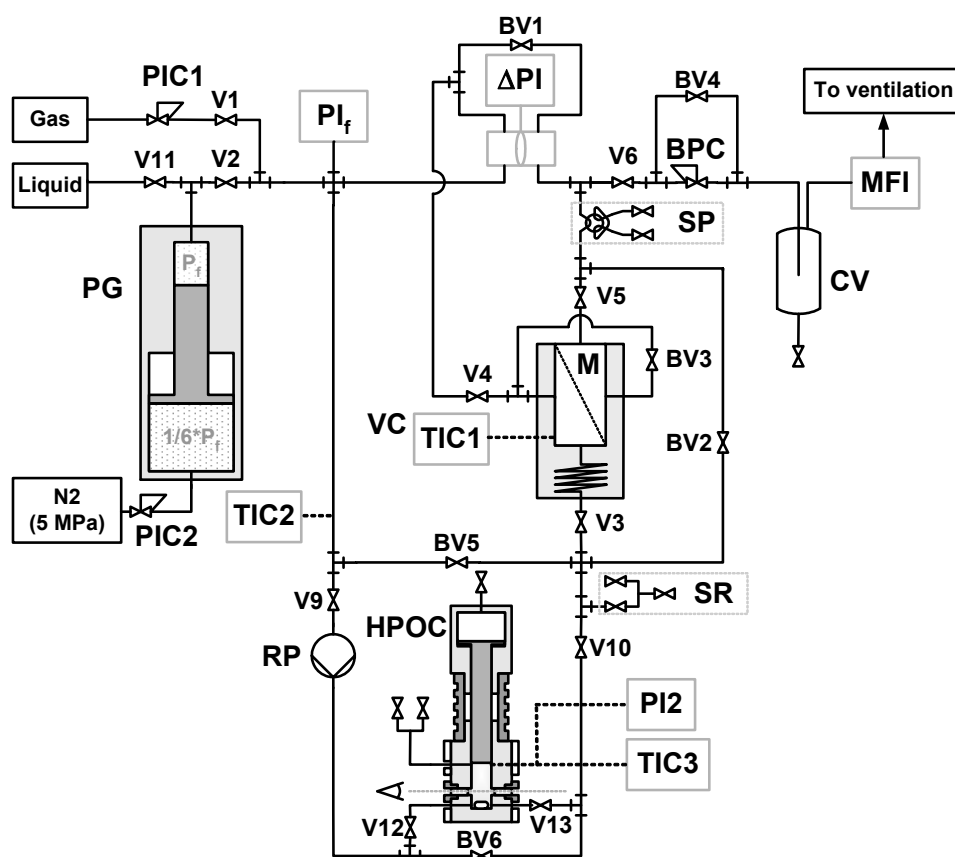


Figure 2. PIC1 pressure reducing valve (0-1.5 MPa), PIC2 digital pressure indicator controller (0.1-5 MPa), BPC back-pressure-controller (0.1-40 MPa), PI_f feed pressure indicator, ΔPI Pressure difference indicator, TIC1 temperature indicator controller membrane module, TIC2 temperature indicator controller tracing, TI1 temperature indicator, PG pressure generator, SP sampling point permeate, SR sampling point retentate, V valve, BV bypass valve, CV collection vessel, MFI mass flow indicator, M membrane module imbedded in a heating mantle, HPOC high-pressure optical cell, PI2 pressure indicator, TIC3 temperature indicator controller.

Table 1. Conditions during continuous hydroformylation of 1-octene.

T [°C]	50
P _{feed} [MPa]	22
Initial concentration [mol L ⁻¹]:	
CO	0.48
H ₂	0.71
CO ₂	15
1-octene ^[a]	0.25
[Rh(CO) ₂ acac] ^[b]	1.7×10 ⁻⁴
PPh(3,5-(CF ₃) ₂ -C ₆ H ₃) ₂ ^[b]	1.4×10 ⁻²

^[a] A similar systematic error occurred as observed for the concentration measurements of octane dissolved in CO₂ (see Chapter 7). The total sum of the concentration of 1-octene and the aldehyde products, determined by GC analysis, varied between 0.052-0.122 mol L⁻¹ at the retentate side.

^[b] The initial concentration is determined by dividing the amount of catalyst precursor by the total volume of the retention section of the setup, which is 0.072 L.

During this time **HPOC** was charged with the catalyst precursors, carbon monoxide, hydrogen and carbon dioxide up to a pressure of 22 MPa at 50 °C. Before permeation was started, **V4** was opened and **BV1** and **BV3** were closed. In this way the circulation was restricted to the retentate/feed side of the membrane. Then **BPC** was adjusted carefully in order to generate a pressure difference across the membrane. In Figure 3 the applied pressure difference and the volume flow as a function of the number of reactor volumes permeated through the membrane is depicted. Initially the pressure difference was 1 MPa, corresponding to an average volume flow (F_v) of 0.52 mL min⁻¹ at 22 MPa and 50 °C (determined by the volume indicator on **PG**). Samples were taken from the retentate and permeate side at the respective sample points **SR** and **SP**. During the remaining three days a pressure difference of 0.5 MPa was applied, corresponding to a volume flow of 0.3 mL min⁻¹ and a residence time of about 4 h. After 1.5 reactor volumes were permeated the contents of **HPOC** was connected in series with the membrane by opening **V12** and **V13** and closing **BV6**. In total the catalyst was isolated for about 3.5 h before release at the retentate side. At the end of the day permeation was stopped by adjusting **BPC** and closing **V2**. The reactor part was allowed to cool down. **PG** was refilled with reaction mixture and was left to equilibrate overnight, so that it was ready for use the next day. The pump **PG** (Figure 2) can contain 300 mL of the high-pressure feed mixture. At a feed rate of 0.5 mL min⁻¹ (F_v) the setup can be continuously operated for 10 h.

The next day heating was turned on again and when the reaction temperature was reached **V2** was opened. Again **BPC** was adjusted to generate a pressure difference in order to start permeation through the membrane. In total 27.5 h of operation was achieved over four consecutive days. During reaction a one-phase system was observed by visual inspection of **HPOC**.

Membrane reactor for homogeneous hydroformylation:

Results and discussion

In Figure 4 the conversion and the *n:iso* ratio are given as a function of reactor volumes permeated across the membrane. Before the addition of catalyst a blank conversion of about 0.5 % is observed. The low *n:iso* ratio confirms that the blank reaction activity is not caused by phosphine-rhodium complexes.

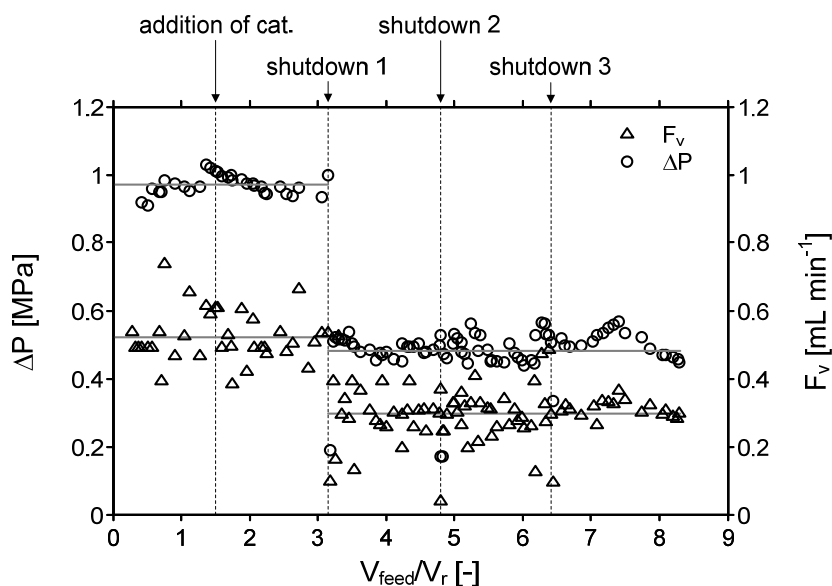


Figure 3. Applied pressure difference, ΔP , and the volume flow, F_v (at 22 MPa and 50 °C), as a function of the number reactor volumes permeated through the membrane, V_{feed}/V_r . The grey lines indicate the average values of pressure difference and the volumetric flow (at 22 MPa and 50 °C). The residence time is 2.3 h between the addition of catalyst and shutdown 1. Between shutdown 1 till $V_{\text{feed}}/V_r = 8.3$ the residence time is about 4 h.

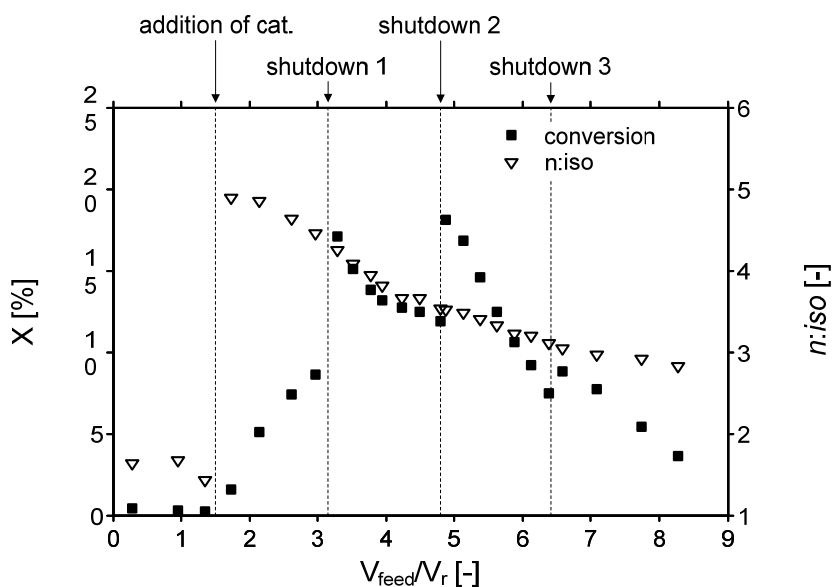


Figure 4. Conversion and the *n:iso* ratio as a function of the number of reactor volumes permeated across the membrane.

The blank activity has to be caused by the stainless steels of the various parts of the setup, because metal precursors like $[\text{Rh}(\text{CO})_2\text{acac}]$ have not been charged to this setup before. After addition of the catalyst, the *n:iso* ratio increases to a value of 5. Between the addition of the

catalyst and the first shutdown the conversion gradually increases to a value of about 9 %, while the *n:iso* ratio decreases from 5 to about 4.5. When the reactor is shut down it takes over 2 h for the membrane module and the high-pressure optical cell to cool down to room temperature, and as a result the reaction is not stopped immediately. Therefore, it is to be expected that the starting conversion on the next day is higher than the conversion at shut down. The first measurement after the first shutdown, at a V_{feed}/V_r value of 3.3, shows a conversion of 17%. During the second day of reaction the conversion decreases from 17% to 12%, and the *n:iso* ratio decreases from 4.2 to 3.5. The third day, after the second shutdown, a similar behavior is observed as after the first shutdown. The conversion starts at 18%, which is higher than the final conversion observed the day before, and decreases to a value of 7.5%. In this case, the *n:iso* ratio decreases from a value of 3.5 to 3.1. On the last day the first measurement yields a value of 9% for the conversion, which decreases to a value of 3.6%. The *n:iso* ratio continues to decrease, and at a $V_{\text{feed}}/V_r = 8.3$ a value of 2.8 is obtained.

The main reaction products, measured with GC, are as expected nonanal and 2-methyloctanal. Isomers of 1-octene or octane have not been detected. This implies that the chemoselectivity during the complete course of reaction has been close to 100%.

The fact that during the hydroformylation the conversion and *n:iso* ratio change is probably caused by the limited retention of the catalyst by the titania membrane. There are several indications that the rhodium species and the ligand are not completely retained by the titania membrane. After adding the catalyst and excess ligand to the retentate side, a clear peak could be identified from the GC-analysis results, which probably could be assigned to the free phosphine ligand. This peak was present in the GC-analysis results of both the retentate and permeate samples. The peak areas assigned to the ligand were similar for the samples taken at the retentate and permeate side at the same time, which indicated a limited retention of ligand. At the start of the second measurement interval (at a V_{feed}/V_r value of 3.2) the area of the peak we associated with the ligand was about 5 % of the area we measured initially (at a V_{feed}/V_r value of 1.7). In the subsequent samples the ligand peak area reduced further. In the collection vessel, **CV**, a yellow colored liquid, containing mainly 1-octene, product aldehydes, and residues of the catalyst accumulated during reaction. The products of aldol condensation reactions of the aldehydes can cause the yellow color of the permeate liquid. Therefore, the color of the permeate is not a decisive indication of the presence of catalyst. The decrease in *n:iso* ratio during the whole reaction is most likely a result of a

decrease in ligand to rhodium ratio. In general, a decrease in ligand to rhodium ratio leads to a decrease in regioselectivity and thus in *n:iso* ratio.^[1]

The averaged reaction rate values observed during the four intervals of reaction are subsequently 0.93×10^{-4} , 2.2×10^{-4} , 2.6×10^{-4} , and 1.1×10^{-4} mol_{aldehyde} h⁻¹, which corresponds to a turnover-frequency, TOF, of about 7.7, 19, 22, and 8.9 mol_{aldehyde} mol_{Rh}⁻¹ h⁻¹, respectively, when a constant Rh concentration is assumed. The fourth day of reaction the averaged reaction rate is more than a factor of two lower than the day before. This is another indication of catalyst loss. Finally, the observed reaction rates are much lower than expected. The corresponding batch experiment has not been carried out, but it is estimated that the TOF should be in the order of 100 to 300 mol_{aldehyde} mol_{Rh}⁻¹ h⁻¹. Besides a loss of activity as result of catalyst leaching, deactivation of the catalyst by impurities cannot be ruled out considering the duration of the complete experiment of about 72 h. The 72 h of operation consisted of 27.5 h of permeation and reaction. The intermittent shutdowns and startups (taking up about 44.5 h) could have a detrimental effect on catalyst stability as well. All in all, it is not likely that the catalyst deactivation alone can account for the observed conversion profiles. Another aspect, which could contribute to the low catalytic activity is the possible adsorption of catalytic species on the membrane. However, the temperature of 50 °C and the presence of a sufficient amount of ligand, either carbon monoxide or phosphine, will probably suppress the occurrence of adsorption.^[2]

Future perspectives for membrane reactors for homogeneous hydroformylation

The combination of the ceramic membrane and the homogeneous hydroformylation catalyst does not perform as well as observed previously for other cases where homogeneous catalysis and membrane separation have been integrated. For example, Jacobs and co-workers obtained for the continuous enantioselective hydrogenation of dimethylitaconate with a Ru-BINAP^[3] catalyst a conversion level above 95% during 40 h of operation.^[4] They applied a dimethylitaconate concentration of 4×10^{-7} mol L⁻¹ in methanol, a retention volume of 14 mL in which 3.6×10^{-5} mol catalyst was dissolved at a temperature of 37 °C and 1 MPa total pressure as a result of the hydrogen present. The example, which is most comparable to the case presented here, is the continuous hydrogenation of 1-butene with a fluoros version of the Wilkinson catalyst. In that case also carbon dioxide was used as the solvent and a

microporous silica membrane was used to retain the catalyst. The conversion was above 30% during 32 permeated reactor volumes.^[5,6]

Improvements of the performance of the current membrane reactor system can be achieved in two ways. First, the retention characteristics of the microporous titania membrane have to be better understood and improved. The pore size distribution has to be narrower in order to minimize the permeation of the larger catalyst molecules through the membrane. In order to obtain a smaller pore size distribution the number of defects in the membrane toplayer, but also of the supporting layers has to be reduced.^[7,8]

The second way to improve the performance is through modification of the catalyst. In particular, in order to increase the size of the catalyst molecule larger ligands have to be used. As demonstrated in Chapters 5 and 6, the application of different ligands has subtle effects on the activity and selectivity. There are several possibilities to increase the size of a soluble catalyst in order to improve the separation. It is to be expected that monodentate phosphines with larger fluorine tails than the trifluoromethyl group will be better retained by the membrane. A number of researchers have reported on the application of monodentate phosphines with fluorine tails in supercritical carbon dioxide.^[5,6,9-12] Bidentate phosphines ligands such as the well-known BINAP or Xantphos have a larger size and a more rigid structure than the triphenylphosphine based ligands.^[3,13] Furthermore, these bidentate ligands are less prone to dissociate completely from the metal centre. Fluorine versions of these ligands have been applied in CO₂-rich reaction environments.^[14-18] In the earliest reports on homogeneously catalyzed reactions integrated with membrane separation, dendritic versions, which are well-defined macromolecular structures, of homogeneous catalysts have been applied.^[19,20] Dendrimers can be used as “hosts” for the solubilization of catalyst in supercritical carbon dioxide.^[21-23] Another strategy to obtain macromolecular homogeneous catalysts, is to attach ligands to a polymer backbone.^[24] This approach has also been applied to rhodium based hydrogenation and hydroformylation catalysts, which have been attached to CO₂ soluble polymers.^[25,26]

In the case of the hydroformylation of 1-octene a good match between membrane retention characteristics and the size of the catalyst and its precursors has not been found yet. However, it should be noted that this has been the first reaction experiment performed with the newly developed high-pressure membrane setup. Before the reaction experiment the

membrane has been used for a large number of measurements under a great variety of conditions, as discussed in Chapter 7.

Relation between pressure, selectivity, and phase behavior

In Chapter 2 it has been illustrated that in particular for fast batch reactions the reactor pressure can provide information on the reaction rate and the extent of the reaction. In the case where the amount of ligand was varied, the correlation between chemoselectivity and pressure could not be established very clearly. However, there is a clear indication that the chemoselectivity changes when the ligand to rhodium ratio is varied (see Chapter 3).

To illustrate that the reactor pressure can be a measure of the chemoselectivity, the pressure observed for the experiments with the four different catalysts, i.e. using ligand **I** to **IV**, is evaluated. The chemoselectivity and regioselectivity for these four cases has been extensively evaluated in Chapter 5 and 6. In Figure 5a the pressure during reaction for the different ligands is plotted against time. Clearly, the pressure decreases faster when the less basic triphenylphosphine analogue is applied. For ligand **I** the pressure “drops” by about 20 MPa in the first 15 min of reaction.

In Figure 5b the pressure and the selectivity for aldehydes are plotted as a function of conversion for the four cases in which the ligand has been varied. It can be seen that there is a subtle difference between the pressure profile for the different ligands. The observed pressure profile for ligand **I** is clearly higher than the other pressure profiles. The correlation with the measured chemoselectivity for aldehydes as a function of the conversion is clear; the higher the chemoselectivity during reaction the lower the pressure. It could be expected that this correlation should exist. The chemoselectivity is mainly determined by the contribution of the hydroformylation and the main side reaction. The main side reaction of the hydroformylation of 1-octene is the formation of 2-octene, and in this isomerization reaction no syngas is consumed. As a result, for catalysts with a higher isomerization rate a smaller decrease in pressure is to be expected.

Another aspect that is important for optimal operation is knowledge on the phase behavior of the reaction mixture. This requires a sufficiently accurate thermodynamic description of multicomponent mixture under reaction conditions. Literature data on the phase behavior of, in particular, “supercritical” multicomponent systems is limited. A reason for this is that the phase behavior of a multicomponent mixture becomes considerably more complex

as a function of the number of components.^[27-31] Therefore, studies dealing with fluid phase equilibria usually consider systems containing not more than three substances.

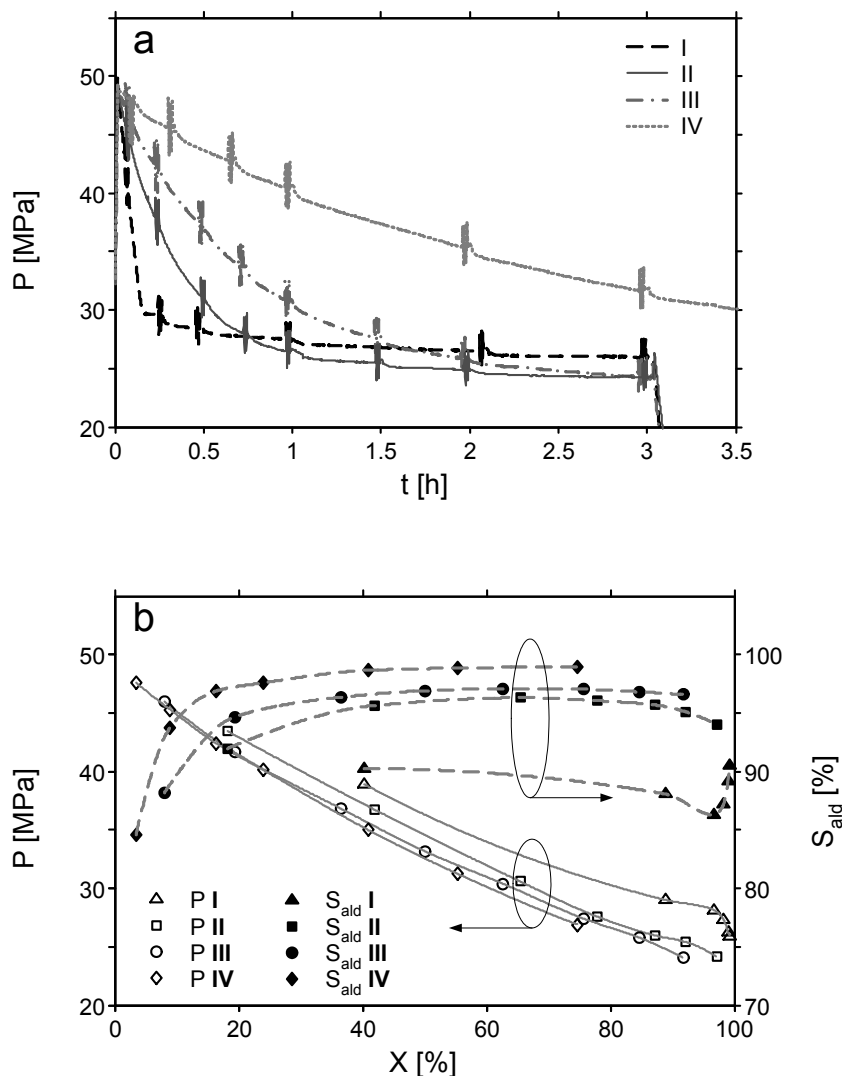


Figure 5. a) The reactor pressure as a function of time for the hydroformylation of 1-octene performed in a carbon dioxide enriched one-phase system. The initial concentration of reactants and solvent are similar the ligand is varied: **I** $P(C_6H_3-3,5-(CF_3)_2)_3$, **II** $PPh(C_6H_3-3,5-(CF_3)_2)_2$, **III** $P(C_6H_4-3-CF_3)_3$, and **IV** $P(C_6H_5)_3$; b) the pressure and the total selectivity for aldehydes at the time of sampling as a function of conversion.

In Figure 6 calculated pressure-temperature and density-temperature envelopes are depicted for reaction mixtures at five different conversion levels during the hydroformylation of 1-octene in $scCO_2$. The formation of nonanal from 1-octene, hydrogen, and carbon monoxide is used as the model reaction. The data for these graphs have been generated using the property analysis tool available in Aspen Plus. The thermodynamic behavior of this five-

component system is predicted using the Peng-Robinson equation of state with a minimum number of 10 binary interaction parameters. Consequently, Figure 6a and 6b only serve as an illustration of how the phase behavior of a reaction mixture may develop as a function of the conversion. The area inside the envelope represents the range of conditions where a two-phase system is present. The area outside the envelope corresponds to the conditions where a one-phase system is present.

Near the critical point and outside the envelope it can be expected that the system is a one-phase supercritical fluid. At lower temperatures the one-phase fluid is a liquid and at high temperature the fluid is a gas. Clearly, the phase behavior during reaction can change considerably, which is illustrated by the shifting pressure-temperature and density-temperature envelopes as a function of the conversion.

For the batch reactions the phase behavior during reaction is best derived using a density-temperature envelope. In the case of a continuous reaction with the hypothetical initial composition given in Figure 6, applying a total pressure of about 25 MPa would ensure a one-phase system irrespectively of the temperature. For an isothermal batch reaction a high enough density has to be applied. Therefore, it is a prerequisite that the reactor has a sufficient range in working pressure, in order to investigate batch reactions as a function of temperature at a similar density. This has been discussed in detail in Chapter 3. At 50 °C a maximum pressure of about 30 MPa was reached just after addition of the substrate. At 70 °C a maximum pressure of about 40 MPa was reached at corresponding concentrations of solvent and reactants applied at 50 °C.

The results presented in Figure 5 and in Chapter 2 can have implications for the screening of new homogeneous catalysts in unconventional solvents like carbon dioxide. In batch reactions following the pressure as a function of time can provide information on the activity and the chemoselectivity of a catalyst. However, analysis of the reaction mixture composition in time remains the preferred method to obtain the most conclusive information on catalyst activity and selectivity. This has been illustrated in Chapters 3, 4, 5 and 6. The phase behavior can have a significant influence on the catalysis, see for example references.^[32-34] In a continuous reaction the phase behavior can be conveniently altered by adjusting the pressure or temperature.^[35] This is a further incentive to “scale-up” homogeneously catalyzed reactions in carbon dioxide from a batch process to a continuously operated process.

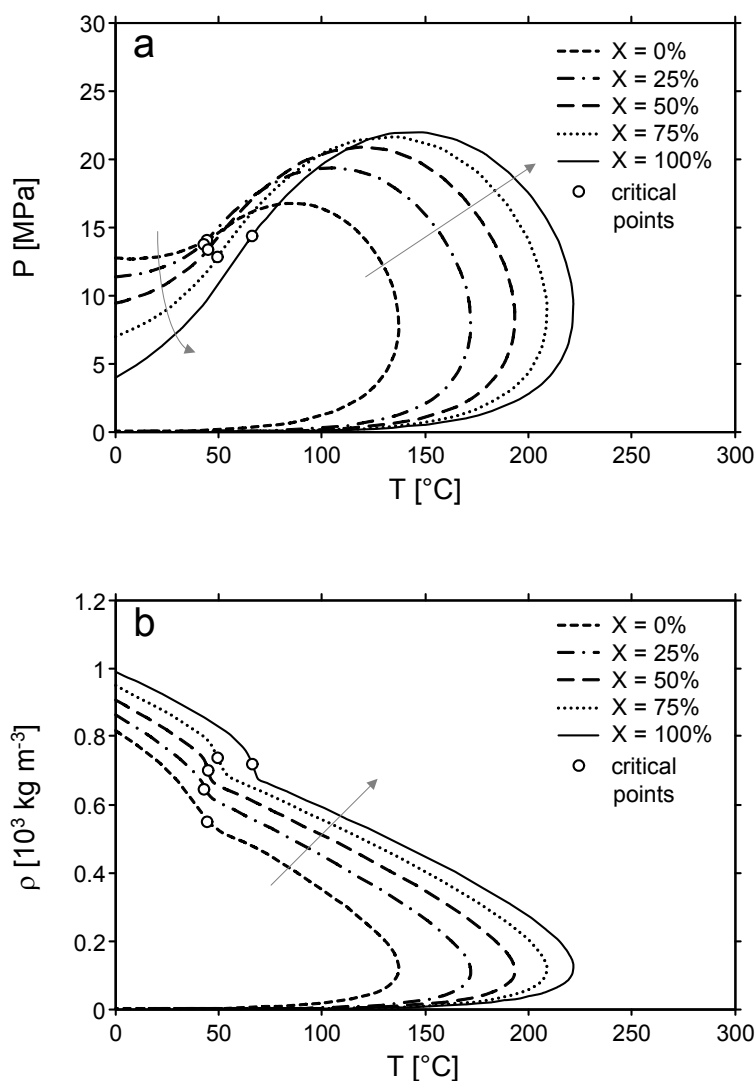


Figure 6. Pressure-temperature envelope (a) and density-temperature-envelope (b) for a reaction mixture as a function of conversion, X . Initial composition of the mixture, in mol fractions, at $X = 0$ %: $x_{\text{CO}} = 0.06$, $x_{\text{H}_2} = 0.06$, $x_{\text{CO}_2} = 0.83$, $x_{1\text{-octene}} = 0.05$. The arrows indicate the direction of the increase in conversion.

Carbon dioxide as a solvent for hydroformylation reactions

Subtle differences in activity and selectivity have been observed when the same catalyst is applied in the solvents carbon dioxide, hexane, and toluene. In particular, the difference in catalyst performance appears to be small when CO_2 and hexane are compared. In Chapter 6 the comparison has been extended by considering the “solventless” case. In that case the combination of the substrate 1-octene and the product aldehyde acts as the solvent. Clearly,

with a similar reactor volume, similar amounts of reactant and catalyst precursors, a considerably higher activity is found for the solventless or “neat” case than for the case with carbon dioxide as the solvent. The overall chemoselectivity and regioselectivity are comparable for these two cases. However, when a closer look is taken at the observed intrinsic or differential selectivity at low carbon monoxide concentration, the solvent carbon dioxide offers the highest differential regioselectivity.

Another advantage of diluting the reaction mixture is the possible reduction of unwanted side products, referred to as “heavy ends”, which can be formed during the hydroformylation of 1-octene. Aldehyde products can form dimers and trimers by aldol addition and condensation reactions. In particular for Co-catalyzed hydroformylation of long chain alkenes about 5 to 15% of the alkene can be converted to heavy ends.^[36] The rate of aldol formation depends on the concentration of aldehyde.^[37]

For a number of reactions conducted in scCO₂ a so-called pressure effect has been observed. One way to describe this is by using transition state theory to take the difference in molar volumes of reactants and the transition states into account as explained in Chapter 3. Alternatively, a pressure effect can also occur because of changes in the thermodynamic properties of the fluid. In Figure 6 the fugacity coefficient of carbon monoxide and hydrogen is plotted against the total pressure and the carbon dioxide concentration for a ternary mixture of CO₂-CO-H₂. The data for Figure 6 have been obtained with Aspen Plus using the Peng-Robinson equation of state in conjunction with the Van der Waals mixing rules. For each binary system one single interaction parameter has been used as input. The values for the interaction parameters are given in Chapter 2. The beginning of the lines at the left hand side of the graph corresponds to an equimolar mixture of carbon monoxide and hydrogen, both with a concentration of 1 mol L⁻¹, at 70 °C and 5.8 MPa. Moving to the right in the graph, carbon dioxide is added up to a pressure of about 32 MPa, which corresponds to a mixture of carbon monoxide, hydrogen, and carbon dioxide with a concentration of 1, 1 and 14.5 mol L⁻¹, respectively. This composition has been frequently used as starting point in the hydroformylation experiments. By increasing the CO₂ concentration, not only the density of the system increases but also the fugacity of carbon monoxide and hydrogen increase.*^[38]

* The fugacity of a gas represents the effective pressure of a gas. The fugacity of a species *i*, f_i , is related to the partial pressure of *i*, p_i , in the following way: $f_i = \phi_i \times p_i$. ϕ_i is the (dimensionless) fugacity coefficient.

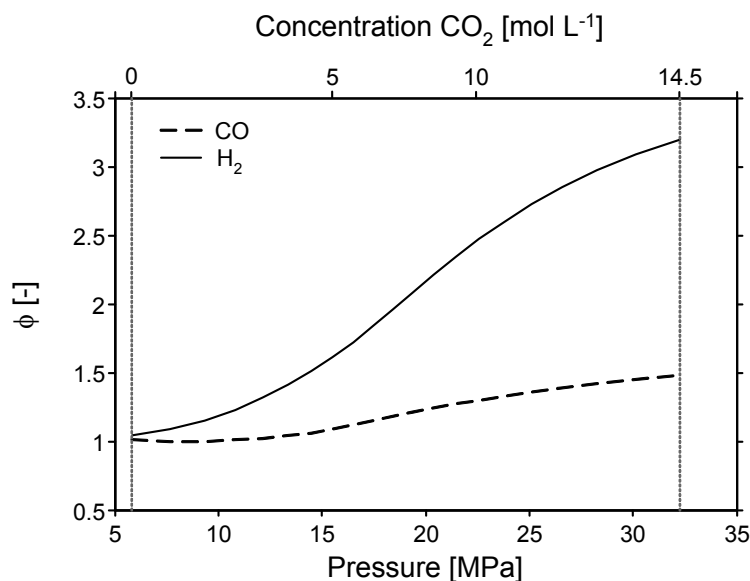


Figure 6. Fugacity coefficients of carbon monoxide and hydrogen as a function of total pressure and carbon dioxide concentration at 70 °C. The concentration of carbon monoxide and hydrogen is 1 mol L⁻¹. The carbon dioxide concentration corresponding to the pressure is given on the second (top) x-axis.

This simultaneous change of the fugacity of carbon monoxide and hydrogen will probably have only a subtle influence on the reaction rate. For the catalyst based on tris(bis-3,5-(trifluoromethyl)phenyl)phosphine and [Rh(CO)₂acac] a higher fugacity of carbon monoxide retards the reaction rate and a higher fugacity of hydrogen can enhance the reaction rate. With regard to the regioselectivity of the hydroformylation reaction, however, it is known that the concentration of carbon monoxide has a substantial effect on the regioselectivity, while the effect of hydrogen concentration is negligible. The fugacity of the reactant gases can be altered by the presence of carbon dioxide and this can be used to influence the regioselectivity for hydroformylation reactions.

Solventless hydroformylation of 1-octene with fluoros phosphine modified rhodium catalyst is an attractive option, certainly when the catalyst retention can be accomplished by membrane separation. On the other hand, the addition of carbon dioxide to expand 1-octene or completely homogenize the reaction mixture can offer some advantages, like increased regioselectivity at low syngas concentrations. Furthermore, from an engineering point of view, the application of a one-phase supercritical reaction mixture allows for a good mass transfer, also on a larger scale. This can result in a more facile process control of the exothermic hydroformylation. To establish whether the application of carbon dioxide in the

hydroformylation as a solvent on an industrial scale can be successful, more research efforts are necessary. Two “extreme cases” have been studied, the one-phase supercritical case and the two-phase “neat” case. It would be interesting to determine how the regioselectivity during the hydroformylation develops in a carbon dioxide expanded 1-octene/aldehyde phase. This system could potentially combine the best of the two extreme cases; a high regioselectivity (supercritical case) and a high activity (neat case).

Concluding remarks

Using a membrane for retention of a homogeneous catalyst in combination with the application of carbon dioxide as a solvent for the continuous hydroformylation of 1-octene has great potential. The proposed membrane reactor concept has a generic character, which will make continuously operated catalytic processes in supercritical fluids possible. Asymmetric hydrogenation is such a commercially relevant example in which very expensive soluble organometallic catalysts are used.^[39-42] As a result of the experimental methods described in this thesis the potential benefits of using carbon dioxide as an environmentally benign alternative to organic solvents can be further extended.

References

- [1] P. W. N. M. van Leeuwen, in *Homogeneous Catalysis: Understanding the Art*, Kluwer Academic Publishers, Dordrecht, **2004**, p. 139-174.
- [2] T. Djekić, A.G.J. van der Ham, A.B. de Haan, *J. Chromatography A* **2007**, *1142*, 32-38.
- [3] R. Noyori, H. Takaya, *Acc. Chem. Res.* **1990**, *23*, 345-350.
- [4] K. de Smet, S. Aerts, E. Ceulemans, I. F. J. Vankelecom, P. A. Jacobs, *Chem. Commun.* **2001**, 597-598.
- [5] L. J. P. van den Broeke, E. L. V. Goetheer, A. W. Verkerk, E. de Wolf, B.-J. Deelman, G. van Koten, J. T. F. Keurentjes, *Angew. Chem. Int. Ed.* **2001**, *40*, 4473-4474.
- [6] E. L. V. Goetheer, A. W. Verkerk, L. J. P. van den Broeke, E. de Wolf, B.-J. Deelman, G. van Koten, J. T. F. Keurentjes, *J. Catal.* **2003**, *219*, 126-133.
- [7] T. van Gestel, C. Vandecasteele, A. Buekenhoudt, C. Dotremont, J. Luyten, R. Leysen, B. van der Bruggen, G. Maes, *J. Membrane Sci.* **2002**, *207*, 73-89.
- [8] T. van Gestel, H. Kruidhof, D. H. A. Blank, H. J. M. Bouwmeester, *J. Membrane Sci.* **2006**, *284*, 128-136.
- [9] S. Kainz, D. Koch, W. Baumann, W. Leitner, *Angew. Chem. Int. Ed.* **1997**, *15*, 1628-1630.
- [10] D. Koch, W. Leitner, *J. Am. Chem. Soc.* **1998**, *120*, 13398-13404.
- [11] A. M. Banet Osuna, W. Chen, E. G. Hope, R. D. W. Kemmitt, D. R. Paige, A. M. Stuart, J. Xiao, L. Xu, *Dalton Trans.* **2000**, *22*, 4052-4055.
- [12] D. J. Adams, J. A. Bennett, D. J. Cole-Hamilton, E. G. Hope, J. Hopewell, J. Kight, P. Pogorzelec, A. M. Stuart, *Dalton Trans.*, **2005**, 3862-3867.
- [13] M. Kranenburg, Y. E. M. van der Burgt, P. C. J. Kamer, P. W. N. M. van Leeuwen, *Organometallics* **1995**, *14*, 3081-3089.

- [14] J. Xiao, S. C. A. Nefkens, P. G. Jessop, T. Ikariya, R. Noyori, *Tetrahedron Lett.* **1996**, *37*, 2813-2816.
- [15] P. G. Jessop, R. R. Stanley, R. A. Brown, C. A. Eckert, C. L. Liotta, T. T. Ngo, P. Pollet, *Green Chem.* **2003**, *5*, 123-128.
- [16] Y. Hu, D. J. Birdsall, A. M. Stuart, E. G. Hope, J. Xiao, *J. Mol. Catal. A.* **2004**, *219*, 57-60.
- [17] M. Berthod, G. Mignani, M. Lemaire, *Tetrahedron: Asymmetry* **2004**, *15*, 1121-1126.
- [18] D. J. Adams, D. J. Cole-Hamilton, D. A. J. Harding, E. G. Hope, P. Pogorzelec, A. M. Stuart, *Tetrahedron* **2004**, *60*, 4079-4085.
- [19] N. J. Ronde, D. Vogt, in *Catalyst Separation, Recovery and Recycling, Chemistry and Process Design*, Eds. D. J. Cole-Hamilton, R. P. Tooze, Springer, Dordrecht, **2006**, p.73-104.
- [20] R. Kreiter, A. W. Kleij, R. J. M. Klein Gebbink, G. van Koten, *Topics in Current Chemistry* **2001**, *217*, 163-199.
- [21] E. L. V. Goetheer, M. W. P. L. Baars, L. J. P. van den Broeke, E. W. Meijer, J. T. F. Keurentjes, *Ind. Eng. Chem. Res.* **2000**, *39*, 4634-4640.
- [22] R. M. Crooks, M. Zhao, L. Sun, V. Chechnik, L. K. Yeung, *Acc. Chem. Res.* **2001**, *34*, 181-190.
- [23] L. K. Yeung, C. T. Lee Jr., K. P. Johnston, R. M. Crooks, *Chem. Commun.* **2001**, 2290-2291.
- [24] D. E. Bergbreiter, *Chem. Rev.* **2002**, *102*, 3345-3384.
- [25] I. Kani, M. A. Omary, M. A. Rawashdeh-Omary, Z. K. Lopez-Castillo, R. Flores, A. Akgerman, J. P. Fackler Jr., *Tetrahedron* **2002**, *58*, 3923-3928.
- [26] Z. K. Lopez-Castillo, R. Flores, I. Kani, J. P. Fackler Jr., A. Akgerman, *Ind. Eng. Chem. Res.* **2003**, *42*, 3893-3899.
- [27] J. Ke, B. Han, M. W. George, H. Yan, M. Poliakoff, *J. Am. Chem. Soc.* **2001**, *123*, 3661-3670.
- [28] J. Ke, M. W. George, M. Poliakoff, B. Han, H. Yan, *J. Phys. Chem. B* **2002**, *106*, 4496-4502.
- [29] C. J. Peters, K. Gauter, *Chem. Rev.* **1999**, *99*, 419-431.
- [30] J. O. Valderrama, *Ind. Eng. Chem. Res.* **2003**, *42*, 1603-1618.
- [31] J. Ke, R. M. Oag, P. J. King, M. W. George, M. Poliakoff, *Angew. Chem. Int. Ed.* **2004**, *43*, 5192-5195.
- [32] S. Kainz, W. Leitner, *Catal. Lett.* **1998**, *55*, 223-225.
- [33] R. S. Oakes, A. A. Clifford, K. D. Bartle, M. Thornton Pett, C. M. Rayner, *Chem. Commun.* **1999**, 247-248.
- [34] M. Burgener, R. Furrer, T. Mallat, A. Baiker, *Appl. Catal. A* **2004**, *268*, 1-8.
- [35] J. R. Hyde, P. Licence, D. Carter, M. Poliakoff, *Appl. Catal. A* **2001**, *222*, 119-131.
- [36] C. D. Frohning, C. W. Kohlpaintner, H.-W. Bohnen, in *Applied Homogeneous Catalysis*, 2nd ed., Vol. 1, (Eds.: B. Cornils, W. A. Herrmann), Wiley-VCH, Weinheim, **2002**, p. 31-103.
- [37] G. Montrasi, G. Pagani, G. Gregorio, P. Cavalieri d'Oro A. Andreetta, *Chim. Ind.* **1980**, *62*, 737-742.
- [38] J. M. Smith, H. C. Van Ness, M. M. Abbott, *Introduction to Chemical Engineering Thermodynamics*, McGraw-Hill, 5th ed., New York, **1996**, p. 315-365.
- [39] H. U. Blaser, F. Spindler, M. Studer, *Appl. Catal. A*, **2001**, *221*, 119-143.
- [40] S. Kainz, A. Brinkmann, W. Leitner, A. Pfaltz, *J. Am. Chem. Soc.* **1999**, *121*, 6421-6429.
- [41] H.-U. Blaser, B. Pugin, F. Spindler, in *Applied Homogeneous Catalysis with Organometallic Compounds*, 2nd ed., Vol. 3, (Eds.: B. Cornils, W. A. Herrmann), Wiley-VCH, Weinheim, **2002**, p. 1131-1147.
- [42] J. G. de Vries, C. J. Elsevier (Eds.), *The Handbook of Homogeneous Hydrogenation* Wiley-VCH, Weinheim, **2007**.

Summary

Homogeneously Catalyzed Hydroformylation in Supercritical Carbon Dioxide: Kinetics, Thermodynamics, and Membrane Reactor Technology for Continuous Operation

The increased awareness for environmental issues and concomitant environmentally conscious governmental policies has prompted the chemical process industry to implement “greener” production and synthesis methods. In particular, the reduction of the emission of harmful, often organic, substances, reduction of the production of waste, and increasing the energy efficiency are three important aspects in the development of environmentally benign chemical production processes. For the chemical and chemical engineering academic community this has given rise to a new direction, where the concept of “green chemistry” is being explored.

Supercritical fluids have been established as promising substitutes to organic solvents. Carbon dioxide is of particular interest as an alternative solvent as it has a low toxicity, is non-flammable and has an accessible critical temperature and pressure. In addition, catalysis is an important tool for the optimization of atom efficiency of a chemical conversion, and therefore for the reduction of waste production. Additionally, catalysis allows for reactions to take place under milder conditions, which can also contribute to an increase in energy efficiency. In particular, soluble molecular organometallic catalysts allow chemical conversions with a higher rate and a better selectivity than their heterogeneous counterparts. The difficult separation of a homogeneous catalyst from reaction products, without deactivating the catalyst, is one of the main obstacles for their application on an industrial scale. Nanofiltration using a microporous ceramic membrane has the potential to be a solution to this problem. A large enough catalyst molecule will be retained while reaction products and solvent can permeate across the membrane. In the field of separation technology membranes have emerged as an energy efficient alternative to conventional separation methods, like distillation and extraction. Ceramic membranes are seen as one of the most promising candidates to purify process streams under demanding conditions.

The main objectives of this thesis are the evaluation of the possible advantages of using supercritical carbon dioxide as a solvent as an alternative for organic solvents, and the

investigation into the potential of membrane technology for the retention of homogeneous catalysts. The hydroformylation of 1-octene, which is an example of a homogeneously catalyzed reaction on an industrial scale, is considered as a model reaction.

To perform the hydroformylation in supercritical carbon dioxide an experimental procedure has been developed, which allows for catalyst preparation under hydroformylation conditions and for carrying out the hydroformylation reaction with a well-defined starting point. It has been demonstrated that with this experimental procedure it is possible to obtain highly reproducible results. Furthermore, a relationship between the change in pressure and the change in reaction mixture composition as a function of time has been established. Using this experimental procedure the effect of total pressure, temperature, concentration of reactants, and concentration of catalyst precursors on the reaction rate, chemoselectivity, and the regioselectivity of the hydroformylation of 1-octene has been studied. The concentration of carbon dioxide had an effect on the regioselectivity of the reaction. Therefore, the same density of solvent has been used for each experiment rather than the more common approach of applying the same total pressure for each experiment. Based on the results obtained by the variation of the reaction parameters a kinetic model has been developed. An optimization method has been applied to find the model parameter values that best describe the experimental data. The observed kinetics for the catalyst based on rhodium(I) dicarbonyl acetylacetonate and tris(3,5-bis(trifluoromethyl)phenyl)phosphine shows resemblance to that observed for the hydroformylation where bulky phosphites have been used as the ligand. For this catalyst a high activity in the order of 5×10^3 to $12 \times 10^3 \text{ mol}_{1\text{-octene}} \text{ mol}_{\text{Rh}}^{-1} \text{ h}^{-1}$ has been observed at 70 °C.

Organometallic complexes based on rhodium with phosphine ligands with a varying number of trifluoromethyl groups have been screened for their activity and selectivity for the hydroformylation of 1-octene. Furthermore, the effect of the type of solvent: carbon dioxide, hexane, and toluene has been included in this study. An increase in the number of trifluoromethyl substituents on the triphenylphosphine ligand results in an increase in 1-octene conversion rate and a decrease in the overall selectivity towards aldehydes. This behaviour is observed in all three solvents. For supercritical carbon dioxide or hexane, as the solvent, the outcome of the hydroformylation reaction in terms of activity and selectivity shows great similarity.

By following the hydroformylation of 1-octene in time, it was observed that during batch operation rhodium catalysts with trifluoromethyl-substituted triarylphosphines showed a higher differential regioselectivity than based on the overall regioselectivity at the end of the reaction. For the hydroformylation in carbon dioxide this effect was most pronounced. Both the mode of operation, batch or semi batch, and the type of solvent had a significant influence on this phenomenon.

The transport of a supercritical fluid across a microporous alumina supported titania membrane has been investigated. The dependence of the permeation of carbon dioxide across the titania membrane on the feed pressure is similar to what has been previously observed for microporous alumina supported silica membranes. At high feed pressure viscous flow appears to be the main mechanism of mass transport across the membrane. Furthermore, the titania membrane shows a reasonable stability over a period of operation of about at least six months in varying conditions.

Finally, the first continuously operated experiment has been performed, in which hydroformylation of 1-octene and separation of the catalyst have been integrated using a membrane reactor. During a 27.5 h of operation of the membrane reactor, spread over four consecutive days, a maximum conversion of 17 % and a maximum regioselectivity of 5 in terms of *n*:*iso* ratio has been observed. The conversion and the *n*:*iso* ratio, which is the ratio between the linear and branched aldehyde product, decrease as a function of the number of permeated reactor volumes indicating a loss of catalyst. Permeation of free ligand and the catalytic species through the membrane appear to be the main reasons for the decrease in activity and selectivity. A good match between membrane retention characteristics and the size of the catalyst and its precursors is not found yet. However, a number of feasible improvements can be made to improve the retention of the catalyst.

Using a membrane for retention of a homogeneous catalyst in combination with the application of carbon dioxide as a solvent for the continuous hydroformylation of 1-octene has great potential. Successful application of the envisioned membrane reactor process can have implications for other homogeneously catalyzed reactions of which asymmetric hydrogenation is a commercially relevant example. As a result of the experimental methods used in this thesis the potential benefits of using carbon dioxide as an environmentally benign alternative to organic solvents could be further extended.

Samenvatting

Het groeiende bewustzijn voor het milieu en de daarmee samenhangende strikter wordende wetgeving zorgen ervoor dat de chemische industrie “groenere”, dat wil zeggen schonere, productie en synthese methoden moet gaan implementeren. Het terugdringen van emissies van bijvoorbeeld vluchtige organische stoffen, de reductie van de productie van afvalstoffen en het vergroten van de energie-efficiëntie zijn drie belangrijke aspecten in de ontwikkeling van milieuvriendelijkere productieprocessen. Dit heeft er toe geleid dat de academische gemeenschap op het gebied van chemie en chemische technologie meer en meer het concept “groene chemie” is gaan verkennen.

Superkritische fluida zijn een veelbelovend alternatief voor organische oplosmiddelen. Vooral koolstofdioxide is interessant als een alternatief oplosmiddel vanwege de lage toxiciteit, onbrandbaarheid, en de toegankelijke kritische temperatuur en druk. Daarnaast speelt katalyse een zeer belangrijke rol om de atoomefficiëntie van een chemische omzetting te maximaliseren om zo een reductie in afvalstoffenproductie te realiseren. Bovendien kan er met behulp van katalyse bij mildere reactiecondities gewerkt worden, zodat de energie-efficiëntie eventueel ook verbeterd kan worden. Voor vergelijkbare reacties levert het gebruik van oplosbare moleculaire organometalkatalysatoren (een belangrijke klasse van homogene katalysatoren) vaak een betere produktselectiviteit en reactiesnelheid op dan het gebruik van een heterogene niet oplosbare katalysator. Over het algemeen is het moeilijk homogene katalysatoren te scheiden van de reactieproducten zonder de katalysator te deactiveren en dit is een groot obstakel voor de toepassing van deze katalysatoren op industriële schaal. Nanofiltratie, waarbij gebruik wordt gemaakt van een microporeus keramisch membraan, is een eventuele oplossing voor dit probleem. De relatief grote katalysatormoleculen worden tegengehouden door het membraan terwijl de relatief kleine product- en oplosmiddelmoleculen door het membraan kunnen permeëren. Membraanscheiding is een alternatief voor de meer traditionele scheidingstechnieken, zoals destillatie en extractie. Vooral keramische membranen worden gezien als een goede kandidaat voor de zuivering van processtromen onder veeleisende condities.

De hoofddoelen van dit werk zijn de evaluatie van de eventuele voordelen van het gebruik van “superkritisch” koolstofdioxide ten opzichte van organische oplosmiddelen en het inzicht verkrijgen in het potentieel van het toepassen van keramische membranen om homogene katalysatoren te scheiden. De hydroformylering van 1-octeen, een voorbeeld van een homogeen gekatalyseerd productieproces op industriële schaal, wordt hierbij gebruikt als modelreactie.

Voor de uitvoering van de hydroformyleringsreactie met koolstofdioxide als oplosmiddel in een batchreactor is er een experimentele procedure ontwikkeld waarbij de katalysator gevormd wordt onder hydroformyleringscondities en waarbij het startpunt van de reactie goed bepaald kan worden. Met deze procedure is het mogelijk resultaten te behalen met een hoge reproduceerbaarheid. Er is een verband gevonden tussen de verandering in reactordruk en de verandering in de samenstelling van het reactiemengsel. Gebruikmakende van de ontwikkelde procedure is het effect van totaal druk, temperatuur, concentratie van reactanten en de concentratie van katalysatorprecursoren op de reactiesnelheid, chemoselectiviteit en regioselectiviteit van de hydroformylering van 1-octeen onderzocht. Er is een effect van de concentratie van koolstofdioxide op de regioselectiviteit van de reactie waargenomen. Om deze reden is voor elk experiment een zelfde concentratie van koolstofdioxide toegepast in plaats van de meer gebruikelijke aanpak waarbij de totale initiële reactordruk per experiment gelijk wordt gehouden. Op basis van de resultaten verkregen met experimenten waarbij de initiële concentraties van de reactanten en katalysator gevarieerd zijn is een mathematische beschrijving van de kinetiek van de reactie opgesteld. Er is een optimalisatieroutine toegepast om de waarden van modelparameters te bepalen waarmee het beste de experimentele resultaten te beschrijven zijn.

Het is gebleken dat de kinetiek van de hydroformyleringsreactie voor de katalysator gebaseerd op rhodium(I)dicarbonylacetylacetaat en tris(3,5-bis(trifluoromethyl)phenyl)-phosphine gelijkenis vertoont met de reactiekinetiek gevonden met een rhodium katalysator met zeer sterische gehindere phosphieten als ligand. Deze katalysator heeft een hoge activiteit. De waarden voor de initiële reactiesnelheid liggen tussen 5×10^3 en 12×10^3 mol_{1-octeen} mol_{Rh}⁻¹ u⁻¹ bij 70 °C.

Rhodium katalysatoren in situ gesynthetiseerd met rhodium(I)dicarbonylacetylacetaat en phosphines met een variërend aantal trifluormethyl substituenten zijn onderzocht op hun activiteit en selectiviteit voor de hydroformylering van 1-octeen. Bovendien is hierbij ook het

effect van het oplosmiddel, koolstofdioxide, hexaan en toluen bekeken. Het gebruik van een triphenylphosphine ligand met een toenemend aantal trifluoromethyl substituenten resulteert in een hogere reactiesnelheid en een lagere chemoselectiviteit voor het aldehyde. Deze verschijnselen zijn waargenomen in alle drie bovengenoemde oplosmiddelen. Qua katalysatoractiviteit en selectiviteit vertonen de resultaten verkregen met koolstofdioxide en hexaan als oplosmiddel een grote gelijkenis.

Door het volgen van de hydroformylering van 1-octeen in de tijd bleek dat gedurende de batchreactie gebruikmakende van rhodium katalysatoren met trifluoromethyl gesubstitueerde triarylphosphine liganden de differentiele regioselectiviteit bij hoge conversie groter was dan de cumulatieve regioselectiviteit op het eind van de reactie. Bij de batchreactie met koolstofdioxide was dit verschijnsel het duidelijkst waarneembaar. De uitvoering van de reactie, batch of semi-batch, en het oplosmiddel hebben beide een significant effect op de regioselectiviteit gedurende de reactie.

Het massatransport van superkritische fluida door een titania membraan is onderzocht. De afhankelijkheid van de voedingsdruk van koolstofdioxide permeatie door een titania membraan is vergelijkbaar met wat eerder waargenomen is voor microporeuze silica membranen. Bij een hoge voedingsdruk lijkt visceus transport het overheersende transport mechanisme te zijn. Bovendien is er een redelijke stabiliteit waargenomen gedurende een periode van zes maanden onder variërende condities.

Ten slotte is er een continu experiment uitgevoerd waarbij getracht is de hydroformylering van 1-octeen en de scheiding van de katalysator te combineren. Gedurende een totale periode van 27.5 u verspreid over 4 opeenvolgende dagen is er een maximum conversie van 17 % en een maximum regioselectiviteit, *n:iso* ratio (*n*-nonanal/*iso*-aldehyden), van 5 waargenomen. De conversie en de *n:iso* ratio namen af als functie van het aantal reactorvolumes wat door het membraan permeëerde. Dit is een indicatie dat er katalysatorverlies is opgetreden. Het is aannemelijk dat permeatie van vrij ligand en katalysator door het membraan de belangrijkste oorzaak is van de afname in activiteit en selectiviteit. Een goede afstemming tussen de membraankarakteristieken (o. a. de gemiddelde poriegrootte) en de grootte van de katalysator en katalysatorprecursoren is nog niet gevonden. Desalniettemin, zijn er voldoende opties om de retentie van de katalysator te verbeteren.

Het gebruik van een membraan voor het tegenhouden van een homogene katalysator in combinatie met het gebruik van koolstofdioxide als oplosmiddel biedt nieuwe mogelijkheden

om de hydroformylering van 1-octeen continu uit te voeren. Als het hier onderzochte membraanreactor concept werkt voor de hydroformylering van 1-octeen dan kan dit concept ook toegepast worden in andere homogeen gekatalyseerde processen. Bijvoorbeeld in asymetrische hydrogenering wat een commercieel interessant proces is. Op basis van de resultaten beschreven in dit proefschrift kunnen de mogelijke voordelen van het toepassen van koolstofdioxide als milieuvriendelijk alternatief voor oplosmiddelen verder worden uitgewerkt.

Curriculum Vitae

Ard Koeken werd geboren op 18 oktober 1978 te Oosterhout. In 1997 behaalde hij zijn diploma op het Newmancollege in Breda. Vervolgens startte hij zijn opleiding bij de Faculteit Scheikundige Technologie aan de Technische Universiteit Eindhoven. Na de afronding van een stage bij Roche Vitamins and Fine Chemicals (toen een divisie van F. Hoffmann – La Roche Ltd) in Basel, Zwitserland, begon hij met afstuderen binnen de capaciteitsgroep Procesontwikkeling. In maart 2003 werd het afstudeerwerk getiteld: “Evaluation of a heterogeneously catalysed hydrogenation reaction in supercritical CO₂” voltooid. Aansluitend startte hij met zijn promotieonderzoek onder de supervisie van prof. dr. ir. J.T.F. Keurentjes en dr. L.J.P. van den Broeke op gebied van homogene katalyse gebruikmakende van koolstofdioxide als het oplosmiddel. Het onderzoek werd uitgevoerd in samenwerking met Arkema Vlissingen B. V. en ECN (Energieonderzoek Centrum Nederland).

Ard Koeken was born on the 18th of October 1978 in Oosterhout. In 1997 he obtained his secondary school diploma at the Newmancollege in Breda. Next, he started his study at the Chemical Engineering and Chemistry department at Eindhoven University of Technology. After completing an internship at Roche Vitamins and Fine Chemicals (at that time a division of F. Hoffmann – La Roche Ltd) in Basel, Switzerland, he started his graduation within the Process Development group. In March 2003 the graduation project titled “Evaluation of a heterogeneously catalysed hydrogenation reaction in supercritical CO₂” was completed. Subsequently, he began his doctoral research under the supervision of prof. dr. ir. J.T.F. Keurentjes and dr. L.J.P. van den Broeke in the field of homogeneous catalysis in supercritical fluids. The research was carried out in cooperation with Arkema Vlissingen B. V. and ECN (Energy research Centre of the Netherlands).

Dankwoord

Na mijn afstudeerproject binnen de capaciteitsgroep procesontwikkeling werd ik in de gelegenheid gesteld om een promotieonderzoek te doen met een prachtig en ambitieus onderwerp waar vele wetenschappelijke gebieden binnen de chemische technologie verenigd in konden worden. Daar ik tijdens een afstudeeropdracht eigenlijk slechts de tijd had een vleugje mee krijgen wat wetenschappelijk onderzoek inhield, wilde ik me graag inzetten voor een wat langer “onderzoeksavontuur”. Ik wil mijn promotor prof. dr. ir. Jos Keurentjes hartelijk danken dat hij mij die kans gegeven heeft. Ik het begin van het onderzoek moest ik wennen aan de vrijheid die ik daarbij had, maar tijdens de besprekingen kreeg ik altijd het vertrouwen. Dit alles resulteerde in een plezierige en leerzame samenwerking.

Dr. L. J. P. van den Broeke wil ik hartelijk danken voor al de hulp bij de totstandkoming van dit werk en de zeer prettige samenwerking. Peter, je was altijd welwillend om mijn dagelijkse beslommeringen aan te horen, je wist alles in perspectief te plaatsen, je kwam altijd met goede suggesties, en je wist mijn soms wat ingewikkelde Engels te ontrafelen.

Verder wil ik de leden van de kerncommissie, prof. dr. P. A. Jacobs, prof. dr. J. G. de Vries en prof. dr. ir. J. C. Schouten bedanken voor hun constructieve commentaar en goede suggesties.

Dit proefschrift is een resultaat van een onderzoeksproject waarbij ik samen heb gewerkt met Berth-Jan Deelman en Michiel van Vliet op het gebied van de katalyse (hoofdstuk 2-6, 8) en met Luci Correia, Paul Pex en Jaap Vente op het gebied keramische membranen (hoofdstuk 7 en 8). Ik heb de samenwerking als zeer leerzaam, productief en prettig ervaren. Dank hiervoor.

Naast goede begeleiding ontvangen te hebben, heb ik ook de eer gehad om een aardig groepje afstudeerders te begeleiden. Ik wil Marc Niessen, Jurjen Meeuwissen, Mariska de la Mar, Stefan de Bakker, Hester Costerus, Arjan Spaapen, Paul van Bavel en Paul Schouten van harte bedanken voor hun inzet, doorzettingsvermogen en de plezierige samenwerking. Ook al zijn jullie bijdragen niet altijd direct terug te vinden in het proefschrift, ze zijn onmisbaar geweest voor het voltooiën ervan. Jullie werk heeft veel inzicht verschaft.

Bij dezen wil ik ook alle anderen bedanken die op wat voor manier dan ook op het wetenschappelijke of praktische vlak betrokken zijn geweest bij dit promotieonderzoek en de totstandkoming van dit proefschrift.

Om onderzoeksvragen te beantwoorden moet je een aantal metingen kunnen verrichten. Om metingen te verrichten heb je experimentele opstellingen nodig. Graag wil ik volgende technici en ingenieurs van diverse vakgebieden bedanken die van essentieel belang zijn geweest bij de totstandkoming van de opstellingen: Anton Bombeek, Karel Janssen, Chris Luyk, Hans Wijtvliet, Jan Heerebeek, Madan Bindraban, Paul Aendenrooier, Jovita Moerel, Dolf van Liempt en alle anderen.

Mijn collega en oud-collega SPD'ers hebben altijd voor een heel prettige en gezellige sfeer gezorgd. De studiereizen naar Brazilië en Zuid-Afrika waren onvergetelijk en onverbeterlijk. De korte-gang-uitjes met de korte-gang-luitjes waren altijd zeer gemakkelijk en ontspannend. Hartelijk dank hiervoor. In het bijzonder wil ik Ana en Tom bedanken dat ze het met mij in het kantoor zo goed uitgehouden hebben. Earl Goetheer en Tjerk de Vries wil ik bedanken. Zij hebben in het begin van het afstudeer- en promotieonderzoek mij van veel advies met betrekking tot hogedruk experimenten voorzien. Dit heeft mij een vliegende start gegeven.

Ook buiten de universiteit zijn er de nodige mensen te bedanken. Ten eerste, mijn oud-mede-TU/e-studenten Tim, Twan, Sander en Maurice. Zij hebben er mede aan bijgedragen dat ik met voldoende kennis aan het promotieonderzoek heb kunnen beginnen. Daarnaast hebben we er voor gezorgd dat we, ondanks de drukke agenda's, de afgelopen jaren leuke bijeenkomsten hebben gehad. Mónica wil ik bedanken voor de mooie vriendschap die we hebben, dat heeft mij veel geholpen tijdens het promotieonderzoek.

Handbal en de handbalploeg/vriendenclub hebben altijd voor een onontbeerlijke bron van onspanning gezorgd. Zo is mijn "verstand" de afgelopen jaren voldoende keren "gereset" en ik denk absoluut dat dit voor de nodige "heldere momenten" heeft gezorgd.

Als laatste wil ik familie, vrienden en in het bijzonder mijn ouders, mijn broer en zus bedanken voor al hun steun, interesse en hun volste vertrouwen in mij. Het moge duidelijk zijn dat jullie een onmisbare basis zijn.

Ard Koeken